

緩衝材に係わる固溶体モデル 及び核種拡散挙動に関する研究

(動力炉・核燃料開発事業団 研究委託内容報告書)

1994年 2 月

三菱マテリアル株式会社

この資料は、動燃事業団の開発業務を進めるため、限られた関係者だけに配布するものです。従って、その取扱には十分注意を払って下さい。なお、この資料の供覧、複製、転載、引用等には事業団の承認が必要です。また今回の配布目的以外のことには使用しないよう注意して下さい。

This document is not intended for publication. No public reference nor disclosure to the third party should be made without prior written consent of Power Reactor and Nuclear Fuel Development Corporation.

本資料についての問合せは下記に願います。

〒107 東京都港区赤坂 1 - 9 - 13

動力炉・核燃料開発事業団

技術管理部 技術情報室

緩衝材に係わる固溶体モデル及び核種拡散挙動に関する研究

浅野 闘一*

要 旨

緩衝材による化学的緩衝作用は、粘土鉱物のイオン交換反応により支配される。また、核種の移行挙動は、緩衝材との相互作用及び緩衝材の空隙特性によって支配される。

本年度は、粘土鉱物（スメクタイト）のイオン交換反応モデルに関する研究を進めるとともに、クニゲルV1を用いてUとAmの実効拡散係数を測定した。

1. 固溶体モデル開発のための試験研究及びモデル研究

(1) スメクタイトのイオン交換反応モデルに関する検討

Na型スメクタイトについて、 K^+ 、 Ca^{2+} 、 Mg^{2+} 、 H^+ とのイオン交換平衡定数を測定した。その結果、それぞれのイオン交換平衡定数 ($\ln K_{ex}$) は、1.19, -0.25, 0.64, 1.17と求まった。

またPHRBEQE を用いてイオンの分配平衡を計算し、実測値との比較検討を行った。その結果、 K^+ 及び H^+ との分配平衡については、理想固溶体モデルによりほぼ推定可能であることがわかった。 Ca^{2+} 及び Mg^{2+} については、塩化物イオン ($CaCl^+$ 、 $MgCl^+$) によるイオン交換反応を考慮する必要がある。

(2) 平成4年度のイオン交換試験データ及び固溶体モデルのレビュー

平成4年度に実施したNa型スメクタイトのイオン交換試験の結果と、MX-80 について取得されたSposito のイオン交換平衡定数を用いて計算した結果を比較した。

その結果、両者はほぼ一致することから、Sposito のイオン交換平衡定数を用いて、Na型スメクタイトのイオン交換平衡を推定することはほぼ可能であることが示された。

2. ベントナイト中での核種の実効拡散係数の測定

(1) Uの実効拡散係数の測定

クニゲルV1を用いてUの実効拡散係数を測定した。クニゲルV1の乾燥密度が0.4, 1.0, 1.4, 2.0 g/cm³の場合、実効拡散係数はそれぞれ 4.0×10^{-11} , 1.2×10^{-11} , 2.6×10^{-12} , 3.5×10^{-12} m²/sと測定された。

(2) Amの実効拡散係数の測定

試験容器への吸着が問題となったため、試験溶液を酸性 (pH 2) に調整して実効拡散係数を測定した。クニゲルV1の乾燥密度が0.8, 1.4, 1.8 g/cm³の場合、実効拡散係数はそれぞれ 7.4×10^{-11} , 5.2×10^{-11} , 1.8×10^{-11} m²/sと測定された。

本報告書は、三菱マテリアル株式会社が動力炉・核燃料開発事業団の委託により実施した研究の成果である。

契約番号 : 050D0225

事業団担当課及び担当者 : 環境技術開発推進本部 処分研究グループ 園部一志

*原子力技術センター 技術第2部

Development of Solid-solution model on Buffer Materials
and Diffusion Behavior of Nuclides

Toichi Asano *

Abstract

1. Development of solid-solution model on buffer materials

(1) Development of solid-solution model on smectite

Ion-exchange equilibrium constants were measured about Na-smectite. Ion-exchange equilibrium constants ($\ln K_{ex}$) of K^+ , Ca^{2+} , Mg^{2+} and H^+ were estimated 1.19, -0.25, 0.64, 1.17, respectively.

Distributions of between Na-smectite and K^+ , Ca^{2+} , Mg^{2+} and H^+ were agreed to calculated distribution by ionexchange equilibrium constants.

The real solid-solution model can apply to estimation of ionic distributions. Ion-exchange equilibrium constants of $CaCl^+$ and $MgCl^+$ were needed for estimation of behavior of Ca and Mg.

(2) Review of the purpose of solid-solution models

Measured distribution data of Na-smectite in 1993 were agreed to calculated distribution by ion-exchange equilibrium constants of MX-80.

And the purpose of solid-solution models were reviewed.

2. Measurement of effective diffusion coefficient in bentonite

(1) Effective diffusion coefficient of U

Effective diffusion coefficients of U were measured in Kunigeru-V1. Dry density of Kunigeru-V1 were 0.4, 1.0, 1.4, 2.0 g/cm³. Effective diffusion coefficients of U were measured 4.0×10^{-11} , 1.2×10^{-11} , 2.6×10^{-12} , 3.5×10^{-12} m²/s, respectively.

(2) Effective diffusion coefficient of Am

Effective diffusion coefficients of Am were measured in Kunigeru-V1. pH condition was about 2. Dry density of Kunigeru-V1 were 0.8, 1.4, 1.8g/cm³. Effective diffusion coefficients of Am were measured 7.4×10^{-11} , 5.2×10^{-11} , 1.8×10^{-11} m²/s, respectively.

Work performed by Mitsubishi Materials Corporation under with Power Reactor and Nuclear Fuel Development Corporation.

Contract No.050D0225

PNC Lieson : Hitoshi Sonobe, Isolation System Reserch Program,
Radioactive Waste Management Project

*Waste Management Technology Department, Nuclear Technology Center.

目 次

要旨

第1章 研究計画

1.1	目的	1
1.2	実施内容	1
1.2.1	スメクタイトのイオン交換反応モデルに関する検討	1
1.2.2	平成4年度のイオン交換試験データ及び固溶体モデルのレビュー	2
1.2.3	ベントナイト中での実効拡散係数の測定	2

第2章 スメクタイトのイオン交換反応モデルに関する研究

2.1	イオン交換平衡定数の測定	
2.1.1	陽イオン交換容量の測定	3
2.1.2	イオン交換平衡定数の測定	11
2.2	2成分系分配平衡への適用性の検討	
2.2.1	計算方法	24
2.2.2	正則溶液モデルによる固相の活量係数	27
2.2.3	評価結果	33
2.3	3成分系分配平衡への適用性の検討	
2.3.1	分配試験	37
2.3.2	計算評価	38
2.3.3	測定値と計算結果の比較	41
2.4	まとめ	51

第3章 平成4年度のイオン交換試験データ及び固溶体モデルのレビュー

3.1	イオン交換試験データのレビュー	53
3.2	固溶体モデルの調査	56

第4章 ベントナイト中での実効拡散係数の測定

4.1	拡散係数の定義	
4.1.1	拡散係数の種類	57
4.1.2	実効拡散係数測定の方法	58
4.2	ベントナイト中でのウランの実効拡散係数測定	
4.2.1	試験内容	59
4.2.2	解析方法	66
4.2.3	ウランの定常拡散試験結果	68
4.3	ベントナイト中でのアメリカシウムの実効拡散係数測定	
4.3.1	吸着を起こさない試験装置材料および雰囲気の設定	73
4.3.2	定常拡散試験内容	79
4.3.3	アメリカシウムの定常拡散試験結果	82
4.4	考察	86

巻末資料1

- (1) Thermodynamic modelling of ion exchange reaction at the Na-smectite/water interface.
- (2) Review of the purpose of solid solution models and their potential applicability in predictive geochemical modelling.

巻末資料2

ウランの定常拡散試験データ

アメリカシウムの定常拡散試験データ

表目次

Table 2.1.1	Conditions of isothermal absorption test	4
Table 2.1.2 (1)	Result of isothermal absorption test about Na-smectite (K ⁺ + Na-smectite)	5
Table 2.1.2 (2)	Result of isothermal absorption test about Na-smectite (Ca ²⁺ + Na-smectite)	5
Table 2.1.2 (3)	Result of isothermal absorption test about Na-smectite (Mg ²⁺ + Na-smectite)	6
Table 2.1.2 (4)	Result of isothermal absorption test about Na-smectite (H ⁺ + Na-smectite)	6
Table 2.1.2 (5)	Result of isothermal absorption test about H-smectite (Na ⁺ + H-smectite)	6
Table 2.1.3	Results of calculation for CEC of smectite samples	10
Table 2.1.4	Conditions of ion-exchange equilibrium constant measurement	11
Table 2.1.5 (1)	Kielland plot data in K ⁺ + Na-smectite system	16
Table 2.1.5 (2)	Kielland plot data in Ca ²⁺ + Na-smectite system	17
Table 2.1.5 (3)	Kielland plot data in Mg ²⁺ + Na-smectite system	18
Table 2.1.5 (4)	Kielland plot data in H ⁺ + Na-smectite system	19
Table 2.1.5 (5)	Kielland plot data in Na ⁺ + H-smectite system	20
Table 2.1.6	Relation of between E _B and K _G	23
Table 2.1.7	Estimated ion-exchange equilibrium constants	23
Table 2.2.1	Conditions of estimation for ion-exchange equilibrium	25
Table 2.2.2	Ion-exchange equilibrium constants of Na-smectite	25
Table 2.2.3	Ion-exchange equilibrium constants of Na-smectite (PHREEQE format)	26
Table 2.2.4 (1)	Relation of equivalent fraction and activity coefficient in solid phase (K ⁺ + Na-smectite)	28
Table 2.2.4 (2)	Relation of equivalent fraction and activity coefficient in solid phase (Ca ²⁺ + Na-smectite)	28
Table 2.2.4 (3)	Relation of equivalent fraction and activity coefficient in solid phase (Mg ²⁺ + Na-smectite)	29
Table 2.2.4 (4)	Relation of equivalent fraction and activity coefficient in solid phase (H ⁺ + Na-smectite)	29

Table 2.2.5	Equation of relation equivalent fraction and activity coefficient about solid phase 32
Table 2.3.1 (1)	Conditions of ion-exchange equilibrium constant measurement (ternary system) 37
Table 2.3.1 (2)	Conditions of initial solutions (ternary system) 38
Table 2.3.2 (1)	Measured data of ionexchange equilibrium in $K^+ + H^+ + Na$ -smectite system 39
Table 2.3.2 (2)	Measured data of ionexchange equilibrium in $Ca^{2+} + H^+ + Na$ -smectite system 40
Table 2.3.3	Conditions of estimation for ion-exchange equilibrium (ternary system) 41
Table 4.2.1	Dry density of bentonite and the number of times of Uranium diffusion experiments 59
Table 4.2.2	Improvement point of steady-state diffusion experiment method 59
Table 4.2.3	Conditions of steady-state diffusion experiment of Uranium 60
Table 4.2.4	Chemical composition of Kunigeru-V1 61
Table 4.2.5	Mineral components of Kunigeru-V1 61
Table 4.2.6	Chemical composition of synthetic pore water for Kunigeru-V1 62
Table 4.2.7	Effective diffusivities of Uranium in compacted bentonite 68
Table 4.3.1	Results of the sorption tests for the purpose of decrease of Americium sorption on the equipment 75
Table 4.3.2	Dry density of bentonite and the number of times of Americium diffusion experiment 79
Table 4.3.3	Conditions of steady-state diffusion experiment of Americium 79
Table 4.3.4	Concentration of leaching cation after treatments of bentonite with HCl 80
Table 4.3.5	Effective diffusivities of Americium in compacted bentonite 82

目次

Fig. 2. 1. 1 (1) Isothermal absorption line of K^+ on Na-smectite (K^+ + Na-smectite) 7
Fig. 2. 1. 1 (2) Isothermal absorption line of Ca^{2+} on Na-smectite (Ca^{2+} + Na-smectite) 7
Fig. 2. 1. 1 (3) Isothermal absorption line of Mg^{2+} on Na-smectite (Mg^{2+} + Na-smectite) 8
Fig. 2. 1. 1 (4) Isothermal absorption line of H^+ on Na-smectite (H^+ + Na-smectite) 8
Fig. 2. 1. 1 (5) Isothermal absorption line of Na^+ on H-smectite (Na^+ + H-smectite) 9
Fig. 2. 1. 2 Flow chart of measurement for ion-exchange equilibrium constant 12
Fig. 2. 1. 3 (1) kielland plot of K^+ on Na-smectite 21
Fig. 2. 1. 3 (2) kielland plot of Ca^{2+} on Na-smectite 21
Fig. 2. 1. 3 (3) kielland plot of Mg^{2+} on Na-smectite 22
Fig. 2. 1. 3 (4) kielland plot of H^+ on Na-smectite 22
Fig. 2. 2. 1 (1) Relation of between $(1-E_M)^2$ and LnG_M (K^+ + Na-smectite system) 30
Fig. 2. 2. 1 (2) Relation of between $(1-E_M)^2$ and LnG_M (Ca^{2+} + Na-smectite system) 30
Fig. 2. 2. 1 (3) Relation of between $(1-E_M)^2$ and LnG_M (Mg^{2+} + Na-smectite system) 31
Fig. 2. 2. 1 (4) Relation of between $(1-E_M)^2$ and LnG_M (H^+ + Na-smectite system) 31
Fig. 2. 2. 2 (1) Equivalent fraction of K^+ between aqueous and solid phase (K^+ + Na-smectite system) 34
Fig. 2. 2. 2 (2) Equivalent fraction of Ca^{2+} between aqueous and solid phase (Ca^{2+} + Na-smectite system) 34
Fig. 2. 2. 2 (3) Equivalent fraction of Mg^{2+} between aqueous and solid phase (Mg^{2+} + Na-smectite system) 35
Fig. 2. 2. 2 (4) Equivalent fraction of H^+ between aqueous and solid phase (H^+ + Na-smectite system) 35

Fig. 2. 3. 1 (1)	Equivalent fraction of K^+ between aqueous and solid phase ($K^+ + H^+ + Na$ -smectite system, $H^+ : 0.001\text{mol}/\ell$ constant)	.. 43
Fig. 2. 3. 1 (2)	Equivalent fraction of K^+ between aqueous and solid phase ($K^+ + H^+ + Na$ -smectite system, $H^+ : 0.005\text{mol}/\ell$ constant)	.. 43
Fig. 2. 3. 1 (3)	Equivalent fraction of K^+ between aqueous and solid phase ($K^+ + H^+ + Na$ -smectite system, $H^+ : 0.01\text{mol}/\ell$ constant)	.. 44
Fig. 2. 3. 1 (4)	Equivalent fraction of K^+ between aqueous and solid phase ($K^+ + H^+ + Na$ -smectite system, $H^+ : 0.05\text{mol}/\ell$ constant)	.. 44
Fig. 2. 3. 1 (5)	Equivalent fraction of H^+ between aqueous and solid phase ($K^+ + H^+ + Na$ -smectite system, $K^+ : 0.001\text{mol}/\ell$ constant)	.. 45
Fig. 2. 3. 1 (6)	Equivalent fraction of H^+ between aqueous and solid phase ($K^+ + H^+ + Na$ -smectite system, $K^+ : 0.005\text{mol}/\ell$ constant)	.. 45
Fig. 2. 3. 1 (7)	Equivalent fraction of H^+ between aqueous and solid phase ($K^+ + H^+ + Na$ -smectite system, $K^+ : 0.01\text{mol}/\ell$ constant)	.. 46
Fig. 2. 3. 1 (8)	Equivalent fraction of H^+ between aqueous and solid phase ($K^+ + H^+ + Na$ -smectite system, $K^+ : 0.05\text{mol}/\ell$ constant)	.. 46
Fig. 2. 3. 2 (1)	Equivalent fraction of K^+ between aqueous and solid phase ($K^+ + Ca^{2+} + Na$ -smectite system, $Ca^{2+} : 0.0005\text{mol}/\ell$ constant)	.. 47
Fig. 2. 3. 2 (2)	Equivalent fraction of K^+ between aqueous and solid phase ($K^+ + Ca^{2+} + Na$ -smectite system, $Ca^{2+} : 0.0025\text{mol}/\ell$ constant)	.. 47
Fig. 2. 3. 2 (3)	Equivalent fraction of K^+ between aqueous and solid phase ($K^+ + Ca^{2+} + Na$ -smectite system, $Ca^{2+} : 0.005\text{mol}/\ell$ constant)	.. 48
Fig. 2. 3. 2 (4)	Equivalent fraction of K^+ between aqueous and solid phase ($K^+ + Ca^{2+} + Na$ -smectite system, $Ca^{2+} : 0.025\text{mol}/\ell$ constant)	.. 48
Fig. 2. 3. 2 (5)	Equivalent fraction of Ca^{2+} between aqueous and solid phase ($K^+ + Ca^{2+} + Na$ -smectite system, $K^+ : 0.001\text{mol}/\ell$ constant)	.. 49
Fig. 2. 3. 2 (6)	Equivalent fraction of Ca^{2+} between aqueous and solid phase ($K^+ + Ca^{2+} + Na$ -smectite system, $K^+ : 0.005\text{mol}/\ell$ constant)	.. 49
Fig. 2. 3. 2 (7)	Equivalent fraction of Ca^{2+} between aqueous and solid phase ($K^+ + Ca^{2+} + Na$ -smectite system, $K^+ : 0.01\text{mol}/\ell$ constant)	.. 50
Fig. 2. 3. 2 (8)	Equivalent fraction of Ca^{2+} between aqueous and solid phase ($K^+ + Ca^{2+} + Na$ -smectite system, $K^+ : 0.05\text{mol}/\ell$ constant)	.. 50
Fig. 3. 1. 1 (1)	Equivalent fraction of K^+ between aqueous and solid phase ($K^+ + Na$ -smectite system) [Measured data in 1993]	.. 54
Fig. 3. 1. 1 (2)	Equivalent fraction of Ca^{2+} between aqueous and solid phase ($Ca^{2+} + Na$ -smectite system) [Measured data in 1993]	.. 54
Fig. 3. 1. 1 (3)	Equivalent fraction of Mg^{2+} between aqueous and solid phase ($Mg^{2+} + Na$ -smectite system) [Measured data in 1993]	.. 55
Fig. 3. 1. 1 (4)	Equivalent fraction of H^+ between aqueous and solid phase ($H^+ + Na$ -smectite system) [Measured data in 1993]	.. 55

Fig. 4. 1. 1	Conceptual concentration profile in steady-state diffusion experiment 58
Fig. 4. 2. 1	Schematic drawing of apparatus for steady-state diffusion test 63
Fig. 4. 2. 2	Schematic drawing of apparatus for compressing sample 63
Fig. 4. 2. 3	Amounts of Uranium diffusing through filters as a function of time at dry density of 0.4g/cm ³ 69
Fig. 4. 2. 4	Amounts of Uranium diffusing through bentonite as a function of time at dry density of 0.4g/cm ³ 69
Fig. 4. 2. 5	Amounts of Uranium diffusing through filters as a function of time at dry density of 1.0g/cm ³ 70
Fig. 4. 2. 6	Amounts of Uranium diffusing through bentonite as a function of time at dry density of 1.0g/cm ³ 70
Fig. 4. 2. 7	Amounts of Uranium diffusing through filters as a function of time at dry density of 1.4g/cm ³ 71
Fig. 4. 2. 8	Amounts of Uranium diffusing through bentonite as a function of time at dry density of 1.4g/cm ³ 71
Fig. 4. 2. 9	Amounts of Uranium diffusing through filters as a function of time at dry density of 2.0g/cm ³ 72
Fig. 4. 2. 10	Amounts of Uranium diffusing through bentonite as a function of time at dry density of 2.0g/cm ³ 72
Fig. 4. 3. 1	Ratio of adsorption of Americium onto acrylic acid resin and stainless 76
Fig. 4. 3. 2	Ratio of adsorption of Americium onto acrylic acid resin by adding Europium or by surface treatment 76
Fig. 4. 3. 3	Ratio of Americium adsorption onto various materials 77
Fig. 4. 3. 4	Ratio of adsorption of Americium onto acrylic acid resin and stainless in pH2-HCl solution 77
Fig. 4. 3. 5	Speciation of Americium in synthetic pore water ¹⁾ 78
Fig. 4. 3. 6	Amounts of Americium diffusing through filters as a function of time at dry density of 0.8g/cm ³ 83
Fig. 4. 3. 7	Amounts of Americium diffusing through bentonite as a function of time at dry density of 0.8g/cm ³ 83
Fig. 4. 3. 8	Amounts of Americium diffusing through filters as a function of time at dry density of 1.4g/cm ³ 84
Fig. 4. 3. 9	Amounts of Americium diffusing through bentonite as a function of time at dry density of 1.4g/cm ³ 84
Fig. 4. 3. 10	Amounts of Americium diffusing through filters as a function of time at dry density of 1.8g/cm ³ 85

Fig. 4. 3. 11	Amounts of Americium diffusing through bentonite as a function of time at dry density of 1.8g/cm ³	85
Fig. 4. 4. 1	Relation between apparent density of bentonite and effective diffusivities of nuclides	87

第1章 研究計画

1.1 目的

緩衝材による地下水の化学的緩衝作用は、主要構成成分である粘土鉱物（スメクタイト鉱物）のイオン交換反応により支配される。また、核種の移行挙動は、核種と緩衝材との相互作用及び緩衝材の空隙特性によって支配される。

本年度は昨年度に引き続き、粘土鉱物（スメクタイト鉱物）のイオン交換反応のモデル化に関する研究を進めるとともに、UとAmの実効拡散係数を測定した。

1.2 実施内容

1.2.1 スメクタイトのイオン交換反応モデルに関する検討

本年度はNa型スメクタイトを研究対象にイオン交換平衡定数を測定し、イオンの分配平衡を予測する際の適用性について検討した。

(1) イオン交換平衡定数の測定

Na型スメクタイトと K^+ 、 Ca^{2+} 、 Mg^{2+} 及び H^+ イオンのイオン交換平衡定数を評価した。イオン交換平衡定数を解析する際に必要なパラメータである陽イオン交換容量は、等温吸着線から各イオン種ごとに評価した。また、 Na^+ と H^+ のイオン交換平衡定数については、H型スメクタイトを用いての評価も行った。

(2) 2成分系分配平衡への適用性の検討

Na型スメクタイトを用いて K^+ 、 Ca^{2+} 、 Mg^{2+} 及び H^+ の分配試験を行い、取得されたイオン交換平衡定数による計算結果と比較した。また、本検討では、スメクタイト相に吸着したイオンの分率に対する活量補正の必要性、また、MX-80について測定されているイオン交換平衡定数による計算評価も合わせて実施した。

(3) 3成分系分配平衡への適用性の検討

$K^+ + H^+ + Na$ 型スメクタイト系及び $K^+ + Ca^{2+} + Na$ 型スメクタイト系を対象に分配試験を行い、多成分系に対するイオン交換平衡定数の適用性について検討を行った。

1.2.2 平成4年度のイオン交換試験データ及び固溶体モデルのレビュー

以下の内容について、スイスのMB T社への委託により検討を行った。

(1) 平成4年度に取得したイオン交換試験データのレビュー

平成4年度に実施したNa型スメクタイトの吸着試験データを用いて、イオン交換平衡モデル（Wannerモデル）の適用性について検討を行った。

(2) 固溶体モデルの調査

固溶体に吸着したイオンの活量補正方法を中心に、固溶体モデルについて調査を行った。

1.2.3 ベントナイト中での実効拡散係数の測定

(1) Uの定常拡散試験

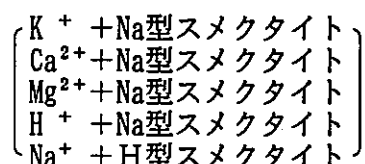
大気雰囲気において、クニゲルV1中でのUの実効拡散係数を測定した。
クニゲルV1の乾燥密度は 0.4及び1.4g/cm³であった。

(2) Amの定常拡散試験

Uと同様に、Amの実効拡散係数を測定した。
クニゲルV1の乾燥密度は 0.8, 1.4 及び1.8g/cm³であった。

第2章 スメクタイトのイオン交換反応モデルに関する研究

スメクタイトのイオン交換反応のモデル化について検討を行うためには、信頼性の高いイオン交換平衡定数データを取得することが必要である。平成4年度に実施した測定手法の検討結果を踏まえて、Na型スメクタイトを対象により信頼性の高いイオン交換平衡定数を測定した。なお、測定したのは以下の4種類のイオン交換反応である。NaとHの交換反応については、Na型スメクタイト及びH型スメクタイトの双方を用いての測定を試みた。



Na型及びH型スメクタイト試料は動燃事業団より支給されたものを使用した。なお、Na型スメクタイトは、平成4年度の研究において使用した試料と同じものである。

2.1 イオン交換平衡定数の測定

2.1.1 陽イオン交換容量の測定

等温吸着線（Langmuirプロット）を測定し、陽イオン交換容量を評価した。

(1) 測定方法

等温吸着線の測定はバッチ式吸着試験により行った。Na型及びH型のスメクタイト試料は、あらかじめ110°Cで1晩以上乾燥させてから試験に使用した。

試験溶液中の K^+ 、 Ca^{2+} 、 Mg^{2+} 及び H^+ 濃度は、それぞれKCl、 $CaCl_2$ 、 $MgCl_2$ 、HClを用いて0.001～0.1eq/lに調整した。

試験溶液100mlにNa型及びH型スメクタイト1.00gを接液させ、スターラで24時間攪拌し、その後24時間静置した。pHを測定した後、上澄液を採取して遠心分離（2000rpm、90分）を行い、さらにシリンジ加圧式限外ろ過フィルター（分画分子量10000、ミリポア社TGC-1型）を用いて限外ろ過を行った。溶液中のNa及びK濃度は原子吸光分析、Ca及びMgはICP発光分光分析、 H^+ 濃度は電極式pH計によりそれぞれ測定した。分配係数は2.1.1式により算出した。

$$K_d \text{ (eq/g)} = \frac{C_0 - C}{C} \times \frac{\text{溶液の体積 (100ml)}}{\text{固相の質量 (1.00g)}} \quad (2.1.1)$$

K_d : 分配係数
 C_0 : 初期の元素濃度 (eq/ml)
 C : 吸着後の元素濃度 (eq/ml)

また、陽イオン交換容量は2.1.2式により算出した。

$$\frac{i}{K_d} = \frac{C + A}{\text{CEC}} \quad (2.1.2)$$

K_d : 分配係数
 CEC : 陽イオン交換容量
 C : 平衡後の液相中のイオン濃度
 A : 定数 (解離速度/吸着速度)

以上、試験条件を表2.1.1にまとめて示す。

Table 2.1.1 Conditions of isothermal absorption test

項目	測定条件
固相試料	Na型及びH型スメクタイト
吸着イオン種	K^+ , Ca^{2+} , Mg^{2+} , H^+ (Na型スメクタイト) Na^+ (H型スメクタイト)
吸着イオンの濃度	0.001 ~ 0.1eq/l (表2参照)
固液比	1.0g/100ml
接触時間	48時間 (振とう24時間)
温度	室温
固液の分離	遠心分離 + 限外ろ過 (分画分子量 10000) 00)
分析方法	Na, K 濃度 原子吸光分析 Ca, Mg濃度 ICP分析 H^+ 電極式pH計
繰り返し試験数	1回/条件

(2) 測定結果

吸着試験の結果を表2.1.2(1)~(5)に示す。また、各イオンについて、吸着平衡後の液相中の濃度と分配係数の逆数をプロット (Langmuirプロット) した結果を図2.1.1(1)~(5)に示す。H型スメクタイトについてはNaがほとんど吸着しなかったため、陽イオン交換容量の評価は不可能であった。

Langmuirプロットにより、液相中の濃度と分配係数の逆数の傾きを求め、陽イオン交換容量の算出を行った。

その結果を表2.1.3に示す。イオン交換容量は、 K^+ で91.0meq/100g, Ca^{2+} で91.0 meq/100g, Mg^{2+} で91.0meq/100g, H^+ では91.0meq/100gと求まった。イオン交換容量のイオン種による大小関係は $Ca > Mg \geq K > H$ の順であり、Caについては他のイオン種と比較して特に大きいことがわかった。

Table 2.1.2(1) Result of isothermal absorption test about Na-smectite ($K^+ + Na$ -smectite)

K 設定値 (eq/ℓ)	初期濃度		吸着平衡後の液相中の濃度		分配係数 (ml/g)	分配係数の 逆数 (g/ml)
	K (eq/ml)	pH	K (eq/ml)	Na (eq/ml)		
0.001	9.51×10^{-7}	6.77	4.09×10^{-8}	1.24×10^{-6}	2.23×10^3	4.49×10^{-4}
0.005	3.66×10^{-6}	6.29	1.05×10^{-6}	4.24×10^{-6}	2.49×10^2	4.02×10^{-3}
0.01	8.70×10^{-6}	5.74	3.68×10^{-6}	6.65×10^{-6}	1.36×10^2	7.35×10^{-3}
0.025	2.05×10^{-5}	4.78	1.33×10^{-5}	6.87×10^{-6}	5.42×10^1	1.84×10^{-2}
0.05	4.99×10^{-5}	4.68	4.17×10^{-5}	1.00×10^{-5}	1.96×10^1	5.09×10^{-2}
0.075	7.80×10^{-5}	4.47	6.91×10^{-5}	9.04×10^{-6}	1.30×10^1	7.71×10^{-2}
0.1	9.72×10^{-5}	4.43	8.82×10^{-5}	1.07×10^{-5}	1.01×10^1	9.86×10^{-2}

Table 2.1.2(2) Result of isothermal absorption test about Na-smectite ($Ca^{2+} + Na$ -smectite)

Ca設定値 (eq/ℓ)	初期濃度		吸着平衡後の液相中の濃度		分配係数 (ml/g)	分配係数の 逆数 (g/ml)
	Ca (eq/ml)	pH	Ca (eq/ml)	Na (eq/ml)		
0.001	9.73×10^{-7}	6.38	2.50×10^{-9}	$< 10^{-8}$	3.89×10^4	2.57×10^{-5}
0.005	4.95×10^{-6}	5.85	2.89×10^{-8}	5.22×10^{-6}	1.70×10^4	5.87×10^{-5}
0.01	9.93×10^{-6}	5.19	1.05×10^{-6}	9.35×10^{-6}	8.43×10^2	1.19×10^{-3}
0.025	2.46×10^{-5}	5.31	1.23×10^{-5}	9.04×10^{-6}	1.00×10^2	9.96×10^{-3}
0.05	4.87×10^{-5}	4.57	3.55×10^{-5}	1.01×10^{-5}	3.71×10^1	2.69×10^{-2}
0.075	7.44×10^{-5}	5.00	6.04×10^{-5}	3.67×10^{-5}	2.31×10^1	4.32×10^{-2}
0.1	9.78×10^{-5}	4.50	8.38×10^{-5}	1.00×10^{-5}	1.67×10^1	6.00×10^{-2}

Table 2.1.2(3) Result of isothermal absorption test about Na-smectite
(Mg²⁺+Na-smectite)

Mg設定値 (eq/ℓ)	初期濃度	吸着平衡後の液相中の濃度			分配係数 (ml/g)	分配係数の 逆数 (g/ml)
	Mg (eq/ml)	pH	Mg (eq/ml)	Na (eq/ml)		
0.001	9.30×10^{-7}	6.22	4.11×10^{-9}	1.26×10^{-6}	2.25×10^4	4.44×10^{-5}
0.005	4.52×10^{-6}	5.90	2.90×10^{-8}	5.30×10^{-6}	1.55×10^4	6.47×10^{-5}
0.01	9.21×10^{-6}	5.24	9.79×10^{-7}	8.91×10^{-6}	8.41×10^2	1.19×10^{-3}
0.025	1.88×10^{-5}	4.61	1.11×10^{-5}	7.78×10^{-6}	6.89×10^1	1.45×10^{-2}
0.05	4.97×10^{-5}	4.59	4.06×10^{-5}	1.04×10^{-5}	2.23×10^1	4.49×10^{-2}
0.075	6.46×10^{-5}	4.42	5.51×10^{-5}	9.83×10^{-6}	1.72×10^1	5.83×10^{-2}
0.1	9.38×10^{-5}	4.40	8.47×10^{-5}	1.02×10^{-5}	1.07×10^1	9.36×10^{-2}

Table 2.1.2(4) Result of isothermal absorption test about Na-smectite
(H⁺+Na-smectite)

H 設定値 (eq/ℓ)	初期濃度	吸着平衡後の液相中の濃度			分配係数 (ml/g)	分配係数の 逆数 (g/ml)
	H (eq/ml)	pH	H (eq/ml)	Na (eq/ml)		
0.001	9.55×10^{-7}	5.51	3.09×10^{-9}	1.21×10^{-6}	3.08×10^4	3.25×10^{-5}
0.005	4.68×10^{-6}	3.07	8.51×10^{-7}	4.35×10^{-6}	4.50×10^2	2.22×10^{-3}
0.01	9.55×10^{-6}	2.40	3.98×10^{-6}	6.74×10^{-6}	1.40×10^2	7.15×10^{-3}
0.025	2.45×10^{-5}	1.78	1.66×10^{-5}	8.61×10^{-6}	4.79×10^1	2.09×10^{-3}
0.05	4.47×10^{-5}	1.42	3.63×10^{-5}	9.13×10^{-6}	2.30×10^1	4.34×10^{-2}
0.075	6.31×10^{-5}	1.20	5.50×10^{-5}	1.03×10^{-5}	1.48×10^1	6.75×10^{-2}
0.1	8.71×10^{-5}	1.10	7.94×10^{-5}	9.78×10^{-6}	9.65	1.04×10^{-1}

Table 2.1.2(5) Result of isothermal absorption test about H-smectite
(Na⁺+H-smectite)

Na設定 値 (eq/ℓ)	初期濃度	吸着平衡後の液相中の濃度			分配係数 (ml/g)	分配係数 の逆数 (g/ml)
	Na (eq/ml)	pH	Na (eq/ml)	H (eq/ml)		
0.001	1.17×10^{-6}	3.97	1.40×10^{-6}	1.07×10^{-7}	-1.64×10^1	-6.09×10^{-2}
0.005	4.78×10^{-6}	3.71	4.88×10^{-6}	1.95×10^{-7}	-2.05	-4.88×10^{-1}
0.01	1.12×10^{-5}	3.59	1.15×10^{-5}	2.57×10^{-7}	-2.61	-3.83×10^{-1}
0.025	2.13×10^{-5}	3.43	2.17×10^{-5}	3.72×10^{-7}	-1.84	-5.43×10^{-1}
0.05	4.92×10^{-5}	3.34	4.97×10^{-5}	4.57×10^{-7}	-1.01	-9.94×10^{-1}
0.075	7.05×10^{-5}	3.30	7.22×10^{-5}	5.01×10^{-7}	-2.35	-4.25×10^{-1}
0.1	9.66×10^{-5}	3.27	9.87×10^{-5}	5.37×10^{-7}	-2.13	-4.70×10^{-1}

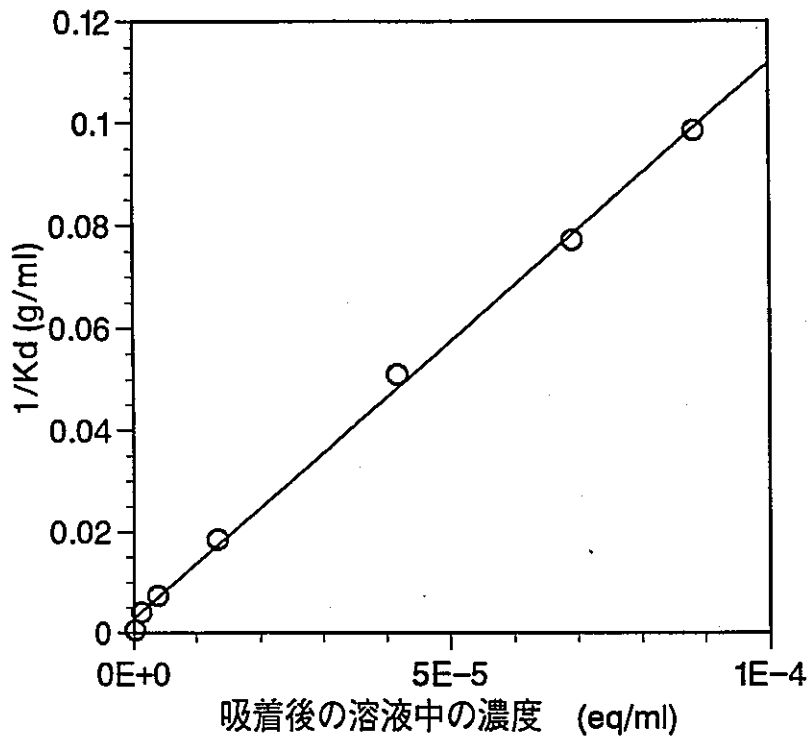


Fig. 2.1.1(1) Isothermal absorption line of K^+ on Na-smectite

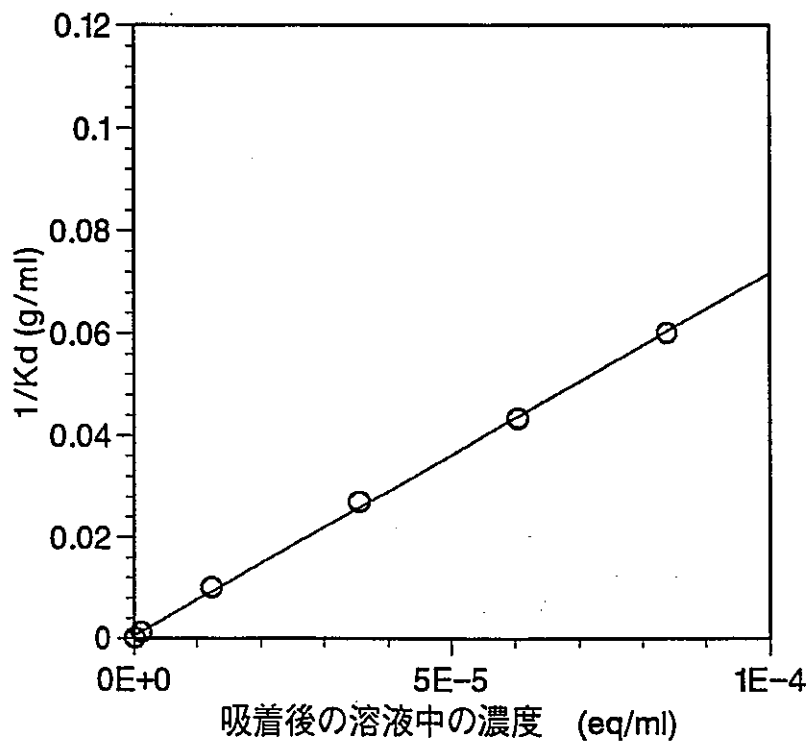


Fig. 2.1.1(2) Isothermal absorption line of Ca^{2+} on Na-smectite

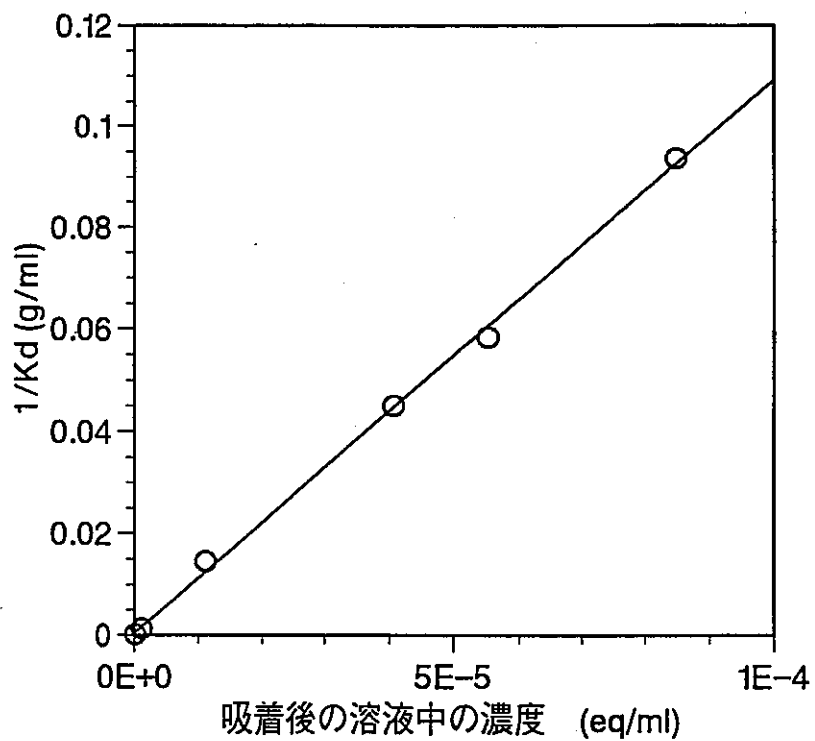


Fig. 2.1.1(3) Isothermal absorption line of Mg^{2+} on Na-smectite

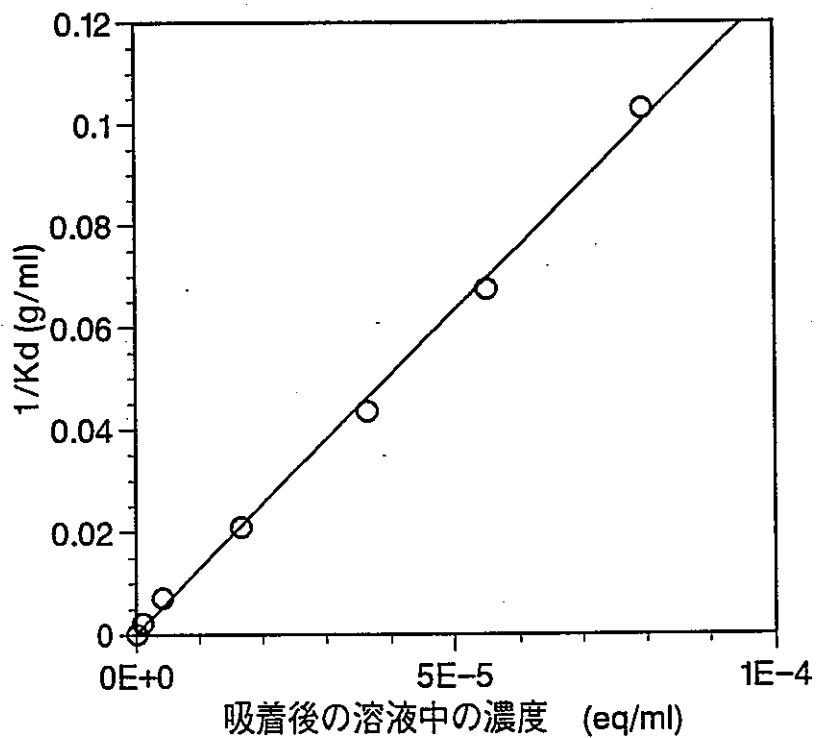


Fig. 2.1.1(4) Isothermal absorption line of H^+ on Na-smectite

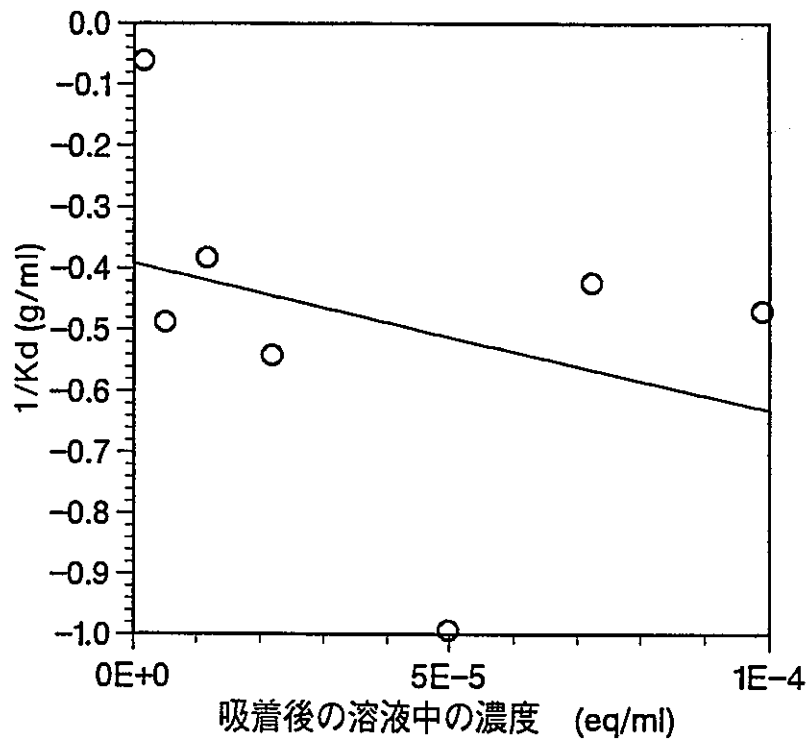


Fig. 2.1.1(5) Isothermal absorption line of Na⁺ on H-smectite

Table 2.1.3 Results of calculation for CEC of smectite samples

イオン交換反応	Langmuirプロットの回帰式 (y : l/Kd, x : 吸着体の濃度)	相関係数 (r^2)	イオン交換容量 (meq/100g)
K^+ + Na型ス멕タイト	$y = 1.091 \times 10^3 x + 2.87 \times 10^{-3}$	0.998	91.7
Ca^{2+} + Na型ス멕タイト	$y = 7.129 \times 10^2 x + 5.36 \times 10^{-4}$	0.999	140.3
Mg^{2+} + Na型ス멕タイト	$y = 1.088 \times 10^3 x + 4.39 \times 10^{-4}$	0.999	91.9
H^+ + Na型ス멕タイト	$y = 1.266 \times 10^3 x + 2.23 \times 10^{-4}$	0.997	79.0
Na^+ + Na型ス멕タイト	評価不能	——	——

2.1.2 イオン交換平衡定数の測定

Na型スメクタイトと K^+ 、 Ca^{2+} 、 Mg^{2+} 及び H^+ イオンとのイオン交換平衡定数を測定した。イオン交換平衡定数の評価はKiellandプロット法によった。

(1) 測定方法

バッチ式の分配試験により、Na型スメクタイトのイオン交換平衡定数を測定した。イオン交換平衡定数の測定対象イオン種は K^+ 、 Ca^{2+} 、 Mg^{2+} 及び H^+ である。また、H型スメクタイトを用いて Na^+ とのイオン交換平衡定数についても測定した。

K^+ 、 Ca^{2+} 、 Mg^{2+} 及び H^+ 濃度を、それぞれ0.001 ~ 0.1eq/lに調整し、試験溶液を作製した。 K^+ 、 Ca^{2+} 、 Mg^{2+} 及び H^+ 濃度はKCl、 $CaCl_2$ 、 $MgCl_2$ 、HClをそれぞれ用いて調整した。さらにNaClを加え、試験溶液中のイオン強度を0.1に調整した。

その他の試験条件、操作手順は、2.1.1に記述した陽イオン交換容量測定試験と同様とした。試験条件を表2.1.4に、操作手順を図2.1.2に示す。

Table 2.1.4 Conditions of ion-exchange equilibrium constant measurement

項目	測定条件
固相試料	Na型スメクタイト H型スメクタイト
交換性イオン種	K^+ 、 Ca^{2+} 、 Mg^{2+} 、 H^+ (Na型スメクタイト) Na^+ (H型スメクタイト)
交換性イオンの濃度	0.001 ~ 0.1eq/l
固液比	1.0g/100ml
接触時間	48時間 (振とう24時間)
温度	室温
固液の分離	遠心分離+限外ろ過 (分画分子量 10000)
分析方法	Na, K 原子吸光法 Ca, Mg ICP分析法 H^+ pH測定

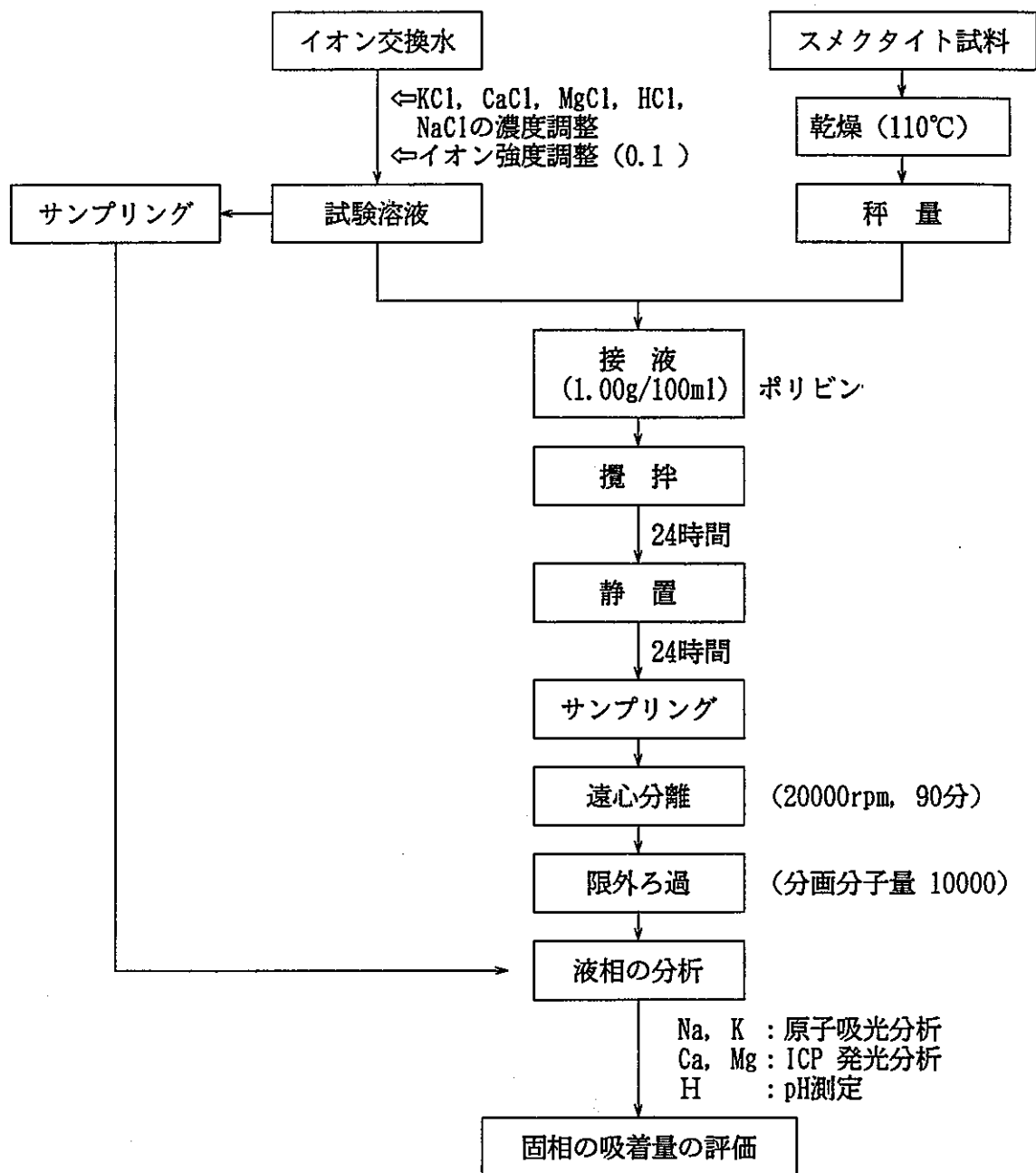


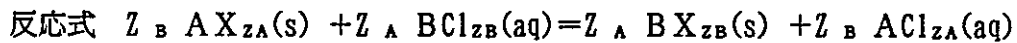
Fig. 2.1.2 Flow chart of measurement for ion-exchange equilibrium constant

(2) 解析方法

イオン交換平衡定数は、選択係数を固相に吸着したイオンの当量分率で積分することにより求めた。イオン交換平衡定数の算出に係わる各定数の定義及び関係式を以下にまとめる。

(a) イオン交換平衡定数 (K_{ex})

スメクタイトのイオン交換反応を以下のように仮定すると、イオン交換平衡定数は2.1.3式で表される。



$$K_{ex} = \frac{[B X_{Z_B}(s)]^{Z_A} [A Cl_{Z_A}(aq)]^{Z_B}}{[A X_{Z_A}(s)]^{Z_B} [B Cl_{Z_B}(aq)]^{Z_A}} \quad (2.1.3)$$

K_{ex} : イオン交換平衡定数
 $M X_{Z_M}$: イオンが吸着している固相 (スメクタイト相)
 $M Cl_{Z_M}$: 塩化物の溶液種
 Z_M : イオンの電荷数
[] : 活量

(b) 選択係数 (K_G)

イオン交換平衡定数を当量分率を用いて表し、固相の活量を1と仮定したものを選択係数として定義する。

$$K_G = \frac{E_B^{Z_A} [A Cl_{Z_A}]^{Z_B}}{E_A^{Z_B} [B Cl_{Z_B}]^{Z_A}} \quad (2.1.4)$$

E_M : 固相に吸着したイオンの当量分率

(c) イオン交換平衡定数の算出式

イオン交換平衡定数は、選択係数を固相中の当量分率で積分して得られることが知られている。

$$\ln K_{ex} = (Z_A - Z_B) + \int_0^1 (\ln K_G) dE_B \quad (2.1.5)$$

(d) 固相の活量係数

固相に吸着したイオンの当量分率に対する活量係数は、2.1.6及び2.1.7式により得られることが知られている。

$$Z_B \ln g_A = - (Z_A - Z_B) E_B + E_B \ln K_G - \int_0^{E_B} \ln K_G dE_B \quad (2.1.6)$$

$$Z_A \ln g_B = (Z_A - Z_B) (1 - E_B) - (1 - E_B) \ln K_G + \int_{E_B}^1 \ln K_G dE_B \quad (2.1.7)$$

本試験では、選択係数と固相中のイオンの当量分率を求め、2.1.5式によりイオン交換平衡定数を算出することとした。

また、固相中のイオンの当量分率 (E_B) は2.1.8式により評価することとした。

$$\begin{aligned} E_B &= \frac{Z_B Q_B}{Z_A Q_A + Z_B Q_B} \\ &= \frac{Z_B Q_B}{CEC} \\ &= \frac{Z_B [C_0(B) - C(B)] \times V / M}{CEC} \end{aligned} \quad (2.1.8)$$

Q_M : 固相に吸着したイオンの濃度 (mol/kg)
 C_0 : 初期の液相中のイオンの当量濃度 (eq/l)
 C : 平衡後の液相中のイオンの当量濃度 (eq/l)
 V : 液相の体積 (l)
 M : 固相の質量 (g)
 CEC : 陽イオン交換容量 (eq/g)

液相中のイオンの平均活量係数 (γ_{MC1}) は、1.2.7式に示すDaviesの式により評価した。

$$\text{Log } \gamma_{MC1} = -A |Z_+ Z_-| \frac{\sqrt{I}}{1 + \sqrt{I}} - 0.3 I \quad (2.1.9)$$

I : イオン強度

(3) 測定及び解析結果

Na型スメクタイトの分配試験の結果を整理し、選択係数 ($\ln K_G$) まで解析した結果を表2.1.5(1)~(4)にまとめて示す。また、H型スメクタイトについては、陽イオン交換容量の測定の場合と同様、 Na^+ とのイオン交換反応が起こらないことからイオン交換平衡定数の評価は不可能であった。

表2.1.5(1)~(4)より、Kiellandプロットを行った結果を図2.1.3(1)~(4)に示す。図中でx軸は固相に吸着したイオンの当量分率 (E_B)、y軸は選択係数 ($\ln K_G$) である。2.1.5式により、 $\ln K_G$ を E_B で積分してイオン交換平衡定数を算出するため、 E_B と $\ln K_G$ の相関式を求めた。 K^+ 、 Mg^{2+} 及び H^+ は1次式により相関式を求めた。 Ca^{2+} については $\ln K_G$ が極大を示すような傾向に見られたため、2次式により評価することにした。その結果、最小自乗法により求められた相関式を表2.1.6に示す。

2.1.5式により、求められた相関式を用いて $\ln K_G$ を E_B で積分し、各イオン交換平衡定数の算出を行った。その結果を表2.1.7に示す。Na型スメクタイトの K^+ 、 Ca^{2+} 、 Mg^{2+} 及び H^+ に対するイオン交換平衡定数 ($\ln K_{\cdot x}$) は、それぞれ1.19、-0.25、0.64、1.17と求められた。

Table 2.1.5(1) Kielland plot data in K⁺+Na-smectite system

設定値 (eq/ℓ)		初期溶液			平衡後の溶液								平衡後の固相				選択係数 Ln K ₀	
		測定濃度 (mol/ℓ)			測定濃度 (mol/ℓ)			活量		活量係数 (Log γ)		イオン強度	陽イオン 交換容量 (meq/100g)	固相中の分率		分率の活量係数		
K ⁺	Na ⁺	pH	K ⁺	Na ⁺	pH	K ⁺	Na ⁺	K ⁺	Na ⁺	K ⁺	Na ⁺			E _K	E _{Na}	Ln g _K	Ln g _{Na}	
0.001	0.099	5.41	9.97×10 ⁻⁴	1.01×10 ⁻¹	4.78	7.88×10 ⁻⁴	1.02×10 ⁻¹	6.14×10 ⁻⁴	7.97×10 ⁻²	-0.108	-0.108	0.103	91.7	0.023	0.977	0.075	-0.002	1.111
		5.41	1.29×10 ⁻³	1.02×10 ⁻¹	4.64	1.07×10 ⁻³	1.08×10 ⁻¹	8.31×10 ⁻⁴	8.39×10 ⁻²	-0.110	-0.110	0.109	91.7	0.024	0.976	0.272	-0.007	0.909
0.0025	0.0975	5.41	2.97×10 ⁻³	9.92×10 ⁻²	4.63	2.11×10 ⁻³	1.06×10 ⁻¹	1.64×10 ⁻³	8.24×10 ⁻²	-0.109	-0.109	0.108	91.7	0.094	0.906	-0.418	0.043	1.649
0.005	0.095	5.38	5.17×10 ⁻³	9.78×10 ⁻²	4.62	4.25×10 ⁻³	1.04×10 ⁻¹	3.30×10 ⁻³	8.08×10 ⁻²	-0.110	-0.110	0.108	91.7	0.100	0.900	0.165	-0.018	1.004
		5.38	4.99×10 ⁻³	1.00×10 ⁻¹	4.73	3.25×10 ⁻³	9.78×10 ⁻²	2.54×10 ⁻³	7.64×10 ⁻²	-0.107	-0.107	0.101	91.7	0.190	0.810	-0.621	0.145	1.953
0.0075	0.0925	5.38	7.67×10 ⁻³	9.43×10 ⁻²	4.61	6.29×10 ⁻³	1.01×10 ⁻¹	4.89×10 ⁻³	7.85×10 ⁻²	-0.109	-0.109	0.107	91.7	0.151	0.849	0.120	-0.021	1.046
0.01	0.09	5.38	9.97×10 ⁻³	9.35×10 ⁻²	4.83	8.18×10 ⁻³	9.57×10 ⁻²	6.38×10 ⁻³	7.46×10 ⁻²	-0.108	-0.108	0.104	91.7	0.195	0.805	0.116	-0.028	1.043
		5.38	1.14×10 ⁻²	9.17×10 ⁻²	4.60	8.29×10 ⁻³	1.04×10 ⁻¹	6.43×10 ⁻³	8.06×10 ⁻²	-0.111	-0.111	0.112	91.7	0.339	0.661	-0.446	0.229	1.863
0.025	0.075	5.30	2.55×10 ⁻²	7.71×10 ⁻²	4.54	2.30×10 ⁻²	8.70×10 ⁻²	1.79×10 ⁻²	6.75×10 ⁻²	-0.110	-0.110	0.110	91.7	0.273	0.727	0.609	-0.229	0.350
		5.30	2.50×10 ⁻²	7.91×10 ⁻²	4.62	2.12×10 ⁻²	8.26×10 ⁻²	1.65×10 ⁻²	6.44×10 ⁻²	-0.108	-0.108	0.104	91.7	0.410	0.590	0.113	-0.079	0.996
0.05	0.05	5.30	4.99×10 ⁻²	5.22×10 ⁻²	4.58	4.35×10 ⁻²	5.65×10 ⁻²	3.40×10 ⁻²	4.42×10 ⁻²	-0.107	-0.107	0.100	91.7	0.706	0.294	0.014	-0.035	1.138

Table 2.1.5(2) Kielland plot data in Ca²⁺+Na-smectite system

設定値 (eq/ℓ)		初期溶液			平衡後の溶液								平衡後の固相				選択係数 Ln K _c	
		測定濃度 (mol/ℓ)			測定濃度 (mol/ℓ)			活量		活量係数 (Log γ)		イオン強度	陽イオン 交換容量 (meq/100g)	固相中の分率		分率の活量係数		
Ca ²⁺	Na ⁺	pH	Ca ²⁺	Na ⁺	pH	Ca ²⁺	Na ⁺	Ca ²⁺	Na ⁺	Ca ²⁺	Na ⁺					E _{Ca}	E _{Na}	Ln g _{Ca}
0.001	0.099	5.42	2.87×10 ⁻⁴	9.91×10 ⁻²	4.74	2.18×10 ⁻⁴	1.00×10 ⁻¹	1.13×10 ⁻⁴	7.81×10 ⁻²	-0.214	-0.107	0.101	140.3	0.010	0.990	-0.252	0.001	-0.783
		5.42	4.68×10 ⁻⁴	9.66×10 ⁻²	4.63	2.12×10 ⁻⁴	1.01×10 ⁻¹	1.29×10 ⁻⁴	7.88×10 ⁻²	-0.215	-0.108	0.102	140.3	0.037	0.963	-1.617	0.029	0.638
0.0025	0.0975	5.36	1.25×10 ⁻³	9.43×10 ⁻²	4.63	5.85×10 ⁻⁴	9.92×10 ⁻²	3.57×10 ⁻⁴	7.75×10 ⁻²	-0.215	-0.107	0.101	140.3	0.095	0.905	-1.561	0.071	0.666
0.005	0.095	5.30	2.46×10 ⁻³	9.24×10 ⁻²	4.61	1.25×10 ⁻³	9.78×10 ⁻²	7.62×10 ⁻⁴	7.64×10 ⁻²	-0.215	-0.108	0.102	140.3	0.173	0.827	-1.463	0.116	0.656
		5.30	2.50×10 ⁻³	9.70×10 ⁻²	4.69	1.28×10 ⁻³	9.87×10 ⁻²	7.79×10 ⁻⁴	7.70×10 ⁻²	-0.216	-0.108	0.103	140.3	0.173	0.827	-1.463	0.116	0.657
0.01	0.09	5.45	4.83×10 ⁻³	8.87×10 ⁻²	4.61	2.70×10 ⁻³	9.40×10 ⁻²	1.64×10 ⁻³	7.34×10 ⁻²	-0.215	-0.108	0.102	140.3	0.304	0.696	-1.395	0.180	0.718
		5.45	4.97×10 ⁻³	9.22×10 ⁻²	4.71	2.75×10 ⁻³	9.78×10 ⁻²	1.66×10 ⁻³	7.61×10 ⁻²	-0.218	-0.109	0.106	140.3	0.317	0.683	-1.482	0.208	0.860
0.025	0.075	5.59	1.20×10 ⁻²	7.39×10 ⁻²	4.52	7.79×10 ⁻³	8.14×10 ⁻²	4.73×10 ⁻³	6.34×10 ⁻²	-0.217	-0.108	0.105	140.3	0.600	0.400	-1.388	0.406	1.162
		5.59	1.29×10 ⁻²	7.39×10 ⁻²	4.65	8.56×10 ⁻³	8.48×10 ⁻²	5.15×10 ⁻³	6.58×10 ⁻²	-0.220	-0.110	0.110	140.3	0.615	0.385	-1.406	0.441	1.251
0.05	0.05	5.72	2.50×10 ⁻²	5.30×10 ⁻²	4.53	2.00×10 ⁻²	6.17×10 ⁻²	1.19×10 ⁻²	4.76×10 ⁻²	-0.226	-0.113	0.122	140.3	0.711	0.289	-1.068	0.230	0.490
		5.72	2.47×10 ⁻²	5.10×10 ⁻²	4.46	1.93×10 ⁻²	5.92×10 ⁻²	1.15×10 ⁻²	4.58×10 ⁻²	-0.224	-0.112	0.117	140.3	0.770	0.230	-1.142	0.433	0.971
0.075	0.025	5.81	3.70×10 ⁻²	2.52×10 ⁻²	4.44	3.09×10 ⁻²	3.38×10 ⁻²	1.83×10 ⁻²	2.60×10 ⁻²	-0.228	-0.114	0.127	140.3	0.870	0.130	-0.968	0.709	0.639
0.1	0	5.89	4.92×10 ⁻²	0.00	4.43	4.25×10 ⁻²	1.00×10 ⁻²	2.48×10 ⁻²	7.64×10 ⁻³	-0.233	-0.117	0.138	140.3	0.955	0.045	-0.833	0.322	0.118

Table 2.1.5(3) Kielland plot data in $Mg^{2+}+Na$ -smectite system

設定値 (eq/ℓ)		初期溶液			平衡後の溶液								平衡後の固相				選択係数 Ln K _G	
		測定濃度 (mol/ℓ)			測定濃度 (mol/ℓ)			活量		活量係数 (Log γ)		イオン強度	陽イオン 交換容量 (meq/100g)	固相中の分率		分率の活量係数		
Mg ²⁺	Na ⁺	pH	Mg ²⁺	Na ⁺	pH	Mg ²⁺	Na ⁺	Mg ²⁺	Na ⁺	Mg ²⁺	Na ⁺					E _{Mg}	E _{Na}	Ln g _{Mg}
0.001	0.099	5.44	3.72×10 ⁻⁴	9.69×10 ⁻²	4.72	1.80×10 ⁻⁴	1.03×10 ⁻¹	1.09×10 ⁻⁴	8.03×10 ⁻²	-0.216	-0.108	0.104	91.9	0.042	0.958	0.659	-0.725	0.986
		5.44	4.53×10 ⁻⁴	1.00×10 ⁻¹	4.75	2.56×10 ⁻⁴	1.00×10 ⁻¹	1.56×10 ⁻⁴	7.81×10 ⁻²	-0.215	-0.107	0.101	91.9	0.043	0.957	1.033	-0.731	0.598
0.0025	0.0975	5.43	1.02×10 ⁻³	9.48×10 ⁻²	4.71	5.10×10 ⁻⁴	1.01×10 ⁻¹	3.10×10 ⁻⁴	7.88×10 ⁻²	-0.216	-0.108	0.103	91.9	0.111	0.889	0.698	-0.569	1.033
0.005	0.095	5.41	2.16×10 ⁻³	9.23×10 ⁻²	4.70	1.19×10 ⁻³	9.83×10 ⁻²	7.25×10 ⁻⁴	7.67×10 ⁻²	-0.215	-0.108	0.102	91.9	0.211	0.789	0.818	-0.355	1.013
		5.41	2.37×10 ⁻³	9.48×10 ⁻²	4.74	1.31×10 ⁻³	9.70×10 ⁻²	7.98×10 ⁻⁴	7.57×10 ⁻²	-0.215	-0.107	0.101	91.9	0.231	0.769	0.821	-0.311	1.032
0.01	0.09	5.35	4.57×10 ⁻³	8.91×10 ⁻²	4.72	2.93×10 ⁻³	9.78×10 ⁻²	1.77×10 ⁻³	7.61×10 ⁻²	-0.218	-0.109	0.107	91.9	0.357	0.643	0.917	-0.055	1.037
		5.35	4.39×10 ⁻³	8.79×10 ⁻²	4.68	2.55×10 ⁻³	9.57×10 ⁻²	1.55×10 ⁻³	7.46×10 ⁻²	-0.216	-0.108	0.103	91.9	0.400	0.600	0.735	0.100	1.386
0.025	0.075	5.34	9.37×10 ⁻³	7.34×10 ⁻²	4.62	5.96×10 ⁻³	8.35×10 ⁻²	3.63×10 ⁻³	6.52×10 ⁻²	-0.215	-0.107	0.101	91.9	0.742	0.258	0.639	1.203	2.568
		5.34	1.19×10 ⁻²	7.61×10 ⁻²	4.61	8.19×10 ⁻³	8.48×10 ⁻²	4.94×10 ⁻³	6.58×10 ⁻²	-0.220	-0.110	0.109	91.9	0.814	0.186	0.653	1.563	3.034
0.05	0.05	5.34	2.03×10 ⁻²	5.01×10 ⁻²	4.53	1.61×10 ⁻²	6.28×10 ⁻²	9.69×10 ⁻³	4.87×10 ⁻²	-0.221	-0.110	0.111	91.9	0.914	0.086	0.790	1.980	3.406
0.075	0.025	5.34	3.11×10 ⁻²	2.52×10 ⁻²	4.48	2.70×10 ⁻²	3.49×10 ⁻²	1.62×10 ⁻²	2.70×10 ⁻²	-0.223	-0.112	0.116	91.9	0.892	0.108	0.980	0.957	1.240
0.1	0	5.41	4.24×10 ⁻²	0.00	4.46	3.79×10 ⁻²	1.03×10 ⁻²	2.25×10 ⁻²	7.93×10 ⁻³	-0.227	-0.114	0.124	91.9	0.979	0.021	0.948	1.382	1.838

Table 2.1.5(4) Kielland plot data in H⁺+Na-smectite system

設定値 (eq/ℓ)		初期溶液			平衡後の溶液								平衡後の固相				選択係数 Ln K _c	
		測定濃度 (mol/ℓ)			測定濃度 (mol/ℓ)			活量		活量係数 (Log γ)		イオン強度	陽イオン 交換容量 (meq/100g)	固相中の分率		分率の活量係数		
H ⁺	Na ⁺	pH	H ⁺	Na ⁺	pH	H ⁺	Na ⁺	H ⁺	Na ⁺	H ⁺	Na ⁺			E _H	E _{Na}	Ln g _H	Ln g _{Na}	
0.001	0.099	3.04	9.12×10 ⁻⁴	1.04×10 ⁻¹	3.60	2.51×10 ⁻⁴	1.02×10 ⁻¹	2.51×10 ⁻⁴	7.97×10 ⁻²	0	-0.108	0.102	79.0	0.084	0.916	-4.876	-0.019	3.367
		3.04	9.12×10 ⁻⁴	9.78×10 ⁻²	3.76	1.74×10 ⁻⁴	9.92×10 ⁻²	1.74×10 ⁻⁴	7.76×10 ⁻²	0	-0.107	0.099	79.0	0.093	0.907	-5.295	0.024	3.829
0.0025	0.0975	2.64	2.29×10 ⁻³	9.66×10 ⁻²	3.08	8.32×10 ⁻⁴	9.92×10 ⁻²	8.32×10 ⁻⁴	7.75×10 ⁻²	0	-0.107	0.100	79.0	0.185	0.815	-4.592	-0.052	3.050
0.005	0.095	2.34	4.57×10 ⁻³	9.35×10 ⁻²	2.61	2.46×10 ⁻³	1.01×10 ⁻¹	2.46×10 ⁻³	7.87×10 ⁻²	0	-0.108	0.103	79.0	0.268	0.732	-4.126	-0.173	2.462
		2.33	4.68×10 ⁻³	9.66×10 ⁻²	2.61	2.46×10 ⁻³	9.92×10 ⁻²	2.46×10 ⁻³	7.74×10 ⁻²	0	-0.108	0.102	79.0	0.281	0.719	-4.162	-0.157	2.514
0.0075	0.0925	2.15	7.08×10 ⁻³	9.55×10 ⁻²	2.34	4.57×10 ⁻³	9.73×10 ⁻²	4.57×10 ⁻³	7.59×10 ⁻²	0	-0.108	0.102	79.0	0.318	0.682	-3.832	-0.296	2.046
0.01	0.09	2.04	9.12×10 ⁻³	9.35×10 ⁻²	2.19	6.46×10 ⁻³	9.57×10 ⁻²	6.46×10 ⁻³	7.47×10 ⁻²	0	-0.108	0.102	79.0	0.337	0.663	-3.651	-0.389	1.772
		2.02	9.55×10 ⁻³	9.24×10 ⁻²	2.17	6.76×10 ⁻³	9.40×10 ⁻²	6.76×10 ⁻³	7.34×10 ⁻²	0	-0.107	0.101	79.0	0.353	0.647	-3.660	-0.390	1.780
0.025	0.075	1.64	2.29×10 ⁻²	7.83×10 ⁻²	1.70	2.00×10 ⁻²	8.03×10 ⁻²	2.00×10 ⁻²	6.28×10 ⁻²	0	-0.107	0.100	79.0	0.374	0.626	-2.944	-0.822	0.632
		1.64	2.29×10 ⁻²	7.91×10 ⁻²	1.73	1.86×10 ⁻²	8.04×10 ⁻²	1.86×10 ⁻²	6.29×10 ⁻²	0	-0.107	0.099	79.0	0.543	0.457	-3.417	-0.537	1.390
0.05	0.05	1.35	4.47×10 ⁻²	4.78×10 ⁻²	1.40	3.98×10 ⁻²	5.65×10 ⁻²	3.98×10 ⁻²	4.43×10 ⁻²	0	-0.106	0.096	79.0	0.615	0.385	-3.057	-0.992	0.576
0.075	0.025	1.18	6.61×10 ⁻²	2.50×10 ⁻²	1.22	6.03×10 ⁻²	3.35×10 ⁻²	6.03×10 ⁻²	2.63×10 ⁻²	0	-0.105	0.094	79.0	0.736	0.264	-2.916	-1.229	0.197

Table 2.1.5(5) Kielland plot data in Na⁺+H-smectite system

設定値 (eq/ℓ)		初期溶液			平衡後の溶液								平衡後の固相				選択係数 Ln K _c	
		測定濃度 (mol/ℓ)			測定濃度 (mol/ℓ)			活量		活量係数 (Log γ)		イオン強度	陽イオン 交換容量 (meq/100g)	固相中の分率		分率の活量係数		
Na ⁺	H ⁺	pH	Na ⁺	H ⁺	pH	Na ⁺	H ⁺	Na ⁺	H ⁺	Na ⁺	H ⁺					E _{Na}	E _H	Ln g _{Na}
0.001	0.099	1.04	1.04×10 ⁻³	9.12×10 ⁻²	1.06	1.44×10 ⁻³	8.71×10 ⁻²	1.14×10 ⁻³	8.71×10 ⁻²	-0.103	0	0.089	94.3	-0.042	1.042	—	—	—
0.0025	0.0975	1.02	2.71×10 ⁻³	9.55×10 ⁻²	1.08	3.04×10 ⁻³	8.32×10 ⁻²	2.40×10 ⁻³	8.32×10 ⁻²	-0.102	0	0.086	94.3	-0.035	1.035	—	—	—
0.005	0.095	1.05	5.44×10 ⁻³	8.91×10 ⁻²	1.08	5.73×10 ⁻³	8.32×10 ⁻²	4.52×10 ⁻³	8.32×10 ⁻²	-0.103	0	0.089	94.3	-0.031	1.031	—	—	—
0.0075	0.0925	1.05	8.70×10 ⁻³	8.91×10 ⁻²	1.09	8.70×10 ⁻³	8.13×10 ⁻²	6.85×10 ⁻³	8.13×10 ⁻²	-0.104	0	0.090	94.3	0	1	—	—	—
0.01	0.09	1.07	1.04×10 ⁻²	8.51×10 ⁻²	1.11	1.04×10 ⁻²	7.76×10 ⁻²	8.20×10 ⁻³	7.76×10 ⁻²	-0.103	0	0.088	94.3	0	1	—	—	—
0.025	0.075	1.14	2.79×10 ⁻²	7.24×10 ⁻²	1.18	2.83×10 ⁻²	6.61×10 ⁻²	2.22×10 ⁻²	6.61×10 ⁻²	-0.105	0	0.094	94.3	-0.042	1.042	—	—	—
0.05	0.05	1.32	5.48×10 ⁻²	4.79×10 ⁻²	1.37	5.48×10 ⁻²	4.27×10 ⁻²	4.29×10 ⁻²	4.27×10 ⁻²	-0.106	0	0.097	94.3	0	1	—	—	—
0.075	0.025	1.62	8.04×10 ⁻²	2.40×10 ⁻²	1.71	8.04×10 ⁻²	1.95×10 ⁻²	6.28×10 ⁻²	1.95×10 ⁻²	-0.107	0	0.100	94.3	0	1	—	—	—
0.1	0	5.46	9.57×10 ⁻²	3.47×10 ⁻²	3.23	9.57×10 ⁻²	5.89×10 ⁻²	7.50×10 ⁻²	5.89×10 ⁻²	-0.106	0	0.096	94.3	0	1	—	—	—

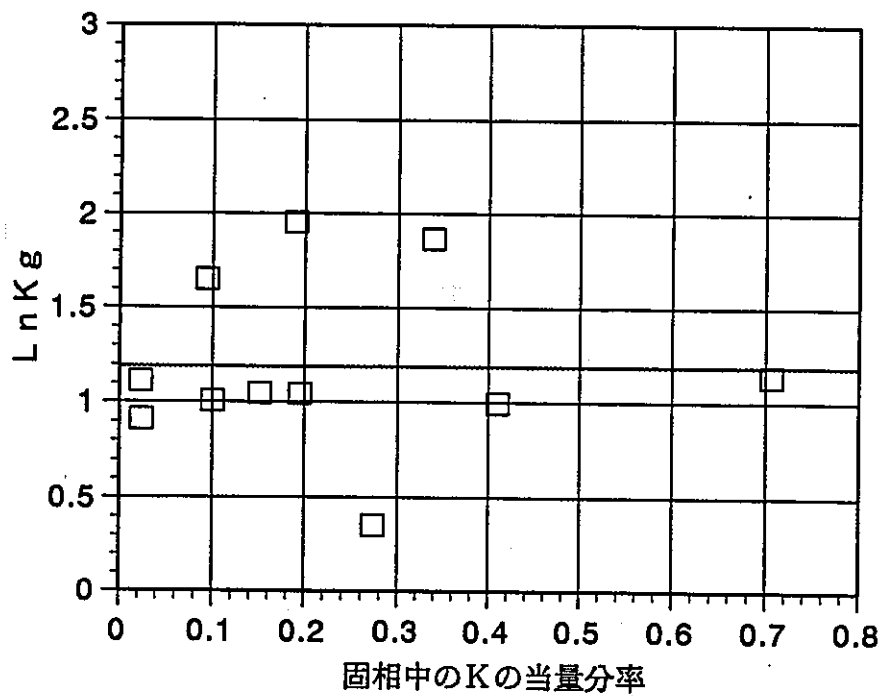


Fig. 2.1.3(1) Kielland plot of K^+ on Na-smectite

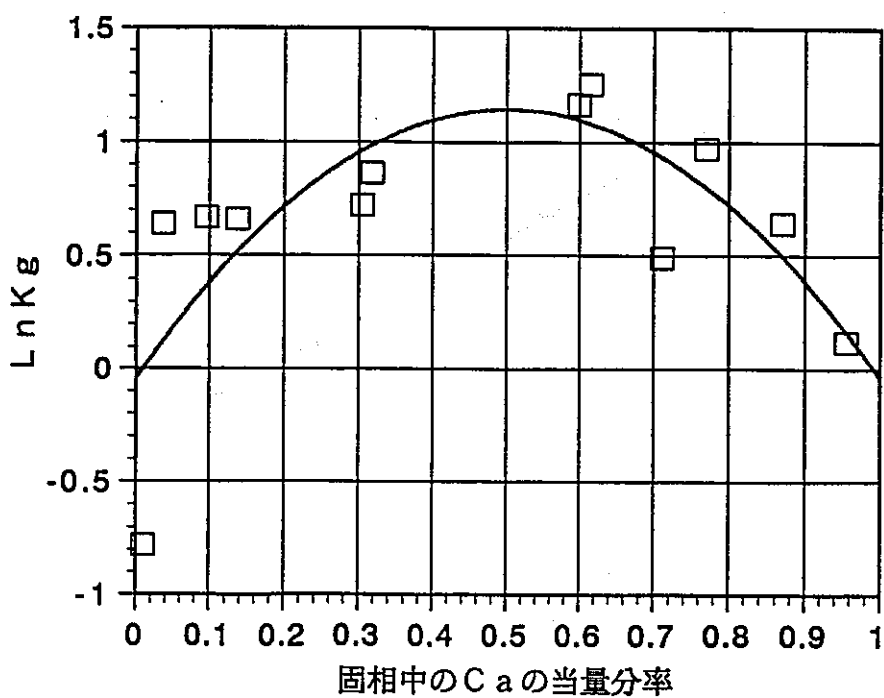


Fig. 2.1.3(2) Kielland plot of Ca^{2+} on Na-smectite

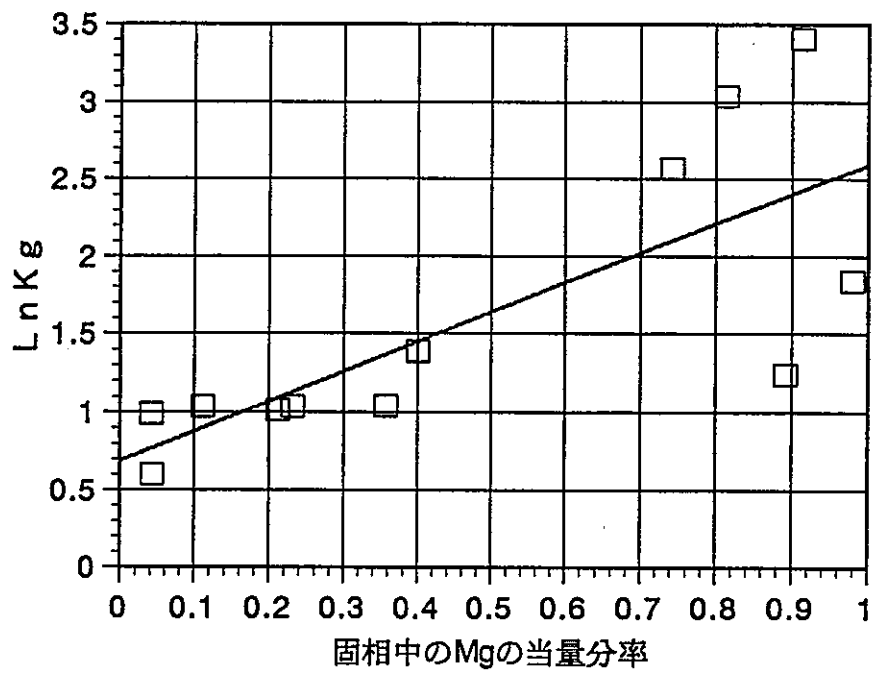


Fig. 2.1.3(3) Kielland plot of Mg^{2+} on Na-smectite

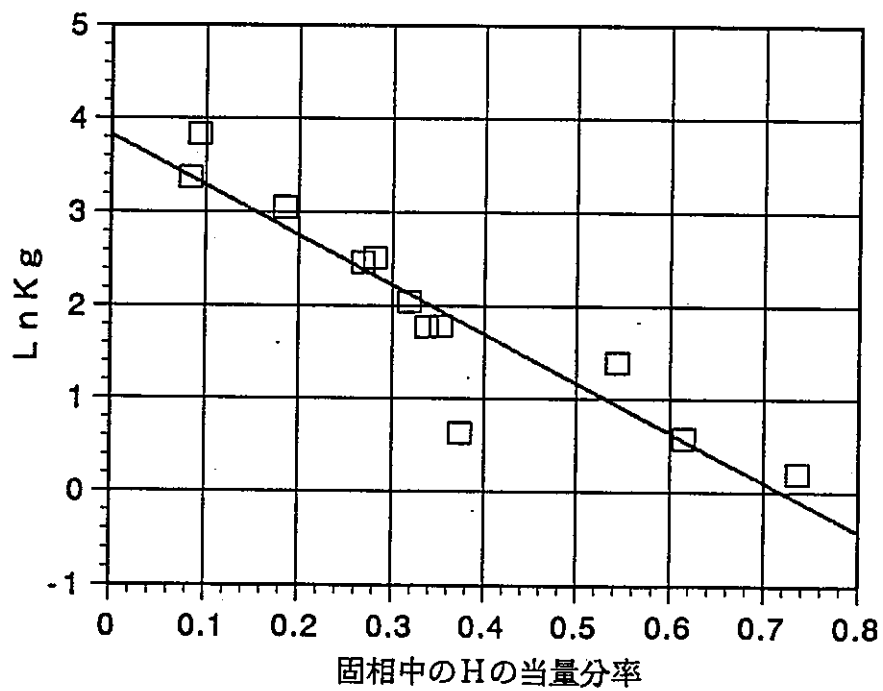


Fig. 2.1.3(4) Kielland plot of H^+ on Na-smectite

Table 2.1.6 Relation of between E_B and K_G

イオン交換反応	Kiellandプロットの回帰式 ($y : K_G, x : E_B$)	相関係数 (r^2)
$K^+ + Na$ 型スワイト	$y = -1.249 \times 10^{-3} x + 1.188$	2.915×10^{-7}
$Ca^{2+} + Na$ 型スワイト	$y = -4.741 x^2 + 4.749 x - 4.555 \times 10^{-2}$	5.627×10^{-1}
$Mg^{2+} + Na$ 型スワイト	$y = 1.907 x + 6.860$	5.797×10^{-1}
$H^+ + Na$ 型スワイト	$y = -5.311 x + 3.821$	8.493×10^{-1}
$Na^+ + H$ 型スワイト	評価不可	—————

Table 2.1.7 Estimated ion-exchange equilibrium constants

イオン交換反応	本試験による 測定値 ($\ln K_{ex}$)	平成4年度の取得 データ ($\ln K_{ex}$)
$K^+ + Na$ 型スワイト	1.19	0.59
$Ca^{2+} + Na$ 型スワイト	-0.25	1.08
$Mg^{2+} + Na$ 型スワイト	0.64	0.68
$H^+ + Na$ 型スワイト	1.17	2.26
$Na^+ + H$ 型スワイト	—————	—————

2.2 2成分系分配平衡への適用性の検討

固溶体モデルを検討する場合、その中心となるのはイオン交換平衡モデル（Wannerモデル）である。そこでまず、イオン交換平衡モデルの適用性について調べることにした。

ここでは2成分系を対象として、2.1.2で実施した分配試験の結果を用いて各モデルによる計算結果と比較を行った。さらに、MX-80について得られているイオン交換平衡定数を用いてNa型スメクタイトの分配平衡を計算し、固溶体割合が変化した場合のイオン交換平衡定数の適用性についても調べた。

2.2.1 計算方法

分配平衡の計算は、Na型スメクタイトと K^+ 、 Ca^{2+} 、 Mg^{2+} 及び H^+ の各2成分系について実施した。計算を行ったケースは以下の3ケースである。

- ①理想固溶体モデルによる計算（MMC データ、固相の活量補正なし）
- ②正則溶液モデルによる計算（MMC データ、固相の活量補正あり）
- ③理想固溶体モデルによる計算（文献値、固相の活量補正なし）

以下に、それぞれのケースにおける計算条件を記述する。

(1) 理想固溶体モデルによる計算（MMC データ、固相の活量補正なし）

2.1.2で取得されたイオン交換平衡定数を用い、固相に吸着したイオンの当量分率に対する活量補正は行わない条件（理想固溶体モデル）で、Na型スメクタイトのイオンの分配平衡を計算した。

計算条件を表2.2.1に示す。計算コードにはPHREEQE 60を使用した。大気雰囲気条件とするため、 $pH\ 7.0$ $p_e+5.9$ 、 CO_2 ガス分圧 $10^{-3.5}atm$ に設定した。固液比条件は、セミマイクロシヨールンベハガー法によるイオン交換容量の測定値 $108meq/100g$ と分配試験の固液比条件 $1.0g/100ml$ より、 $10.8meq/l$ として入力した。液相中のイオンについては、PHREEQE 60の中でDebye-Huckelの式により活量補正を行った。

計算に使用したイオン交換平衡定数を表2.2.2、PHREEQE 60の入力形式とした値を表2.2.3にそれぞれ示した。PHREEQE 60の入力形式への換算に際しては、 $Na^+ + Z^- \Rightarrow NaZ$ の平衡定数を文献値より 10^{20} と仮定した。

Table 2.2.1 Conditions of estimation for ion-exchange equilibrium

項目	計算条件
計算コード	PHREEQE 60
化学的雰囲気条件	・ pH 7.0 ・ pe+5.9 (Eh+350mV)
ガス平衡	大気雰囲気 (CO ₂ ガス 10 ^{-3.5} atm)
固液比	10 g / 1 l (10.8 meq / l)
液相の活量補正式	Debye-Huckelの式
固相の活量	1 と仮定 (理想固溶体モデル)
データベース	PHREEQE オリジナルデータベース
イオン交換平衡定数	表 2.2.2 参照

Table 2.2.2 Ion-exchange equilibrium constants of Na-smectite

イオン交換反応	K _{ex}	
	本試験測定結果	Sposito data*
Na-smec + K ⁺ ⇌ K-smec + Na ⁺	3.28	1.8
Na-smec + H ⁺ ⇌ H-smec + Na ⁺	3.21	1.26
2 Na-smec + Ca ²⁺ ⇌ Ca-2 smec + 2 Na ⁺	0.78	1.48
2 Na-smec + Mg ²⁺ ⇌ Mg-2 smec + 2 Na ⁺	1.90	1.48
Na-smec + Ca ²⁺ + Cl ⁻ ⇌ CaCl-smec + Na ⁺	—	193
Na-smec + Mg ²⁺ + Cl ⁻ ⇌ MgCl-smec + Na ⁺	—	181

* : MX-80 について測定されたデータ

Table 2.2.3 Ion-exchange equilibrium constants of Na-smectite (PHREEQE format)

イオン交換反応	本試験の測定結果		Sposito data*	
	K	Log K	K	Log K
$\text{Na}^+ + \text{smec}^- \rightleftharpoons \text{Na-smec}$	1.00×10^{20}	20.00	1.00×10^{20}	20.00
$\text{K}^+ + \text{smec}^- \rightleftharpoons \text{K-smec}$	3.28×10^{20}	20.52	1.8×10^{20}	20.26
$\text{H}^+ + \text{smec}^- \rightleftharpoons \text{H-smec}$	3.21×10^{20}	20.51	1.26×10^{20}	20.10
$\text{Ca}^{2+} + 2 \text{smec}^- \rightleftharpoons \text{Ca-2 smec}$	0.78×10^{40}	39.89	1.48×10^{40}	40.17
$\text{Ca}^{2+} + \text{Cl}^- + \text{smec}^- \rightleftharpoons \text{CaCl-smec}$	————	—	193×10^{20}	22.29
$\text{Mg}^{2+} + 2 \text{smec}^- \rightleftharpoons \text{Mg-2 smec}$	1.90×10^{40}	40.28	1.48×10^{40}	40.17
$\text{Mg}^{2+} + \text{Cl}^- + \text{smec}^- \rightleftharpoons \text{MgCl-smec}$	————	—	181×10^{20}	22.26

* : MX-80 について測定されたデータ

(2) 正則溶液モデルによる計算 (MMC データ, 固相の活量補正あり)

固溶体に吸着したイオンの活量補正に対するモデルは, 現在不明である。

ここでは固相中の活量補正モデルとして最も一般的である正則溶液 (Regular solution) モデルを選定し, その適用性について検討することとした。

正則溶液モデルは合金を溶融する場合などに適用される活量補正モデルであり, 2成分系では固相中の分率に対する活量係数 ($\text{Ln } g_M$) と $(1-E_M)^2$ の間に, 以下の式のような一次関係にあることが知られている。また, その比例係数 (α/RT) はイオン種に依らず同じであることが仮定されている。

$$\begin{cases} \text{Ln } g_A = (\alpha/RT) \cdot E_B^2 = (\alpha/RT) \cdot (1-E_A)^2 \\ \text{Ln } g_B = (\alpha/RT) \cdot E_A^2 = (\alpha/RT) \cdot (1-E_B)^2 \end{cases} \quad (2.2.1)$$

Na型スメクタイトについては, 各イオン交換系について $(1-E_M)^2$ と $\text{Ln } g_M$ の関係をプロットし, 最小自乗法により傾き (α/RT) を求めて, 各分率において活量補正を行うこととした。

(3) 理想固溶体モデルによる計算（文献値，固相の活量補正なし）

Sposito ら¹¹⁾により測定されたMX-80 のイオン交換平衡定数を用いて，Na型スメクタイトの分配平衡を計算した。Sposito らによるイオン交換平衡定数を表 2.2.2 及び表 2.2.3 に併記する。

計算に使用したモデルは(1)で実施する計算結果と比較するため，理想固溶体モデルとし，固相中のイオンの活量補正は行わなかった。イオン交換平衡定数以外の計算条件はすべて(1)に記述した条件と同じとした。

2.2.2 正則溶液モデルによる固相の活量係数

正則溶液モデルを用いて固相に吸着したイオンに対する活量補正を行うため，表 2.1.5 (1)~(4)に示したNa型スメクタイトの分配試験の結果から $(1-E_M)^2$ 及び $\ln g_M$ を計算し，表 2.2.4 (1)~(4)にまとめた。また， $(1-E_M)^2$ と $\ln g_M$ についてプロットし，図 2.1 (1)~(4)に示した。

K^+ + Na型スメクタイト系では， K^+ 及び Na^+ とともに活量係数 ($\ln g_M$) のバラつきが大きく，一様な傾向は見られなかった。 Ca^{2+} + Na型スメクタイト系では， Ca^{2+} の活量係数 ($\ln g_M$) は $-1.62 \sim -0.25$ の範囲で吸着分率によらずマイナス側であったが， Na^+ の活量係数 ($\ln g_M$) はプラス側であった。 Mg^{2+} + Na型スメクタイト系では， Mg^{2+} の活量係数 ($\ln g_M$) は $0.6 \sim 0.9$ 付近ではほぼ一定であったが， Na^+ の活量係数 ($\ln g_M$) は吸着分率の減少とともに活量係数は大きく上昇する傾向にあった。 H^+ + Na型スメクタイト系では， H^+ は吸着分率の減少とともに活量係数も大きく減少する傾向にあった。

以上の結果より，正則溶液モデルでは $(1-E_M)^2$ と $\ln g_M$ の相関がイオン種間で一致することが仮定されているが，各試験系とも各イオン種間で相関は一致しないことから，正則溶液モデルの適用性には問題がある可能性があることがわかった。

各試験系において，各イオン種ごとに $(1-E_M)^2$ と $\ln g_M$ の相関式を求めた結果を表 2.2.5 に示す。

ここでは交換性のイオン種である K^+ ， Ca^{2+} ， Mg^{2+} 及び H^+ のみに着目し，その比例係数 (α/RT) を 2.2.1 式に代入して固相に吸着したイオンの活量補正を行うこととした。 K^+ ， Ca^{2+} ， Mg^{2+} 及び H^+ の比例係数は，それぞれ 6.07×10^{-2} ， -1.22×10^{-1} ， 1.52×10^{-3} ， -2.94 と求められた。

Table 2.2.4(1) Relation of equivalent fraction and activity coefficient in solid phase ($K^+ + Na$ -smectite)

設定値(eq/ℓ)		K^+		Na^+	
K^+	Na^+	$(1-E_K)^2$	$\ln g_K$	$(1-E_{Na})^2$	$\ln g_{Na}$
0.001	0.099	9.55×10^{-1}	0.075	5.23×10^{-4}	-0.002
		9.53×10^{-1}	0.272	5.76×10^{-4}	-0.007
0.0025	0.0975	8.21×10^{-1}	-0.418	8.80×10^{-3}	0.043
0.005	0.095	8.09×10^{-1}	0.165	1.01×10^{-2}	-0.018
		6.57×10^{-1}	-0.621	3.60×10^{-2}	0.145
0.0075	0.0925	7.21×10^{-1}	0.120	2.27×10^{-2}	-0.021
0.01	0.09	6.48×10^{-1}	0.116	3.81×10^{-2}	-0.028
		4.37×10^{-1}	-0.446	1.15×10^{-1}	0.229
0.025	0.075	5.29×10^{-1}	0.609	7.44×10^{-2}	-0.229
		3.48×10^{-1}	0.113	1.68×10^{-1}	-0.079
0.05	0.05	8.65×10^{-2}	0.014	4.98×10^{-1}	-0.035

Table 2.2.4(2) Relation of equivalent fraction and activity coefficient in solid phase ($Ca^{2+} + Na$ -smectite)

設定値(eq/ℓ)		Ca^{2+}		Na^+	
Ca^{2+}	Na^+	$(1-E_{Ca})^2$	$\ln g_{Ca}$	$(1-E_{Na})^2$	$\ln g_{Na}$
0.001	0.099	9.81×10^{-1}	-0.252	9.57×10^{-5}	0.001
		9.28×10^{-1}	-1.617	1.33×10^{-3}	0.029
0.0025	0.0975	8.19×10^{-1}	-1.561	8.99×10^{-3}	0.071
0.005	0.095	6.85×10^{-1}	-1.463	2.98×10^{-2}	0.116
		6.84×10^{-1}	-1.463	3.00×10^{-2}	0.116
0.01	0.09	4.85×10^{-1}	-1.395	9.22×10^{-2}	0.180
		4.67×10^{-1}	-1.482	1.00×10^{-1}	0.208
0.025	0.075	1.60×10^{-1}	-1.388	3.60×10^{-1}	0.406
		1.48×10^{-1}	-1.406	3.79×10^{-1}	0.441
0.05	0.05	8.32×10^{-2}	-1.068	5.06×10^{-1}	0.230
		5.29×10^{-2}	-1.142	5.93×10^{-1}	0.433
0.075	0.025	1.70×10^{-2}	-0.968	7.56×10^{-1}	0.709
0.1	0	2.00×10^{-3}	-0.833	9.13×10^{-1}	0.322

Table 2.2.4(3) Relation of equivalent fraction and activity coefficient in solid phase ($Mg^{2+}+Na$ -smectite)

設定値(eq/ℓ)		Mg^{2+}		Na^+	
Mg^{2+}	Na^+	$(1-E_{Mg})^2$	$\ln g_{Mg}$	$(1-E_{Na})^2$	$\ln g_{Na}$
0.001	0.099	9.18×10^{-1}	0.659	1.75×10^{-3}	-0.725
		9.16×10^{-1}	1.033	1.82×10^{-3}	-0.731
0.0025	0.0975	7.90×10^{-1}	0.698	1.23×10^{-2}	-0.569
0.005	0.095	6.22×10^{-1}	0.818	4.45×10^{-2}	-0.355
		5.91×10^{-1}	0.821	5.33×10^{-2}	-0.311
0.01	0.09	4.14×10^{-1}	0.917	1.27×10^{-1}	-0.055
		3.60×10^{-1}	0.735	1.60×10^{-1}	0.100
0.025	0.075	6.66×10^{-2}	0.639	5.50×10^{-1}	1.203
		3.44×10^{-2}	0.653	6.63×10^{-1}	1.563
0.05	0.05	7.42×10^{-3}	0.790	8.35×10^{-1}	1.980
0.075	0.025	1.16×10^{-2}	0.980	7.96×10^{-1}	0.957
0.1	0	4.36×10^{-4}	0.948	9.59×10^{-1}	1.382

Table 2.2.4(4) Relation of equivalent fraction and activity coefficient in solid phase ($H^+ + Na$ -smectite)

設定値(eq/ℓ)		H^+		Na^+	
H^+	Na^+	$(1-E_H)^2$	$\ln g_H$	$(1-E_{Na})^2$	$\ln g_{Na}$
0.001	0.099	8.40×10^{-1}	-4.876	7.00×10^{-3}	-0.019
		8.22×10^{-1}	-5.295	8.74×10^{-3}	0.024
0.0025	0.0975	6.65×10^{-1}	-4.592	3.41×10^{-2}	-0.052
0.005	0.095	5.36×10^{-1}	-4.126	7.18×10^{-2}	-0.173
		5.16×10^{-1}	-4.162	7.92×10^{-2}	-0.157
0.0075	0.0925	4.66×10^{-1}	-3.832	1.01×10^{-1}	-0.296
0.01	0.09	4.39×10^{-1}	-3.651	1.14×10^{-1}	-0.389
		4.18×10^{-1}	-3.660	1.25×10^{-1}	-0.390
0.025	0.075	3.91×10^{-1}	-2.944	1.40×10^{-1}	-0.822
		2.09×10^{-1}	-3.417	2.95×10^{-1}	-0.537
0.05	0.05	1.48×10^{-1}	-3.057	3.78×10^{-1}	-0.992
0.075	0.025	6.96×10^{-2}	-2.916	5.42×10^{-1}	-1.229

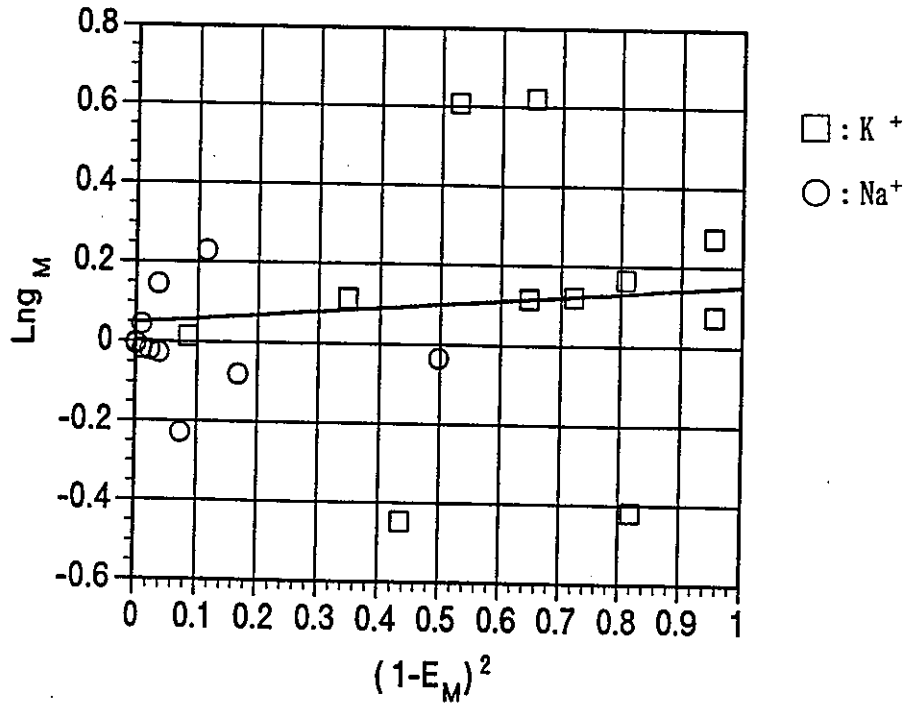


Fig. 2.2.1(1) Relation of between $(1-E_M)^2$ and $Ln g_M$
 ($K^+ + Na$ -smectite system)

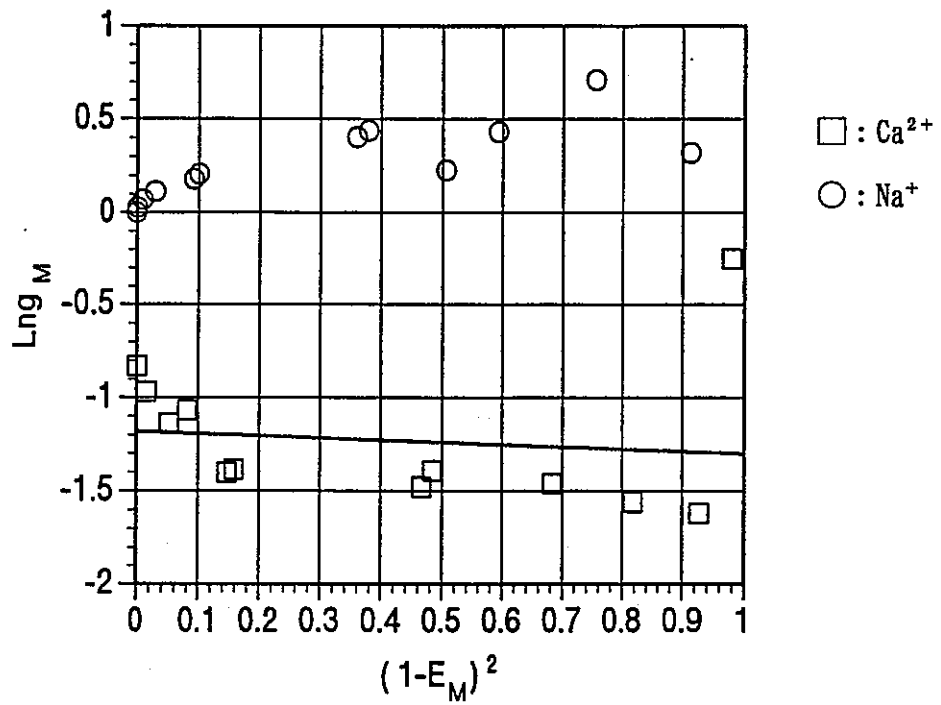


Fig. 2.2.1(2) Relation of between $(1-E_M)^2$ and $Ln g_M$
 ($Ca^{2+} + Na$ -smectite system)

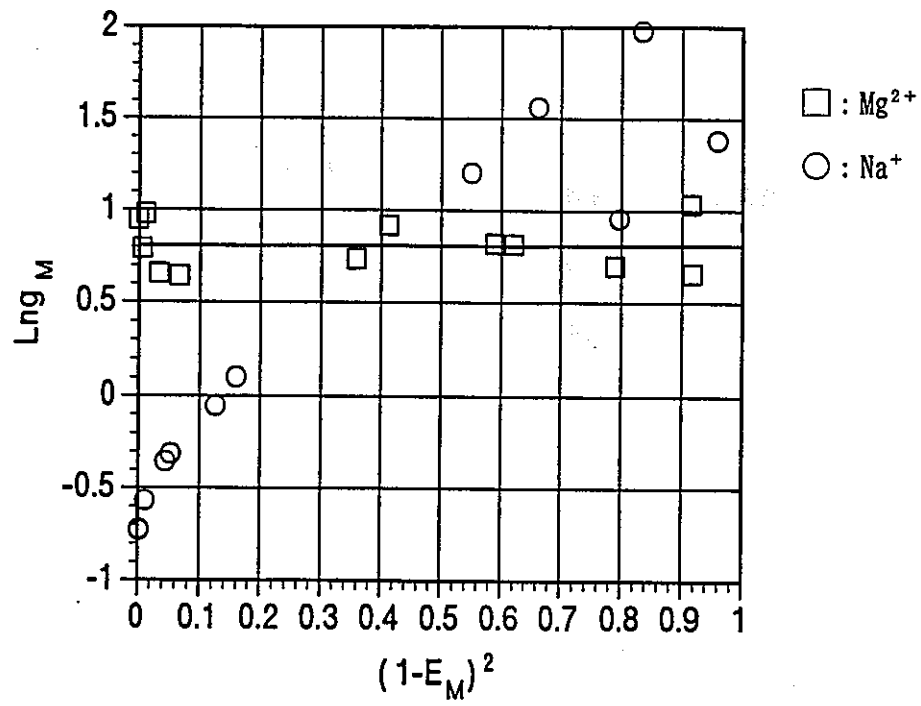


Fig. 2.2.1(3) Relation of between $(1-E_M)^2$ and Lng_M
 ($\text{Mg}^{2+} + \text{Na}$ -smectite system)

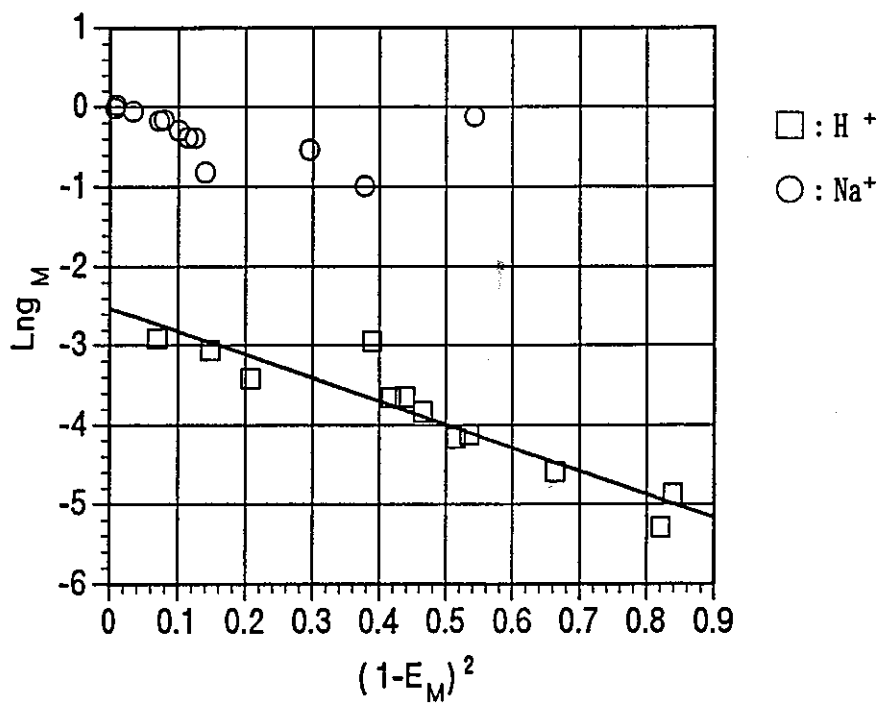


Fig. 2.2.1(4) Relation of between $(1-E_M)^2$ and Lng_M
 ($\text{H}^+ + \text{Na}$ -smectite system)

Table 2.2.5 Equation of relation of equivalent fraction and activity coefficient about solid phase

イオン 交換反応	データ の種類	相関式		相関係数 (r^2)
		$y : \text{Ln} g_M$	$x : (1 - E_M)^2$	
$\text{K}^+ +$ Na型スモクタイト	K 単独	$y = 6.07 \times 10^{-2} x - 3.86 \times 10^{-2}$		2.04×10^{-3}
	Na 単独	$y = -8.14 \times 10^{-2} x - 7.07 \times 10^{-3}$		1.03×10^{-2}
	K + Na	$y = 1.00 \times 10^{-2} x - 3.77 \times 10^{-3}$		1.82×10^{-4}
$\text{Ca}^{2+} +$ Na型スモクタイト	Ca 単独	$y = -1.22 \times 10^{-1} x - 1.18$		1.37×10^{-2}
	Na 単独	$y = 5.08 \times 10^{-1} x + 1.04 \times 10^{-1}$		6.30×10^{-1}
	Ca + Na	$y = -2.97 \times 10^{-1} x - 3.85 \times 10^{-1}$		1.57×10^{-2}
$\text{Mg}^{2+} +$ Na型スモクタイト	Mg 単独	$y = 1.52 \times 10^{-3} x + 8.07 \times 10^{-1}$		1.69×10^{-5}
	Na 単独	$y = 2.46 x - 4.91 \times 10^{-1}$		8.91×10^{-1}
	Mg + Na	$y = 1.30 x + 1.06 \times 10^{-1}$		4.30×10^{-1}
$\text{H}^+ +$ Na型スモクタイト	H 単独	$y = -2.94 x - 2.52$		8.66×10^{-1}
	Na 単独	$y = -2.27 x - 6.15 \times 10^{-2}$		8.44×10^{-1}
	H + Na	$y = -5.94 x - 3.14 \times 10^{-1}$		6.55×10^{-1}

2.2.3 評価結果

Na型スメクタイトと K^+ 、 Ca^{2+} 、 Mg^{2+} 及び H^+ イオンの分配平衡について、測定結果と各モデルによる計算結果の比較を図2.2.2(1)~(4)に示した。図中でx軸は液相中の当量分率、y軸は固相中の当量分率である。

(1) 理想固溶体モデルと正則溶液モデルの比較

理想固溶体モデルと正則溶液モデルを比較した場合、 K^+ +Na型スメクタイト系ではほとんど差はなく、どちらもほぼ測定値と一致することがわかった。これは正則溶液モデルで評価した固相中の K^+ の活量係数(g_M)が分率に依らず1に近いためである。 Ca^{2+} +Na型スメクタイト系及び Mg^{2+} +Na型スメクタイト系については、理想固溶体及び正則溶液モデルとも測定値と一致しないことがわかった。しかし、理想固溶体モデルにより計算されたSpositoらによる計算結果は測定値とほぼ一致することから、2.1.2で得られたNa型スメクタイトのイオン交換平衡定数に問題があるものと考えられた。 H^+ +Na型スメクタイト系については、理想固溶体モデルでは測定値とほぼ一致するが、正則溶液モデルでは測定値と大きく相違することがわかった。正則溶液モデルでは、固相中の分率(E_M)が小さい場合、活量係数(g_M)が小さくなり、実際の分率よりもかなり大きく評価されることが原因である。

以上のことから、理想固溶体モデルにより、各イオンの分配平衡を予測することは一応可能であることがわかった。正則溶液モデルにより固相中のイオンの活量補正を行った場合、 K^+ 、 Ca^{2+} 及び Mg^{2+} では理想固溶体モデルとほとんど差がないものの、 H^+ については大きく相違する可能性があった。正則溶液モデルについては、2.2.2に記述したように $(1-E_M)^2$ と $\ln g_M$ の相関性についても問題がある。

よって、イオンの分配平衡を評価する場合、理想固溶体モデルにより評価することが適切であるものと判断した。

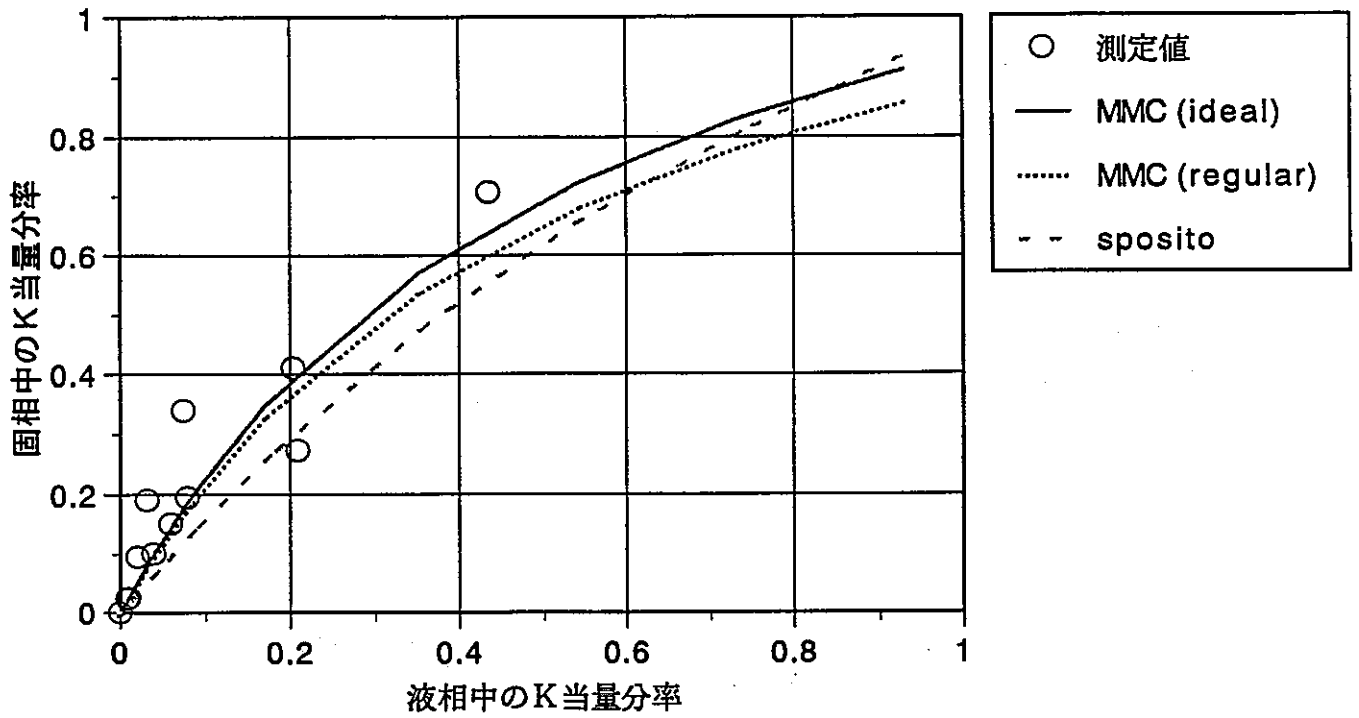


Fig. 2.2.2(1) Equivalent fraction of K^+ between aqueous and solid phase
($K^+ + Na$ -smectite system)

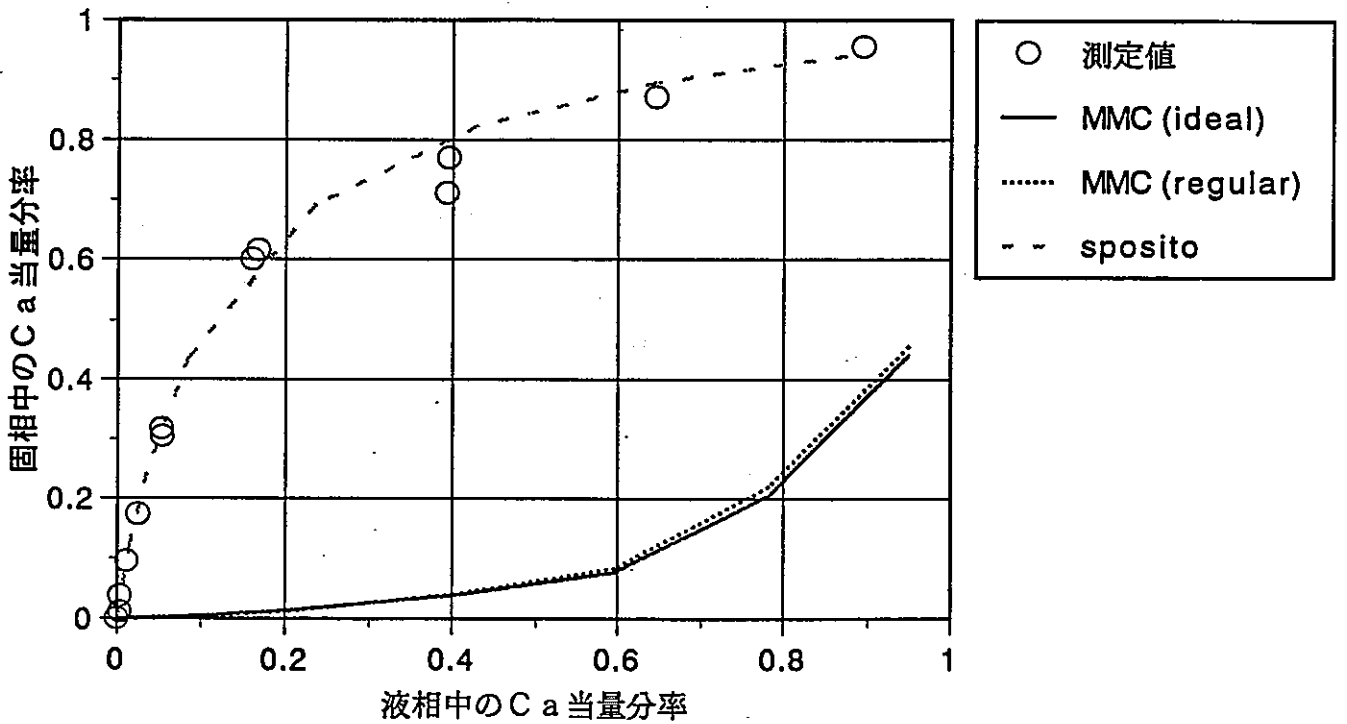


Fig. 2.2.2(2) Equivalent fraction of Ca^{2+} between aqueous and solid phase
($Ca^{2+} + Na$ -smectite system)

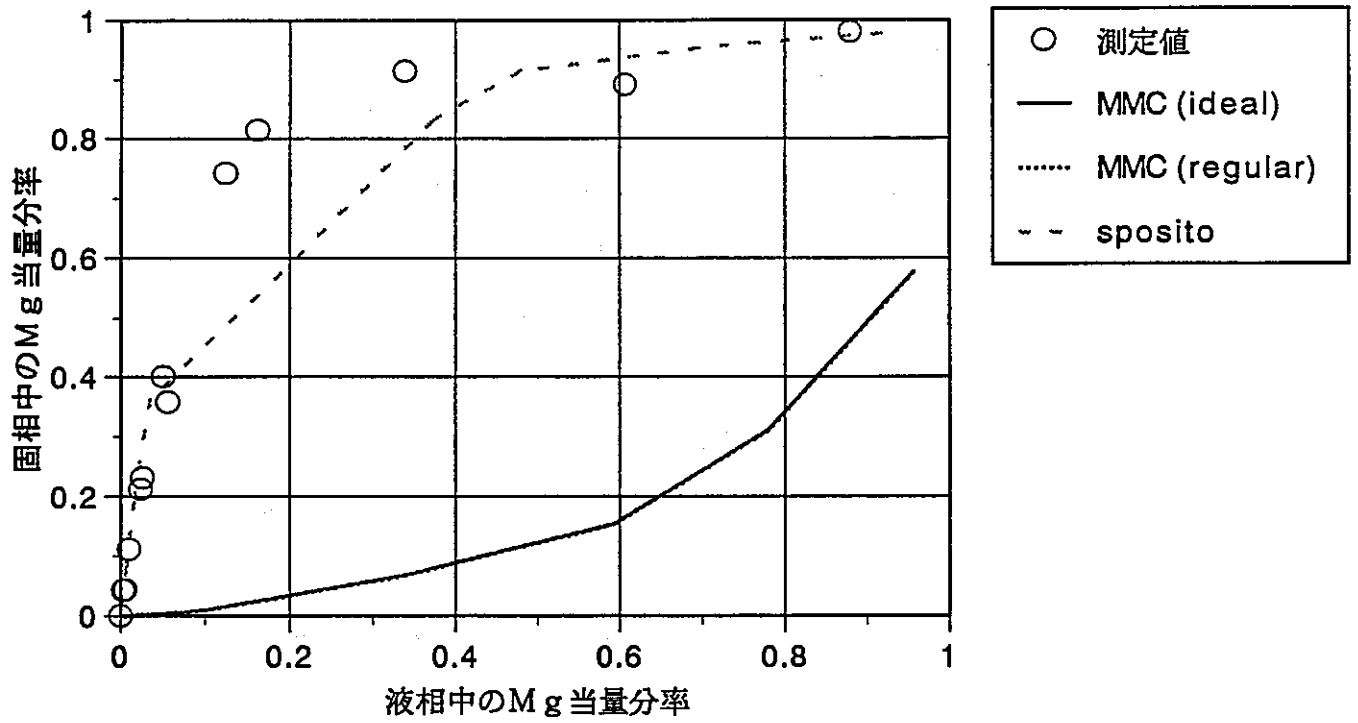


Fig. 2.2.2(3) Equivalent fraction of Mg^{2+} between aqueous and solid phase
 ($Mg^{2+} + Na$ -smectite system)

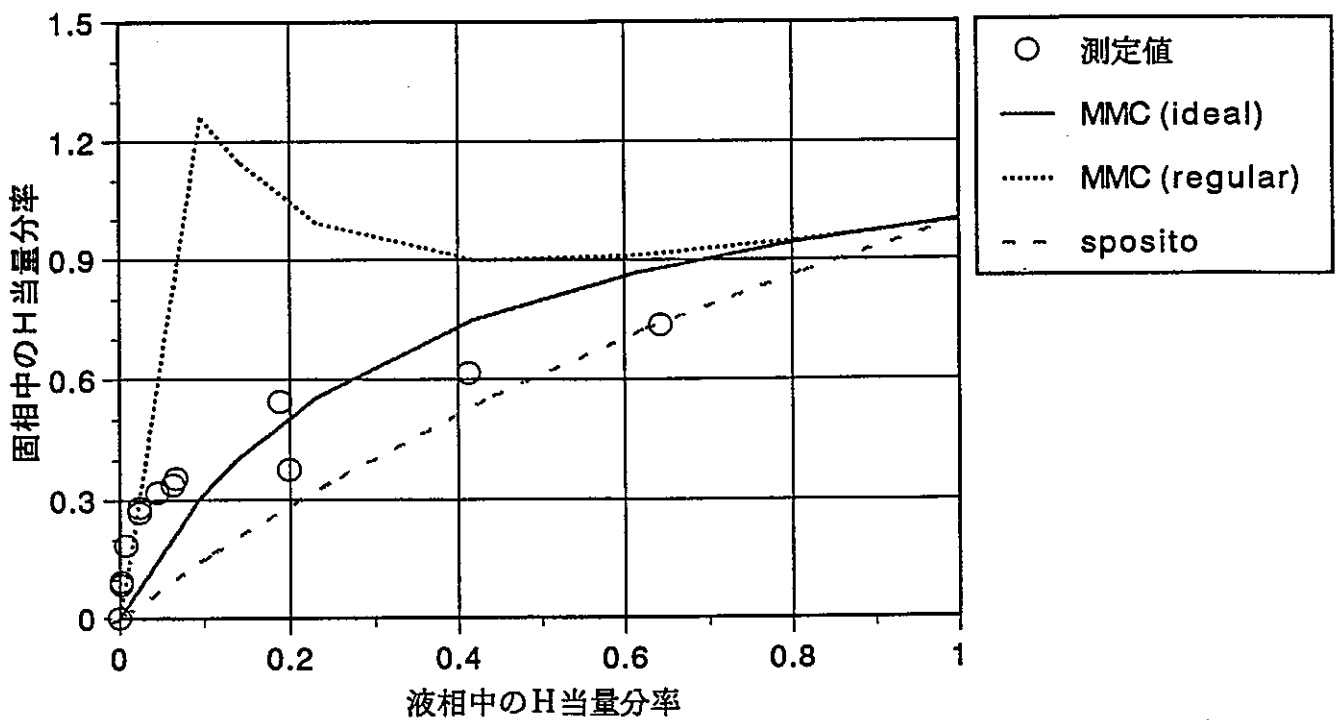


Fig. 2.2.2(4) Equivalent fraction of H^+ between aqueous and solid phase
 ($H^+ + Na$ -smectite system)

(2) Na型スメクタイトとMX-80のイオン交換平衡定数の比較

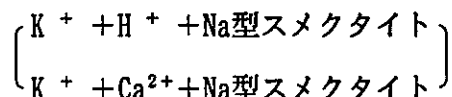
2.1.2.で得られたNa型スメクタイトのイオン交換平衡定数とSpositeらによるMX-80のイオン交換平衡定数を用いて計算し、その結果を比較した。

その結果、 K^+ + Na型スメクタイト系では、MX-80の平衡定数の方が若干低い傾向にあったが、どちらも測定値のバラツキの範囲内で一致することがわかった。 Ca^{2+} 及び Mg^{2+} + Na型スメクタイト系については、どちらもMX-80の平衡定数による結果のみ測定値と一致する結果であった。この原因は2.1.2.で測定されたイオン交換平衡定数において、 $CaCl^+$ 及び $MgCl^+$ による平衡定数が評価されていないためと考えられる。 H^+ + Na型スメクタイト系については、 K^+ + Na型スメクタイト系と同様、どちらも測定値のバラツキの範囲内でほぼ一致することがわかった。

以上の結果から、MX-80について測定されたイオン交換平衡定数を用いても、Na型スメクタイトの分配平衡が、測定値のバラツキの範囲内で評価できることがわかった。スメクタイトの固溶割合の変化によるイオン交換平衡定数への影響は少ない可能性がある。

2.3 3成分系分配平衡への適用性の検討

イオン交換平衡モデル (Wannerモデル) の多成分系への適用性を検討するため, 3成分系についても分配試験を行い, 理想固溶体モデルによる計算結果と比較した。検討対象としたのは, 以下の3成分系である。



2.3.1 分配試験

(1) 試験方法

バッチ式分配試験を行った。Na型スメクタイト試料は2.1.1に記述した試料と同じとした。KCl, CaCl₂ 及び, HCl を用いて, 試験溶液中のK⁺, Ca²⁺及びH⁺濃度を0.001 ~0.05 eq/ℓに調整した。さらにNaClを加え, 試験溶液中のイオン強度を0.1に調整した。(表2.3.1(2)参照)

試験溶液100ml にNa型スメクタイト1.00g を接液させ, スターラで24時間攪拌後, 24時間静置した。

pHを測定後, 上澄液を採取して遠心分離 (20000rpm, 90分) を行い, 分画分子量10000 のシリンジ加圧式限外ろ過フィルタ (ミリポア社, TGC-1 型) を用いて, ろ過した。溶液中のNa及びK濃度は原子吸光法, CaはICP 発光分光分析法, H⁺濃度はpH計によりそれぞれ測定を行った。試験条件を表2.3.1(1)~(2)に示す。

Table 2.3.1(1) Conditions of ion-exchange equilibrium constant measurement (ternary system)

項目	測定条件
固相試料	Na型スメクタイト
交換性イオン種	K ⁺ , H ⁺ K ⁺ , Ca ²⁺
交換性イオンの濃度	0.001 ~0.05eq/ℓ
固液比	1.0g/100ml
接触時間	48時間 (振とう24時間)
温度	室温
固液の分離	遠心分離+限外ろ過 (分画分子量 10000)
分析方法	Na, K 原子吸光法 Ca ICP分析法 H ⁺ pH測定

Table 2.3.1(2) Conditions of initial solutions (ternary system)

(mol/ℓ)

K ⁺ +H ⁺ +Na型スメクタイト系			K ⁺ +Ca ²⁺ +Na型スメクタイト系		
KCl	HCl	NaCl	KCl	CaCl ₂	NaCl
0.001	0.001	0.098	0.001	0.0005	0.098
	0.005	0.094		0.0025	0.094
	0.01	0.089		0.005	0.089
	0.05	0.049		0.025	0.049
0.005	0.001	0.094	0.005	0.0005	0.094
	0.005	0.090		0.0025	0.090
	0.01	0.085		0.005	0.085
	0.05	0.045		0.025	0.045
0.01	0.001	0.089	0.01	0.0005	0.089
	0.005	0.085		0.0025	0.085
	0.01	0.08		0.005	0.08
	0.05	0.04		0.025	0.04
0.05	0.001	0.049	0.05	0.0005	0.049
	0.005	0.045		0.0025	0.045
	0.01	0.04		0.005	0.04
	0.05	0.0		0.025	0.0

(2) 試験結果

3成分系での分配試験の結果を整理し、表2.3.2(1)~(2)に示した。

2.3.2 計算評価

(1) 計算条件

3成分系での分配平衡の計算は、以下の2ケースについて行った。

- ① Na型スメクタイトのイオン交換平衡定数による評価
- ② MX-80のイオン交換平衡定数による評価

Na型スメクタイト及びMX-80のイオン交換平衡定数については、2.2に記述した2成分系での検討と同様とした。

Table 2.3.2(1) Measured data of ionexchange equilibrium in $K^+ + H^+ + Na$ -smectite system

設定値 (mol/l)			初期溶液				平衡後の液相											交換強度
			測定濃度 (mol/l)				測定濃度 (mol/l)				活量			活量係数 (Log γ)				
KCl	HCl	NaCl	pH	K	H	Na	pH	K	H	Na	K ⁺	H ⁺	Na ⁺	K ⁺	H ⁺	Na ⁺		
0.001	0.001	0.098	3.04	1.24×10^{-3}	9.12×10^{-4}	9.87×10^{-2}	3.67	9.87×10^{-4}	2.14×10^{-4}	1.03×10^{-1}	7.69×10^{-4}	1.67×10^{-4}	8.03×10^{-2}	-0.108	-0.108	-0.108	0.104	
	0.005	0.094	2.34	1.24×10^{-3}	4.57×10^{-3}	9.57×10^{-2}	2.57	1.07×10^{-3}	2.69×10^{-3}	9.92×10^{-2}	8.35×10^{-3}	2.10×10^{-3}	7.74×10^{-2}	-0.108	-0.108	-0.108	0.103	
	0.01	0.089	2.04	1.23×10^{-3}	9.12×10^{-3}	9.24×10^{-2}	2.17	1.05×10^{-3}	6.76×10^{-3}	9.57×10^{-2}	8.19×10^{-3}	5.27×10^{-3}	7.46×10^{-2}	-0.108	-0.108	-0.108	0.104	
	0.05	0.049	1.34	1.21×10^{-3}	4.57×10^{-2}	8.61×10^{-2}	1.38	1.06×10^{-3}	4.17×10^{-2}	5.74×10^{-2}	8.28×10^{-3}	3.26×10^{-2}	4.49×10^{-2}	-0.107	-0.107	-0.107	0.100	
0.005	0.001	0.094	3.02	4.91×10^{-3}	9.55×10^{-4}	9.24×10^{-2}	3.59	4.58×10^{-3}	2.57×10^{-4}	9.67×10^{-2}	3.58×10^{-3}	2.01×10^{-4}	7.55×10^{-2}	-0.108	-0.108	-0.108	0.102	
	0.005	0.090	2.34	5.22×10^{-3}	4.57×10^{-3}	9.17×10^{-2}	2.55	4.78×10^{-3}	2.82×10^{-3}	9.67×10^{-2}	3.72×10^{-3}	2.20×10^{-3}	7.53×10^{-2}	-0.108	-0.108	-0.108	0.104	
	0.01	0.085	2.04	5.32×10^{-3}	9.12×10^{-3}	8.79×10^{-2}	2.17	4.83×10^{-3}	6.76×10^{-3}	9.24×10^{-2}	3.76×10^{-3}	5.27×10^{-3}	7.20×10^{-2}	-0.108	-0.108	-0.108	0.104	
	0.05	0.045	1.35	5.22×10^{-3}	4.47×10^{-2}	4.63×10^{-2}	1.37	4.75×10^{-3}	4.27×10^{-2}	5.31×10^{-2}	3.71×10^{-3}	3.33×10^{-2}	4.15×10^{-2}	-0.107	-0.107	-0.107	0.101	
0.01	0.001	0.089	3.03	1.14×10^{-2}	9.33×10^{-4}	8.96×10^{-2}	3.56	8.70×10^{-3}	2.75×10^{-4}	9.41×10^{-2}	6.78×10^{-3}	2.15×10^{-4}	7.34×10^{-2}	-0.108	-0.108	-0.108	0.103	
	0.005	0.085	2.35	1.14×10^{-2}	4.47×10^{-3}	8.70×10^{-2}	2.54	9.21×10^{-3}	2.88×10^{-3}	9.24×10^{-2}	7.18×10^{-3}	2.25×10^{-3}	7.20×10^{-2}	-0.108	-0.108	-0.108	0.104	
	0.01	0.080	2.04	1.09×10^{-2}	9.12×10^{-3}	8.26×10^{-2}	2.16	9.41×10^{-3}	6.92×10^{-3}	8.73×10^{-2}	7.34×10^{-3}	5.39×10^{-3}	6.81×10^{-2}	-0.108	-0.108	-0.108	0.104	
	0.05	0.040	1.34	1.02×10^{-2}	4.57×10^{-2}	4.18×10^{-2}	1.37	9.41×10^{-3}	4.27×10^{-2}	4.82×10^{-2}	7.35×10^{-3}	3.33×10^{-2}	3.77×10^{-2}	-0.107	-0.107	-0.107	0.100	
0.05	0.001	0.049	3.04	4.80×10^{-2}	9.12×10^{-4}	4.96×10^{-2}	3.44	4.49×10^{-2}	3.63×10^{-4}	5.65×10^{-2}	3.50×10^{-2}	2.83×10^{-4}	4.41×10^{-2}	-0.108	-0.108	-0.108	0.102	
	0.005	0.045	2.35	4.91×10^{-2}	4.47×10^{-3}	4.63×10^{-2}	2.50	4.61×10^{-2}	3.16×10^{-3}	5.55×10^{-2}	3.59×10^{-2}	2.46×10^{-3}	4.32×10^{-2}	-0.108	-0.108	-0.108	0.105	
	0.01	0.040	2.05	5.12×10^{-2}	8.91×10^{-3}	4.23×10^{-2}	2.14	4.76×10^{-2}	7.24×10^{-3}	5.05×10^{-2}	3.71×10^{-2}	5.64×10^{-3}	3.93×10^{-2}	-0.109	-0.109	-0.109	0.105	
	0.05	0	1.34	5.12×10^{-2}	4.57×10^{-2}	0	1.38	4.76×10^{-2}	4.17×10^{-2}	1.02×10^{-2}	3.72×10^{-2}	3.26×10^{-2}	7.79×10^{-3}	-0.107	-0.107	-0.107	0.099	

当量濃度分率						平衡後の固相			
当量濃度分率			当量活量分率			固相中の当量分率			陽イオン 交換容量 (meq/100g)
K ⁺	H ⁺	Na ⁺	K ⁺	H ⁺	Na ⁺	E _K	E _H	E _{Na}	
0.009	0.002	0.988	0.009	0.002	0.988	0.023	0.129	0.847	108.1
0.010	0.026	0.963	0.010	0.026	0.963	0.016	0.348	0.637	108.1
0.010	0.065	0.925	0.010	0.065	0.925	0.017	0.437	0.547	108.1
0.011	0.416	0.573	0.011	0.416	0.573	0.014	0.744	0.242	108.1
0.045	0.003	0.952	0.045	0.003	0.952	0.031	0.129	0.840	108.1
0.046	0.027	0.927	0.046	0.027	0.927	0.041	0.324	0.635	108.1
0.046	0.065	0.889	0.046	0.065	0.889	0.045	0.437	0.518	108.1
0.047	0.424	0.528	0.047	0.424	0.528	0.044	0.372	0.585	108.1
0.084	0.003	0.913	0.084	0.003	0.913	0.250	0.122	0.629	108.1
0.088	0.028	0.884	0.088	0.028	0.884	0.203	0.293	0.505	108.1
0.091	0.067	0.842	0.091	0.067	0.842	0.138	0.407	0.454	108.1
0.094	0.425	0.481	0.094	0.425	0.481	0.073	0.565	0.363	108.1
0.441	0.004	0.555	0.441	0.004	0.555	0.287	0.102	0.612	108.1
0.440	0.030	0.530	0.440	0.030	0.530	0.278	0.241	0.481	108.1
0.452	0.069	0.479	0.452	0.069	0.479	0.333	0.309	0.358	108.1
0.4789	0.419	0.103	0.4789	0.419	0.103	0.333	0.744	-0.077	108.1

Table 2.3.2(2) Measured data of ionexchange equilibrium in Ca²⁺+H⁺+Na-smectite system

設定値 (eq/ℓ)			初期溶液				平衡後の液相											イオン強度
			測定濃度 (mol/ℓ)				測定濃度 (mol/ℓ)				活量			活量係数 (Log γ)				
KCl	CaCl ₂	NaCl	pH	K	Ca	Na	pH	K	Ca	Na	K ⁺	Ca ²⁺	Na ⁺	K ⁺	Ca ²⁺	Na ⁺		
0.001	0.0005	0.098	5.51	1.27×10 ⁻³	4.52×10 ⁻⁴	9.74×10 ⁻²	4.74	9.72×10 ⁻⁴	2.14×10 ⁻⁴	9.78×10 ⁻²	7.60×10 ⁻⁴	1.31×10 ⁻⁴	7.65×10 ⁻²	-0.107	-0.214	-0.107	0.099	
	0.0025	0.094	5.43	1.33×10 ⁻³	2.39×10 ⁻³	9.24×10 ⁻²	4.73	9.87×10 ⁻³	1.26×10 ⁻³	9.48×10 ⁻²	7.72×10 ⁻⁴	7.70×10 ⁻⁴	7.41×10 ⁻²	-0.107	-0.214	-0.107	0.100	
	0.005	0.089	5.53	1.27×10 ⁻³	4.53×10 ⁻³	8.96×10 ⁻²	4.73	1.02×10 ⁻³	2.66×10 ⁻³	9.26×10 ⁻²	7.96×10 ⁻⁴	1.62×10 ⁻³	7.23×10 ⁻²	-0.108	-0.215	-0.108	0.102	
	0.025	0.049	5.64	1.33×10 ⁻³	2.33×10 ⁻²	5.05×10 ⁻²	4.57	1.13×10 ⁻³	1.89×10 ⁻²	5.71×10 ⁻²	8.74×10 ⁻⁴	1.13×10 ⁻²	4.42×10 ⁻²	-0.111	-0.223	-0.111	0.115	
0.005	0.0005	0.094	5.50	5.12×10 ⁻³	4.80×10 ⁻⁴	9.38×10 ⁻²	4.71	4.53×10 ⁻³	2.47×10 ⁻⁴	9.48×10 ⁻²	3.54×10 ⁻³	1.51×10 ⁻⁴	7.41×10 ⁻²	-0.107	-0.214	-0.107	0.100	
	0.0025	0.090	5.51	5.12×10 ⁻³	2.38×10 ⁻³	8.96×10 ⁻²	4.69	4.63×10 ⁻³	1.35×10 ⁻³	9.15×10 ⁻²	3.62×10 ⁻³	8.24×10 ⁻⁴	7.15×10 ⁻²	-0.107	-0.214	-0.107	0.100	
	0.005	0.085	5.54	5.22×10 ⁻³	4.68×10 ⁻³	8.70×10 ⁻²	4.69	4.91×10 ⁻³	2.83×10 ⁻³	8.96×10 ⁻²	3.83×10 ⁻³	1.72×10 ⁻³	6.99×10 ⁻²	-0.108	-0.216	-0.108	0.103	
	0.025	0.045	5.66	5.22×10 ⁻³	2.34×10 ⁻²	4.62×10 ⁻²	4.56	5.29×10 ⁻³	1.91×10 ⁻²	5.39×10 ⁻²	4.09×10 ⁻³	1.14×10 ⁻²	4.17×10 ⁻²	-0.112	-0.224	-0.112	0.116	
0.01	0.0005	0.089	5.43	1.22×10 ⁻²	4.78×10 ⁻⁴	8.87×10 ⁻²	4.68	9.41×10 ⁻³	2.67×10 ⁻⁴	9.40×10 ⁻²	7.33×10 ⁻³	1.62×10 ⁻⁴	7.32×10 ⁻²	-0.108	-0.217	-0.108	0.104	
	0.0025	0.085	5.50	1.14×10 ⁻²	2.38×10 ⁻³	8.46×10 ⁻²	4.65	9.41×10 ⁻³	1.47×10 ⁻³	9.05×10 ⁻²	7.33×10 ⁻³	8.92×10 ⁻⁴	7.05×10 ⁻²	-0.108	-0.217	-0.108	0.104	
	0.005	0.080	5.53	1.14×10 ⁻²	4.57×10 ⁻³	7.86×10 ⁻²	4.66	9.41×10 ⁻³	3.01×10 ⁻³	8.70×10 ⁻²	7.33×10 ⁻³	1.89×10 ⁻³	6.77×10 ⁻²	-0.109	-0.217	-0.109	0.105	
	0.025	0.040	5.64	1.14×10 ⁻²	2.26×10 ⁻²	4.18×10 ⁻²	4.55	9.72×10 ⁻³	1.94×10 ⁻²	5.05×10 ⁻²	7.51×10 ⁻³	1.16×10 ⁻²	3.90×10 ⁻²	-0.112	-0.225	-0.112	0.118	
0.05	0.0005	0.049	5.44	4.84×10 ⁻²	4.70×10 ⁻⁴	4.96×10 ⁻²	4.56	4.60×10 ⁻²	3.53×10 ⁻⁴	5.92×10 ⁻²	3.58×10 ⁻²	2.14×10 ⁻⁴	4.61×10 ⁻²	-0.109	-0.218	-0.109	0.106	
	0.0025	0.045	5.49	4.84×10 ⁻²	2.31×10 ⁻³	4.54×10 ⁻²	4.51	4.55×10 ⁻²	1.75×10 ⁻³	5.48×10 ⁻²	3.54×10 ⁻²	1.06×10 ⁻³	4.27×10 ⁻²	-0.109	-0.217	-0.109	0.106	
	0.005	0.040	5.56	4.80×10 ⁻²	6.91×10 ⁻³	4.04×10 ⁻²	4.50	4.61×10 ⁻²	3.58×10 ⁻³	4.96×10 ⁻²	3.59×10 ⁻²	2.17×10 ⁻³	3.86×10 ⁻²	-0.109	-0.218	-0.109	0.106	
	0.025	0	5.68	4.92×10 ⁻²	2.26×10 ⁻²	0	4.51	4.93×10 ⁻²	2.01×10 ⁻²	1.00×10 ⁻²	3.80×10 ⁻²	1.20×10 ⁻²	7.72×10 ⁻²	-0.113	-0.225	-0.113	0.120	

当量濃度分率						当量活量分率			平衡後の固相			陽イオン 交換容量 (meq/100g)
K ⁺	Ca ²⁺	Na ⁺	K ⁺	Ca ²⁺	Na ⁺	固相中の当量分率						
						E _K	E _{Ca}	E _{Na}				
0.010	0.004	0.986	0.010	0.002	0.988	0.028	0.044	0.928	108.1			
0.010	0.026	0.964	0.010	0.012	0.977	0.032	0.209	0.759	108.1			
0.010	0.054	0.936	0.011	0.026	0.963	0.023	0.346	0.631	108.1			
0.012	0.394	0.595	0.015	0.231	0.754	0.019	0.814	0.167	108.1			
0.045	0.005	0.950	0.045	0.002	0.952	0.055	0.043	0.902	108.1			
0.047	0.027	0.926	0.048	0.013	0.939	0.045	0.191	0.764	108.1			
0.049	0.057	0.894	0.051	0.028	0.922	0.029	0.342	0.629	108.1			
0.054	0.392	0.553	0.069	0.230	0.701	-0.006	0.796	0.211	108.1			
0.091	0.005	0.904	0.091	0.002	0.907	0.258	0.039	0.703	108.1			
0.091	0.029	0.880	0.093	0.014	0.893	0.184	0.168	0.648	108.1			
0.092	0.059	0.849	0.095	0.029	0.877	0.184	0.289	0.527	108.1			
0.098	0.392	0.510	0.124	0.229	0.647	0.155	0.592	0.253	108.1			
0.434	0.007	0.559	0.436	0.003	0.561	0.222	0.022	0.756	108.1			
0.438	0.034	0.528	0.446	0.016	0.538	0.268	0.104	0.628	108.1			
0.438	0.070	0.482	0.465	0.034	0.501	0.176	0.616	0.208	108.1			
0.495	0.404	0.101	0.634	0.238	0.129	-0.009	0.463	0.547	108.1			

計算条件を表2.3.3に示す。計算コードにはPHREEQE 60を使用した。大気雰囲気条件とするため、pH 7.0 $pe+5.9$, CO_2 ガス分圧 $10^{-3.5}atm$ に設定した。固液比条件は、セミマイクロショールンベハガー法によるイオン交換容量の測定値 108meq/100gと分配試験の固液比条件1.0g/100mlより、10.8meq/ℓとして入力した。液相中のイオンについては、PHREEQE 60の中でDebye-Huckelの式により活量補正を行った。

Table 2.3.3 Conditions of estimation for ion-exchange equilibrium (ternary system)

項目	計算条件
計算コード	PHREEQE 60
化学的雰囲気条件	・ pH 7.0 ・ $pe+5.9$ (Eh+350mV)
ガス平衡	大気雰囲気 (CO_2 ガス $10^{-3.5}atm$)
固液比	10 g / 1 ℓ (10.8meq/ℓ)
液相の活量補正式	Debye-Huckelの式
固相の活量	1と仮定 (理想固溶体モデル)
データベース	PHREEQE オリジナルデータベース
イオン交換平衡定数	表2.2.2参照

2.3.3 測定値と計算結果の比較

$K^+ + H^+ + Na$ 型スメクタイト及び $K^+ + Ca^{2+} + Na$ 型スメクタイト系での分配試験の測定結果と計算結果の比較を図2.3.1～図2.3.2に示した。図中でx軸は液相中の当量分率、y軸は固相中の当量分率である。

(1) $K^+ + H^+ + Na$ 型スメクタイト系

図2.3.1(1)～(4)は H^+ 濃度 (pH) を一定にした場合の K^+ の分配を、図2.3.1(5)～(8)は逆に K^+ 濃度を一定にした場合の H^+ の分配を示した。

図2.3.1(1)～(4)より、 K^+ についてはNa型スメクタイト及びMX-80のイオン交換平衡定数による場合ともほぼ同様の結果であった。どちらについても K^+ の分率が低い場合のみ測定値と一致し、 K^+ の濃度が高くなるにつれ、計算では固相中の分率が高く評価される傾向が見られた。

一方、図2.3.1(5)～(8)より、 H^+ については測定値にバラつきが大きいものの、イオン交換平衡定数による計算結果は測定値とほぼ一致することがわかった。また、MX-80のイオン交換平衡定数については、Na型スメクタイトのものと比較して固相中

の分率は低く評価される傾向にあった。

(2) $K^+ + Ca^{2+} + Na$ 型スメクタイト系

図 2.3.2 (1)~(4)は Ca^{2+} 濃度を一定にした場合の K^+ の分配を、図 2.3.2 (5)~(8)は逆に K^+ 濃度を一定にした場合の Ca^{2+} の分配を示した。

図 2.3.2 (1)~(4)より、 K^+ については、 $K^+ + H^+ + Na$ 型スメクタイト系の場合と同様、 K^+ の分率が低いのみ測定値と一致し、 K^+ の濃度が高くなるにつれ、計算では固相中の分率が低く評価される傾向が見られた。

一方、図 2.3.2 (5)~(8)より、 Ca^{2+} についてはMX-80のイオン交換平衡定数による計算結果のみ測定値と一致した。これは2成分系における検討結果と同じ結果である。この原因として、2.1.2で測定されたイオン交換平衡定数において、 $CaCl^+$ による交換反応が評価されていないためと考えられた。

(3) まとめ

以上の結果により、 K^+ については高濃度 (0.01mol/l 以上) 領域でイオン交換定数による解析値と測定値のズレが大きいものの、 H^+ については測定値とほぼ一致することが確認された。また、 Ca^{2+} についても、塩化物イオン ($CaCl^+$) による反応が考慮されているMX-80のイオン交換平衡定数による計算結果では、測定値とほぼ一致することが確認された。よって、3成分系での分配平衡に対してもイオン交換モデルは適用可能であるものと考えられる。また、2成分系での結果と同様、MX-80について測定されたイオン交換平衡定数を用いても、Na型スメクタイトの分配平衡の評価はほぼ可能であることがわかった。

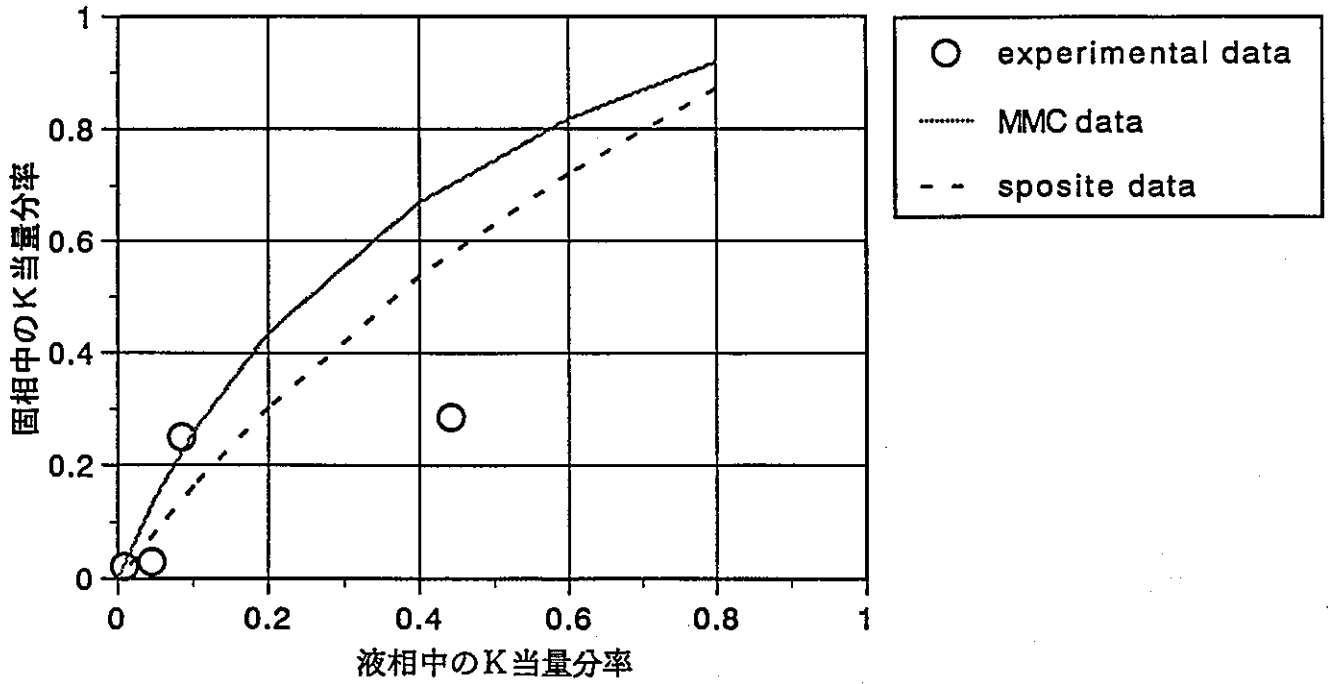


Fig. 2.3.1(1) Equivalent fraction of K^+ between aqueous and solid phase
 (K^+H^+Na -smectite system, $H^+ : 0.001 \text{ mol/l}$ constant)

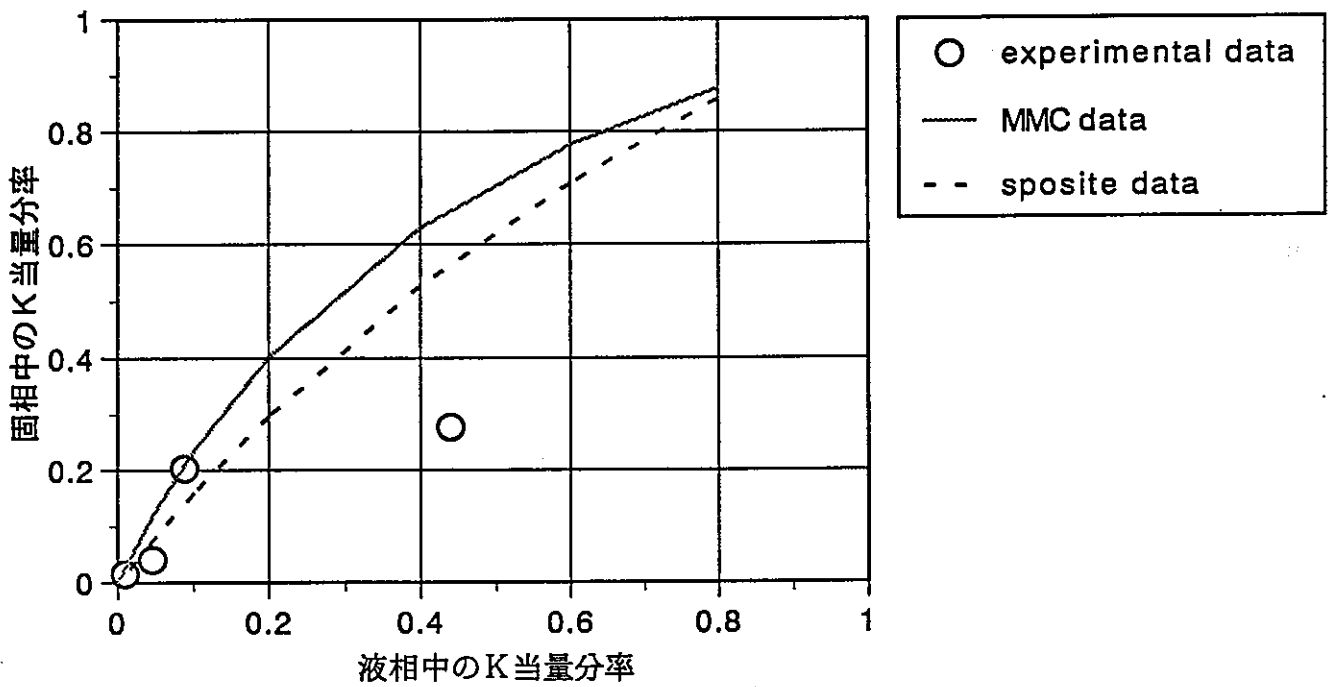


Fig. 2.3.1(2) Equivalent fraction of K^+ between aqueous and solid phase
 (K^+H^+Na -smectite system, $H^+ : 0.005 \text{ mol/l}$ constant)

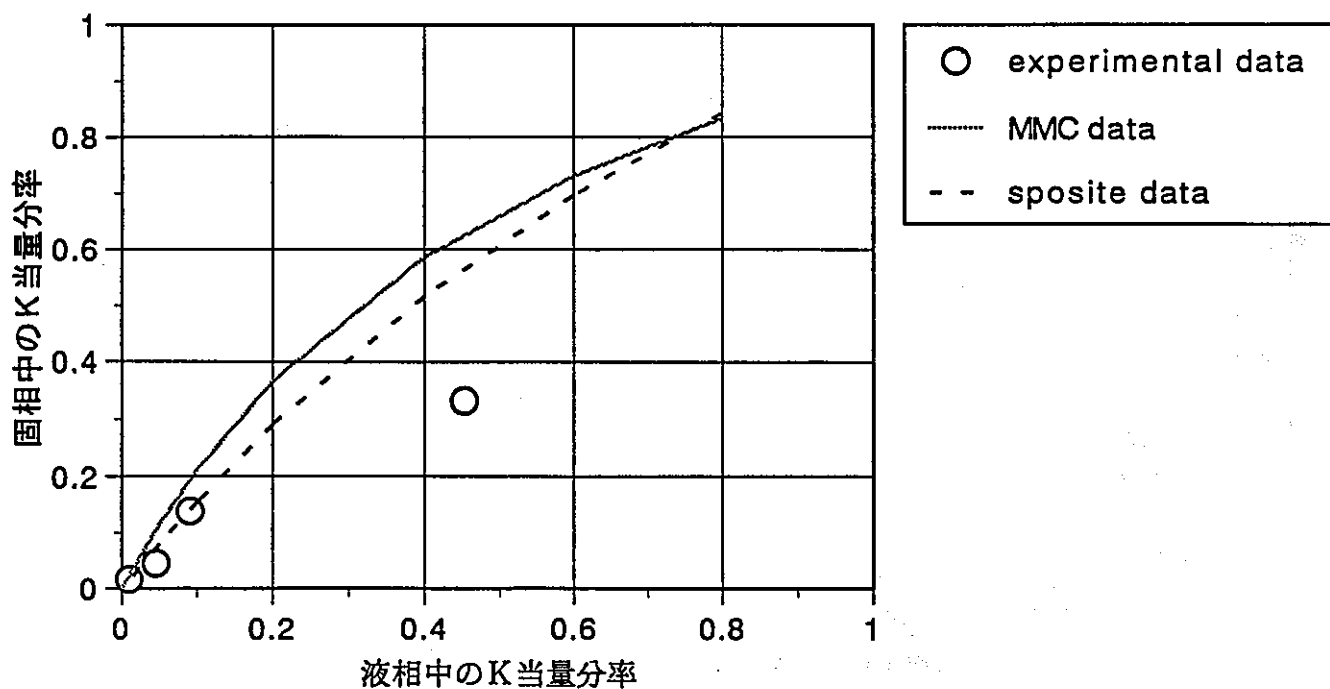


Fig. 2.3.1(3) Equivalent fraction of K^+ between aqueous and solid phase
 (K^+H^+Na -smectite system, $H^+ : 0.01\text{mol}/\ell$ constant)

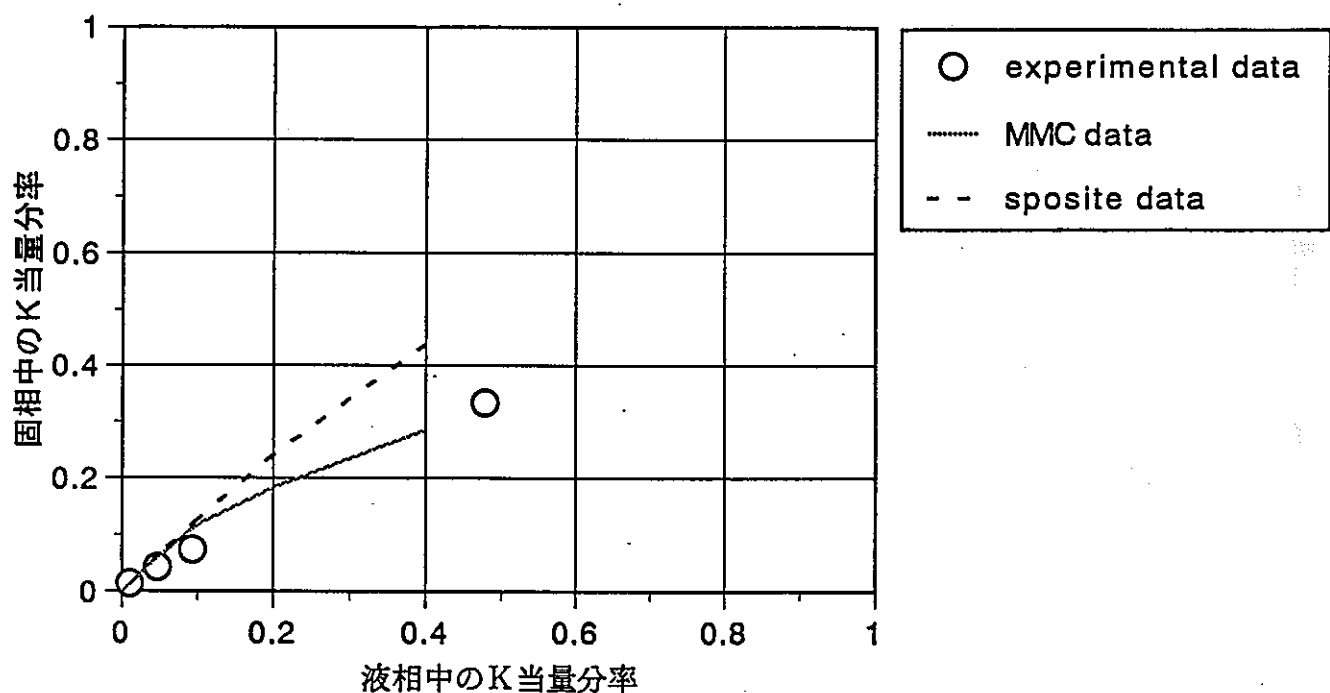


Fig. 2.3.1(4) Equivalent fraction of K^+ between aqueous and solid phase
 (K^+H^+Na -smectite system, $H^+ : 0.05\text{mol}/\ell$ constant)

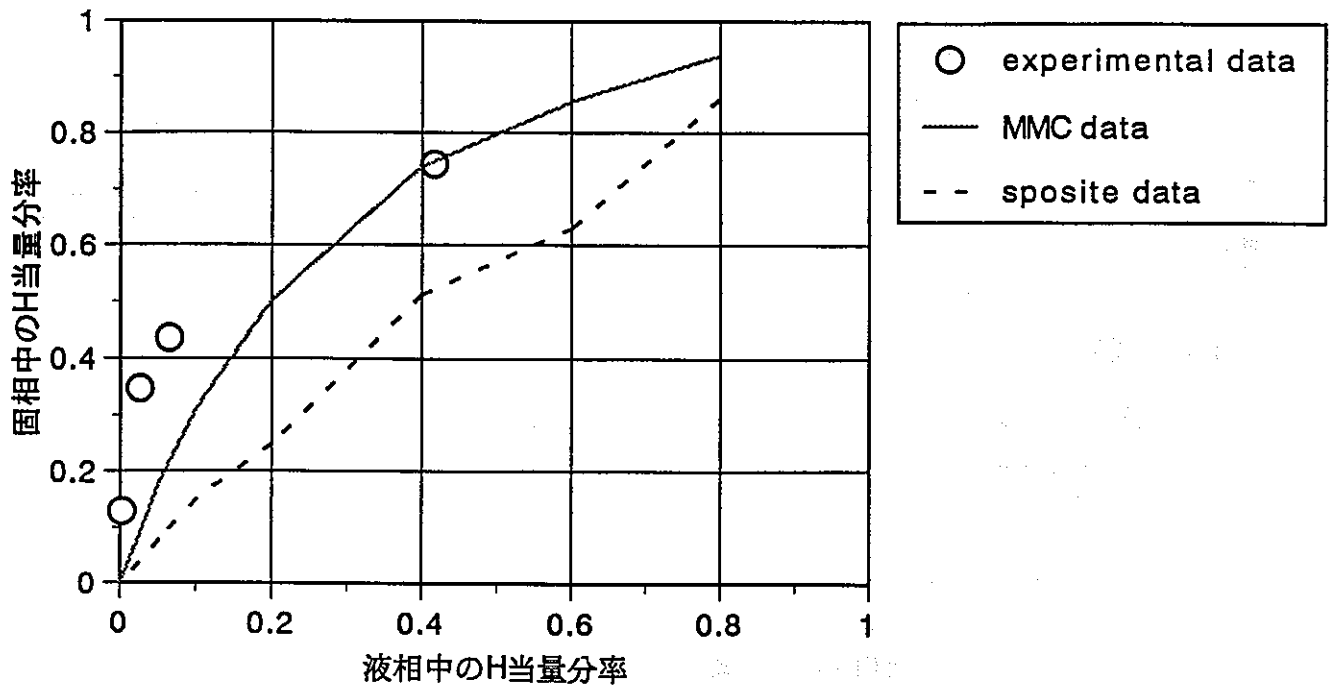


Fig. 2.3.1(5) Equivalent fraction of H⁺ between aqueous and solid phase
 (K⁺+H⁺+Na-smectite system, K⁺: 0.001 mol/ℓ constant)

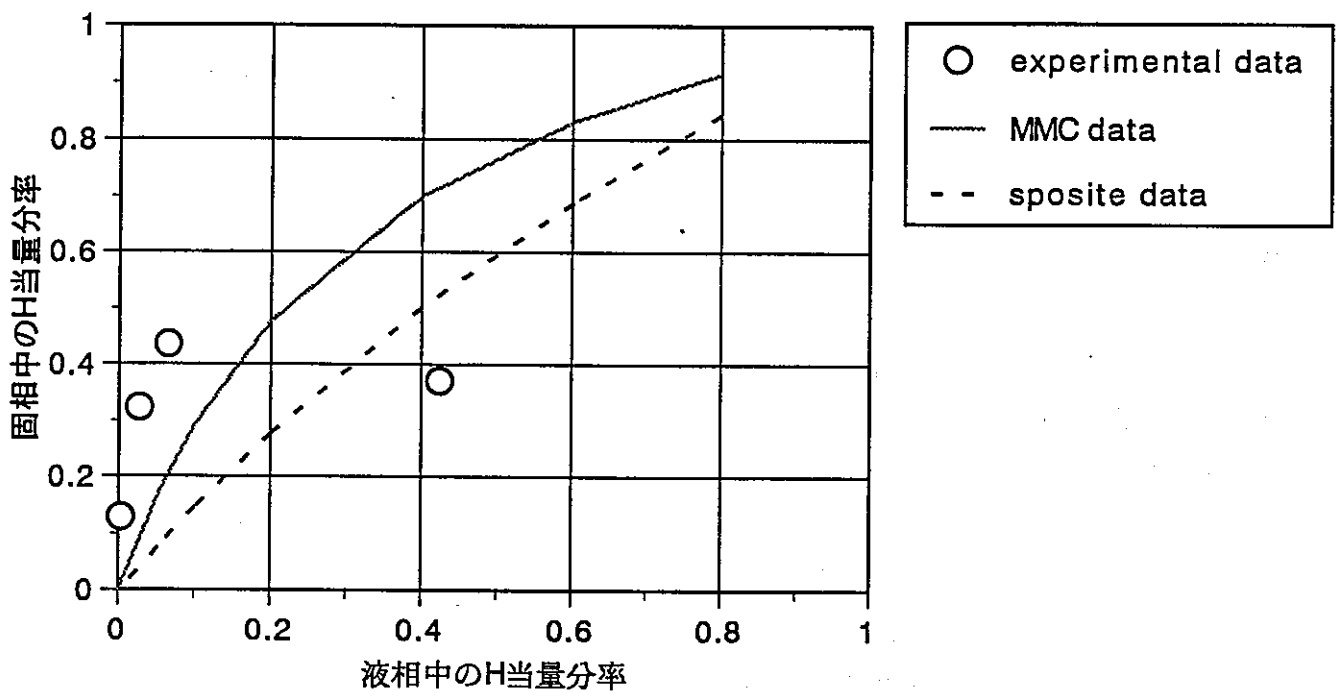


Fig. 2.3.1(6) Equivalent fraction of H⁺ between aqueous and solid phase
 (K⁺+H⁺+Na-smectite system, K⁺: 0.005 mol/ℓ constant)

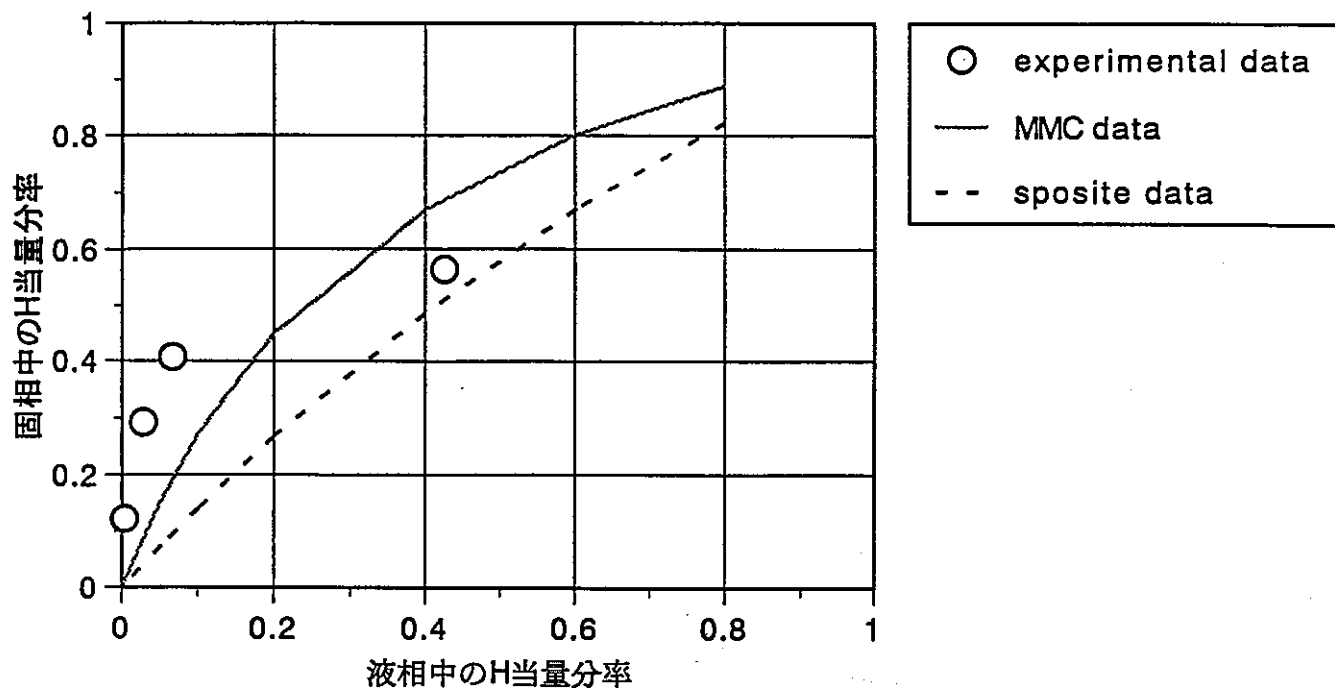


Fig. 2.3.1(7) Equivalent fraction of H^+ between aqueous and solid phase
 ($K^+ + H^+ + Na$ -smectite system, $K^+ : 0.01 \text{ mol}/\ell$ constant)

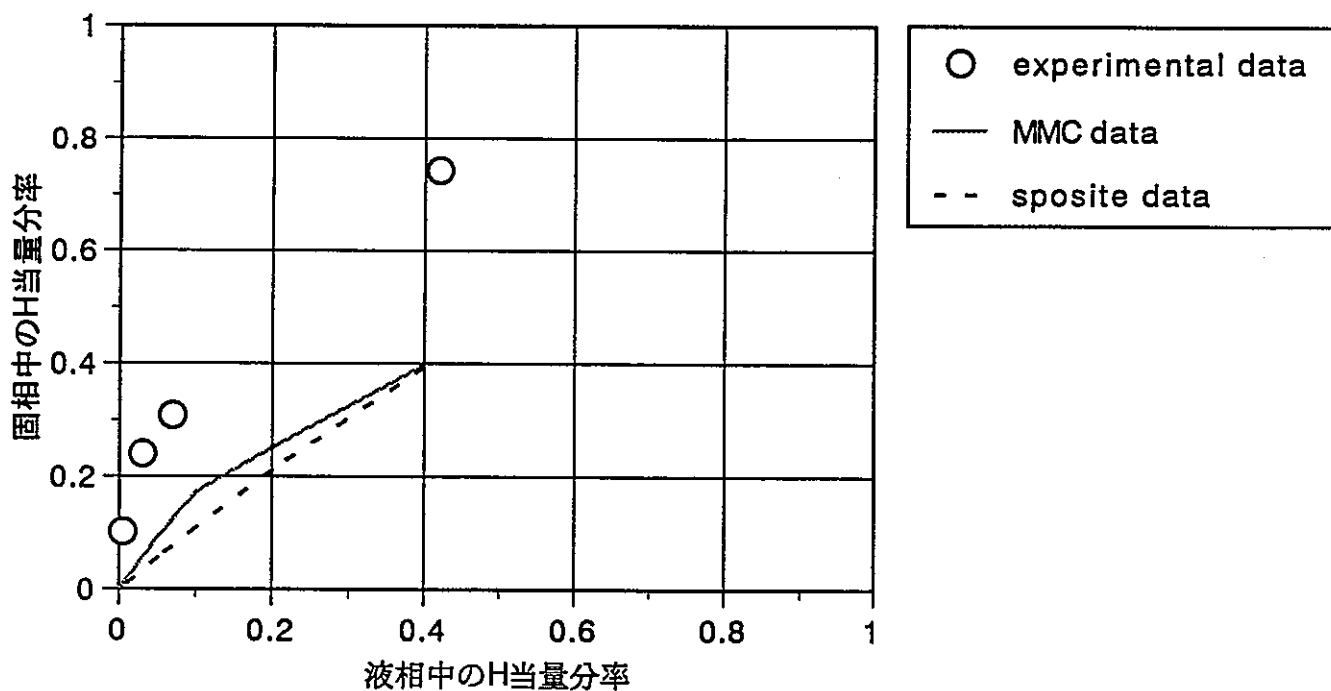


Fig. 2.3.1(8) Equivalent fraction of H^+ between aqueous and solid phase
 ($K^+ + H^+ + Na$ -smectite system, $K^+ : 0.05 \text{ mol}/\ell$ constant)

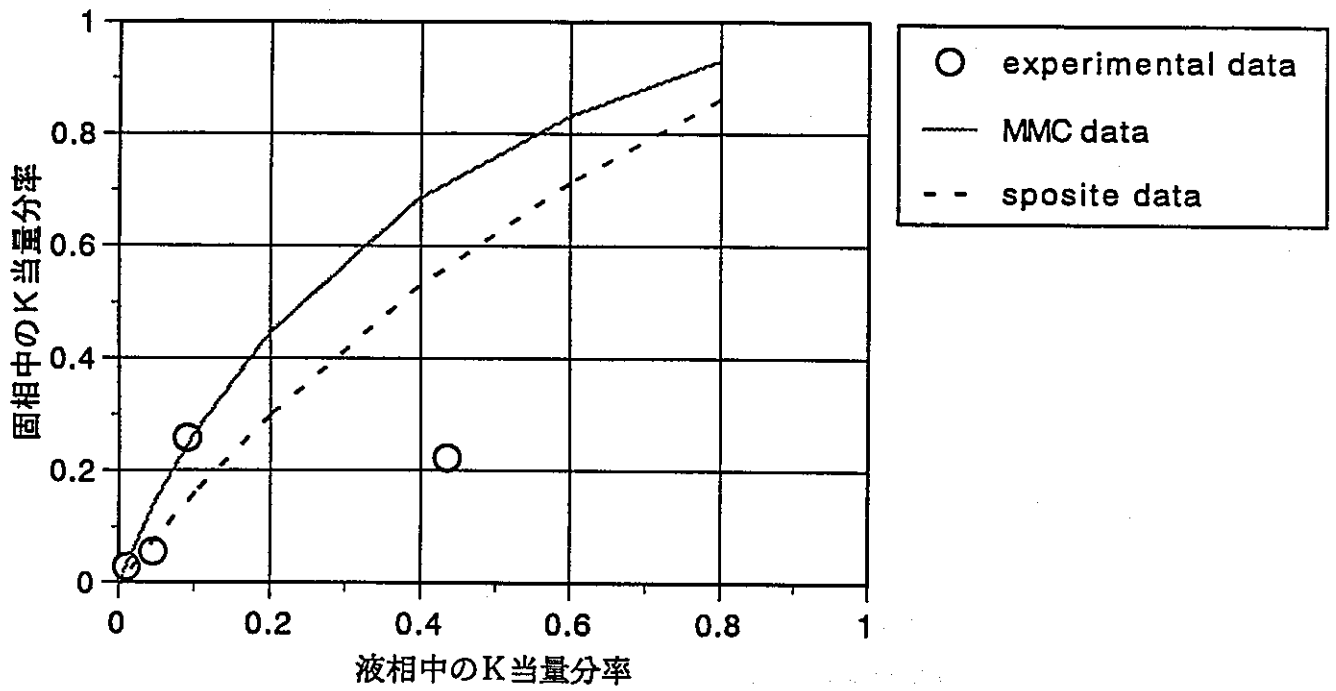


Fig. 2.3.2(1) Equivalent fraction of K^+ between aqueous and solid phase
 ($K^+Ca^{2+}Na$ -smectite system, $Ca^{2+} : 0.0005 \text{ mol/l}$ constant)

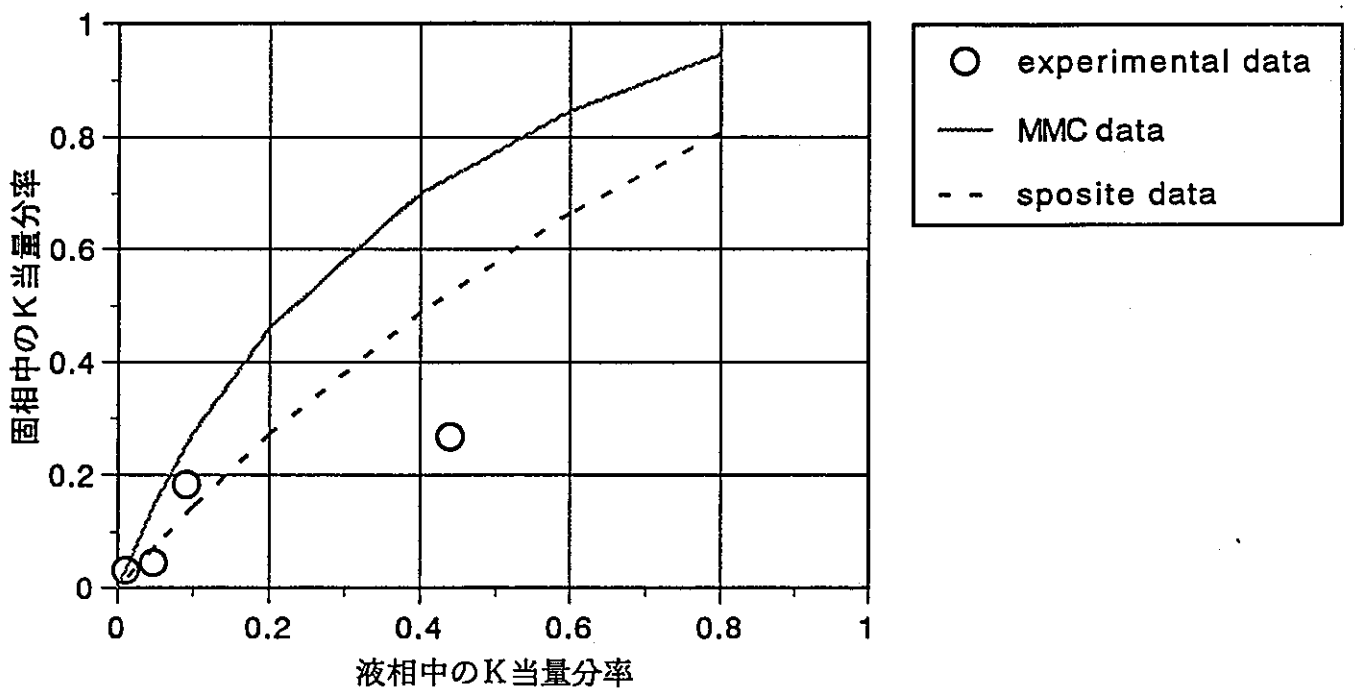


Fig. 2.3.2(2) Equivalent fraction of K^+ between aqueous and solid phase
 ($K^+Ca^{2+}Na$ -smectite system, $Ca^{2+} : 0.0025 \text{ mol/l}$ constant)

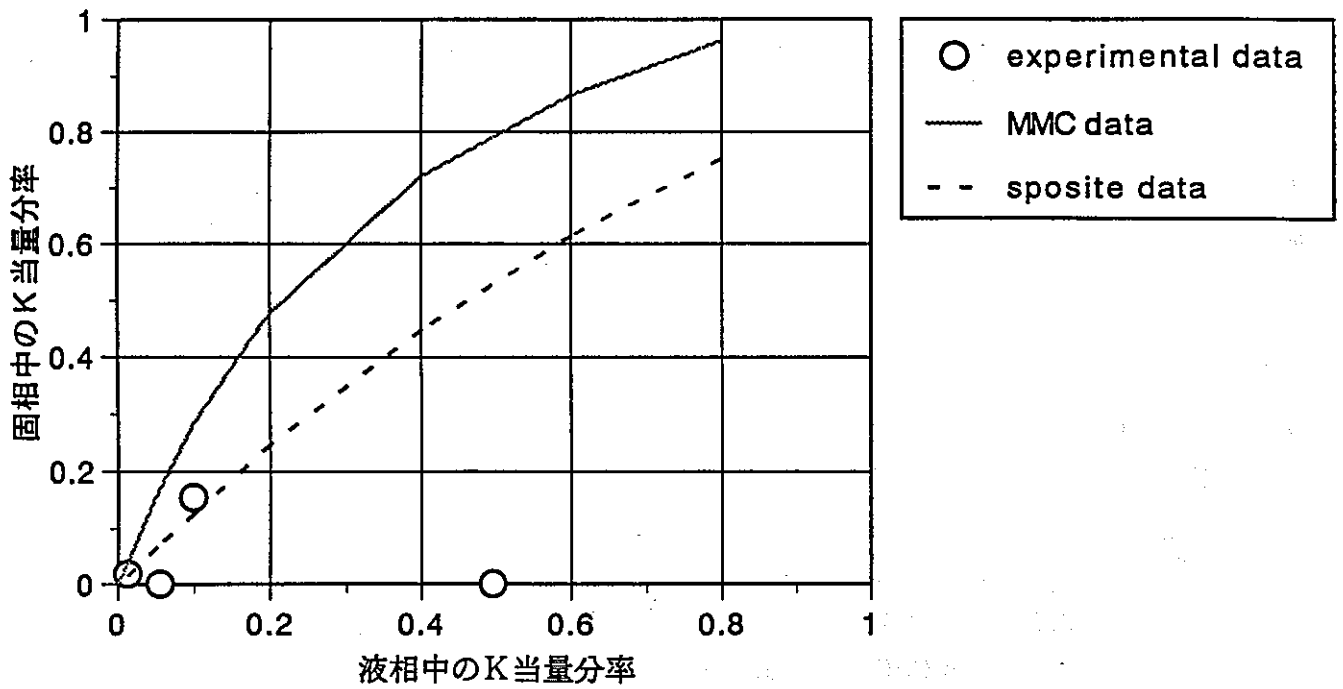


Fig. 2.3.2(3) Equivalent fraction of K^+ between aqueous and solid phase
 ($K^+ + Ca^{2+} + Na$ -smectite system, $Ca^{2+} : 0.005 \text{ mol/l}$ constant)

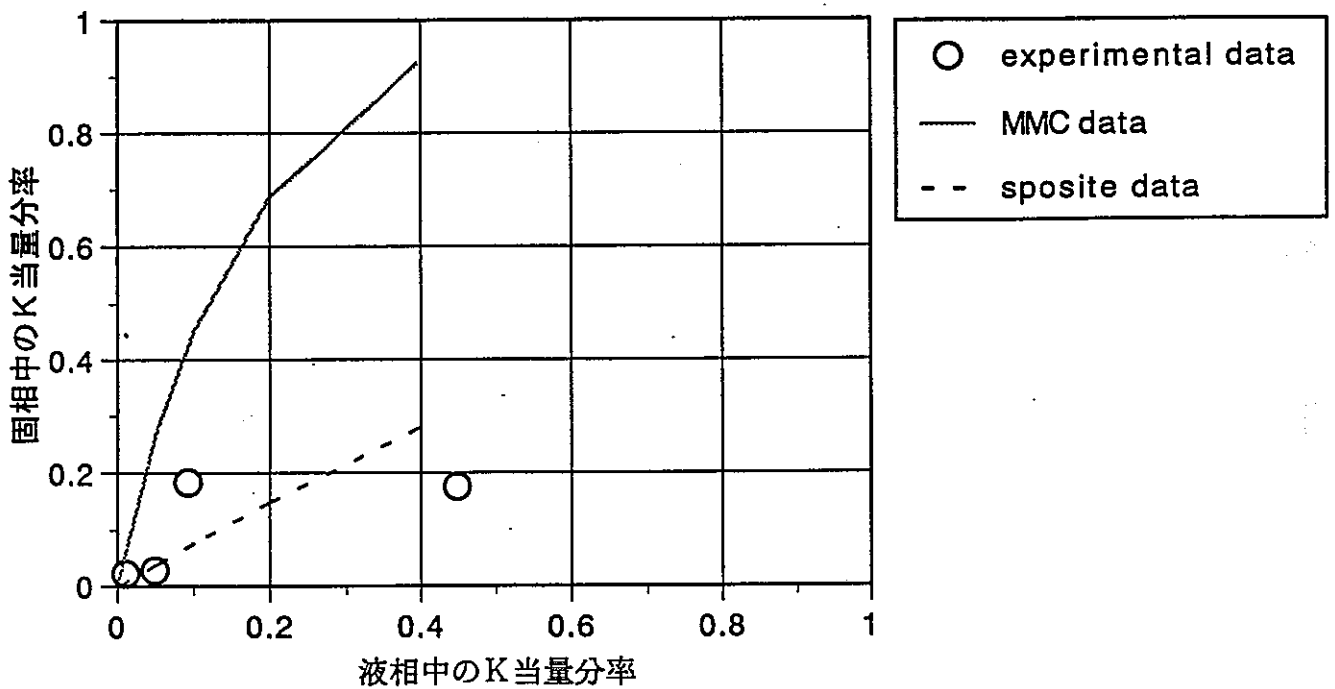


Fig. 2.3.2(4) Equivalent fraction of K^+ between aqueous and solid phase
 ($K^+ + Ca^{2+} + Na$ -smectite system, $Ca^{2+} : 0.025 \text{ mol/l}$ constant)

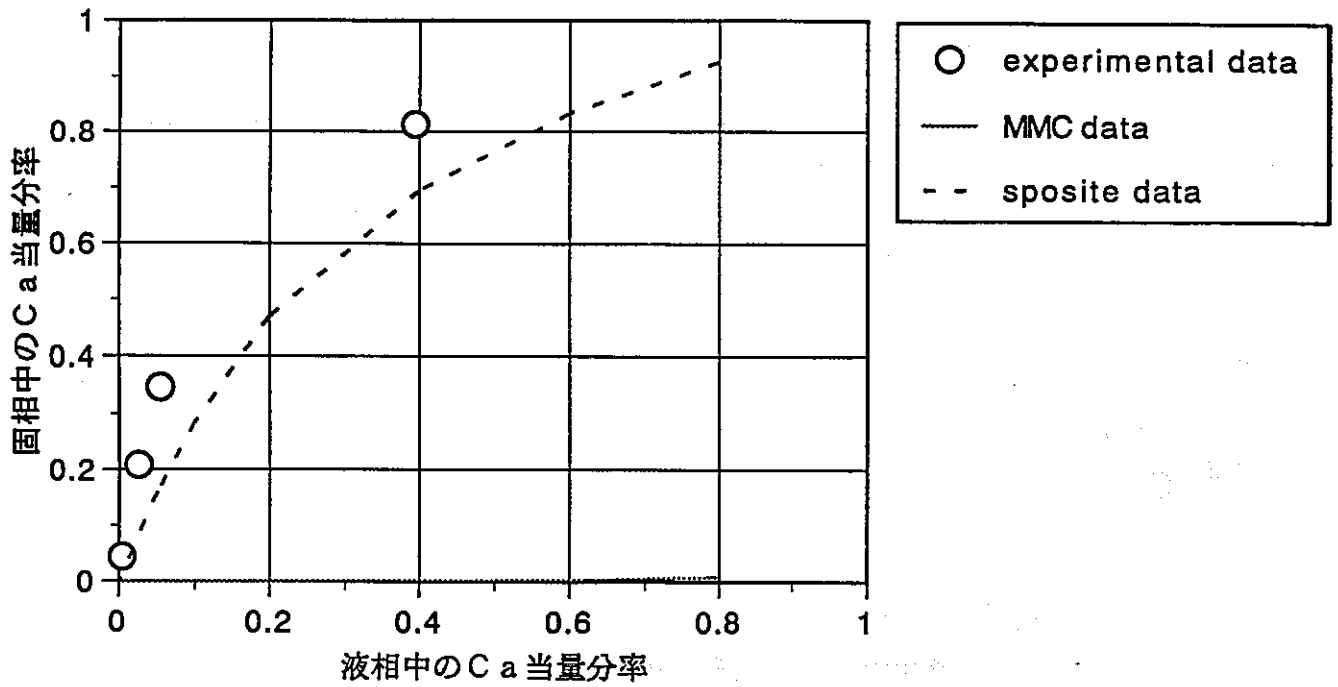


Fig. 2.3.2(5) Equivalent fraction of Ca^{2+} between aqueous and solid phase
 (K^+ + Ca^{2+} + Na -smectite system, $\text{K}^+ : 0.001 \text{ mol/l}$ constant)

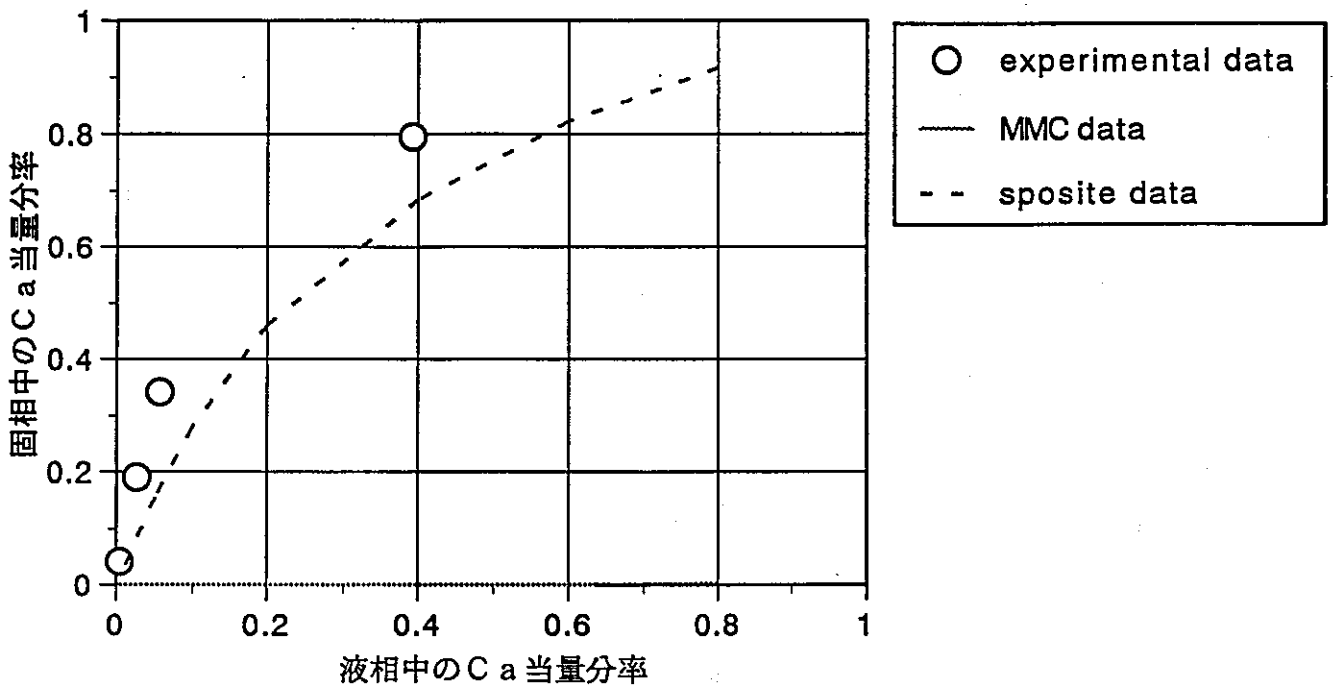


Fig. 2.3.2(6) Equivalent fraction of Ca^{2+} between aqueous and solid phase
 (K^+ + Ca^{2+} + Na -smectite system, $\text{K}^+ : 0.005 \text{ mol/l}$ constant)

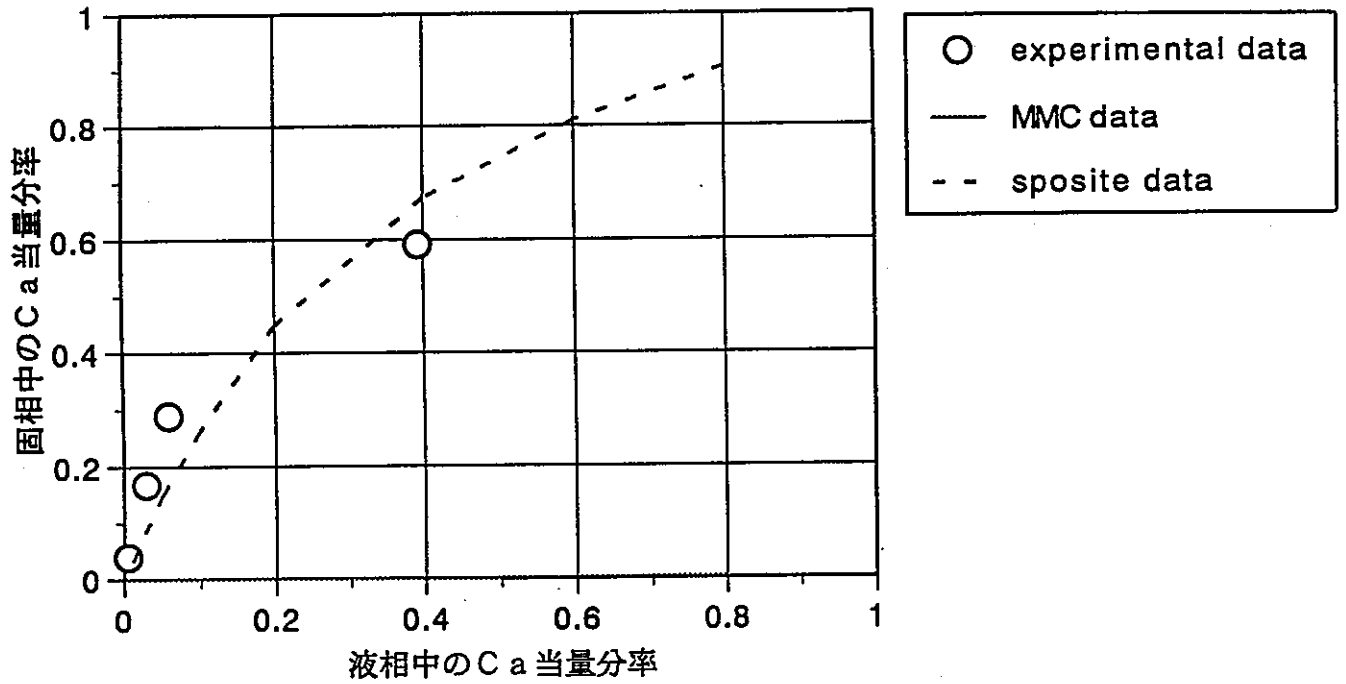


Fig. 2.3.2(7) Equivalent fraction of Ca^{2+} between aqueous and solid phase
($\text{K}^+\text{+Ca}^{2+}\text{+Na}$ -smectite system, $\text{K}^+ : 0.01\text{mol}/\ell$ constant)

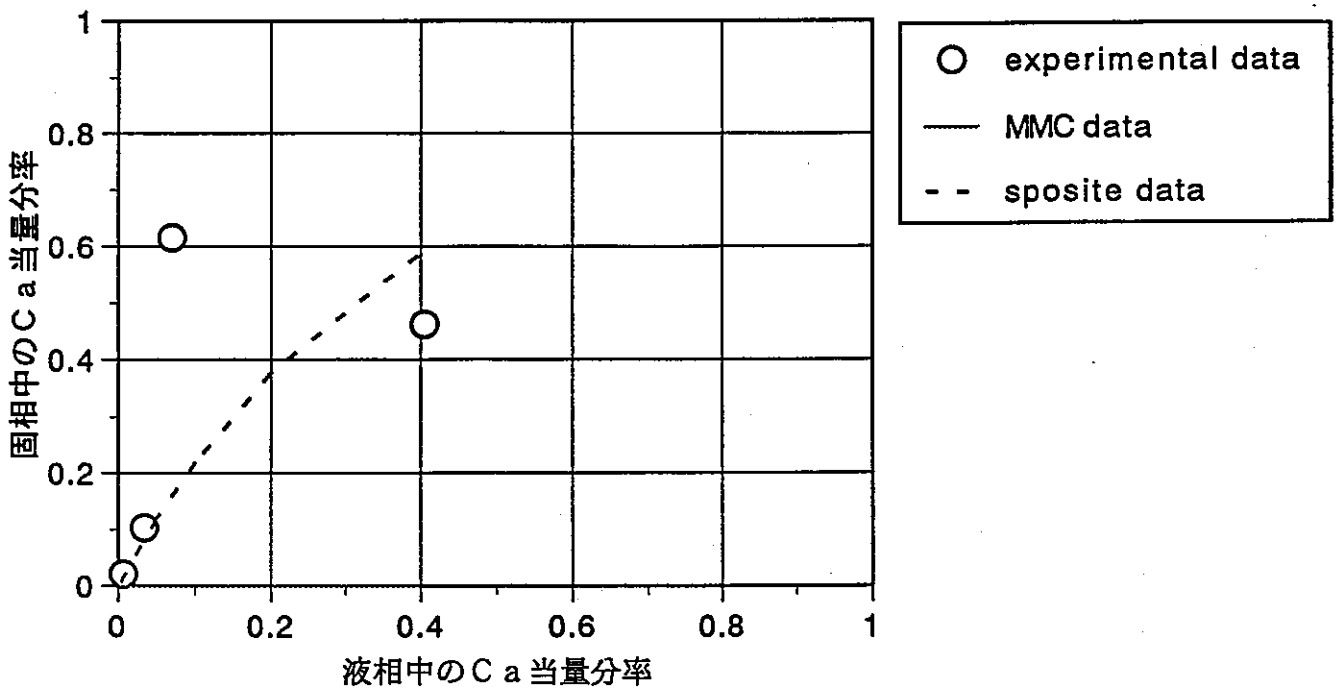


Fig. 2.3.2(8) Equivalent fraction of Ca^{2+} between aqueous and solid phase
($\text{K}^+\text{+Ca}^{2+}\text{+Na}$ -smectite system, $\text{K}^+ : 0.05\text{mol}/\ell$ constant)

2.4 まとめ

2章で行ったイオン交換平衡モデルの検討結果について、以下にまとめる。

- ① Kiellandプロット法により、Na型スメクタイトのイオン交換平衡定数を測定した。その結果、 K^+ 、 Ca^{2+} 、 Mg^{2+} 及び H^+ とのイオン交換平衡定数 ($\ln K_{ex}$) は、それぞれ1.19, -0.25, 0.64, 1.17と求められた。
- ② 固相に吸着したイオンに対する活量補正の必要性について検討するため、正則溶液モデルを用いて計算し、測定値と比較を行った。その結果、正則溶液モデルを用いた場合、 K^+ 、 Ca^{2+} 及び Mg^{2+} では理想固溶体モデルとほとんど差がなかったが、 H^+ については測定値と大きく相違する可能性があった。また、理想固溶体モデルについては、測定値とほぼ一致することを確認した。
よって、スメクタイトの分配平衡を評価する場合、理想固溶体モデルによる評価が適切かつ妥当であると判断した。
- ③ 固溶状態が相違することが考えられるMX-80のイオン交換平衡定数を用いて、Na型スメクタイトのイオンの分配平衡を解析し、測定値と比較を行った。その結果、MX-80のイオン交換平衡定数を用いても、Na型スメクタイトの分配平衡を評価できることがわかった。
- ④ 3成分系についても、イオン交換平衡モデルによりイオンの吸着分配が予測評価できるものと考えられた。しかし、Ca及びMgの分配平衡については、 Ca^{2+} 、 Mg^{2+} の他、塩化物イオン ($CaCl^+$ 、 $MgCl^+$) による交換反応についても考慮しなければならないことがわかった。

参考文献)

- 1) Sposito, G., Holtzclaw, K. M., Jouany, C., and Charlet, L. Cation selectivity in sodium-calcium, sodium-magnesium and calcium-magnesium exchange on Wyoming Bentonite at 298K. *Soil Sci. Soc. Am. J.* 47, 917-921

第3章 平成4年度のイオン交換試験データ及び固溶体モデルのレビュー

平成4年度に実施したイオン交換平衡試験データのレビュー及び固溶体モデルの調査を Dr. Wanner (スイス, MB T社) に委託して実施した。その成果の概要を以下にまとめる。なお、報告書の原文は巻末資料として添付した。

3.1 イオン交換試験データのレビュー

(1) 概要

平成4年度に実施したイオン交換平衡測定試験 (Kiellandプロット試験) のデータについて、Sposito のイオン交換平衡定数を用いて解析した。解析に用いたSposito のイオン交換平衡定数は表2.2.2に示したものと同様である。解析はMIN SURFコードにより行い、理想固溶体と仮定して解析した。

(2) 結果

結果を図3.1.1(1)~(4)に示す。

$K^+ + Na$ 型スメクタイト系では、実験値と解析結果は一致した。

H^+ 系では、実験値と解析結果は一致しなかった。反応式 $[H^+ + Z^- \rightleftharpoons H-Z]$ の平衡定数 (Log K) が20.95であれば、よく一致することが示された。

Ca^{2+} 及び Mg^{2+} 系については、 $CaCl^+$ 及び $MgCl^+$ の反応を考慮すると吸着分率が上昇し、実験値に近くなることがわかった。

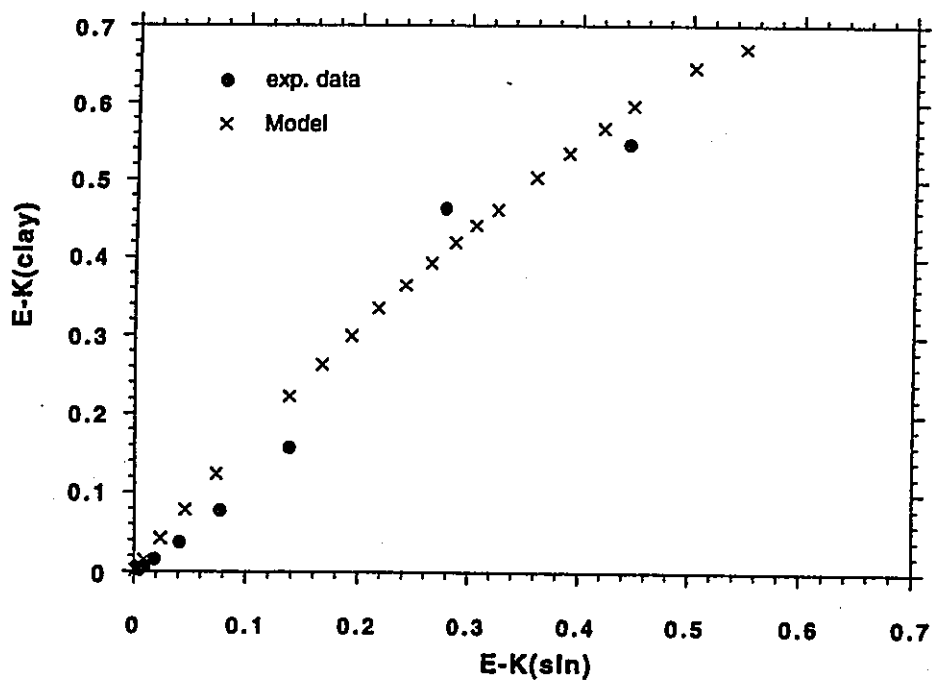


Fig. 3.1.1(1) Equivalent fraction of K^+ between aqueous and solid phase
 ($K^+ + Na$ -smectite system) (Measured data in 1993)

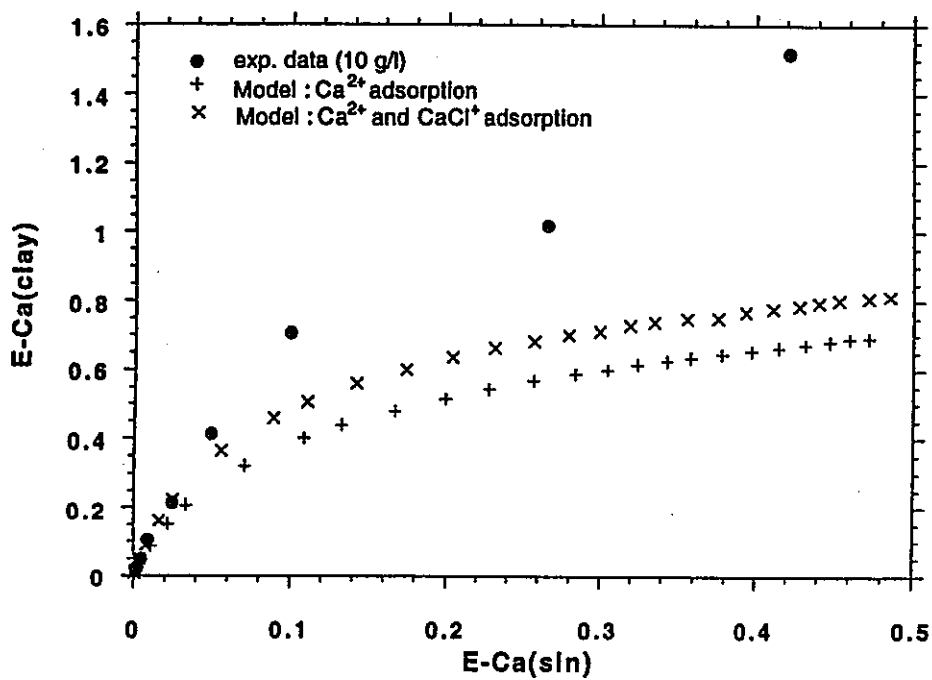


Fig. 3.1.1(2) Equivalent fraction of Ca^{2+} between aqueous and solid phase
 ($Ca^{2+} + Na$ -smectite system) (Measured data in 1993)

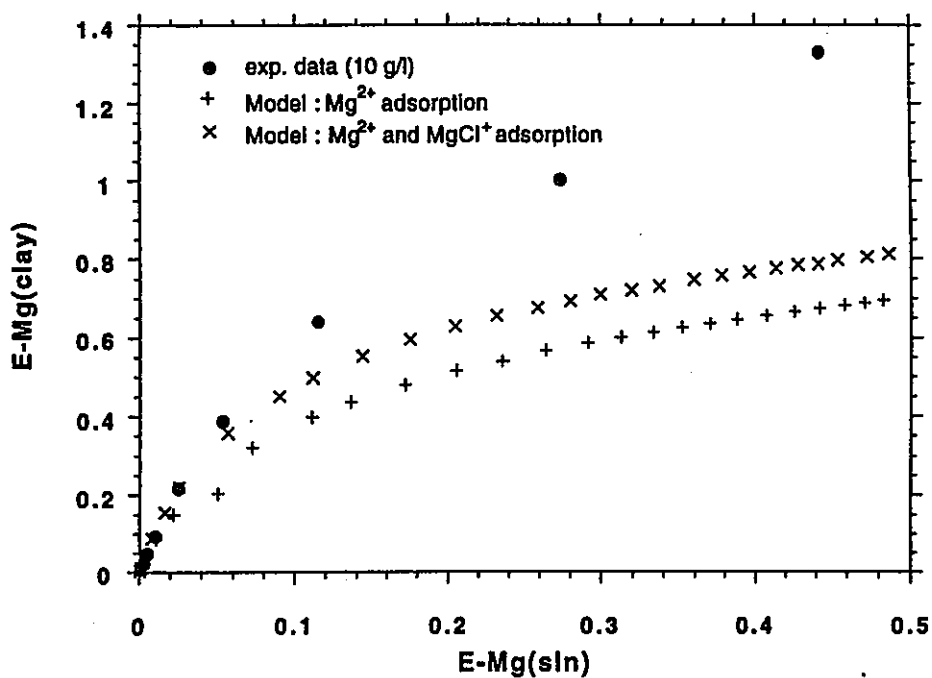


Fig. 3.1.1(3) Equivalent fraction of Mg²⁺ between aqueous and solid phase
(Mg²⁺+Na-smectite system) [Measured data in 1993]

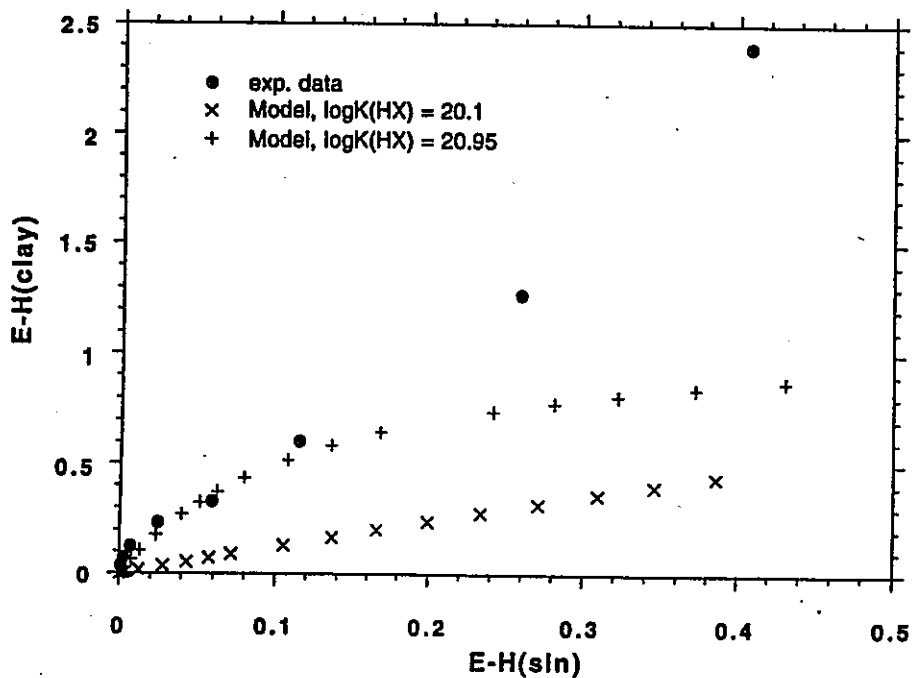


Fig. 3.1.1(4) Equivalent fraction of H⁺ between aqueous and solid phase
(H⁺+Na-smectite system) [Measured data in 1993]

3.2 固溶体モデルの調査

固溶体モデルの調査のうち、固相の活量係数の補正式について以下に示した。

(1) 固溶体の活量係数について

非理想固溶体中の活量係数は、以下の式で表される。

$$\ln f_{NAX} = a_1 X_{KX} + a_2 X_{KX}^2 + a_3 X_{KX}^3 + a_4 X_{KX}^4$$

$$\ln f_{XKX} = a_1 X_{NAX} + a_2 X_{NAX}^2 + a_3 X_{NAX}^3 + a_4 X_{NAX}^4$$

(2) 正則溶液モデル

合金に適用される正則溶液モデルを適用すると、活量係数は以下の式で表される。

(a) 正則溶液モデル (2元系)

$$RT \ln \lambda_1 = A X_2^2 = A (1 - X_1)^2$$

$$RT \ln \lambda_2 = A X_1^2 = A (1 - X_2)^2$$

(b) 正則溶液モデル (3元系)

$$RT \ln \lambda_1 = A_{12} X_2^2 + A_{13} X_3^2 + X_2 X_3 (A_{12} - A_{23} + A_{13})$$

$$RT \ln \lambda_2 = A_{23} X_3^2 + A_{12} X_1^2 + X_1 X_3 (A_{12} - A_{23} - A_{13})$$

$$RT \ln \lambda_3 = A_{13} X_1^2 + A_{23} X_2^2 + X_1 X_2 (-A_{12} + A_{23} + A_{13})$$

第4章 ベントナイト中での実効拡散係数の測定

本年度は、緩衝材中での核種の拡散係数データ整備の一環として、ウランおよびアメリカシウムを対象とし、ベントナイト中での実効拡散係数データを取得した。

4.1 拡散係数の定義

4.1.1 拡散係数の種類

平成4年度までの研究で検討したように、性能評価上必要となる緩衝材中の拡散係数は、核種の放出の段階に応じて以下の2種類に大別される。

(a)見かけの拡散係数

ベントナイト中での拡散が非定常の段階の拡散係数で、微視的には次式のように表現される。

$$D_a = \frac{(\varepsilon_o + \varepsilon_d) \delta_D}{(\varepsilon_o + \varepsilon_d) + (1 - \varepsilon_o - \varepsilon_d - \varepsilon_m) \rho K_d} \frac{D_p}{\tau^2} \quad (4.1.1)$$

ここで、

ε_o :	実効空隙率	δ_D :	狭窄性
ε_d :	デッドエンド空隙率	ρ :	緩衝材密度
ε_m :	マイクロ空隙率	K_d :	核種の分配係数
		τ :	振じれ率
		D_p :	空隙水中の拡散係数

(b)実効拡散係数

ベントナイト中での核種の拡散が定常段階の拡散係数で、微視的には次式のように示される。

$$D_e = \frac{\varepsilon_o \delta_D D_p}{\tau^2} \quad (4.1.2)$$

空隙水中の拡散係数を別にすれば、見掛けの拡散係数には有効空隙、デッドエンド空隙、マイクロ空隙、振じれ率および吸着の効果が考慮されており、一方、実効拡散係数は有効空隙と振じれ率により支配される。

4.1.2 実効拡散係数測定のご概念

本試験研究において取得を目的としているのは4.1.1で示した拡散係数のうち、実効拡散係数である。本試験では、定常拡散試験法(Through-diffusion法)を用い、実効拡散係数を測定した。

定常拡散試験法のご基本的な概念を図4.1.1に示す。試料を挟んで両側に溶液槽を設け、一方の槽には測定対象とするトレーサ元素を比較的高い濃度で調製した溶液を満たす。他方の槽にはトレーサ元素を含まないこと以外は、もう一方の槽と同じ条件で調製された溶液を満たす。このとき、トレーサ元素は高濃度側の槽から低濃度側の槽へ拡散する。定常状態においては、試料中のトレーサ元素の濃度勾配が直線的になる。定常状態が達成された状態での低濃度側の槽へ破過するトレーサのフラックスから4.1.3式に示すフィックの法則を用い、実効拡散係数は算出される。

$$F = -D_e \frac{dC}{dx} = D_e \frac{C_0}{L} \quad (4.1.3)$$

- D_e : 実効拡散係数
- F : 拡散フラックス
- C : トレーサ元素濃度
- C₀ : 高濃度側槽中トレーサ元素濃度
- L : 試料厚み

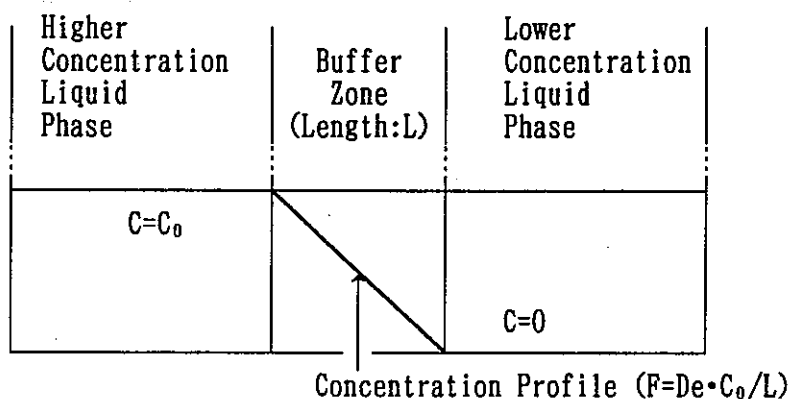


Fig. 4.1.1 Conceptual concentration profile in steady-state diffusion experiment.

4.2 ベントナイト中でのウランの実効拡散係数測定

4.2.1 試験内容

本年度は、ベントナイト密度をパラメータとして、定常拡散試験による実効拡散係数の測定を実施した。表4.2.1に、定常拡散試験を実施したベントナイトの乾燥充填密度および試験件数を示す。ベントナイトの実効拡散係数の決定には、解析上、試験装置に組み込まれているフィルタのみの実効拡散係数も必要となる。フィルタのみの定常拡散試験も含め、1密度あたり、定常拡散試験を2件行った。

Table 4.2.1 Dry density of bentonite and the number of times of Uranium diffusion experiments.

乾燥密度 (g/cm ³)	0.4	0.8	1.4	2.0
試験数*	1 (+1)	1 (+1)	1 (+1)	1 (+1)

* () 内はフィルタの定常拡散試験数である

ウランの定常拡散試験は、基本的には1990年度に実施したウランの定常拡散試験の方法に準拠し実施した。前回実施した定常拡散試験と比較し、変更した点および変更理由を表4.2.2に示す。

Table 4.2.2 Improvement point of steady-state diffusion experiment method.

変更点	変更理由
高濃度側リザーバタンクを排除した。	リザーバタンクを設置し、溶液を循環させることにより、低濃度側リザーバとの間に圧力差が生じ透水が起こる可能性があるため。
溶液中のウランの濃度測定を従来の放射線測定から蛍光光度法にした。	劣化ウランは比放射能が低く、放射線測定の精度が問題となる。今回はより精度の高い蛍光光度法による濃度測定を実施した。

以下に、試験条件および具体的試験方法を示す。

(1)試験条件

ベントナイト中でのウランの定常拡散試験を実施した試験条件を表4.2.3 にまとめる。なお、フィルタのみの定常拡散試験は、ベントナイト中の定常拡散試験からベントナイトを抜いた状態、すなわちフィルタ2枚を重ねた状態で実施した。

Table 4.2.3 Conditions of steady-state diffusion experiment of Uranium.

項目	試験条件
試験方法	定常拡散試験(Through-diffusion法)
試験媒体	ベントナイト: クニゲルV1
試料サイズ	φ20×1 mm
フィルタ	φ20×1 mmステンレス製焼結フィルタ
試料充填密度	0.4 ~2.0 g/cm ³
拡散核種	U (depleted)
試験溶液	ベントナイト模擬空隙水
試験温度	室温
雰囲気	大気雰囲気
試験期間	約40~80日

(2)ベントナイト試料

ベントナイト試料には粒度を0.042 ~0.074 μm に調整したクニミネ工業(株)製クニゲルV1を用いた。クニゲルV1の化学組成及び構成鉱物の分析結果を表4.2.4 および表4.2.5 にそれぞれ示す。含有鉱物及び分析結果から分かるように、主な構成鉱物はモンモリロナイトと石英である。

(3)試験核種

ウランの実効拡散係数を測定するため、定常拡散試験にはトレーサとして劣化ウラン(初期化学形UO₂(NO₃)₂)を使用した。

Table 4.2.4 Chemical composition of Kunigeru-VI

Chemical component	(weight-%)
SiO ₂	70.2
Al ₂ O ₃	14.2
Fe ₂ O ₃	2.5
CaO	2.0
MgO	2.2
Na ₂ O	2.5
K ₂ O	0.2
Ignition loss	4.6

Table 4.2.5 Mineral components of Kunigeru-VI

Mineral component	weight-%
montmorillonite	50 ~55
quartz	30 ~35
feldspar	5 ~10
calcite	1 ~ 3
others	0 ~ 1

(4)試験手順

以下に詳細な試験手順を示す。

①試験装置

試験に用いた装置の概念図を図 4.2.1に示す。試料は、装置中央部に正対して配置された2枚のフィルターにより保持されている。フィルタはフィルタホルダにより拘束され、これらにより圧密したベントナイトの膨潤を抑制している。ベントナイトは、フィルターホルダに開けられた孔を通して両リザーバ中の模擬空隙水と接触しており、膨潤はできないものの湿潤は可能な状態である。フィルターホルダの孔は、1989年度の研究成果を受けて、トレーサの拡散現象に影響しないように合計21個が配置されている。試験を通じて2枚のフィルター及び試験装置の組合せは固定した。また、両リザーバの容量はいずれも 100mlである。

②試料の充填

粒度を 200~350mesh (0.042~0.074mm)に調整したクニゲルV 1を、図 4.2.2に示す充填用治具を用い試料ホルダに充填した。試料の形状は2.0cm ϕ × 厚さ0.1cmとした。充填に際しては、所定の乾燥密度が得られるように秤量した試料をシリンダと試料ホルダ内に投入し、静かにパンチをのせて油圧プレスで加圧・成形した。

③模擬空隙水の作成

模擬空隙水の組成は、種々の固液比で取得したベントナイトと平衡にある溶液の組成から外挿的に求めたものである。本定常拡散試験における模擬空隙水の組成を表4.2.6に示す。

Table 4.2.6 Chemical composition of synthetic pore water for Kunigeru VI.

充填密度 (g/cm ³)	Na ⁺ (mol/l)	Cl ⁻ (mol/l)	SO ₄ ²⁻ (mol/l)
0.4	2.9×10 ⁻²	3.0×10 ⁻⁴	7.8×10 ⁻³
1.0	7.8×10 ⁻²	1.1×10 ⁻³	2.7×10 ⁻²
1.4	1.3×10 ⁻¹	2.1×10 ⁻³	5.0×10 ⁻²
2.0	2.9×10 ⁻¹	6.0×10 ⁻³	1.4×10 ⁻¹

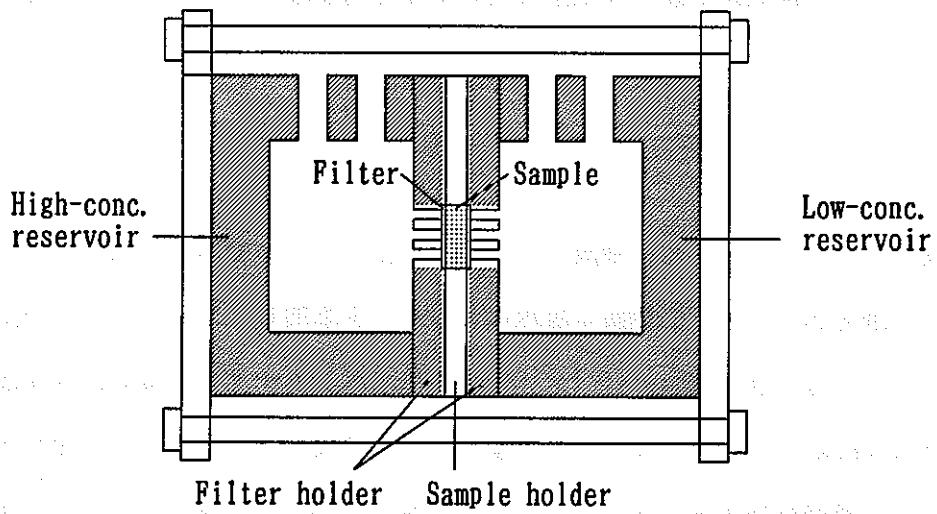


Fig. 4.2.1 Schematic drawing of apparatus for steady-state diffusion test.

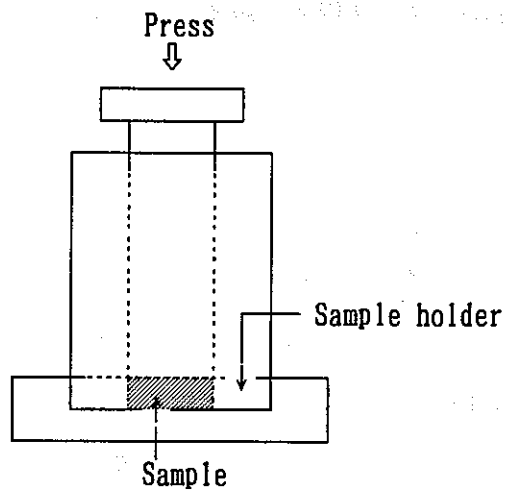


Fig. 4.2.2 Schematic drawing of apparatus for compressing sample.

④試料の脱気・膨潤

試料を充填した試料ホルダを図 4.2.1 に示した試験装置に組み込み、高濃度側、低濃度側の両リザーバを、③で調製した模擬空隙水で満たした。試験装置全体を真空デシケータに入れ、真空に引いた状態で30分間保持することにより試料を脱気した。このとき、模擬空隙水の突沸を防ぐために脱気はロータリポンプを用い、緩やかに行なった。脱気終了後、大気圧に戻して3日間放置し、ベントナイトを膨潤させた。

⑤トレーサの添加

試験に用いたトレーサは、硝酸ウラニル（劣化ウラン）である。試料を膨潤させた後、高濃度側リザーバの模擬空隙水にトレーサを添加し、フィルタの実効拡散係数測定の際はウラン20ppm ($2.1 \times 10^{-4} \text{ mol/l}$)、ベントナイトの実効拡散係数測定の際は50ppm ($5.3 \times 10^{-4} \text{ mol/l}$) に調整した。その後、スターラにより速やかに両リザーバの模擬空隙水を攪拌した。十分に攪拌した時点で、両リザーバから溶液を採取し、初期濃度を測定した。

⑦サンプリング

リザーバ中の濃度測定は、高、低リザーバ中の両溶液を同時に採取し、サンプリング溶液の濃度を測定することにより実施した。サンプリングは、濃度変化を勘案しつつ、1日1回から週1回程度の頻度で行った。1回のサンプリング量は0.4 ml とした。

⑧濃度測定

ウランの濃度測定は蛍光光度法により行った。分析手順を以下に示す。

- 1) 白金皿にサンプリング溶液をとり、蒸発乾固させる。
- 2) 乾固させた皿に、蛍光剤である炭酸ナトリウム、炭酸カリウム、フッ化カリウム、フッ化リチウムの混合物を所定量とり、加熱融解させウランと混合する。
- 3) 室温で放置冷却し試料を固める。
- 4) 試料中でのウランの量を蛍光光度計にて測定する。

⑨高および低濃度リザーバの液調整

定常拡散試験においては、高、低濃度両リザーバ中の濃度を一定に保つ必要がある。このため、高濃度側の濃度が減少した場合はトレーサを添加して一定とし、低濃度側の濃度についても、高濃度側の濃度の1割を越えないように溶液を交換した。またサンプリングにともなうリザーバ液量の減少を考慮し、総量が95mlとなったところで、液量を100mlに戻すこととした。

⑩試験の終了

トレーサ濃度の変化率がほぼ一定となったことを確認した時点で、ベントナイト中の拡散によるフラックスが定常状態に達したと判断し、試験を終了した。試験には、フィルタの拡散試験は1週間程度、ベントナイト試料の拡散試験では40～80日程度の期間を要した。

4.2.2 解析方法

(1)実効拡散係数の解析方法

低濃度側へ単位時間あたり放出されるトレーサ量を $F(t)$ とし、これが定常に達した時の値を F_0 、供試体試料厚さを L 、断面積を S とすると、実効拡散係数 De はフィックの法則より次のような関係で表される。

$$F_0 = SDe \frac{\partial C}{\partial x} = S De \frac{C_0}{L} \quad (4.2.1)$$

また、 $F(t)$ を $t=0 \rightarrow t$ まで積分した量を $Q(t)$ とすると、 $Q(t)$ は次式で表される。

$$\frac{Q(t)}{SLC_0} = \frac{De t}{L^2} - \frac{\alpha}{6} - \frac{2\alpha}{\pi^2} \sum_{n=1}^{\infty} \frac{(-1)^n}{n^2} \exp \left[-\frac{De n^2 \pi^2 t}{L^2 \alpha} \right] \quad (4.2.2)$$

$Q(t)$:積算通過量

α :収着容量

$$= \varepsilon + \rho (1 - \varepsilon) Kd$$

ε :空隙率

ρ :媒体の真密度 (g/cm^3)

Kd :分配係数 (ml/g)

4.2.2 式において $t \rightarrow$ 無限大とおくことにより、定常状態の積算通過量 $Q(t)$ は、次のように近似される。

$$\frac{Q(t)}{SLC_0} = \frac{De t}{L^2} - \frac{\alpha}{6} \quad (4.2.3)$$

4.2.3 式より、 $Q(t)$ を t に対してプロットすれば、 t に対する1 次関数に漸近し、 De は決定される。

(2)フィルタの補正

図4.2.1 の試験体系からも示されるように、高濃度側から低濃度側への拡散はフィルタを介している。ベントナイトの定常拡散試験において取得された実効拡散係数は、別途実施し取得されたフィルタの実効拡散係数を用い、次式により補正を行った。

$$De_r = \frac{L_{ben}}{\frac{L_{total}}{De} - \frac{2 \times L_{fil}}{De_{fil}}} \quad (4.2.4)$$

De_r : ベントナイト中での補正後の実効拡散係数 (m^2/s)

De : 試験により取得されたベントナイト中での実効拡散係数 (m^2/s)

De_{fil} : フィルタ中での実効拡散係数 (m^2/s)

L_{total} : ベントナイト部とフィルタ部を足したカラムの総長 (m)

L_{ben} : ベントナイト部のみの厚さ (m)

L_{fil} : フィルター一枚の厚さ (m)

4.2.3 ウランの定常拡散試験結果

各ベントナイト密度におけるフィルタおよびベントナイト中での定常拡散試験の結果得られたウランの積算通過量の経時変化を図4.2.3～9に示す。ページ上段に示されるのがフィルタ中の定常拡散試験結果、下段に示されるのがベントナイト中での定常拡散試験結果得られたグラフである。

フィルタ中での定常拡散試験およびベントナイト中での定常拡散試験のいずれも、試験開始後100時間以降は、積算通過量が直線的に増加しており、試験は定常に達したものと推察された。図4.2.6に示される乾燥密度 1.4g/cm^3 でのベントナイト中でのウランの定常拡散試験におけるウランの積算通過量の経時変化については、600～1000時間の間は、ほとんど破過が見られなかった。この現象に対する原因は不明であるが、試験はその後再び定常状態に達しており、実効拡散係数の解析においては問題はなかった。

解析の結果得られたベントナイト中でのウランの実効拡散係数を、1990年度に取得されたウランの実効拡散係数とともに表4.2.7に示す。傾向として、乾燥密度の増加とともに実効拡散係数は減少した。

なお、本試験結果により取得された積算通過量の経時変化グラフは1990年年度の取得されたグラフより、データのばらつきが少ない。これはウランの分析方法等の試験方法を変更したためであると考えられる。ベントナイト密度 1.0 及び 2.0g/cm^3 中でのウランの実効拡散係数は、本年度のデータも1990年度の結果もほとんど変わりはないことから本試験は再現性があるものと判断される。

Table 4.2.7 Effective diffusivities of Uranium in compacted bentonite.

ベントナイト 乾燥充填密度 (g/cm^3)	実効拡散係数値 (m^2/s)			
	本年度の結果		1990年度の結果	
	フィルタ中	ベントナイト中	フィルタ中	ベントナイト中
0.4	7.9×10^{-11}	4.0×10^{-11}	—	—
1.0	5.8×10^{-11}	1.2×10^{-11}	3.7×10^{-11}	1.9×10^{-11}
1.4	6.6×10^{-11}	2.6×10^{-12}	—	—
2.0	5.8×10^{-11}	3.5×10^{-12}	3.7×10^{-11}	4.2×10^{-12}

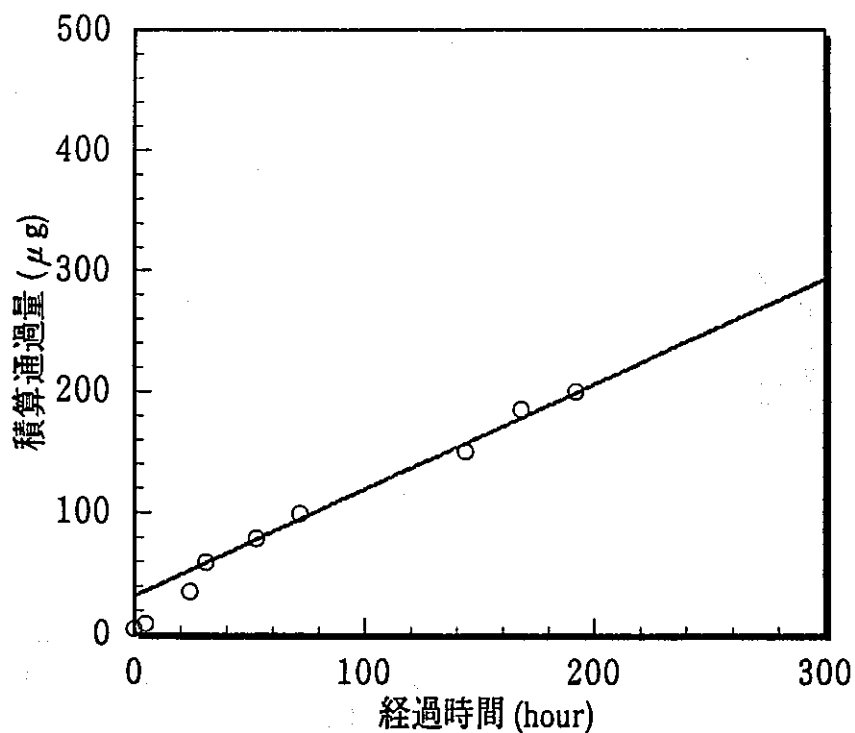


Fig. 4.2.3 Amounts of Uranium diffusing through *filters* as a function of time at dry density of 0.4 g/cm^3 .

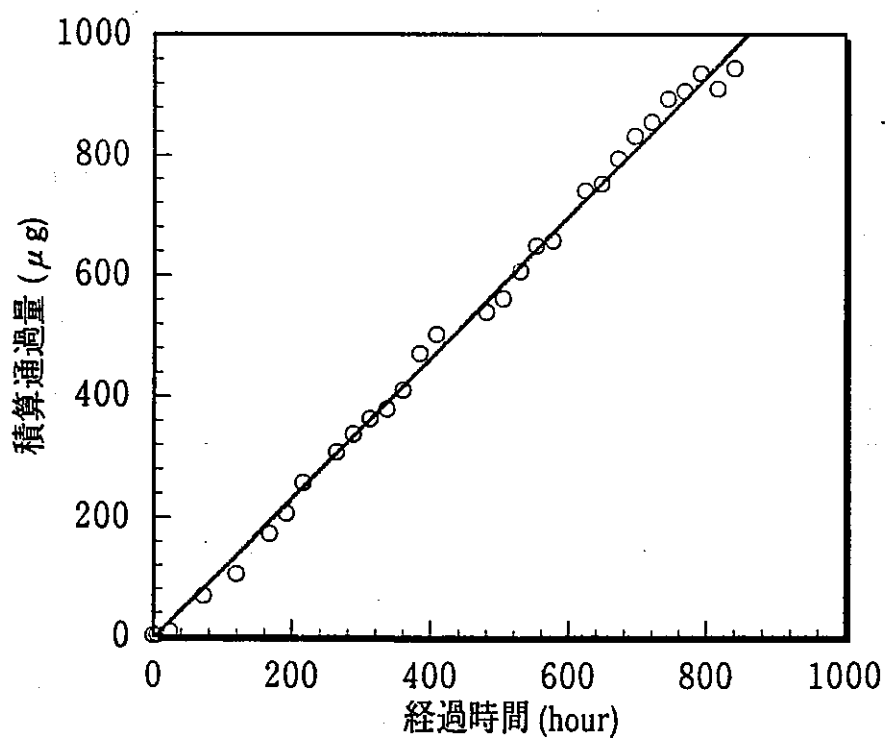


Fig. 4.2.4 Amounts of Uranium diffusing through *bentonite* as a function of time at dry density of 0.4 g/cm^3 .

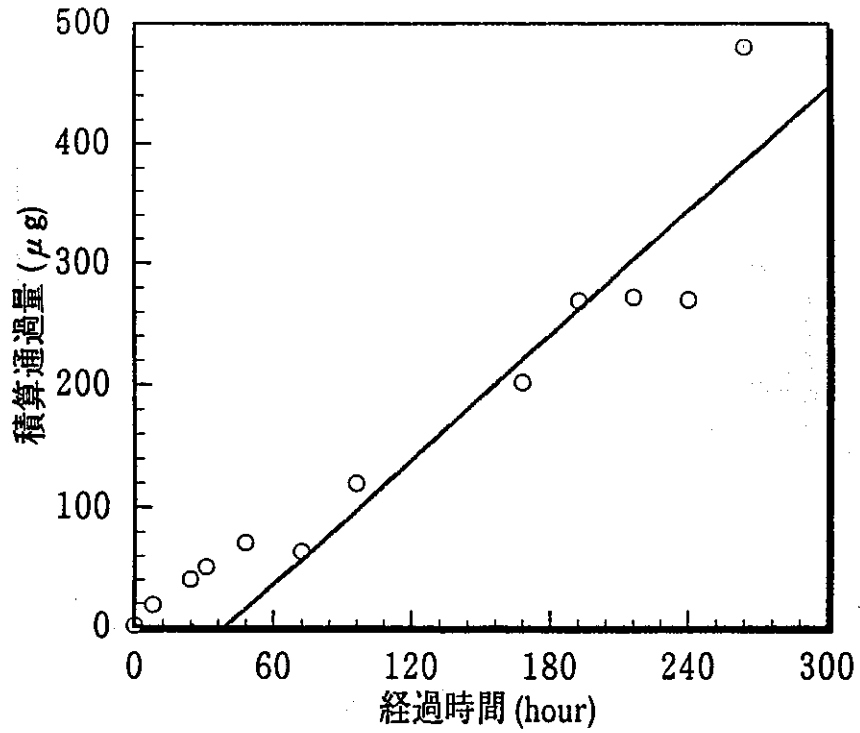


Fig. 4.2.5 Amounts of Uranium diffusing through *filters* as a function of time at dry density of 1.0 g/cm^3 .

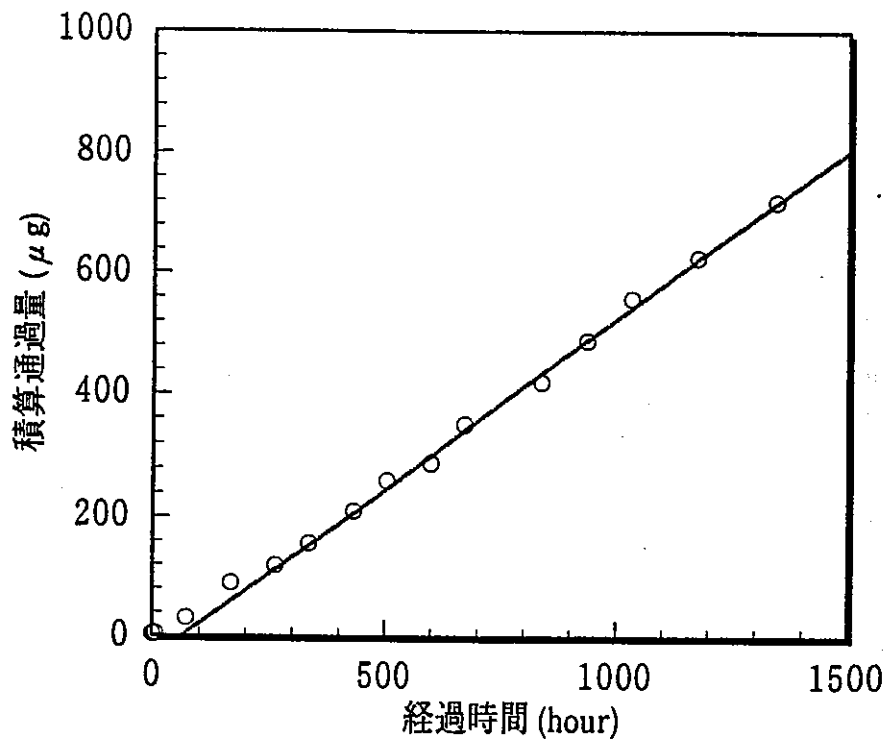


Fig. 4.2.6 Amounts of Uranium diffusing through *bentonite* as a function of time at dry density of 1.0 g/cm^3 .

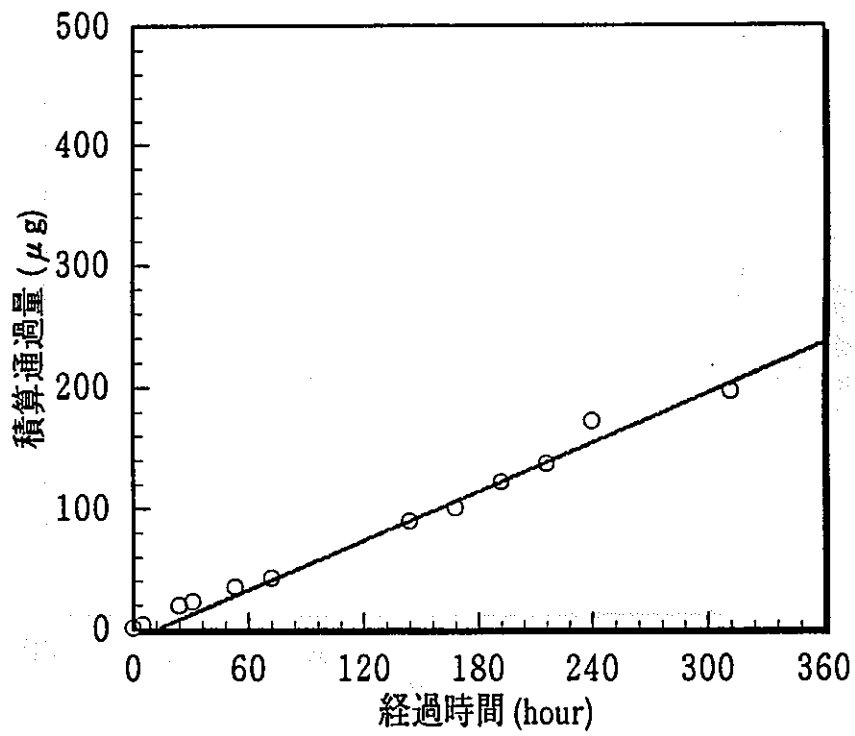


Fig. 4.2.7 Amounts of Uranium diffusing through *filters* as a function of time at dry density of 1.4 g/cm^3 .

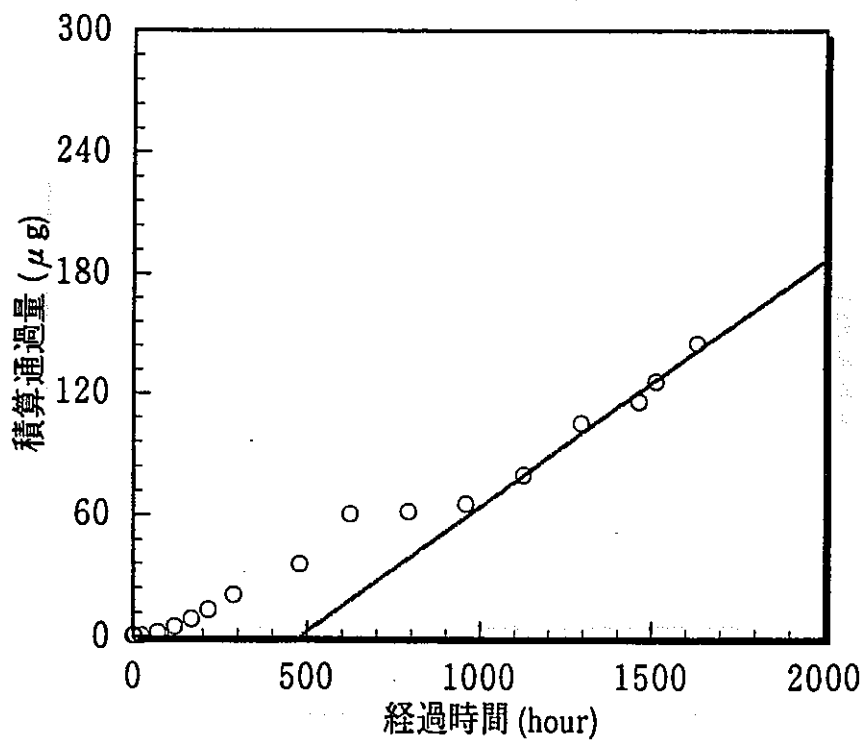


Fig. 4.2.8 Amounts of Uranium diffusing through *bentonite* as a function of time at dry density of 1.4 g/cm^3 .

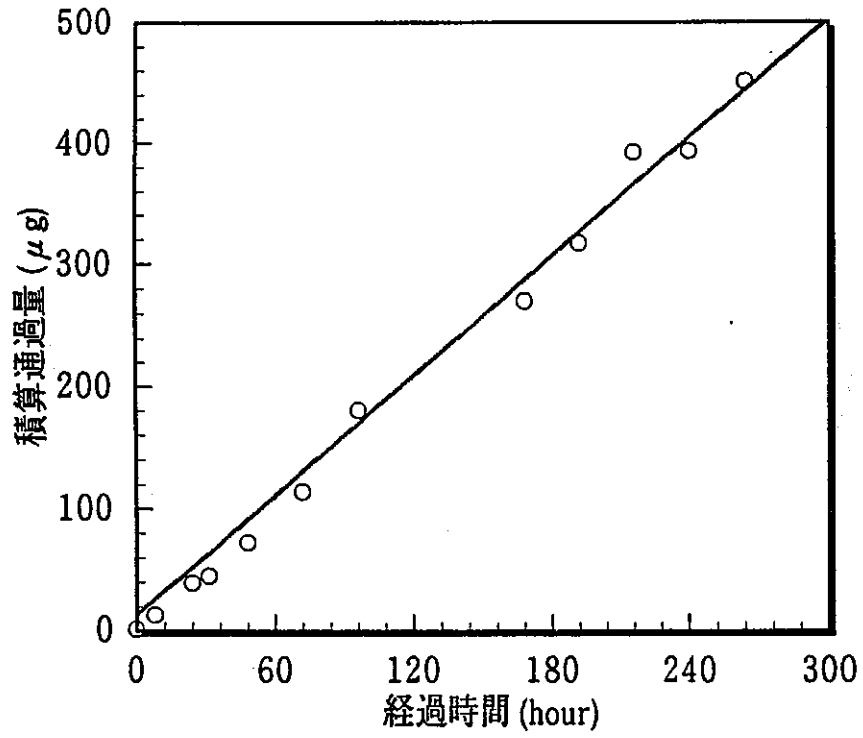


Fig. 4.2.9 Amounts of Uranium diffusing through *filters* as a function of time at dry density of 2.0 g/cm^3 .

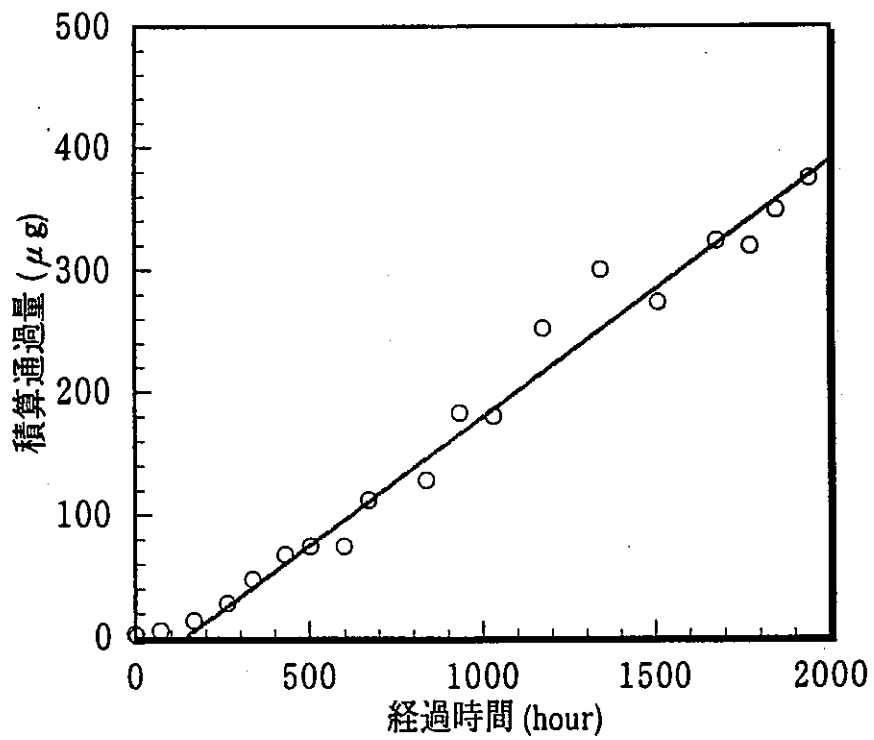


Fig. 4.2.10 Amounts of Uranium diffusing through *bentonite* as a function of time at dry density of 2.0 g/cm^3 .

4.3 ベントナイト中でのアメリカシウムの実効拡散係数測定

アメリカシウムの定常拡散試験は、前節のウランの定常拡散試験と同様、図4.2.1に示される装置を用い、ウランの定常拡散試験に準拠し試験を実施した。その結果、試験装置へのアメリカシウムの吸着が激しく、リザーバ内の濃度は経過時間とともに急激に減少し、試験を遂行することは現実的に不可能となった。そこで、アメリカシウムについては、吸着が起こらないような試験装置材料および雰囲気を設定することにより定常拡散試験を行い、実効拡散係数を取得した。

4.3.1 吸着を起こさない試験装置材料および雰囲気の設定

アメリカシウムの拡散試験装置への吸着が激しく、定常拡散試験を行うことが困難なため吸着の起こらない試験装置材料および雰囲気を選定することを目的として、以下のバッチ式の吸着試験および検討を実施した。

(1) 試験装置への吸着の確認

アメリカシウムが拡散試験装置に吸着していることの確認として、試験装置リザーバの材料であるアクリル及びフィルタホルダとフィルタの材料であるステンレスを対象にバッチ式吸着試験を行った。試験の液性はベントナイト充填密度 1.8g/cm^3 の模擬空隙水とした。試験では吸着量の経時変化を測定した。図4.3.1はアクリル及びステンレスへのアメリカシウムの吸着の経時変化を示したものである。アクリル及びステンレスへのアメリカシウムの吸着は時間とともに増加し、溶液中に存在するアメリカシウムはほとんど吸着してしまった。これにより定常拡散試験装置におけるアクリルおよびステンレスの両材料にアメリカシウムは吸着されたことを確認した。

(2) 担体および表面処理剤による吸着の低減化

アメリカシウムが吸着起こらないような雰囲気にするため、次の2つの方法でリザーバ容器の材料であるアクリルへの吸着の低減化を試みた。

① 担体の添加

アメリカシウムと同属元素のランタノイドで化学的挙動が類似していると考えられ

るユーロピウムを担体として添加し、アメリシウムの吸着を低減化を試みた。

②表面処理剤の使用

表面へのアメリシウムの吸着の低減化を図るため、界面活性剤（シリコナイズ）を容器表面に塗布した。

①の担体の添加については、ユーロピウム濃度が $1 \times 10^{-9} \text{ mol/l}$ になるように調整して添加したが、模擬空隙水の高pHの液性ではコロイド生成及び沈殿が生成したので $0.45 \mu\text{m}$ メンブランフィルタで濾過を行ったところ試験溶液中のユーロピウム濃度は $8.3 \times 10^{-7} \text{ mol/l}$ まで減少していた。

図4.3.2 に試験の結果を示す。いずれの方法においても若干の改善はみられたものの、模擬空隙水液性ではある程度の吸着は起ってしまい、長期に渡ると予想されるアメリシウムの定常拡散試験を実施することは困難であると判断した。

(3)試験装置の材質の変更

次に拡散試験装置の材質を変更し、アメリシウムの吸着を起こさないような材質を検討した。材質としては、市販の試験容器として入手がしやすく、拡散試験装置に加工するのが可能であると考えられるポリエチレン、ポリプロピレン、ポリスチレン、テフロンおよびガラスの5種類を選定した。試験溶液は模擬空隙水とした。これらの材質へのアメリシウムの吸着試験結果を図4.3.3 に示す。アメリシウムの吸着はポリエチレンが最も吸着が少なかったが、ある程度の吸着は起こっており、また時間経過とともに吸着は増加していたため、試験装置の材質の変更による改善は期待できないものと判断した。

(4)アメリシウムの化学形態の変更

(3)までの検討で、模擬空隙水中でのアメリシウムの容器への吸着は改善することが困難であることがわかったため、ここでは模擬空隙水中のアメリシウムの化学形態が、吸着の原因となっているものと考え、アメリシウムそのものの化学形を変化させ吸着の低減を試みた。

模擬空隙中ではpHが高く、炭酸イオン濃度も高いのでアメリシウムの化学形は価数

の多い陰イオンであると考えられる。よってこれとは対象的な陽イオンとなる領域までpHを下げ、吸着挙動に変化があるかを確認した。図4.3.4 に酸性雰囲気(pH2)でのアクリルおよびステンレスへのアメリシウム(III)の吸着試験結果を示す。酸性の雰囲気ではアクリルおよびステンレスへの吸着は起こっていない。これは、pH2の酸性雰囲気ではアメリシウムの化学形は、図4.3.5 に示すグラフから推察されるように+3価の化学形態に変化しており、このことが原因となっているためであると考えられる。以上のように、試験溶液をアルカリ性雰囲気から酸性雰囲気に変更することにより、アメリシウムの化学形が変化し、アクリルおよびステンレスへの吸着はほとんどなくなることが判明した。

表4.3.1 に吸着試験の結果をまとめる。この結果をふまえ、定常拡散試験が実施可能な条件として、本年度のアメリシウムの定常拡散試験はAm(III)が支配的な化学形となるpH2の酸性雰囲気で行い、実効拡散係数を測定することとした。

Table 4.3.1 Results of the sorption tests for the purpose of decrease of Americium sorption on the equipment.

試験	結果
キャリアの添加	ある程度の吸着は起こり、定常拡散試験の実施は困難
表面処理	ある程度の吸着は起こり、定常拡散試験の実施は困難
装置材質の変更	模擬空隙水雰囲気ではいずれもある程度の吸着が起こり、定常拡散試験の実施は困難
試験雰囲気の変更	試験溶液の雰囲気を酸性にすることで、吸着は起こらないことが判明 ⇒ 定常拡散試験に適用

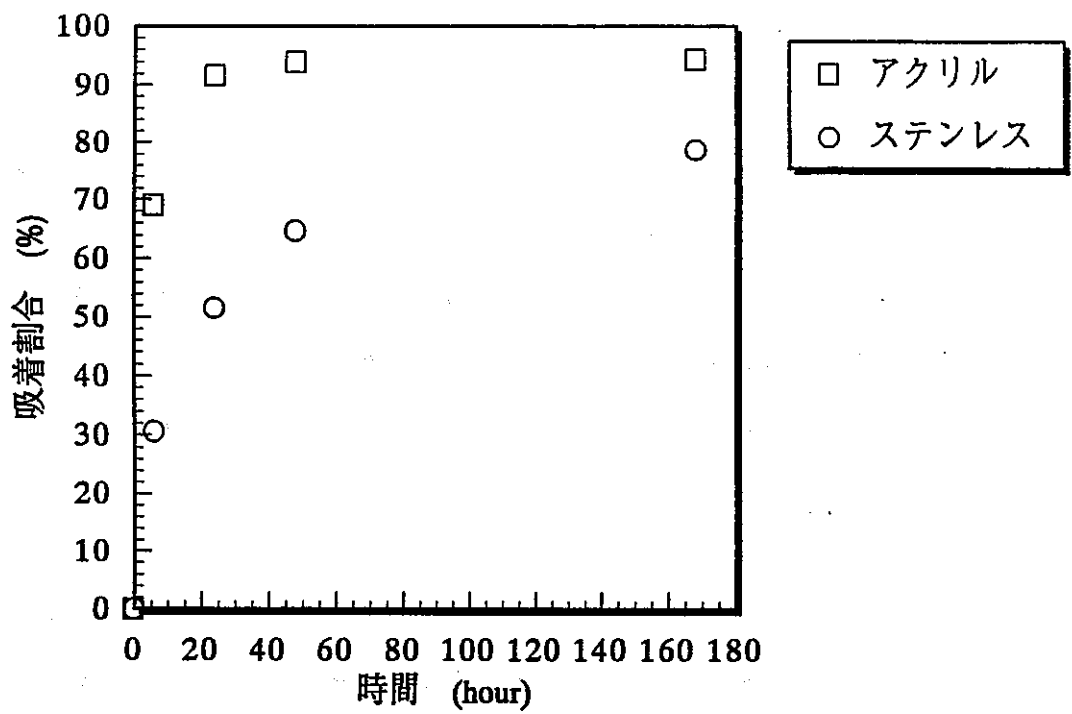


Fig. 4.3.1 Ratio of adsorption of Americium onto acrylic acid resin and stainless.

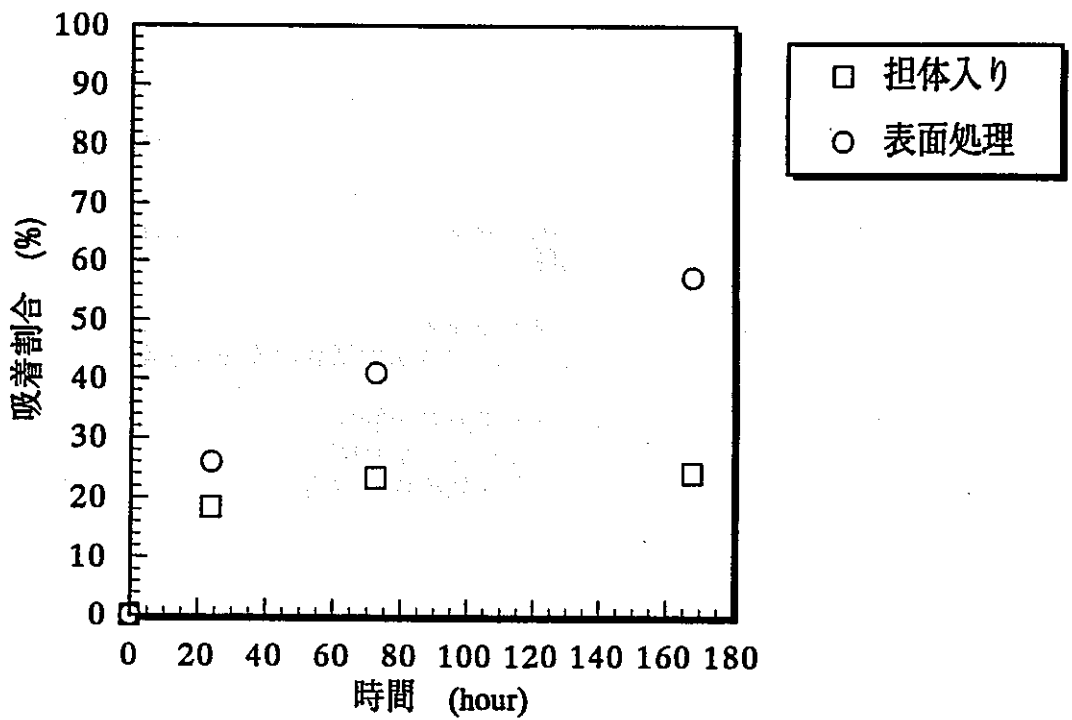


Fig. 4.3.2 Ratio of adsorption of Americium onto acrylic acid resin by adding Europium or by surface treatment.

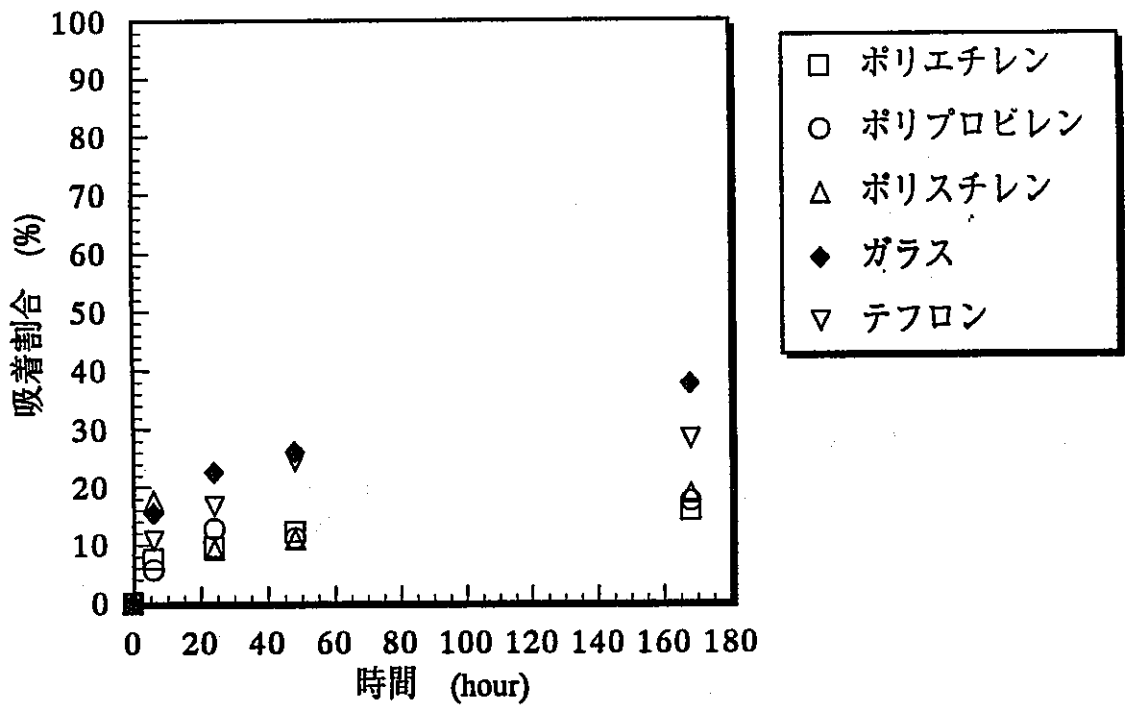


Fig. 4.3.3 Ratio of Americium adsorption onto various materials.

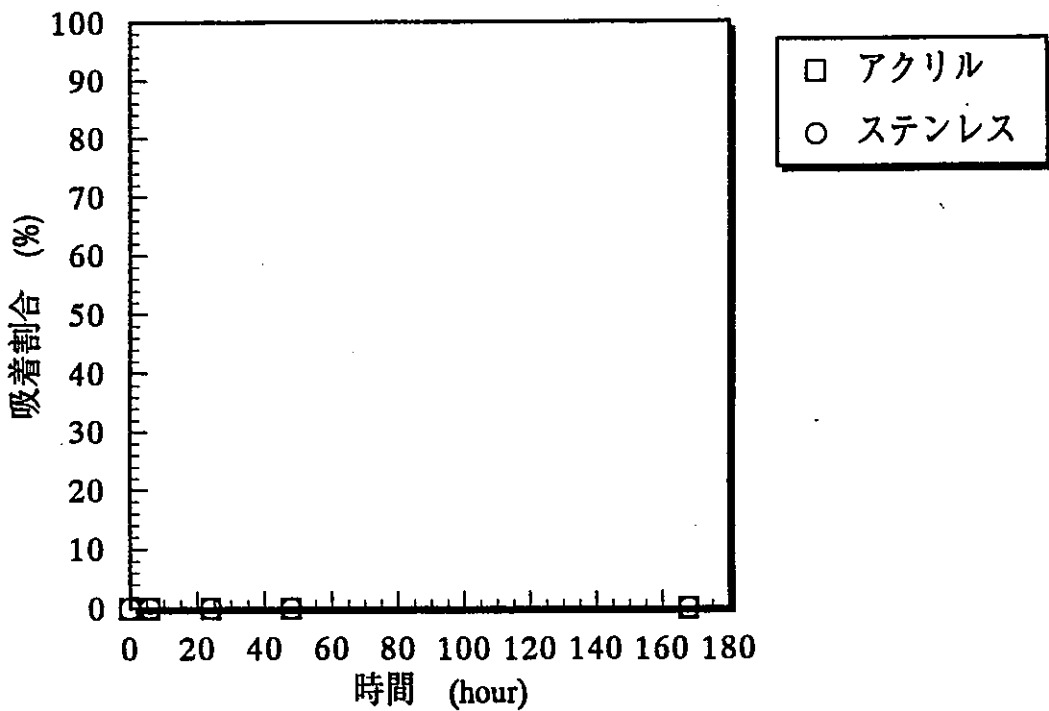


Fig. 4.3.4 Ratio of adsorption of Americium onto acrylic acid resin and stainless in pH2-HCl solution.

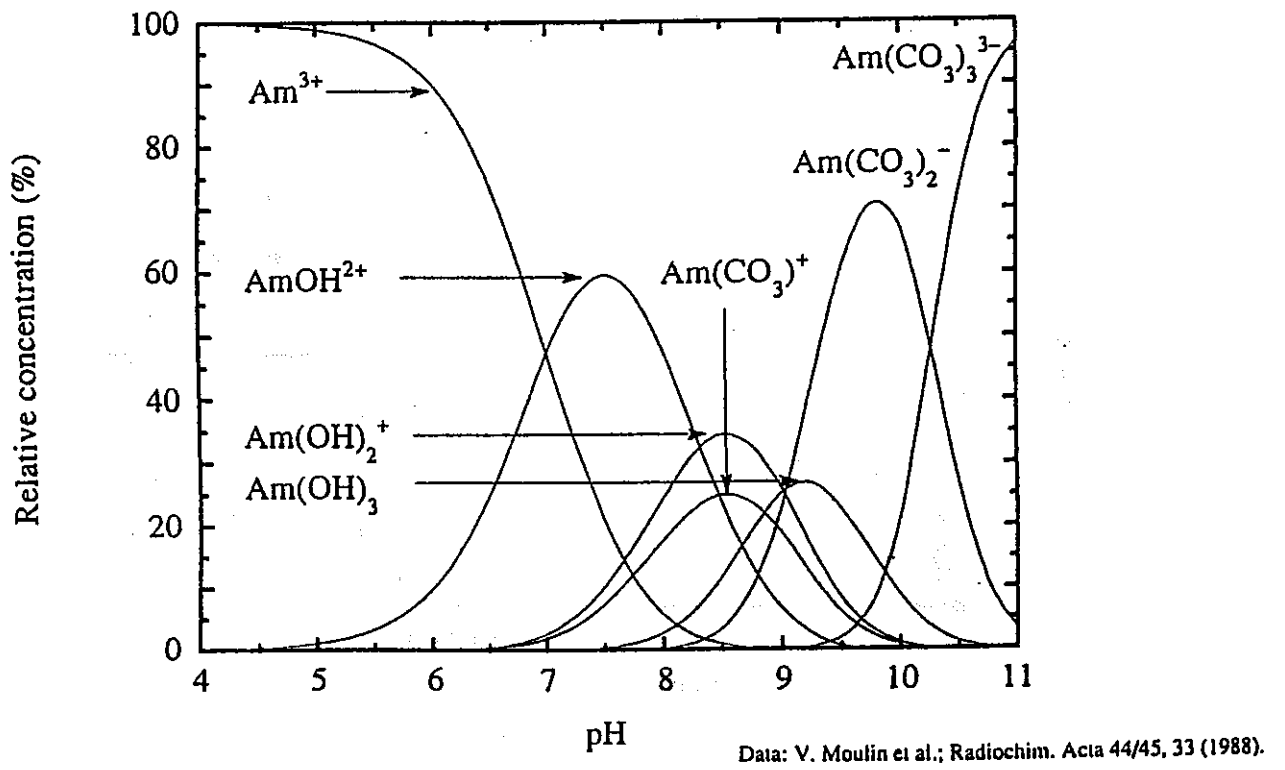


Fig. 4.3.5 Speciation of Americium in synthetic pore water. ¹⁾

4.3.2 定常拡散試験内容

本年度は、ベントナイト密度をパラメータとして、定常拡散試験により実効拡散係数を測定した。表4.3.2 に、定常拡散試験を実施したベントナイトの乾燥充填密度および試験件数を示す。フィルタのみの実効拡散係数を含め、1密度あたり、定常拡散試験を2件行った。

Table 4.3.2 Dry density of bentonite and the number of times of Americium diffusion experiments.

乾燥密度 (g/cm ³)	0.8	1.4	1.8
試験数*	1 (+1)	1 (+1)	1 (+1)

* ()内はフィルタの定常拡散試験数

以下に、試験条件および具体的試験方法を示す。

(1)試験条件

ベントナイト中でのアメリカシウム²⁴¹の定常拡散試験を実施した試験条件を表4.3.3 に示す。

Table 4.3.3 Conditions of steady-state diffusion experiment of Americium.

項目	試験条件
試験方法	定常拡散試験(Through-diffusion法)
試験媒体	ベントナイト: H型クニゲルV1
試料サイズ	φ20×1 mm
フィルタ	φ20×1 mmステンレス製焼結フィルタ
試料充填密度	0.8 ~ 1.8 g/cm ³
試験核種	Am-241
試験溶液	pH2 塩酸酸性溶液
試験温度	室温
雰囲気	大気雰囲気
試験期間	約100 ~130 日

(2)ベントナイト試料

試験を酸性雰囲気で行うため、試験試料としてはクニミネ工業製クニゲルV1を塩酸で処理し、H型としたクニゲルV1を用いた。

H型に処理した手順を以下に示す。

- ① 0.1N-HClとクニゲルV1を固液比10ml/gで懸濁させ50のろ紙でろ過する。この作業を繰り返し3回行った。各段回でのろ液中での Na^+ 、 K^+ 、 Mg^{2+} 、 Ca^{2+} の浸出濃度を分析した。分析結果を表4.3.1中に示す。
- ② 塩酸で処理を行った試料をイオン交換水（固液比10ml/g）で洗浄した。この際①同様に各浸出陽イオンを分析した。分析結果を表4.3.1中に示す。
- ③ 110℃で24時間乾燥させ、乾燥後粉碎し、試料粒径を200～350mesh(0.042～0.074 mm)に調整した。

表4.3.4に懸濁、濾過したのちの浸出イオン濃度を示す。最終的には、イオン交換水中での浸出イオンはほとんどなくなることから、酸処理後のベントナイトはほぼH型に変化したことがわかる。

Table 4.3.4 Concentration of leaching cation after treatments of bentonite with HCl.

	浸出濃度 (ppm)				
	Na^+	K^+	Mg^{2+}	Ca^{2+}	pH
1回目塩酸処理後	930	26.5	167	740	3.3
2回目塩酸処理後	185	9.2	66.8	267	1.1
3回目塩酸処理後	46.0	6.2	49.2	170	1.0
イオン交換水で処理後	8.0	1.4	1.9	6.9	2.0

(3)試験手順

試験の手順は、基本的にウランの定常拡散試験と同じである。試験手順を示すにあたって、特に留意する点のみを示す。

①試験装置

ウランの定常拡散試験と同様、図4.2.1に示す装置を用いた。

②試料の充填

ウランの定常拡散試験と同じく、粒度を調整したH型クニゲルV1を、治具を用いてカラムに充填した。充填した試料の形状は、ウランの場合と同様、2.0cm φ×0.1cmとした。

③試験溶液

試験装置を構成するアクリルおよびステンレス系材料に吸着が起こらないようにするため、試験溶液にはpH2の塩酸溶液を用いた。

④試料の脱気・膨潤

ウランの定常拡散試験と同じ手法で試料の脱気・膨潤を行なった。

⑤トレーサの添加

試験に用いたトレーサは、日本アイソトープ協会を通じてLMR I社より輸入したAm-241（製品番号 AM241-ELSA45）である。これを希釈して約160Bq/ml（計数値約10,000 cpm/ml）とし、試験に供した。

⑥濃度測定

サンプリングは0.5mlづつ行い、アメリカシウム濃度の濃度測定は液体シンチレーションカウンタによる放射線測定により実施した。

⑦その他

その他、高濃度側リザーバ、低濃度側リザーバの濃度及び溶液量調整は、ウランの定常拡散試験と同じ手法により行った。

4.3.3 アメリシウムの定常拡散試験結果

各ベントナイト密度におけるフィルタおよびベントナイト中での定常拡散試験の結果得られたウランの積算通過量の経時変化を図4.3.6～11に示す。ページ上段に示されるのがフィルタ中の定常拡散試験結果、下段に示されるのがベントナイト中での定常拡散試験の結果得られたグラフである。

フィルタ中での定常拡散試験は、試験開始後まもなく積算通過量が直線的に増加しており、試験が定常に達したものと思われる。また、ベントナイト中での定常拡散試験には、試験開始後約2000時間以降は、積算通過量がほぼ直線的に増加しているため、試験は定常に達したものと判断した。

4.2.3 式および4.2.4 式を用いて解析されたベントナイト中でのアメリシウムの実効拡散係数を表4.3.5 に示す。実効拡散係数はベントナイトの乾燥密度の増加とともに小さくなるという傾向を示した。

Table 4.3.5 Effective diffusivities of Americium in compacted bentonite.

ベントナイト 乾燥充填密度 (g/cm ³)	実効拡散係数値 (m ² /s)	
	フィルタ中	ベントナイト中
0.8	4.2 × 10 ⁻¹¹	7.4 × 10 ⁻¹¹
1.4	3.7 × 10 ⁻¹¹	5.2 × 10 ⁻¹¹
1.8	3.3 × 10 ⁻¹¹	1.8 × 10 ⁻¹¹

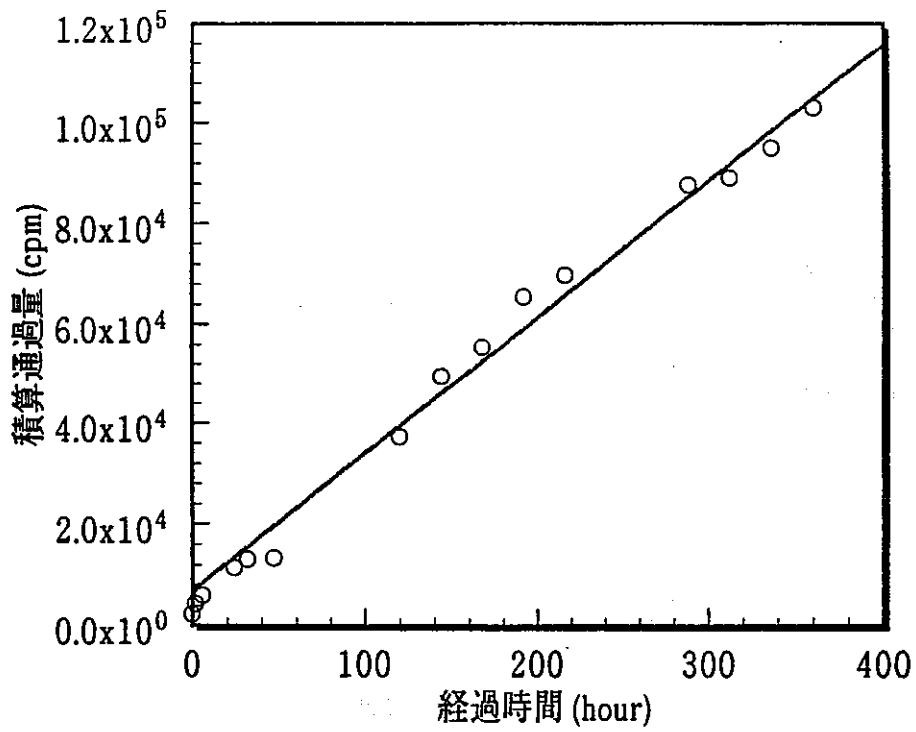


Fig. 4.3.6 Amounts of Americium diffusing through *filters* as a function of time at dry density of 0.8 g/cm^3 .

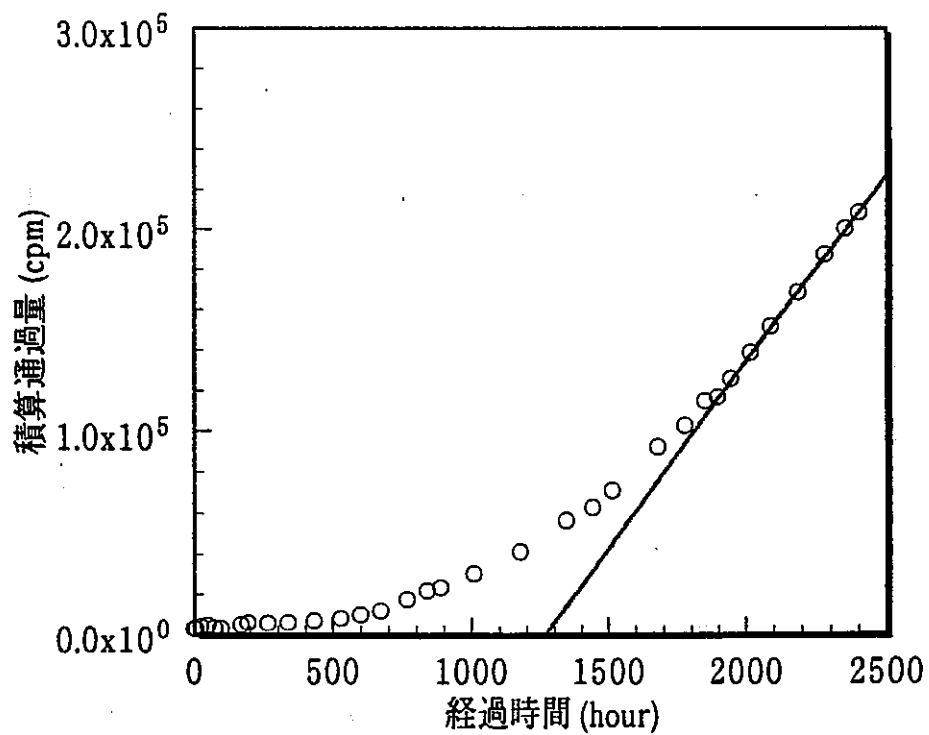


Fig. 4.3.7 Amounts of Americium diffusing through *bentonite* as a function of time at dry density of 0.8 g/cm^3 .

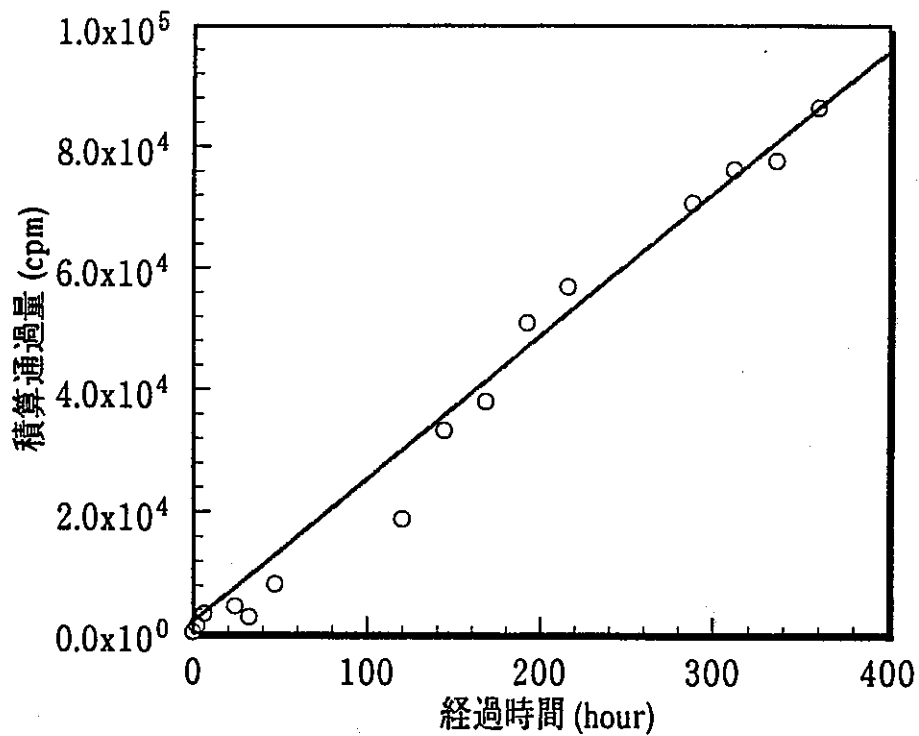


Fig. 4.3.8 Amounts of Americium diffusing through *filters* as a function of time at dry density of 1.4 g/cm^3 .

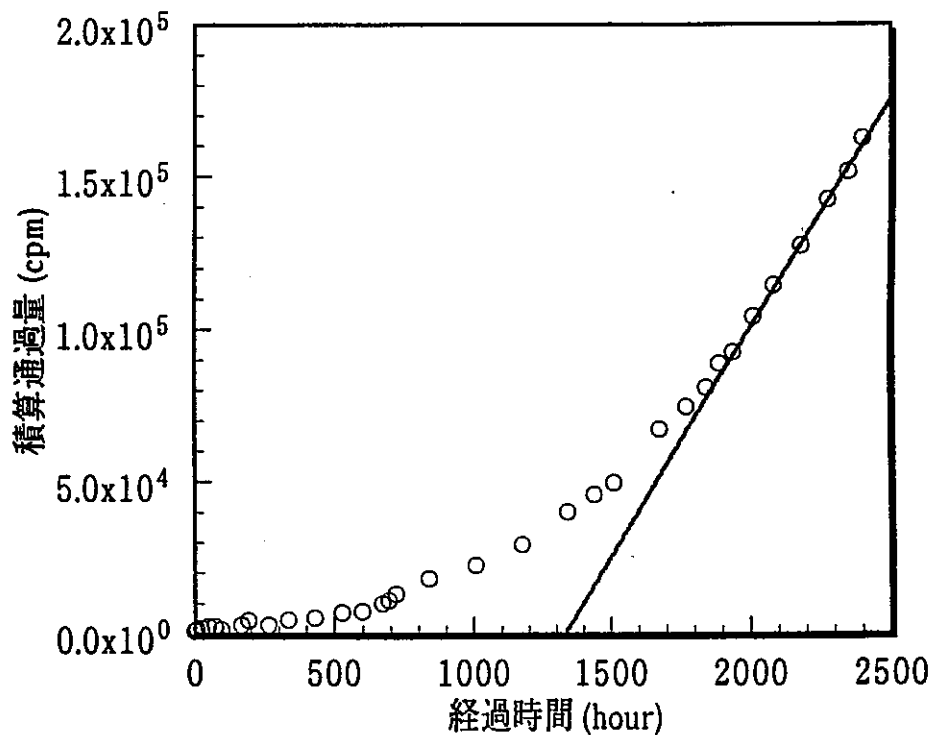


Fig. 4.3.9 Amounts of Americium diffusing through *bentonite* as a function of time at dry density of 1.4 g/cm^3 .

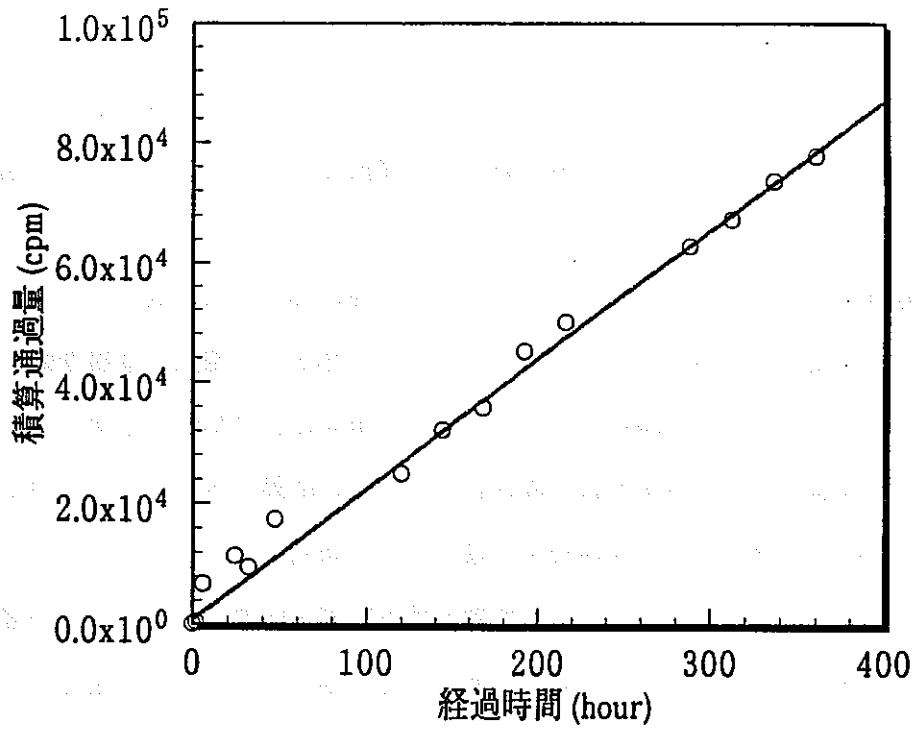


Fig. 4.3.10 Amounts of Americium diffusing through *filters* as a function of time at dry density of 1.8 g/cm^3 .

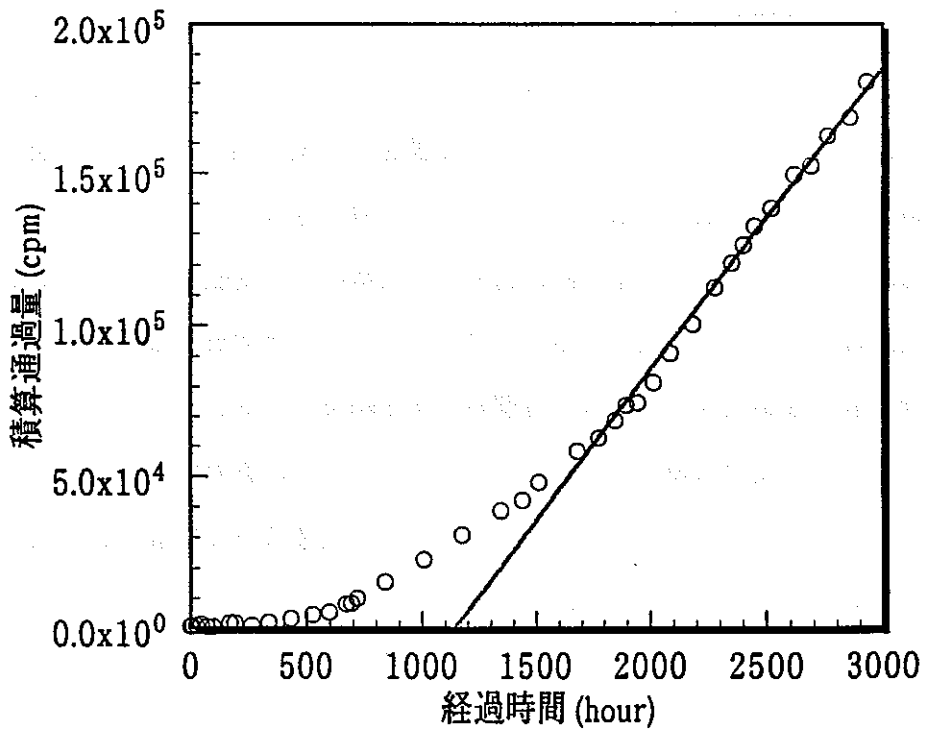


Fig. 4.3.11 Amounts of Americium diffusing through *bentonite* as a function of time at dry density of 1.8 g/cm^3 .

4.4 考察

クニゲルV1を試料として過去に本研究で取得した他核種の実効拡散係数と、本年度取得したウラン、アメリシウムの実効拡散係数を、充填密度に対してプロットし、図4.4.1に示す。

昨年度実施した研究では、ベントナイト中での核種の実効拡散係数は、その核種の荷電状態すなわち中性分子、陽イオンおよび陰イオンの形態から、電気二重層理論により評価されることを示した。この理論によれば、空隙中の電場および粘性の効果により、ベントナイト中での核種の実効拡散係数は評価される。評価の結果、ベントナイト中での核種の実効拡散係数には、陽イオン>中性分子>陰イオンの傾向があることが示された。

本年度のウランおよびアメリシウムの実効拡散係数測定結果を、空隙中での電氣的雰囲気の面から考察する。ウランの実効拡散係数は、他の陽イオンおよび中性分子と比較してオーダ的に小さい。これは、ウランはベントナイト中で炭酸塩系の陰イオン形態をとることが予想され、ベントナイト中ではアニオンイクスクルージョンにより電氣的反発を受けていることが原因であると考えられる。

一方、本研究で試験的に取得されたアメリシウムの実効拡散係数は、ウランにくらべ1桁程度大きい。アメリシウムの実効拡散係数測定には、H型ベントナイトを用い、また試験溶液もpH2としているため、ベントナイトの表面の荷電状態が異なり、普通のベントナイト中で取得された実効拡散係数とは、一概には比較できない。ただし、ベントナイトの表面の荷電が、ベントナイト骨格内部に起因する荷電により支配され、pHの変動による表面荷電の変動は少ないものと仮定すると、アメリシウムの化学形態は陽イオンであることから、実効拡散係数が大きいことは十分理解できる結果となる。

本研究における今後の課題としては、ベントナイト中での実効拡散係数の評価として、本年度取得したウランおよびアメリシウムを含めた各核種の実効拡散係数を電気二重層理論により定量的に評価することが挙げられる。

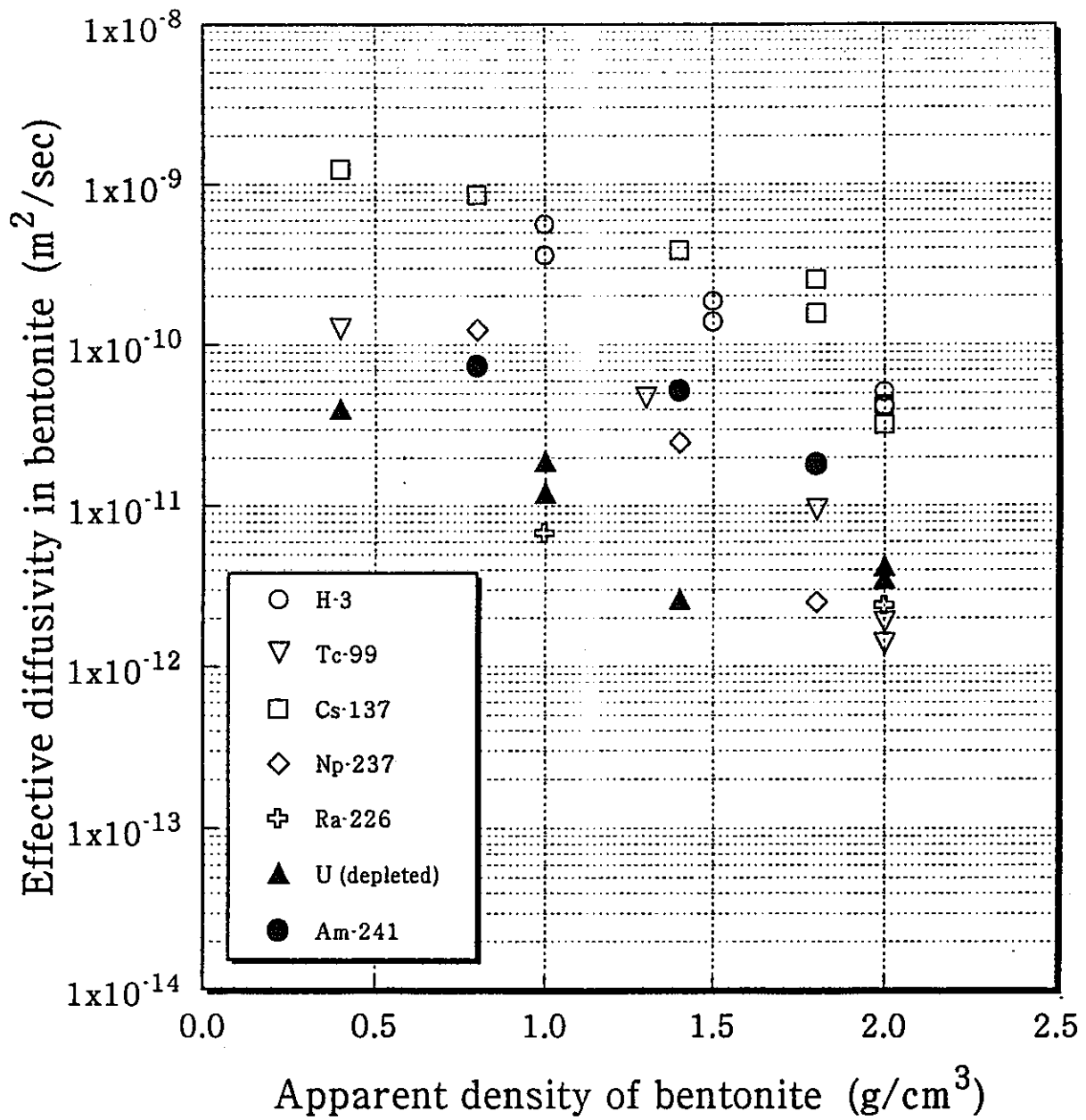


Fig. 4.4.1 Relation between apparent density of bentonite and effective diffusivities of nuclides.

参考文献)

- 1) 長崎晋也, 弥生研究会, p75, (平成5年3月)

卷末資料 1

Technical report

- (1) Thermodynamic modelling of ion exchange reaction at the Na-smectite/water interface.
- (2) Review of the purpose of solid solution models and their potential applicability in predictive geochemical modelling.

**Power Reactor and Nuclear Fuel Development
Corporation (PNC)**

Technical Report

**Review of the purpose of solid solution models and their
potential applicability in predictive geochemical modelling**

Hans Wanner

December 1993



Environmental

MBT Umwelttechnik AG

Vulkanstrasse 110

CH - 8048 Zürich

Abstract

The theory and application of solid solution models are presented and discussed. References are given that allow to follow the development, improvement and scientific discussions of different modelling approaches for solid solutions.

Laboratory experiments with clay minerals under natural environmental conditions can usually be sufficiently well described by using surface interaction models. In the long term, however, alteration of the smectite barrier in the near-field of a high-level nuclear waste repository cannot be excluded. Since the demonstration of safety of a nuclear waste repository requires defensible predictions over geological time scales, potential mineral dissolution/precipitation reactions involving the smectite matrix should therefore be considered.

Solid solution models allow a thermodynamic description of solids of variable composition. The solids are divided into components of constant composition (so-called "end-members") for which solubility products are estimated or derived from laboratory data. The stabilisation of a solid solution with respect to the free end-members is due to the energy of mixing. Deviation from ideality can hardly be modelled for solid solutions consisting of more than three end-members. A large number of end-members are needed to simulate the behaviour of natural clays.

Another field of application of solid solution models is the thermodynamic modelling of coprecipitation reactions. It is probable that the solubilities of radionuclides are not determined by pure, solubility-limiting solid phases, but rather by coprecipitation processes, i.e., by the removal of radionuclides from the solution and inclusion into the lattice of a precipitating bulk solid. This means that the isolated use of chemical speciation models may not be a realistic basis for the prediction of radionuclide mobility, but that coprecipitation processes should be considered and investigated.

It is recommended to use solid solution models to simulate slow, long-term alteration processes of the smectite structure. Surface interaction processes and short-term experiments are simulated best by using ion exchange and surface complexation models such as the Wanner model. It is therefore recommended to combine the solid solution model and the Wanner model to develop a powerful system for clay modelling, both for short-term and long-term processes.

1 Introduction

The existence of mixtures of solid phases is a well known and important fact in technology such as metallurgy and in science such as mineralogy and geology. In order to allow predictions of the behaviour of mixtures of solid phases under various conditions, it is necessary to establish a thermodynamic basis for the energetics and reactivities of such substances.

The reactions between solid and aqueous phases may be divided into two types: (1) reactions taking place on the surface of the solid phases, and (2) dissolution and precipitation reactions involving the solid matrix. Only kinetic considerations allow to distinguish between the two types of reaction. The first type includes reactions such as ion exchange and surface complexation which can be described using, e.g., the Wanner model. The second type can best be described by solid solution models, especially in the case of solids of complex composition such as clay minerals.

Mathematical treatment of the solid/water interactions of various mixed solids started about 25 years ago in the group of Helgeson, where the first theoretical computer model was developed for this purpose. The lack of data limited the practical use of the model at first. However, the great interest in modelling the formation and dissolution of clay minerals and the complex composition of clays was the reason for the need of computer programs to model such reactions. It became obvious that the compositions of clay minerals have to be considered as variable. Two ways had been chosen to take into account such variations in composition: (1) Clays are modelled as well defined compounds, characterised by means of a solubility product. (2) Clays are modelled as solid solutions of a number of mineral phases, and their composition changes continuously during the chemical evolution. In both approaches thermodynamic data are needed to model the dissolution and precipitation reactions of the thermodynamically defined constituents. The first approach was used by Tardy and Fritz (1974, 1976) and Fritz (1975), the second approach was used by Helgeson and Mackenzie (1970) for montmorillonite-illite systems. Tardy and Fritz (1981) concluded later that the first approach is limited in practice because it requires a very extensive data set to cover the whole range of chemical compositions of natural clays, while the second approach is more suitable for modelling the chemical evolution of natural systems. However, in the second approach one has to choose the so called "end-members", i.e., the pure minerals of which the natural system of interest is supposed to consist.

2 The solid solution model

2.1 General

A solid solution of n mineral phases is distinguished from a simple mixture of the same n minerals by the Gibbs energy of mixing, $\Delta_{\text{mix}}G$. The Gibbs energy of formation of a bulk phase containing m_j moles of each constituting mineral M_j is expressed as

mixture" of minerals, each mineral forms its own phase and is characterised only by its mole fraction.

In thermodynamic terms, each mineral (end-member) participating in a solid solution can be assigned a chemical potential, μ_j , of the form

$$\mu_j = RT \ln A_j = RT \ln (\lambda_j X_j) \quad (2)$$

with: A_j : activity of the end member, j, in the solid solution
 λ_j : activity coefficient of the end-member, j, in the solid solution
 X_j : mole fraction of the end-member, j, in the solid solution

The chemical potential, μ_j , has two terms:

$$\mu_j = RT \ln X_j + RT \ln \lambda_j \quad (3)$$

The first term represents the chemical potential in case of ideal mixing, where the activity coefficient is unity:

$$\lambda_j = 1, \quad \text{and} \quad A_j = X_j \quad (4)$$

The second term is called excess chemical potential and describes the energetical difference between the ideal and the non-ideal solid solution. It defines the activity coefficient of the end-member.

2.3 Mass action law

The equilibrium condition between an aqueous solution and a mineral, or end-member, of a solid solution, is written as follows:

$$K_j = \frac{Q_j}{A_j} = \frac{\prod_i [a_i]^{\alpha_{ij}}}{\lambda_j X_j} \quad (5)$$

with: a_i : activity of the aqueous species, i, in the aqueous solution
 α_{ij} : stoichiometric coefficient of the aqueous species, i, in the dissolution reaction of the mineral, j
 K_j : solubility product of the mineral, j
 Q_j : ion activity product of the mineral, j
 A_j , X_j and λ_j : already defined above

In the case of a pure mineral, the equilibrium with the aqueous phase is characterised exclusively by the composition of the aqueous phase, i.e., $K_j = Q_j$. On the other hand, the

$$\Delta_f G = \left(\sum_{j=1}^n m_j \Delta_f G_j \right) + \Delta_{\text{mix}} G \quad (1)$$

If the term $\Delta_{\text{mix}} G$ is negativ, then the bulk phase is more stable than the simple mixture of the same minerals. This means that the bulk phase can be stable under conditions where none of the constituting minerals (= end-members) are stable. This observation is of fundamental importance, e.g.:

- A magnesian calcite may be in equilibrium with aqueous solutions which are undersaturated with both calcite and magnesite.
- An aluminum smectite can be stable under conditions in which the constituting end-members, muscovite and pyrophyllite, are unstable.

A large number of theoretical studies have been devoted to the problem of solid solutions. Binary systems and the derivation of $\Delta_{\text{mix}} G$ have been described by Wagner, Mellgren and Westbrook (1952), Prigogine and Defay (1954), Saxena (1973), Kerrick and Darken (1975), Grover (1976), and Powell (1976). Experimental studies of the solubility of $(\text{Ca},\text{Mg})\text{CO}_3$, leading to a confirmation of the solid solution concept, were published, discussed and criticised by de Boer (1977), Thorstenson and Plummer (1977), Lafon (1978), Garrels and Wollast (1978), and Berner (1978). Meanwhile, a large number of studies have been published applying solid solution models to simulate the evolution of natural systems, presenting improved methods of deriving thermodynamic data of end-members, or reporting experimental studies that allow to improve the quality of the thermodynamic database: e.g., in chronological order: Tardy and Garrels (1974), Chen (1975), Nriagu (1975), Tardy and Garrels (1976, 1977), Pfeifer (1977), Helgeson et al. (1978), Mattigod and Sposito (1978), Stoessel (1979, 1981), Fritz (1981), Tardy and Fritz (1981), Garrels and Tardy (1982), Tardy (1982), Aagaard and Helgeson (1983), Fritz (1985), Fritz and Kam (1985), May et al. (1986), Sposito (1986), Tardy, Duplay and Fritz (1987), Tardy and Touret (1987), Duplay (1988), Clauer, Frappe and Fritz (1989), Crovisier et al. (1992), Michaux et al. (1992), Tardy and Duplay (1992), Ben Baccar and Fritz (1993), Jensen (1993). More references on specific subjects can be found in the publications mentioned.

2.2 Thermodynamic description

An *aqueous* solution is a mixture of pure water and dissolved compounds such as electrolytes, in which all the dissolved species are characterised by their molality and their activity. The molalities describe the mass balance, and the activities describe the mass action, or energetical balance, of the mixture. *Solid* solutions can be described in the same way: A solid solution is a "chemical mixture" of minerals in one single solid phase, in which all the minerals are characterised by their mole fraction and their activity. In contrast, in a "physical

description of the equilibrium of a solid solution with the aqueous phase requires the input of the composition of the solid phase as well. This means that, for a solid solution consisting of n end-members to be in equilibrium with the aqueous phase, n equilibrium relations need to be fulfilled simultaneously, each of them to the degree corresponding to the abundance of the respective end-member in the solid solution.

2.4 Ideal solid solutions

In the case of ideal solid solutions, the activities of the components, A_j , are equal to their mole fractions, X_j , and the equilibrium condition is expressed as:

$$Q_j = X_j K_j \quad (6)$$

This means that, at equilibrium conditions, the degree of saturation of a mineral (or end-member) in the aqueous solution is equal to its mole fraction in the solid solution. This simple expression involves a very important statement: A mineral that is largely undersaturated in an aqueous solution may still be a minor end-member of an ideal solid solution, and a mineral which is close to saturation in an aqueous solution is always a major end-member of an ideal solid solution.

It is worthwhile mentioning that the formation of an ideal solid solution is characterised by a purely entropic energy gain. This can be visualised by considering the solid solution as a solid phase of a defined composition and expressing its ion activity product, Q^* , in terms of Gibbs energy of reaction. Q^* can be expressed in terms of the ion activity products and the mole fractions of the end-members:

$$Q^* = \prod_{j=1}^n Q_j^{X_j} = \prod_{j=1}^n K_j^{X_j} A_j^{X_j} \quad (7)$$

This corresponds to a reaction energy of:

$$\Delta_r G^* = RT \ln Q^* = RT \sum_{j=1}^n X_j \ln K_j + RT \sum_{j=1}^n X_j \ln A_j \quad (8)$$

$$\Delta_r G^* = \underbrace{\sum_{j=1}^n X_j \Delta_r G_j}_{(1)} + RT \underbrace{\sum_{j=1}^n X_j \ln A_j}_{(3)} \quad (9)$$

The term (1) is the free energy of reaction (formation/dissolution) of the solid solution, the term (2) represents a simple combination of the free energies of reaction of the end-members. The terms (1) and (2) differ only by the purely entropic term (3). This term is always negative for an ideal solid solution, and a solid solution is thus always more stable than a simple mixture of its end-members. It is, however, important to mention that Eqs. (7) through (9) are meaningful only if all the n Eqs. (6) are valid, which means that all the n end-members are in

simultaneous equilibrium with the aqueous solution. Eqs. (7) through (9) thus represent the mass action law of the solid solution only if its composition is strictly constant.

2.5 *Non-ideal solid solutions*

Non-ideal solid solutions are the normal case in the real world. In practice, Eq. (4) will not represent a realistic situation, but in some cases the approximation of $\lambda_j \approx 1$ and $A_j \approx X_j$ may be a reasonable assumption. In Eq. (3) the term "RT ln λ_j " represents the chemical excess potential which quantifies the deviation from ideality. Fritz (1981) suggests, like several authors earlier, to express the activity coefficient of each end-member as a function of the mole fractions of all the end-members:

$$RT \ln \lambda_j = f(X_1, X_2, \dots, X_n) \quad (10)$$

In the simplest case, i.e., the regular binary system, only one coefficient, A, needs to be determined:

$$RT \ln \lambda_1 = A X_2^2 = A(1-X_1)^2 \quad (11)$$

$$RT \ln \lambda_2 = A X_1^2 = A(1-X_2)^2 \quad (12)$$

For a regular ternary system the functions become considerably more complicated:

$$RT \ln \lambda_1 = A_{12} X_2^2 + A_{13} X_3^2 + X_2 X_3 (A_{12} - A_{23} + A_{13}) \quad (13)$$

$$RT \ln \lambda_2 = A_{23} X_3^2 + A_{12} X_1^2 + X_1 X_3 (A_{12} + A_{23} - A_{13}) \quad (14)$$

$$RT \ln \lambda_3 = A_{13} X_1^2 + A_{23} X_2^2 + X_1 X_2 (-A_{12} + A_{23} + A_{13}) \quad (15)$$

The number of coefficients, A_{ij} , to be determined for the characterisation of the non-ideality of a regular solid solution with n end-members is equal to $n!/2$. This explains why no thermodynamic data of chemical excess potentials are available for $n > 3$.

2.6 *Variations in the composition of solid solutions*

The composition of a solid solution is likely to change if a perturbation occurs to the system, such as dissolution, evaporation, temperature change, etc. The progress of this variation is described by a new variable, ξ , which is the basic parameter of a kinetic description of the reaction. A theoretical development is given by Clément (1992) who also describes a new computer code for such calculations.

3 Application potential of solid solution models

The potential field of application of solid solution models for radioactive waste management purposes includes two unresolved and critically important problem areas: (1) the long-term behaviour of engineered barriers, such as clays or concrete, and of host rocks; and (2) coprecipitation reactions. The use of solid solution models in these two areas will be shortly discussed in the following sections.

3.1 *Long-term behaviour of engineered barriers such as smectites*

The alteration behaviour of smectites is an important factor in assessing the safety of a final repository of radioactive waste. Smectites are often used as backfill materials providing both physical stability of the repository and a chemical barrier function towards the dispersion of the highly toxic radionuclides into the host rock. The favourable properties of smectites, especially of the sodium type, are mainly based on their swelling capability, leading to the necessary counter-pressure against the rock mass, as well as to an almost complete impermeability for water. In fact, compacted sodium smectite is completely resistant to advective water flow, and transportation of radionuclides thus occur exclusively by diffusion. A mineral transformation of the smectite structure may result in a partial or even complete loss of its favourable properties, and predictions of its long-term behaviour are therefore of prime importance.

Speculations about possible transformation products of smectites have been published by the radioactive waste community over many years. These speculations are characterised by a general disagreement about possible alteration products such as illites, hydrous micas, zeolithes, etc. Predictive modelling has been limited to simplistic estimations, for example a linear reaction rate proportional to the potassium supply for the transformation of smectite into illite, etc.

For the modelling of the retention behaviour of radionuclides in the near field, the surface characteristics of the solid phase are of key importance. The long-term behaviour of the surfaces will be determined not only by the surface reactions but also by the transformation processes of the solid phase, by which new surface types with different chemical behaviour may be created.

It has been recognised that dissolution/precipitation reactions of the clay structure will occur on long time scales, especially since, in a final repository for radioactive waste, the clay backfill will be surrounded by minerals of completely different composition. The groundwater in contact with the clay backfill will not be in equilibrium with the clay either. Therefore, dissolution reactions of the clay structure are very likely to occur.

3.2 Modelling of clays as solid solutions

Solid solution modelling of clays has been the subject of various studies in the past, especially by Fritz and collaborators: Duplay (1988), Fritz (1981, 1985), Fritz and Kam (1985), Garrels and Tardy (1982), Tardy (1982), Tardy, Duplay and Fritz (1987), Tardy and Fritz (1981). Estimated data can also be found in the above publications, as well as in Tardy and Duplay (1992), Tardy and Garrels (1974), and Tardy and Touret (1987). Clay solid solution modelling and data estimation methods published by other groups include Aagaard and Helgeson (1983), Mattigod and Sposito (1978), May et al. (1986), Nriagu (1975), Sposito (1986), and Stoessel (1979, 1981).

The fact that a comparatively large number of publications is available on the solid solution modelling of clays does not mean that the problem is solved, quite on the contrary. It means that there is a strong and worldwide interest in reliable predictions of the behaviour of clays, and that the solid solution approach is considered to be the most promising model to meet this need. Clays are among the most complex minerals because ionic or atomic substitutions can occur at different sites (tetrahedral, octahedral, interstitial) and thus a large number of different end-members have to be considered. The state of the art in the group of Prof. Fritz at Strasbourg is to use 36 different end-members to represent the entire range of clays. It should be mentioned that the spectrum of end-members used considers different occupations of the ion exchange sites and can thus handle ion exchange reactions as well. However, a weak point of this procedure is that dissolution/precipitation reactions of such minerals are slow, whereas ion exchange reactions are fast. This situation can be improved by (1) combining solid solution models with ion exchange and surface complexation models, or (2) by introducing kinetic rate laws into the solid solution model as has been proposed recently by Madé, Clément and Fritz (1990) and Clément (1992).

It is not the purpose of the present note to discuss specific solid solution models for clays in detail. It should nevertheless be mentioned that the models serving to describe the chemical composition of most smectites, vermiculites, illites, etc., in general include the following end-members:

$(\text{Mg}_3^{2+}, \text{Fe}_3^{2+}, \text{Al}_2^{3+}, \text{Fe}_2^{3+})\text{Si}_4\text{O}_{10}(\text{OH})_2$	talc-pyrophyllite (phyllosilicates)
$\text{K}^+(\text{Mg}_3^{2+}, \text{Fe}_3^{2+}, \text{Al}_2^{3+}, \text{Fe}_2^{3+})\text{AlSi}_3\text{O}_{10}(\text{OH})_2$	phlogopite-muscovite (tetrahedral K^+ -micas)
$\text{K}^+(\text{Mg}_{2.5}^{2+}, \text{Fe}_{2.5}^{2+}, \text{Al}_{1.667}^{3+}, \text{Fe}_{1.667}^{3+})\text{Si}_4\text{O}_{10}(\text{OH})_2$	celadonite (octahedral K^+ -micas)

An up-to-date publication for advanced reading, including a method for estimating formation energies of end-members, has recently been published by Tardy and Duplay (1992).

3.3 Coprecipitation reactions

Minerals found in nature usually contain small quantities of other components which had been incorporated during the formation period. Such an incorporation of minor components

can be due to a thermodynamically favoured reaction, or it can as well be due to a temporary availability of the minor component. In the latter case the incorporation need not necessarily be energetically favoured but it can be explained by statistical thermodynamic simulations.

Coprecipitation reactions may be important retardation processes for the migration of radionuclides. They are usually neither considered in sorption models nor in speciation models of solubility limiting phases. It is considered likely that radionuclide solubilities may not be controlled by a solubility limiting solid phase of the radionuclide, but rather by coprecipitation reactions of the radionuclides. The coprecipitation mechanism may be described, in a simplified way, as follows: Solid phases that are in equilibrium with an aqueous solution dissolve and reprecipitate dynamically, at a rate determined by the kinetic rate constant and the equilibrium concentrations according to the rate law. A common example is calcite, CaCO_3 . In a solution that is in equilibrium with calcite, it is possible that minor cations can be built into the calcite structure without requiring a net precipitation of calcite, see Section 2.1 above. Coprecipitation reactions can be simulated by kinetically controlled solid solution models. However, the data are scarce, and the incorporation of statistical thermodynamics could be of valuable help in improving the thermodynamic basis of solid solution models for coprecipitation applications.

3.4 Availability of thermodynamic data for clays

Clays are among the most complex natural minerals to model because of the variability in their composition. Consequently, a large number of end-members are necessary to obtain a reliable solid solution model for clays. Each end-member is characterised by a well defined stoichiometric composition and a solubility product. At an early stage, the solubility products of the end-members were derived from solubility products of well known, crystalline end-members. By using these constants, the stabilities of clays predicted with any type of solid solution models were overestimated considerably compared to the observations in nature and in the laboratory. Hence, the solubility products describing the dissolution thermodynamics of highly crystalline end-members are not appropriate to model solid solutions consisting of less crystalline end-members. Tardy and Fritz (1981) have adjusted the solubility products to correspond to lower stabilities of the end-members, and they thus obtained more reliable predictions of the long-term behaviour of clays.

The procedure of continuously adjusting the solubility products of end-members according to new observations from geology and laboratory experiments has been used ever since. One of the most recent tabulation has been published by Tardy and Duplay (1992).

The temperature dependency of the solubility products of end-members is important to simulate the geological formation of clay minerals as well as to predict their long-term alteration in the near field of a repository for high-level nuclear waste. Estimations of the temperature dependency of the solubility products of end-members are available, e.g., from Tardy, Duplay and Fritz (1987).

More publications containing thermodynamic data for end-members are given in the first paragraph of Section 3.2 above.

4 Conclusions

Clay minerals are metastable compounds that are subject to slow dissolution/precipitation reactions. Surface interaction models are not sufficient to model the long-term behaviour of clays because they do not take into account any structural changes in the clay matrix due to dissolution/precipitation reactions. Solid solution models represent a promising tool for mathematical handling of structural alteration reactions of minerals. Although it is difficult to validate long-term model predictions, tendencies in rock alteration processes are predicted correctly by solid solution models, and in a few cases they have been applied successfully to explain the formation of presently existing minerals, e.g., by Crovisier et al. (1992).

Solubility product data are available from estimation procedures and have been continuously improved in concordance with evidence from geology and laboratory experiments. Estimation methods for the temperature dependency of solubility products up to 200°C are also available.

Theoretically, solid solution models can also handle surface reactions, and the model presented by Tardy and Duplay (1992) does involve ion exchange reactions. However, surface reactions and dissolution/precipitation reactions in clay minerals cannot be distinguished unless kinetic aspects are considered. Short-term surface interaction experiments, such as ion exchange and surface complexation reactions, may therefore not be explained by a solid solution model, because the model would predict structural changes due to dissolution/precipitation reactions, which in practice would only occur in the long term. Surface reaction models seem to be the best tool to simulate short-term laboratory experiments. For the prediction of the long-term development of clays and their retardation behaviour for radionuclides, the most promising modelling tool seems to be a combination of a solid solution model and a surface interaction model.

It is also recognised that solid solution models can be used to model coprecipitation reactions. This is a potentially important retention mechanism for radionuclides, probably more important than the solubility control by a pure solid phase of the radionuclide.

5 Recommendations

1. It is recommended to use solid solution models to simulate slow alteration reactions of the bentonite backfill. The solid solution models successfully used by the group of Prof. Fritz at Strasbourg are the following:

DISSOL: Fritz (1975, 1981, 1985), Tardy and Fritz (1981). Path calculation model to simulate rock-water reactions. This code has been specially adapted to take into account the solid solution behaviour of clay minerals.

THERMAL: Fritz (1981). Effects of temperature on solution equilibria to simulate hydrothermal reactions.

KINDIS: Madé, Clément and Fritz (1990), Clément (1992). This code uses chemical kinetics to account for differences in the dissolution/precipitation and surface interaction rates. The code is at an early stage of testing, and has at present limited applicability due to the scarcity of kinetic data.

2. Reactions taking place on the bentonite surface are best modelled using ion exchange and surface complexation models such as the Wanner model.
3. It is recommended to work in the direction of combining the solid solution model DISSOL and the ion exchange and surface complexation model by Wanner (1986) and Wanner et al. (1993). This procedure will allow to model long-term alteration of the clay while adapting continuously the fast surface reactions to the slowly varying composition of the clay phase.
4. Thermodynamic data to quantify the energetic properties of the end-members have been estimated and adjusted to be compatible with evidence from geology and laboratory data. It is recommended to use these data while continuous adaptation to new experimental findings is essential.
5. Cooperation with highly experienced specialists in the field of solid solution model development and application is recommended. Collaboration with the group of Prof. Fritz at the University of Strasbourg, France, is encouraged as this group has over 20 years experience in solid solution modelling and is still actively devoted to this subject. MBT Environmental (H. Wanner) is willing to act as a coordinator and is in a position to supervise and give the necessary input for the inclusion of the surface interaction model.
6. It is suggested to perform long-term leaching experiments with Japanese bentonites under relevant conditions to obtain an experimental basis for testing solid solution models combined with surface complexation models. Such experiments should be carefully designed at a stage where the boundary conditions of the combination of the solid solution model and the surface interaction model are fully defined.

6 References

- Aagaard, P. and Helgeson, H.C. (1983). Activity/composition relations among silicates and aqueous solutions: II. Chemical and thermodynamic consequences of ideal mixing of atoms on homological sites in montmorillonites, illites, and mixed-layer clays. *Clays Clay Min.*, **31**(3), 207-217.
- Ben Baccar, M. and Fritz, B. (1993). Geochemical modelling of sandstone diagenesis and its consequences on the evolution of porosity. *Applied Geochemistry*, **8**, 285-295.
- Berner, R.A. (1978). Discussion: Equilibrium, kinetics and the precipitation of magnesian calcites from seawater. *Amer. J. Sci.*, **278**, 1475-1477.
- Chen, C.H. (1975). A method of estimation of standard free energies of formation of silicate minerals at 298.15 K. *Amer. J. Sci.*, **275**, 801-817.
- Clauer, N., Frapé, S.K. and Fritz, B. (1989). Calcite veins of the Stripa granite (Sweden) as records of the origin of the groundwaters and their interactions with the granitic body. *Geochim. Cosmochim. Acta*, **53**, 1777-1781.
- Clément, A. (1992). KINDIS: Un logiciel de simulation thermodynamique et cinétique des interactions solution-minéraux à température donnée (0-300°C). *Notes Tech. Inst. Géol. Strasbourg*, no. 21, 74pp, in French.
- Crovisier, J.-L., Honnorez, J., Fritz, B. and Petit J.-C. (1992). Dissolution of subglacial volcanic glasses from Iceland: Laboratory study and modelling. *Applied Geochemistry*, **1** (suppl.), 55-81.
- De Boer, R.B. (1977). Stability of Mg-Ca carbonates. *Geochim. Cosmochim. Acta*, **41**, 265-270.
- Duplay, J. (1988). Géochimie des argiles et géothermométrie des populations monominérales de particules. Ph.D. thesis, University of Strasbourg, France, in French.
- Fritz, B. (1975). Etude thermodynamique et simulation des réactions entre minéraux et solutions. Applications à la géochimie des altérations et des eaux continentales. *Mém. Sci. Géol. Strasbourg*, No. 41, 153pp, in French.
- Fritz, B. (1981). Etude thermodynamique et modélisation des réactions hydrothermales et diagénétiques. *Mém. Sci. Géol. Strasbourg*, No. 65, 202pp, in French.
- Fritz, B. (1985). Multicomponent solid solutions for clay minerals and computer modeling of weathering processes. In: *The Chemistry of Weathering* (ed. J.L. Drever); NATO ASI series, D. Reidel Publishing Co., Vol. 149, pp.19-34.

- Fritz, B. and Kam, M. (1985). Chemical interactions between the bentonite and the natural solutions from the granite near a repository for spent nuclear fuel. SKB TR 85-10, 24pp.
- Fritz, B. and Tardy, Y. (1974). Prediction for mineralogical sequences in tropical soils by a theoretical dissolution model. Proc. Int. Symp. Water-Rock Interactions, Prague, 409-416.
- Fritz, B. and Tardy, Y. (1976). Séquences de minéraux secondaires dans l'altération des granites et roches basiques; modèles thermodynamiques. Bull. Soc. géol. France, **18**, 7-12.
- Garrels, R.M. and Tardy, Y. (1982). Born-Haber cycles for interlayer cations of micas. Int'l Clay Conference Bologna, 1981. In: Developments in sedimentology (H. van Olophen and F. Veniale, eds.), Amsterdam: Elsevier Science Publishers B.V., Vol. 35, pp.423-440.
- Garrels, R.M. and Wollast, R. (1978). Discussion: "Equilibrium criteria for two-components solids reacting with fixed composition in an aqueous phase. Example: the magnesian calcites" by D.C. Torstenson and L.N. Plummer. Amer. J. Sci., **278**, 1469-1474.
- Grover, J. (1976). Chemical mixing in multicomponent solutions: An introduction to the use of Margules and other thermodynamic excess functions to represent non-ideal behaviour. In: Thermodynamics in geology (ed. D.G. Fraser), D. Reidel Publishing Co., pp.67-98.
- Helgeson, H.C., Delany, J.M., Nesbitt, H.W. and Bird, D.K. (1978). Summary and critique of the thermodynamic properties of rock-forming minerals. Amer. J. Sci., **278**, 1-229.
- Helgeson, H.C. and Mackenzie, F.T. (1970). Silicate sea water equilibria in the ocean system. Deep Sea Res., **17**, 877-892.
- Jensen, B.S. (1993). The formation of solid solutions in surface layers: An important adsorption mechanism? J. Contamin. Hydrol., **13**, 231-247.
- Kerrick, D.M. and Darken, L.S. (1975). Statistical thermodynamic models for ideal oxide and silicate solid solutions, with application to plagioclase. Geochim. Cosmochim. Acta, **39**, 1431-1442.
- Lafon, G.M. (1978). Discussion: "Equilibrium criteria for two-components solids reacting with fixed composition in an aqueous phase. Example: the magnesian calcites" by D.C. Torstenson and L.N. Plummer. Amer. J. Sci., **278**, 1455-1468.

- Madé, B, Clément, A. and Fritz, B. (1990). Modélisation cinétique et thermodynamique de l'altération: le modèle géochimique KINDIS. C.R. Acad. Sci. Paris, t.310, Série II, 31-36, in French.
- Mattigod, S.V. and Sposito, G. (1978). Improved method for estimating the standard free energies of formation ($\Delta_f G^{\circ}_{298.15}$) of smectites. *Geochim. Cosmochim. Acta*, **42**, 1753-1762.
- May, H.M., Kinniburgh, D.G., Helmke, P.A. and Jackson, M.L. (1986). Aqueous dissolution, solubilities and thermodynamic stabilities of common aluminosilicate clay minerals: Kaolinite and smectite. *Geochim. Cosmochim. Acta*, **50**, 1667-1677.
- Michaux, L., Mouche, E., Petit, J.-C. and Fritz, B. (1992). Geochemical modelling of the long-term dissolution behaviour of the French nuclear glass R7T7. *Applied Geochemistry*, **1** (suppl.), 41-54.
- Nriagu, J. (1975). Thermochemical approximations for clay minerals. *Amer. Mineral.*, **30**, 834-839.
- Pfeifer, H.R. (1977). A model for fluids in metamorphosed ultramafic rocks. Observations at surface and subsurface conditions (high pH spring waters). *Schweiz. Miner. Petr., Mitt.*, **57**, 361-396.
- Powell, R. (1976). Activity-composition relationships for crystalline solutions. In: *Thermodynamics in geology* (ed. D.G. Fraser), D. Reidel Publishing Co., pp.57-66.
- Prigogine, I. and Defay, R. (1954). *Chemical thermodynamics*. London: Longmans, Green and Co.
- Saxena, S.R. (1973). *Thermodynamics of rock-forming crystalline solutions*. New York: Springer Verlag.
- Sposito, G. (1986). On the polymer model of thermodynamical clay mineral stability. *Clays Clay Min.*, **34**, 198-203.
- Stoessel, R.K. (1979). A regular solution site mixing model for illites. *Geochim. Cosmochim. Acta*, **43**, 1151-1159.
- Stoessel, R.K. (1981). Refinements in a site mixing model for illites: Local electrostatic balance at the quasi chemical approximation. *Geochim. Cosmochim. Acta*, **45**, 1733-1741.
- Tardy, Y. (1982). Kaolinite and smectite stability in weathering conditions. *Estudios Geológicos*, **38**, 295-312.

- Tardy, Y. and Duplay, J. (1992). A method of estimating the Gibbs free energies of formation of hydrated and dehydrated clay minerals. *Geochim. Cosmochim. Acta*, **56**, 3007-3029.
- Tardy, Y., Duplay, J. and Fritz, B. (1987). Stability fields of smectites and illites as a function of temperature and chemical composition. SKB TR 87-20, 34pp.
- Tardy, Y. und Fritz, B. (1981). An ideal solid solution model for calculating solubility of clay minerals. *Clay Minerals*, **16**, 361-373.
- Tardy, Y. and Garrels, R.M. (1974). A method of estimating the Gibbs energy of formation of layer silicates. *Geochim. Cosmochim. Acta*, **38**, 1101-1116.
- Tardy, Y., and Garrels, R.M. (1976). Prediction of Gibbs energies of formation: I. Relationship among Gibbs energies of formation of hydroxides, oxides and aqueous ions. *Geochim. Cosmochim. Acta*, **40**, 1051-1056.
- Tardy, Y., and Garrels, R.M. (1977). Prediction of Gibbs energies of formation: II. Monovalent and divalent metal silicates. *Geochim. Cosmochim. Acta*, **41**, 87-92.
- Tardy, Y. and Touret, O. (1987). Hydration energies of smectites: A model for glauconite, illite, and corrensite formation. In: *Proc. Int'l Clay Conf., Denver, Colorado, 1985* (L.G. Schultz, H. van Olphen and F.A. Mumpton, eds.), pp.46-52.
- Thorstenson, D.C. and Plummer, L.N. (1977). Equilibrium criteria for two component solids reacting with fixed composition in an aqueous phase. Example: The magnesian calcites. *Amer. J. Sci.*, **277**, 1203-1223.
- Wagner, C., Mellgren, S. and Westbrook, J.H. (1952). *Thermodynamics of alloys*. Reading, Massachusetts: Addison Wesley Publishing Co. Inc., 161pp.
- Wanner, H. (1986). Modelling interaction of deep groundwaters with bentonite and radionuclide speciation, Nagra NTB 86-21, 103pp.
- Wanner, H., Albinsson, Y., Karnland, O., Wersin, P., Wieland, E. (1993). The surface properties of montmorillonite. Presentation at Migration '93 conference, Charleston, South Carolina, USA, 12-17 December 1993. Submitted for publication at *J. Contam. Hydrology*.

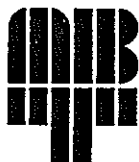
**Power Reactor and Nuclear Fuel Development Corporation
(PNC)**

Technical Report

**Thermodynamic modelling of ion exchange
reactions at the Na-smectite/water interface**

Hans Wanner and Erich Wieland

December 1993



Environmental

MBT Umwelttechnik AG

Vulkanstrasse 110

CH - 8048 Zürich

Abstract

The experimental results of the investigation of the ion exchange behaviour of Na-smectite, provided by Mitsubishi Materials Corporation (Yajima, 1993), are analysed and interpreted with the help of a classical thermodynamic model. The model is based on the concept of hypothetical surface complex formation and can be used to predict ion exchange equilibria and speciation in solution and at the solid/water interface. The experimental results reported by Yajima (1993) are compared with the exchange isotherms of K^+ , H^+ , Ca^{2+} and Mg^{2+} as predicted from model computations for the special conditions used in the experiments. The experimental results are successfully interpreted by the model. The model computations correctly predict the exchange isotherm for K^+ on Na-smectite in a chloride background medium of increasing ionic strength. The model suggests that the interaction of K^+ with the layer sites of Na-smectite is independent of pH under neutral and alkaline conditions, and that the contribution from negatively charged edge sites is negligible. Protonation and deprotonation reactions occurring at both layer and edge sites are of crucial importance and should be taken into account in the acid as well as in the neutral and alkaline pH range. Modelling of Na/Ca and Na/Mg exchange reactions in chloride background medium emphasizes the role of $CaCl^+$ and $MgCl^+$ as adsorbing species. The experimental results indicate that the Na/K exchange exhibits ideal behaviour on Na-smectite; this allows the assumption that the activity coefficients for the surface species are unity.

In addition, the experimental results on the interaction of bentonite and water, provided by PNC (Sasaki, 1993), are analysed and interpreted. These measurements are compatible with our model, and they are used to evaluate the amounts of soluble impurities present in Kunipia F and Kunigel V1. The soluble impurities found in Kunipia F are 0.005% KCl, 0.07% NaCl and 0.69% $CaSO_4$. In Kunigel V1 we find 0.004% KCl, 0.001% NaCl and 0.38% $CaSO_4$. The knowledge of these impurities is important for the interpretation of experimental results, especially in the case of low ionic strength, because they influence the ion exchange reactions and can thus have a significant effect on the retardation of certain actinides and fission products.

Table of Contents

1	Introduction	
2	Ion exchange on Na-smectite	
2.1	Theory	
2.1.1	Presentation of the experimental data	
2.1.2	Presentation of the ion exchange equilibria	
2.1.3	Modelling of ion exchange reactions	
2.2	Results and Discussion	
2.2.1	$\text{Na}^+ \rightarrow \text{K}^+$ and $\text{Na}^+ \rightarrow \text{H}^+$ exchange reactions	
2.2.2	$\text{Na}^+ \rightarrow \text{Ca}^{2+}$ and $\text{Na}^+ \rightarrow \text{Mg}^{2+}$ exchange reactions	
2.2.3	$\text{Na}^+ \rightarrow \text{K}^+$ exchange reactions at layer and edge sites	
3	Ion exchange selectivity and activity coefficients	
3.1	Thermodynamics of ion exchange reactions	
3.2	The solid solution model	
3.2.1	Definition of the activity-concentration relationship	
3.2.2	The Vanselow selectivity coefficient	
3.2.3	Determination of the rational activity coefficients in the solid solution model	
3.2.3.1	Ideal solid solution models : Ion exchange on montmorillonite	
3.2.3.2	Real mixtures of solid solution	
3.3	Empirical cation exchange models	
3.4	Applicability of cation exchange models	
4	Leaching of purified bentonite (Na-smectite), Kunipia F and Kunigel V1 bentonite in distilled water	
4.1	Purified bentonite (Na-smectite)	
4.2	Kunipia F and Kunigel V1 bentonite	
5	Conclusions and Recommendations	
6	Acknowledgments	
7	References	

Glossary

a_j :	activity of species i
c_j :	concentration of species i
c_s :	solid concentration [g/l]
CEC:	cation exchange capacity [eq/kg]
$E_i(\text{clay})$:	equivalent fraction of the adsorbed species i on clay (denoted as $E-i(\text{clay})$ in the figures)
$E_i(\text{sln})$:	equivalent fraction of species i in solution (denoted as $E-i(\text{sln})$ in the figures)
f_j :	rational activity coefficient of surface species
γ_i :	single-ion activity coefficient of aqueous species
g_i :	activity coefficient in the Gaines - Thomas conventional formulation
K_X° :	thermodynamic ion exchange constant
K_X :	conditional ion exchange constant
K_{GT} :	conditional ion exchange constant (Gaines - Thomas convention)
K_V :	(conditional) Vanselow selectivity coefficient
m_j^0 :	initial molality of species i
m_j :	molality of species i in the supernatant
M_S :	weight of dry clay
M_{T1} :	weight of sample before extraction of the supernatant
M_{T2} :	weight of sample after extraction of the supernatant
M_{TW} :	total mass of water per kg dry clay mineral
M_W :	gravimetric water content of the slurry (kg water per kg dry clay)
n_j :	total moles of species i per kg of slurry
q_j :	moles of species i adsorbed per kg dry clay
Q :	sum of the moles of adsorbed species
x_i :	mole fraction of species i
Z_i :	charge of a species i

1 Introduction

Bentonite has been chosen as a candidate backfill material for nuclear repositories by many countries, mainly because of its favourable physical properties. These include its high swelling properties and its effectiveness as a barrier for the migration of hazardous material. The active component in the bentonite responsible for these favourable properties is montmorillonite. One can distinguish between different types of montmorillonite in terms of the major exchangeable ion. A common type is Na-montmorillonite which has extremely good swelling properties. In a compacted form no advective water flow is possible, and any movement across water-saturated, compacted bentonite will take place by diffusion and will therefore be very slow. It can thus be expected that the interactions between dissolved species and the surface of the solid phase will be controlled by equilibrium reactions. It is important to quantify these surface reactions thermodynamically, in order to enable predictions of the retardation of radionuclides in the near field.

The first step in the quantification of surface reactions includes the identification of any type of reaction that may take place on the surface of montmorillonite. The identification of possible impurities and their reactivities is also an important part of the first step. In this way it will be possible to make reliable predictions for bentonites of different compositions.

The careful experimental measurements provided by MMC (Yajima, 1993) and PNC (Sasaki, 1993) are used in the present work to test existing surface reaction models and to quantify the soluble impurities in two Japanese bentonite: Kunipia F and Kunigel VI.

2 Ion exchange on Na-smectite

2.1 Theory

2.1.1 Presentation of the experimental data

The ion exchange experiments with Na-smectite as exchanger phase were performed as batch-type experiments (Yajima, 1993). The condition of mass balance in a batch system where an initial molality of species i , m_i^0 , in the reactant aqueous solution is mixed with 1 kg of dry clay mineral is given by

$$m_i^0 M_{TW} = n_i + m_i (M_{TW} - M_W) \quad [\text{mol per kg dry clay mineral}] \quad (1)$$

with M_{TW} as the total mass of water in this solution per 1 kg of dry clay mineral, M_W is the gravimetric water content of the slurry (kg water per kg of dry clay), m_i^0 denotes the initial molality of species [mol per kg water], m_i is the molality of the species i in the supernatant [mol per kg water] and n_i is the total moles of species i per 1 kg of slurry (dry mineral plus entrained solution). The chemical analysis of the supernatant solution was carried out after isolating Na-smectite from the reacting solution by centrifugation. This kind of separation requires a concentration correction for the reactant solution entrained with the clay. The moles of chemical species, i , adsorbed per kilogram of dry clay contacting an aqueous solution is calculated with the equation (Sposito, 1981):

$$q_i = n_i - M_W m_i \quad [\text{mol/kg}] \quad (2)$$

where n_i is the total moles of species, i , per kilogram of slurry (dry clay mineral plus entrained solution slurry); M_W is the gravimetric water content of the slurry (kg water per kg dry clay); and m_i is the molality (or molarity) (moles per kg water) of species i in the supernatant solution. This equation represents the surface concentration, q_i , of a chemical species per kilogram of dry clay mineral. Substituting n_i in Eq. (2) by Eq. (1) gives

$$q_i = m_i^0 M_{TW} - m_i M_{TW} \quad [\text{mol/kg}] \quad (3)$$

The weight of the entrained solution, M_W , can be determined experimentally with

$$M_W = M_{T1} - M_{T2} - M_S \quad [\text{kg}] \quad (4)$$

where M_{T1} and M_{T2} are the weights of the sample before and after extraction of the supernatant from the reacting suspension; M_S is the weight of the dry clay mineral in the reacting suspension. The equation ignores contributions to the weight of the entrained solution from dissolved salts, but these contributions are considered negligible in the present context.

Once the surface excess of a species, i , and its concentration in solution has been determined correctly, an exchange isotherm can be constructed. An exchange isotherm is analogous to an adsorption isotherm except that the variables plotted are charge fractions instead of surface concentrations (Sposito, 1981). The equivalent fraction E_i of an adsorbed cation, i , on the surface of a clay mineral is:

$$E_i(\text{clay}) = |Z_i| q_i / \text{CEC} \quad (5)$$

where Z_i is the charge of the cation, i , and q_i is its surface concentration given by Eq. (3). The CEC is defined by

$$\text{CEC} = \sum_k |Z_k| q_k \quad [\text{eq/kg}] \quad (6)$$

with the sum extending over all exchangeable cations, k . Eqs. (3) and (5) can be combined to yield:

$$E_i(\text{clay}) = |Z_i| (m_i^0 M_{TW} - m_i M_{TW}) / \text{CEC} \quad (7)$$

Eq. (7) is identical to the formulation given by Yajima (1993):

$$E_i(\text{clay}) = |Z_i| (c_i^0 - c_i) V / (M_S \text{CEC}) \quad (8)$$

with c_i^0 and c_i equal to m_i^0 and m_i , respectively. V and M_S are the volume of the solution [L] and the dry weight of the clay mineral [g], respectively. Since the ratio V/M_S corresponds to M_{TW} , Eqs. (7) and (8) are identical.

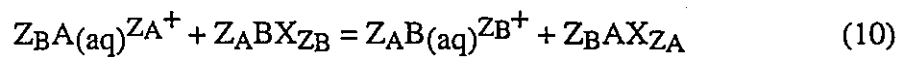
The equivalent fraction of a cation, i , in aqueous solution, $E_i(\text{sln})$, can be expressed:

$$E_i(\text{sln}) = \frac{|Z_i| c_i}{\sum_k |Z_k| c_k} \quad (9)$$

where c_i is the concentration of the exchangeable cation, i , in solution and the sum extends over all cations, k , in solution.

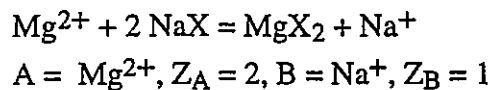
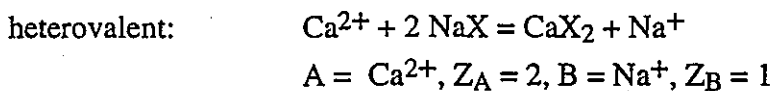
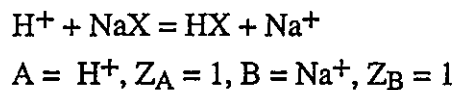
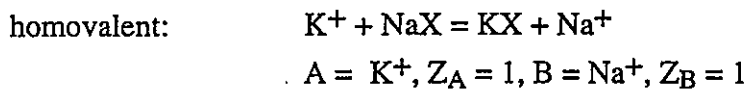
2.1.2 Presentation of the ion exchange equilibria

The concept of hypothetical surface complex formation is used to model ion exchange reactions on clays (Shaviv and Mattigod, 1985; Wanner, 1986; Fletcher and Sposito, 1989). This convention for describing ion exchange is based on the concept of surface complex formation and can be implemented in conventional models such as MINEQL. The reaction equation describing the stoichiometric replacement of ions on the surface of an exchanger phase is :



with Z_A and Z_B as the valence charges of the cations A and B, and X as the solid exchanger.

The ion exchange reactions considered in this study represent the stoichiometric replacement of Na^+ by H^+ , K^+ , Ca^{2+} and Mg^{2+} on Na-smectite:



The thermodynamic equilibrium constant, K_X° , for the ion exchange reactions given above is (see also Sections 3.1 and 3.2):

$$K_x^\circ = \frac{(x_A f_A)^{Z_B} (m_B \gamma_B)^{Z_A}}{(x_B f_B)^{Z_A} (m_A \gamma_A)^{Z_B}} \quad (11)$$

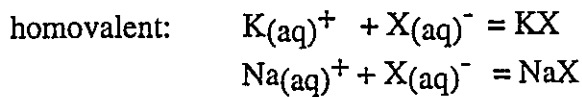
with x_A and x_B as the mole fractions of the cations on the exchanger phase ($x_A = m_{AXZ_A} / (m_{AXZ_A} + m_{BXZ_B})$ and $x_B = m_{BXZ_B} / (m_{AXZ_A} + m_{BXZ_B})$), f_A and f_B as the activity coefficient of the adsorbed species, m_A and m_B as the molalities of ions in the aqueous phase and γ_A and γ_B as the corresponding single-ion activity coefficients, respectively, calculated by the Debye-Hückel expression. The conditional equilibrium constant, K_x , is related to the thermodynamic equilibrium constant, K_x° :

$$K_x^\circ = K_x \frac{(\gamma_B)^{Z_A}}{(\gamma_A)^{Z_B}} \quad (12)$$

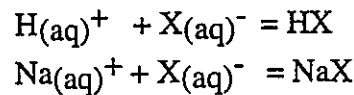
For the subsequent data treatment with MIN_SURF the ion exchange reactions can be formulated in terms of hypothetical complexation reactions of aqueous species by defining the reactive ligand X^- as a hypothetical solution species (Shaviv and Mattigod, 1985; Wanner, 1986; Fletcher and Sposito, 1989).



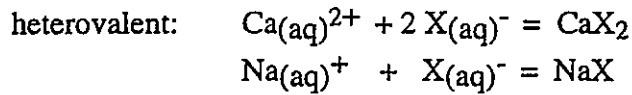
The equilibrium reactions representing the replacement of Na^+ by H^+ , K^+ , Ca^{2+} and Mg^{2+} on Na-smectite are then given by:



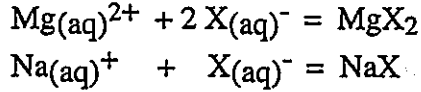
$$A = \text{K}^+, Z_A = 1, B = \text{Na}^+, Z_B = 1$$



$$A = \text{H}^+, Z_A = 1, B = \text{Na}^+, Z_B = 1$$



$$A = \text{Ca}^{2+}, Z_A = 2, B = \text{Na}^{+}, Z_B = 1$$



$$A = \text{Mg}^{2+}, Z_A = 2, B = \text{Na}^{+}, Z_B = 1$$

The equilibrium constants for reactions (13a) and (13b) are defined by:

$$K(\text{AX}_{Z_A}) = \frac{m_{\text{AX}_{Z_A}}}{(m_A \gamma_A)(m_X \gamma_X)^{Z_A}} \quad (14a)$$

$$K(\text{BX}_{Z_B}) = \frac{m_{\text{BX}_{Z_B}}}{(m_B \gamma_B)(m_X \gamma_X)^{Z_B}} \quad (14b)$$

where $m_{\text{AX}_{Z_A}}$ and $m_{\text{BX}_{Z_B}}$ denote the molalities of surface complexes, and m_A , m_B and m_X are the molalities of solution species. The single-ion activity coefficients of the surface complexes, AX and BX, are defined as unity.

The relationship between the thermodynamic equilibrium constant for ion exchange and the two formation constants of the hypothetical surface reactions can be established by eliminating the mole fractions from Eq. (12) and substituting $m_{\text{AX}_{Z_A}}$ and $m_{\text{BX}_{Z_B}}$ using the equilibrium expressions given in Eqs. (14a) and (14b) (Fletcher and Sposito, 1989):

$$K_x^{\circ} = \left(\frac{f_B^{Z_B}}{f_A^{Z_A}} \right) \left(\frac{K(\text{AX}_{Z_A})^{Z_B}}{K(\text{BX}_{Z_B})^{Z_A}} \right) (m_{\text{AX}_{Z_A}} + m_{\text{BX}_{Z_B}})^{(Z_A - Z_B)} \quad (15)$$

The activity coefficients, f_i , of the surface complexes are defined as unity in our modelling approach. This assumption can be justified by the fact that montmorillonite normally shows an ion exchange behaviour which is close to ideality (Sposito, 1981, Fletcher and Sposito, 1989).

Eq. (15) includes the thermodynamic constant K_x° and $(m_{AX_{Z_A}} + m_{BX_{Z_B}})$ as measurable quantities, whereas the formation constants $K(AX_{Z_A})$ and $K(BX_{Z_B})$ are unknown. However, if one of the constants is known, e.g., $K(BX_{Z_B})$, the value of the other constant can then be derived from Eq. (15). In the modelling approach presented in this report, we use a convention by arbitrarily setting the formation constant for the Na surface complex to 10^{20} (Wanner, 1986). In the case of homovalent exchange reactions, the compositional correction term $(m_{AX_{Z_A}} + m_{BX_{Z_B}})^{(Z_A - Z_B)}$ reduces to unity. The formation constants K_I for the homovalent exchange reactions $Na^+ \rightarrow K^+$ and $Na^+ \rightarrow H^+$ are then given by:

$$K(AX_{Z_A}) = K_x^\circ \times K(BX_{Z_B}) \quad (16)$$

However, for heterovalent exchange reactions with $Z_A \neq Z_B$, the ratio of the formation constants, $K(AX_{Z_A})^{Z_B}/K(BX_{Z_B})^{Z_A}$, must be dependent on both the level of exchange $(m_{AX_{Z_A}} + m_{BX_{Z_B}})$ and the total quantity of exchanger (CEC) in the system. The formation constant $K(AX_{Z_A})$ for the heterovalent exchange reaction $Na^+ \rightarrow Ca^{2+}$ is:

$$K(CaX_2) = K_x^\circ \times K(NaX)^2 (m_{CaX_2} + m_{NaX})^{-1} \quad (17)$$

The expression for the corresponding exchange reaction $Na^+ \rightarrow Mg^{2+}$ is analogous.

Eq. (18) relates the molalities of surface complexes to the CEC and the concentration of suspended clay, c_s , [g/l]

$$2 m_{CaX_2} + m_{NaX} = CEC \times c_s \quad [\text{mol/l}] \quad (18)$$

The expression for the corresponding exchange reaction $Na^+ \rightarrow Mg^{2+}$ is again analogous.

2.1.3 Modelling of ion exchange reactions on Na-smectite

In the following, we present predicted exchange isotherms defined as a graph of $E_i(\text{clay})$ against $E_i(\text{sln})$ for an exchangeable cation i at fixed temperature and pressure. The equivalent fractions are calculated with Eqs. (5) and (9). The molalities of surface and solution species of an ion i are computed with the aid of the computer code MIN_SURF (Berner, 1986; Sierro, 1992) which is an extended version of the computer code MINEQL.

Model computations conducted with the computer code MIN_SURF involve the following assumptions and approximations:

- 1) Ion exchange reactions are adequately described using the convention given by Shaviv and Mattigod (1985), Wanner (1986) and Fletcher and Sposito (1989).
- 2) The consistent set of formation constants published for ion exchange reactions on montmorillonite (Fletcher and Sposito, 1989) adequately describes ion exchange reactions on Na-smectite.
- 3) The CEC of Na-smectite (77% montmorillonite, 22% beidellite, 1% nontronite) is 108.1 meq/100g and the proportions of exchangeable cations are 97.1% Na, 0.9% K, 1.3% Ca and 0.7% Mg.
- 4) Impurities in the purified Na-smectite and background concentrations of the relevant cations, Na^+ , K^+ , Mg^{2+} and Ca^{2+} , can be ignored. This assumption is justified because the concentration of background electrolyte, NaCl, and of the exchangeable cations, KCl, HCl, MgCl_2 and CaCl_2 , are at least an order of magnitude higher than the cation concentration measured in leaching experiments.
- 5) The total carbonate concentration, c_T , is set equal to 10^{-5} M which corresponds to the equilibrium concentration at atmospheric partial pressure of CO_2 and $\text{pH} < 5.5$. This assumption implies that the experimental devices are closed systems, and bidistilled water saturated with CO_2 is the only carbonate source. The assumption strictly holds for the experiments carried out at $\text{pH} = 4.5$ and 3, but implicitly indicates that equilibrium with atmospheric CO_2 is not reached in the experiments at $\text{pH} = 11$ within the time scale of the experiments.
- 6) Calcite and magnesite may precipitate if supersaturation occurs.

Based on these assumptions and the ion exchange reactions as defined above, the exchange isotherms for $\text{Na}^+ \rightarrow \text{K}^+$, $\text{Na}^+ \rightarrow \text{H}^+$, $\text{Na}^+ \rightarrow \text{Ca}^{2+}$, and $\text{Na}^+ \rightarrow \text{Mg}^{2+}$ (displayed in Figures 1 to 4) and the isotherms of the $\text{Na}^+ \rightarrow \text{K}^+$ exchange determined at $\text{pH} = 3$ (range 3.0 - 3.3) and at $\text{pH} = 11$ (range 10.8 - 11.0) (shown in Figure 6) are modelled. The model computations are performed for the specific experimental conditions. Therefore, we consider that the ionic strength is not constant in the exchange experiments, but increases with increasing concentrations of the exchangeable cations.

2.2 Results and Discussion

2.2.1 $\text{Na}^+ \rightarrow \text{K}^+$ and $\text{Na}^+ \rightarrow \text{H}^+$ exchange reactions

The formation constant, $K(\text{KX})$, needed in modelling the replacement of K^+ on Na-smectite is taken from Fletcher and Sposito (1989). The formation constant, $K(\text{NaX})$, serves as a reference value and is arbitrarily set equal to 10^{20} (Wanner, 1986).

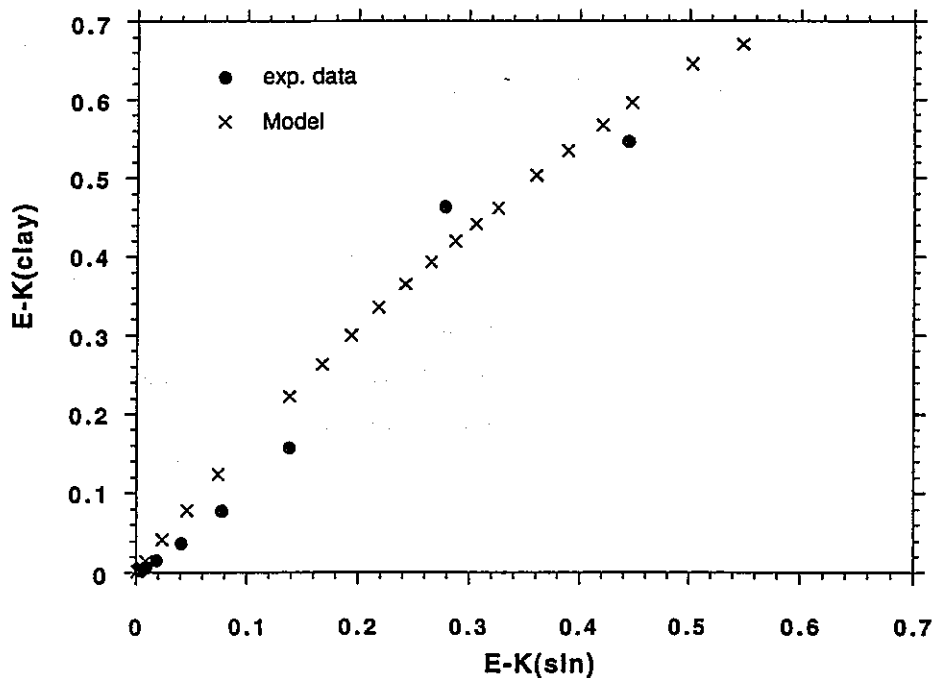
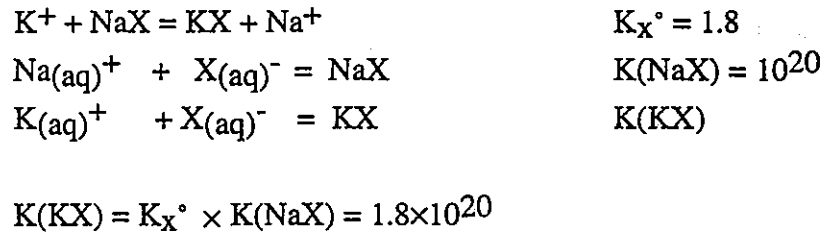
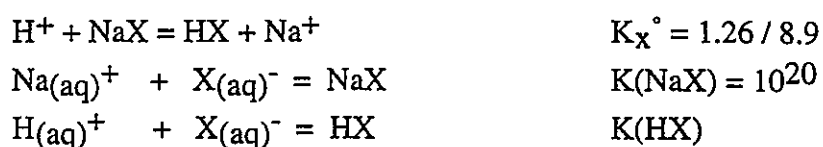


Figure 1 Exchange isotherm for K^+ on Na-smectite in chloride background medium of increasing ionic strength ($I = 0.11 - 0.24 \text{ M}$) at $\text{pH} = 4.5$ (range 4.4 - 4.7). $E\text{-K}(\text{clay})$ and $E\text{-K}(\text{sln})$ represent the equivalent fractions of K on the solid and in solution, respectively.

Figure 1 presents the exchange isotherm for K^+ on Na-smectite. The equivalent fraction of K^+ , E-K(clay), is displayed versus the equivalent fraction of K^+ in the supernatant solution, E-K(sln). Figure 1 shows good agreement of the experimental data and model computations. The difference between experiments and model predictions at low equivalent fractions of K^+ may partially be attributed to the uncertainty in the precision of the experimental data.

The ion exchange reactions used in modelling the replacement of H^+ on Na-smectite are given by:



$$K(HX) = K_X^\circ \times K(NaX) = 1.26 \times 10^{20} \text{ and } 8.9 \times 10^{20}$$

Model computations are performed with two thermodynamic equilibrium constants, K_X° , for the Na/H exchange. Fletcher and Sposito (1989) suggested a value of $K_X^\circ = 1.26$ for the Na/H exchange corresponding to a $\log K(HX) = 20.1$. Figure 2, however, shows that model calculations based on a value of $\log K(HX) = 20.1$ underestimate the replacement of Na with H. The experimental data and model computations agree in the E-H(sln) range 0 to 0.1 if the formation constant is set to $\log K(HX) = 20.95$ corresponding to a thermodynamic ion exchange constant $K_X^\circ = 8.9$. An increase in E-H(sln) from 0 to 0.1 corresponds to a decrease in pH from 4.77 to 1.97. As shown in Figure 2, model calculations underestimate the extent of the Na/H exchange above E-H(sln) = 0.1 (i.e., below pH = 1.97), but fit the experimental data above pH = 1.97. Other types of surface reactions may interfere with the Na/H exchange in the strongly acidic pH range: The deviation of experimental data and model calculations can be attributed to the reaction of protons with edge surface sites and/or dissolution processes occurring at the Na-smectite surface. Both types of surface reactions enhance the apparent surface proton density and, hence, increase the equivalent fraction of H^+ on Na-smectite. However, based on the available experimental data, a further refinement of edge site contributions and proton consumption due to dissolution is not possible to date. An attempt to quantify the effect of the two surface reactions on the proton balance requires an extension of the experimental programme addressing the problem of separating ion exchange reactions and protonation of edge surface sites.

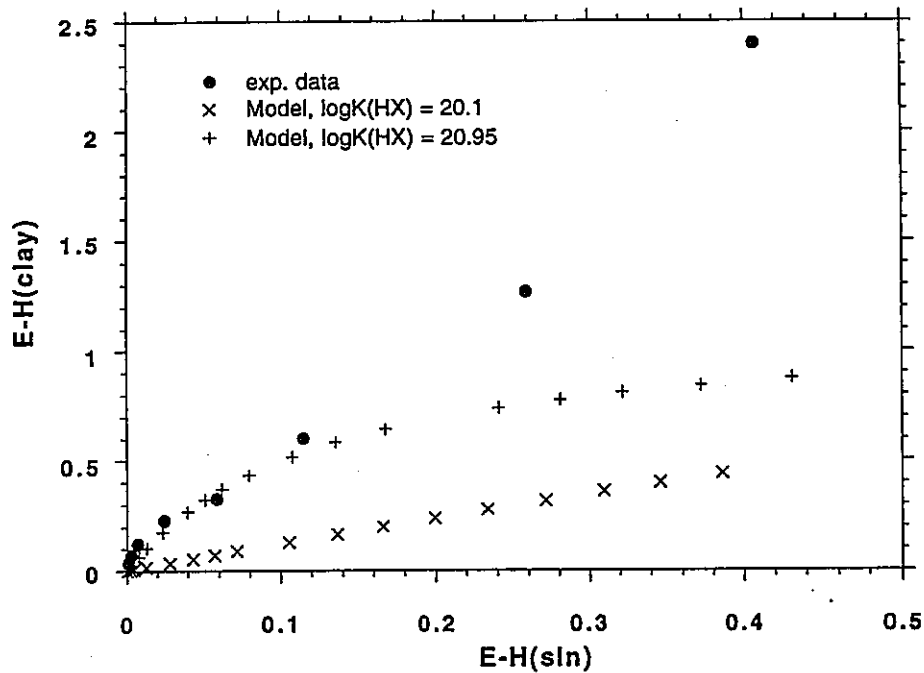
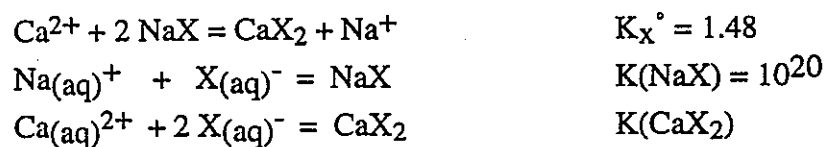


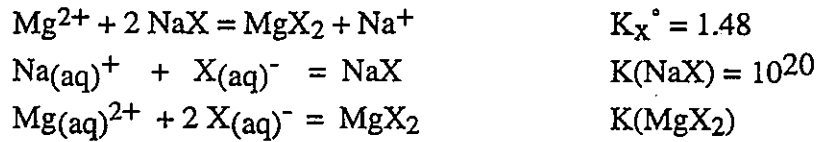
Figure 2 Exchange isotherm for H^+ on Na-smectite in chloride background medium of increasing ionic strength ($I = 0.11 - 0.16$ M). E-H(clay) and E-H(sln) represent the equivalent fractions of H on the solid and in solution, respectively.

2.2.2 $Na^+ \rightarrow Ca^{2+}$ and $Na^+ \rightarrow Mg^{2+}$ exchange reactions

The formation constants, $K(CaX_2)$ and $K(MgX_2)$, for the replacement of Ca^{2+} and Mg^{2+} on Na-smectite used in our model calculations are taken from Fletcher and Sposito (1989):



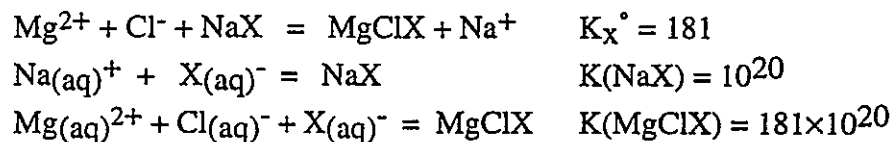
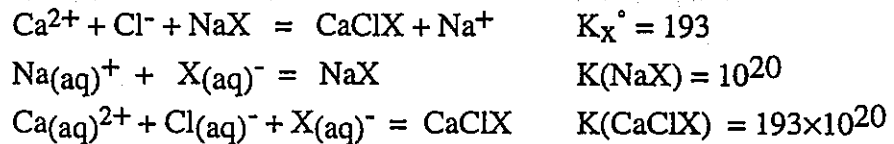
$$K(CaX_2) = K_X^\circ \times K(NaX)^2 (m_{CaX_2} + m_{NaX})^{-1} = 1.48 \times 10^{40} (m_{CaX_2} + m_{NaX})^{-1}$$



$$K(\text{MgX}_2) = K_x^\circ \times K(\text{NaX})^2 (m_{\text{MgX}_2} + m_{\text{NaX}})^{-1} = 1.48 \times 10^{40} (m_{\text{MgX}_2} + m_{\text{NaX}})^{-1}$$

The experimental protocol indicates that the study presented by Yajima (1993) was conducted at constant Na^+ concentrations allowing the electrolyte background concentration to increase from 0.11 M to 0.24 M. The value $(m_{\text{CaX}_2} + m_{\text{NaX}})$ ranges from 0.0108 mol/l to 0.0074 mol/l under the given experimental conditions. For modelling purposes, we assume an average value of $(m_{\text{CaX}_2} + m_{\text{NaX}})$ and $(m_{\text{MgX}_2} + m_{\text{NaX}})$ of 0.0091 mol/l. The formation constant for the Na/Ca and Na/Mg ion exchange reactions can then be estimated to $\log K(\text{MgX}_2) = \log K(\text{CaX}_2) = 42.21$. This value is comparable with the values reported by Wanner (1986) (Na/Ca exchange: $\log K^\circ = 42.4$ and Na/Mg exchange: $\log K^\circ = 41.7$).

Sodium-calcium exchange on Crook County (Wyoming) bentonite has previously been investigated by Sposito et al. (1983a,b). Their results obtained in a montmorillonite suspension with constant 0.05 M perchlorate background and at pH = 7 support a nonpreference model for the Na/Ca and Na/Mg exchange reactions. However, preference for divalent cations has been observed in the presence of chloride as interfering anion. The affinity of the surface for Ca and Mg is significantly enhanced with chloride as background electrolyte (Sposito et al., 1983a). The stoichiometries and the formation constants for the binary ion exchange of Ca^{2+} and Mg^{2+} in the presence of chloride were defined by Fletcher and Sposito (1989) and are adopted here:



In Figures 3 and 4, the exchange isotherms for Ca^{2+} and Mg^{2+} based on the ion exchange equilibria listed above are compared with the experimental data.

In a first attempt, the experimental data are evaluated for a water/bentonite ratio of 100 (Figures 3 and 4, upper graphs). With this assumption, the resulting equivalent fraction E-Ca(clay) at high surface coverages of Ca^{2+} calculated from the experimental data exceeds the CEC. A reevaluation of the equivalent fraction E-Ca(clay) from the experimental data, under the assumption that the water/bentonite ratio in the experimental protocol possibly had been chosen to be 50 instead of 100 (Yajima, 1993), now correctly results in equivalent fractions E-Ca(clay) that are lower than the CEC (Figures 3 and 4, lower graphs). It should be mentioned that supersaturation of Ca^{2+} and Mg^{2+} solutions with respect to mineral phases (e.g., CaCl_2 , MgCl_2 , CaSO_4 , CaCO_3) controlling the free concentration of Ca and Mg can be ruled out. Hence the observation that the maximum surface coverage exceeds the cation exchange capacity for a water/bentonite ratio of 100 can not be attributed to precipitation of Ca^{2+} or Mg^{2+} . Based on this circumstantial evidence, our assumption that the water/bentonite ratio was 50 is reasonable and, hence, the experimental data displayed in the lower plots of Figures 3 and 4 are most likely representative.

The model calculations presented in Figures 3 and 4 are conducted for two different cases: 1) Ca^{2+} or Mg^{2+} are the only species replacing Na^+ on Na-smectite and 2) both Ca^{2+} (or Mg^{2+}) and CaCl^+ (or MgCl^+) could replace Na^+ on Na-smectite. Given the uncertainties in the experimental data and the fact that the thermodynamic constants reported by Fletcher and Sposito (1989) are used without further adjustments, agreement between model predictions and the experimental data (water/bentonite ratio = 50) is good. Implementation of CaCl^+ and MgCl^+ as adsorbable species increases the equivalent fraction of Ca and Mg on Na-smectite. Agreement between the modelling curve and the experimental data appears to be better without inclusion of CaCl^+ and MgCl^+ as sorbing species. Note, however, that a more detailed analysis of the importance of the reactive species is not possible from the experimental data presented by Yajima (1993). A refined evaluation of the formation constants for Ca^{2+} , Mg^{2+} , CaCl^+ and MgCl^+ adsorption onto montmorillonite requires an extension of the experimental programme by including $\text{Na}^+ \rightarrow \text{Ca}^{2+}$ and $\text{Na}^+ \rightarrow \text{Mg}^{2+}$ exchange experiments conducted in non-complexing background electrolyte (e.g., sodium perchlorate).

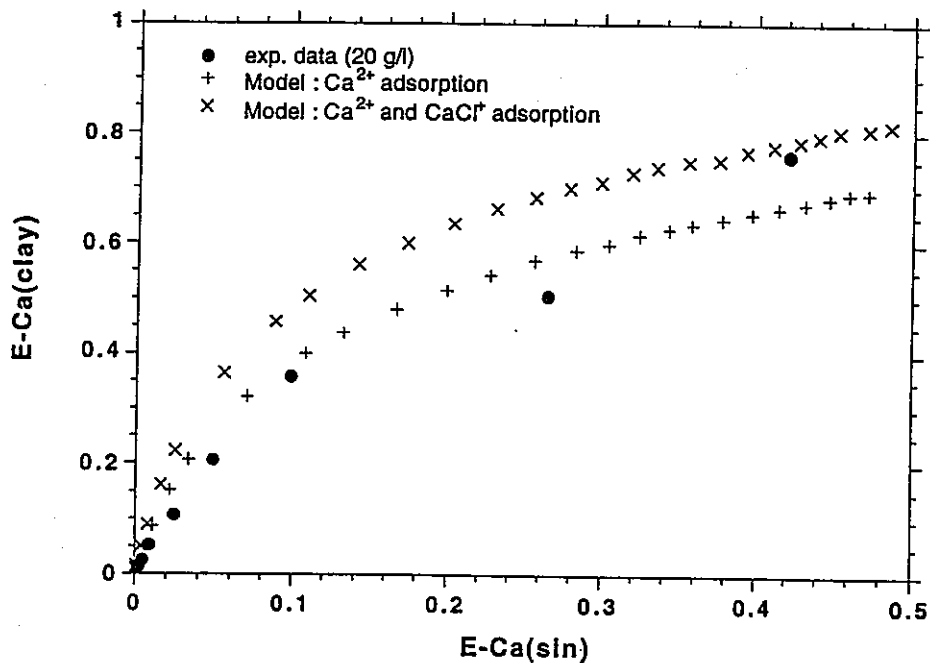
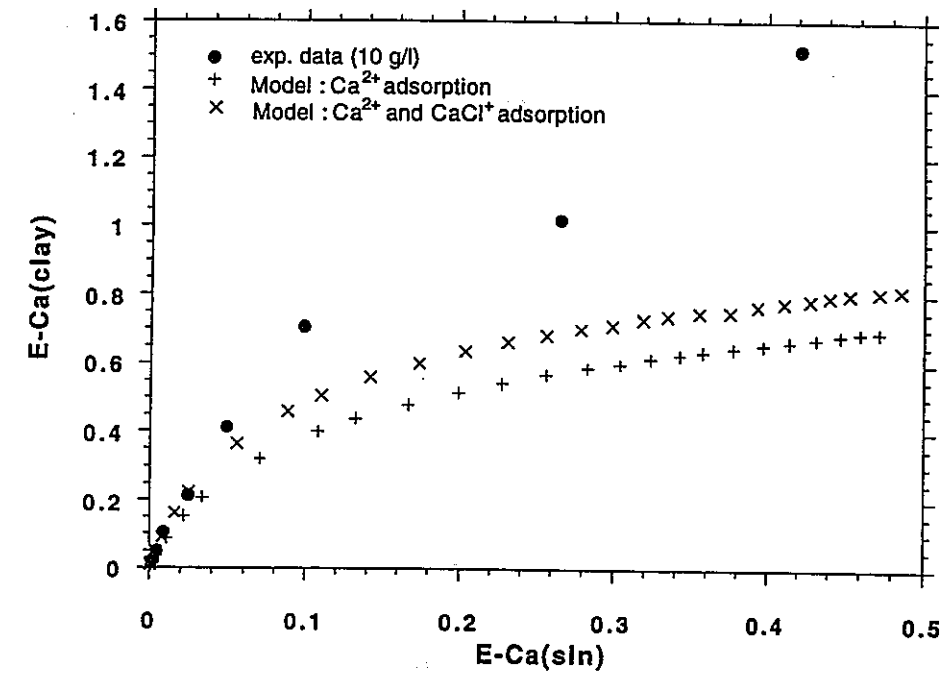


Figure 3 Exchange isotherms for Ca^{2+} on Na-smectite in chloride background medium of increasing ionic strength ($I = 0.11 - 0.24 \text{ M}$). The experimental data are calculated for a water/bentonite ratio of 100 (upper) and 50 (lower). $E\text{-Ca}(\text{clay})$ and $E\text{-Ca}(\text{soln})$ represent the equivalent fractions of Ca on the solid and in solution, respectively.

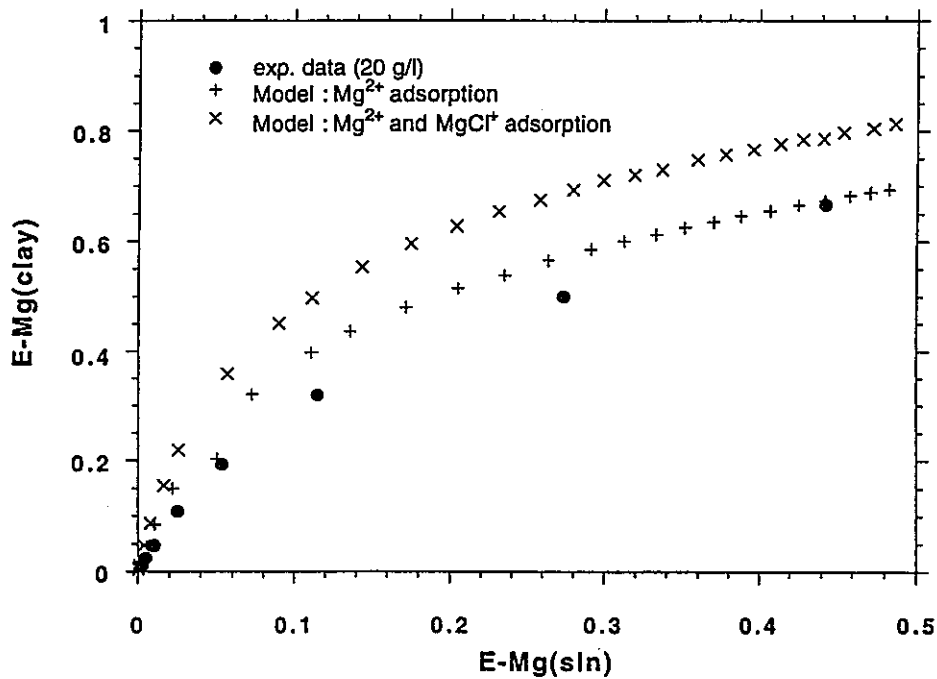
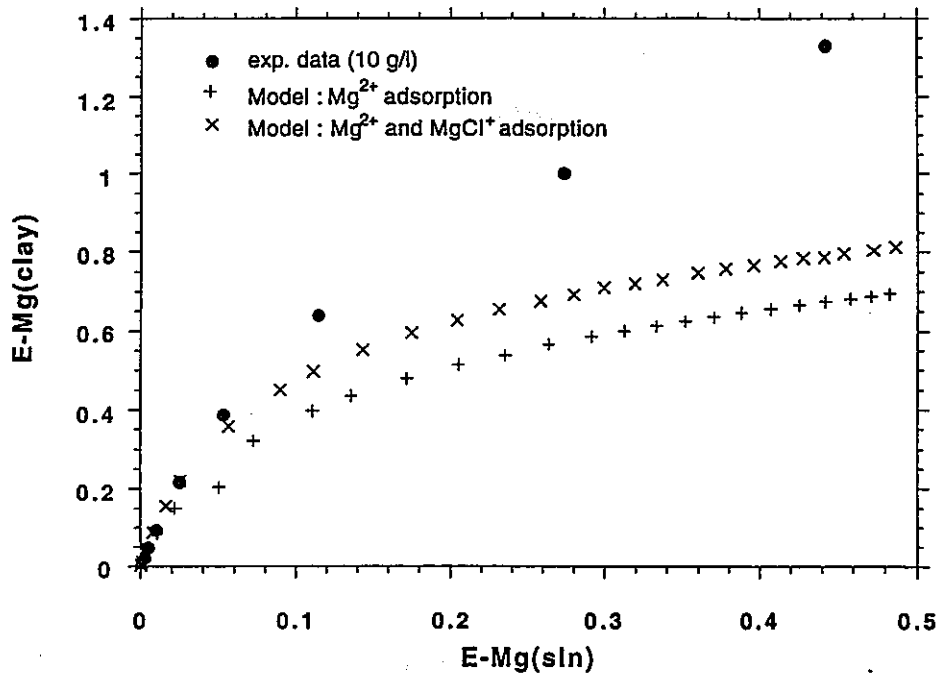


Figure 4 Exchange isotherms for Mg^{2+} on Na-smectite in chloride background medium of increasing ionic strength ($I = 0.11 - 0.24$ M). The experimental data are calculated for a water/bentonite ratio of 100 (upper) and 50 (lower). E-Mg(clay) and E-Mg(sln) represent the equivalent fractions of Mg on the solid and in solution, respectively."

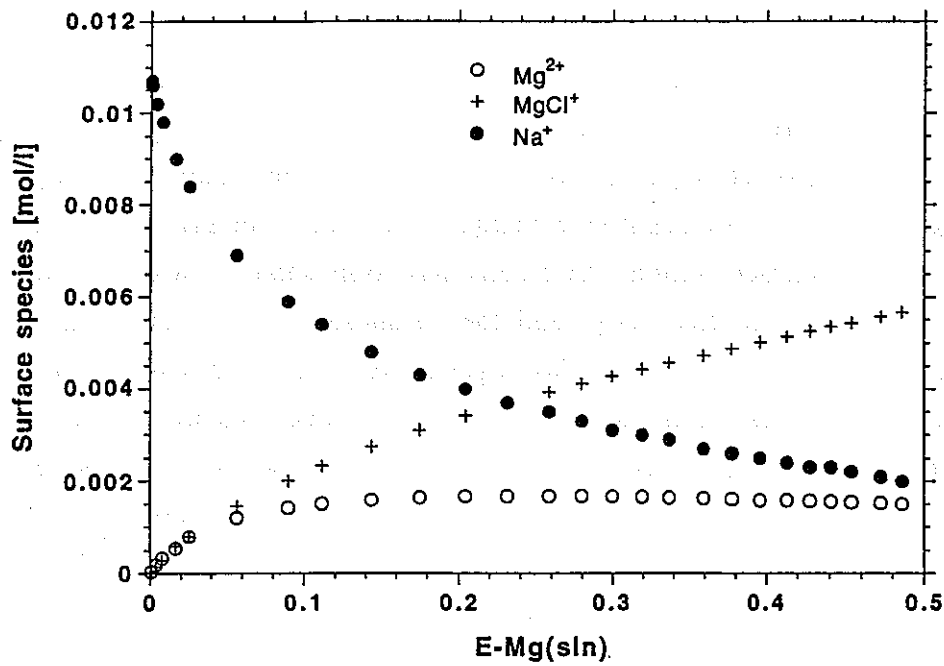
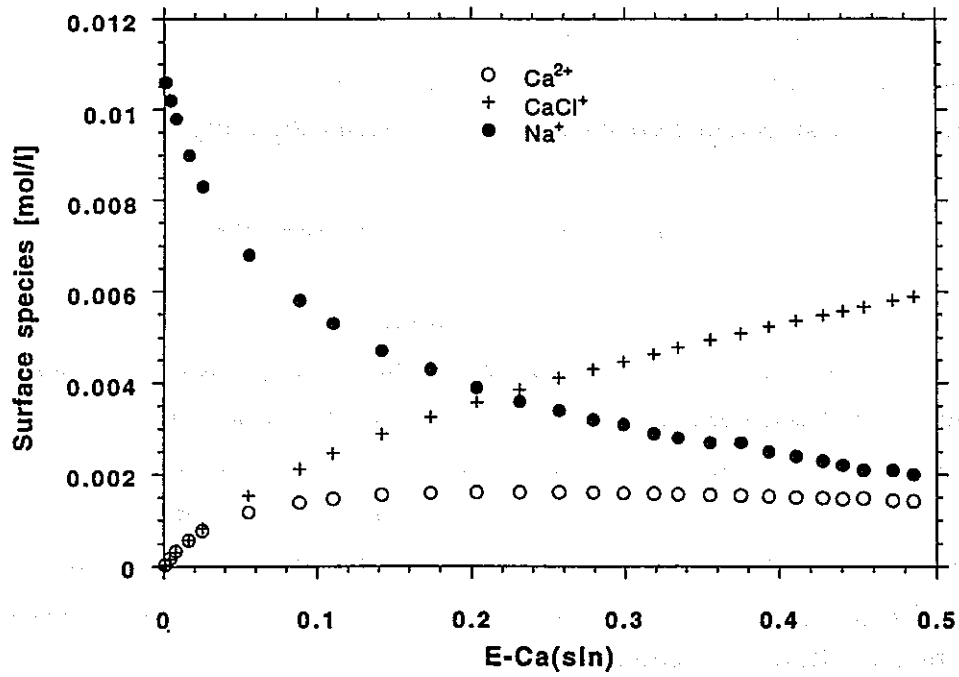
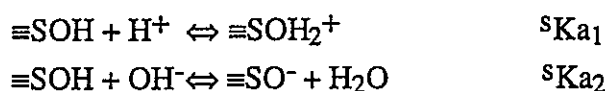


Figure 5 Theoretical distribution of surface species for Ca^{2+} and Mg^{2+} on Na-smectite in chloride background electrolyte ($I = 0.11 - 0.24 \text{ M}$) plotted as function of the normality $E\text{-M(sln)}$ in solution.

The speciation of Ca and Mg on the surface of montmorillonite as a function of the normality E-Ca(sln) and E-Mg(sln) in solution is illustrated in Figure 5. According to the model computations, CaCl⁺ and MgCl⁺ adsorb onto montmorillonite over the entire concentration range. With increasing concentration of the chloride background electrolyte, the concentrations of CaCl⁺ and MgCl⁺ increase in solution, and, hence, these species are adsorbed in preference to the free metal cation (Figure 5).

2.2.3 *Na⁺ → K⁺ exchange reactions at layer and edge sites*

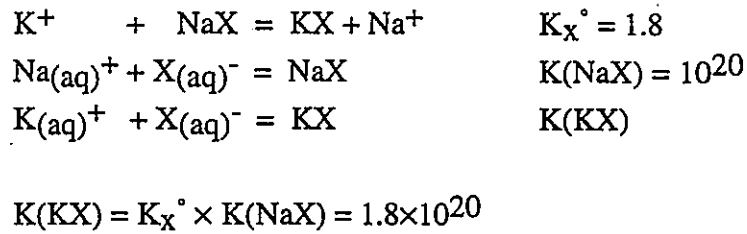
As previously mentioned, the surface of montmorillonite contains two distinctly different types of surface sites: layer sites, i.e. structural-charge sites due to isomorphic substitution at the basal siloxane layer, and edge sites, i.e., surface sites exposed on the edge surface of montmorillonite platelets. Layer sites are accessible for ion exchange reactions and mainly account for the exchanger characteristics of the clay mineral. The nature of the edge surface sites, however, is significantly different: edge sites are hydroxyl (OH) groups and are subject to ionization (i.e., protonation and deprotonation) as shown by the following reactions:



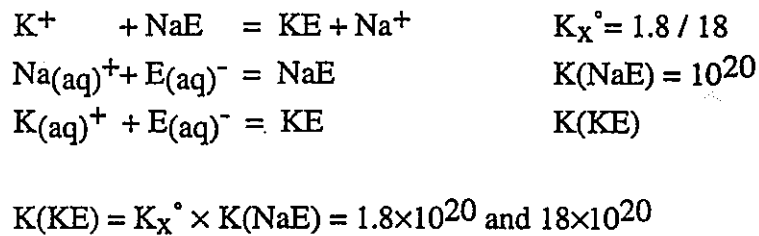
with $\equiv\text{SOH}$ indicating OH groups exposed at the edge surface. The degree of ionization of the amphoteric OH groups depends on pH and ionic strength. Edge OH groups are protonated in the acid pH range and dissociate protons in the alkaline pH range. At pH = 11, edge surface sites are negatively charged and, hence, binding of K⁺ may occur. With this type of surface reaction, OH groups may form stable surface complexes with the cation (e.g., K⁺ in this study) and the formation reaction is termed surface complexation. As pH decreases, the clay edges become saturated with protons and the edge effect becomes less pronounced. At pH = 3, the edge sites are neutral or carry a positive charge, and complex formation with edge sites do not occur. In the following, we discuss the possible effect of K⁺ complexation occurring at edge surface sites.

The constants for the Na/K exchange reactions occurring at layer and edge surface sites of Na-smectite are taken from Fletcher and Sposito (1989):

Ion exchange reactions at layer sites:



Complexation reactions at edge sites:



In Figure 6, the exchange isotherms for K^+ on Na-smectite measured at pH = 3 (range 3.0 - 3.3) and at pH = 11 (range 10.8 - 11.0) are compared with the model calculations. For modelling purposes, we assume that the formation constant of the surface complexes of K^+ with edge surface sites are $K(KE) = 1.8 \times 10^{20}$ ($\log K(KE) = 20.255$ as reported by Fletcher and Sposito, 1989) and $K(KE) = 18 \times 10^{20}$ ($\log K(KE) = 21.255$ as an estimated value). The experimental data taken at pH = 3 and 11 are in good agreement within the scatter of the experimental data. The experimental equivalent fraction for adsorbed K^+ appears to be slightly higher at pH = 11 than at pH = 3. However, it is questionable whether the pH dependence of K^+ adsorption is significant within the limits of experimental uncertainty. Note further that at pH = 3 two ion exchange reactions overlap: the replacement of Na^+ and H^+ by K^+ . The equilibrium constants for the two exchange reactions may be significantly different. We further may assume that the replacement of Na^+ by K^+ is favoured compared to the replacement of H^+ by K^+ . The equivalent fraction for adsorbed K^+ may hence be lower at pH = 3 than at pH = 11. This may explain the difference in the experimental results at pH = 11 and at pH = 3 as well as the composition dependence of the apparent conditional equilibrium constant for the Na/K exchange.

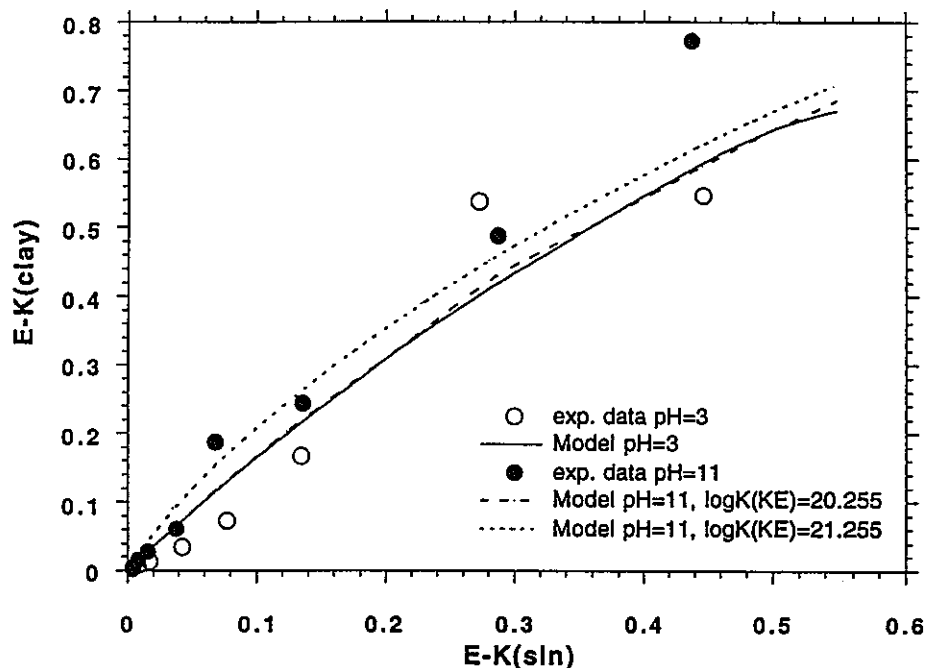


Figure 6 Exchange isotherm for K^+ on Na-smectite at pH = 3 and 11 in chloride background medium of increasing ionic strength ($I = 0.11$ - 0.24 M). The exchange isotherms are predicted from model calculations by including layer and edge surface sites as possible coordinative counterparts for K^+ (see text). E-K(clay) and E-K(sln) represent the equivalent fractions of K on the solid and in solution, respectively.

The experimental data determined at both pH values hence are adequately predicted with the general modelling approach used in this study to simulate the Na-smectite/water interaction. Model computations predict a pH independent exchange isotherm for K^+ on Na-smectite. For the purpose of modelling the interaction of K^+ with edge sites, we assume an edge site density of 10 meq/100 g corresponding to 10% of the cation exchange capacity. Figure 6 shows that the formation of surface complexes between K^+ and edge OH groups increases the equivalent fraction of adsorbed K^+ insignificantly. Hence ion exchange on layer sites determines the extent of K^+ adsorption on Na-smectite in the acid and alkaline pH range. Contributions from the association of K^+ with negatively charged edge OH groups are negligible at the K^+ concentrations considered here. Note, however, that the ionisation of edge surface sites,

i.e., the interaction of protons with edge OH groups, is extremely important when ion exchange reactions overlap with proton displacement at the Na-smectite surface.

3 Ion exchange selectivity and activity coefficients

Various conventions have been applied in the literature to treat the experimental data resulting from ion exchange studies and to establish a consistent set of equilibrium constants. In this section, we would like to compare the quasi-thermodynamic approach, based on the concept of surface complex formation used in our modelling approach, with the Gaines and Thomas convention chosen by Yajima (1993) for presenting the selectivity coefficient as a function of the equivalent fraction of the exchangeable cation. We will demonstrate differences in the data treatment for the homovalent ion exchange reactions (e.g., $\text{Na}^+ \rightarrow \text{K}^+$ exchange) and for the heterovalent ion exchange reactions (e.g., $\text{Na}^+ \rightarrow \text{Ca}^{2+}$ exchange).

3.1 Thermodynamics of ion exchange reactions

The thermodynamic equilibrium constants for homovalent and heterovalent ion exchange reactions can then be expressed as:

homovalent : $A = \text{K}^+, Z_A = 1, B = \text{Na}^+, Z_B = 1$

$$K_x^\circ = \frac{(a_{\text{KX}})(a_{\text{Na}})}{(a_{\text{NaX}})(a_{\text{K}})} = \frac{(a_{\text{KX}})(m_{\text{Na}}\gamma_{\text{Na}})}{(a_{\text{NaX}})(m_{\text{K}}\gamma_{\text{K}})} \quad (19)$$

heterovalent : $A = \text{Ca}^{2+}, Z_A = 2, B = \text{Na}^+, Z_B = 1$

$$K_x^\circ = \frac{(a_{\text{CaX}_2})(a_{\text{Na}})^2}{(a_{\text{NaX}})^2(a_{\text{Ca}})} = \frac{(a_{\text{CaX}_2})(m_{\text{Na}}\gamma_{\text{Na}})^2}{(a_{\text{NaX}})^2(m_{\text{Ca}}\gamma_{\text{Ca}})} \quad (20)$$

The single-ion activity coefficient of solutes in aqueous solution refer to the Infinite Dilution Reference State and can be evaluated from conventional expressions. However, various model approaches have been suggested in the literature to express the activities and the activity coefficient of surface species.

3.2 *The solid solution model*

3.2.1. *Definition of the activity-concentration relationship*

An exchanger phase can be considered as a solid solution, i.e., a macroscopically homogenous mixture, with a variable composition. The activity-concentration relationship for surface species, *i*, of a solid solution is defined by Guggenheim (1952):

$$(i) = f_i x_i \quad (21)$$

where *i* is a surface species such as CaX₂, NaX or KX given in Eqs. (19) and (20), *f* is the rational activity coefficient and *x_i* is the mole fraction of the surface species. The thermodynamic definition of the activity-concentration relationship given by Eq. (21) applies to components of mixtures of solids and non-aqueous solutions. The Reference State is that of the component *i* at *T* = 298.15 K and *P* = 1 bar as *x_i* approaches 1.0. If the rational activity coefficient of each component of a solid solution is equal to 1.0, regardless of the composition of the mixture, the solid solution is said to be ideal.

3.2.2 *The Vanselow selectivity coefficient*

In the Vanselow convention, the stoichiometry of ion exchange reactions is based on chemical equilibria expressed in mole fractions of the exchangeable cations. The stoichiometric replacement of an ion, *i*, on the exchanger surface has already been illustrated in Eq. (11). Eqs. (19) and (20) for homo- and heterovalent ion exchange reactions can be expressed in terms of rational activity coefficients and the Vanselow coefficient:

$$\text{homovalent:} \quad K_x^\circ = K_V \frac{(f_{KX})}{(f_{NaX})} \quad (22a)$$

$$\text{heterovalent:} \quad K_x^\circ = K_V \frac{(f_{CaX_2})}{(f_{NaX})^2} \quad (22b)$$

with *K_V* as the Vanselow selectivity coefficient (Vanselow, 1932) given by:

$$K_V = \frac{(x_{KX})(a_{Na})}{(x_{NaX})(a_K)} \quad (23a)$$

$$K_V = \frac{(x_{CaX_2})(a_{Na})^2}{(x_{NaX})^2(a_{Ca})} \quad (23b)$$

The Vanselow selectivity coefficient is a conditional equilibrium constant which, for non-ideal systems, varies with the composition of the exchanger phase. The cause of the composition dependence of K_V are the interactions between adsorbed species that occur as the adsorbate composition changes. In an ideal solid solution with the rational activity coefficient equal to unity, the thermodynamic constant equals the Vanselow selectivity coefficient as illustrated in Eqs. (22a) and (22b). Solid solutions, however, are often not ideal and the rational activity coefficients in Eqs. (22a) and (22b) are introduced to account for the composition dependence of the conditional exchange constant, K_V , thereby maintaining a constant value of the thermodynamic constant, K_X° .

3.2.3 *Determination of the rational activity coefficients in the solid solution approach*

3.2.3.1 *Ideal solid solutions: Ion exchange on montmorillonite*

According to Sposito (1984) and Fletcher and Sposito (1989), montmorillonite reveals an ideal or near-ideal ion exchange behaviour in many cases. Measurements of the Ca/Na, Mg/Na, Ca/Mg and Na/Cu exchange reactions (Sposito et al., 1981, Sposito et al., 1983a,b,c), of the binary reactions between Na, K and Rb on Wyoming bentonite, and of the binary reactions between Na, Li and NH_4 on Camp Berteau montmorillonite (Gast, 1969; Gast et al. 1969) show ideal or near-ideal behaviour of the exchanger phase. Hence the assumption made in the ideal solid solution model, that the rational activity coefficient $f_{Na} = f_K = f_{Ca} = 1$ in Eqs. (23a) and (23b), seems to be justified in the case of montmorillonite. Experimental data and the model computations further confirm the ideal behaviour of montmorillonite. Note, however, that Cs and Rb exchange reactions on montmorillonite show non-ideal ion exchange behaviour (Gast, 1969), and that derivation from ideal ion exchange behaviour may be not found on clay minerals other than montmorillonite.

3.2.3.2 *Non-ideal solid solutions*

Real mixtures are not ideal and rational activity coefficients hence correct the mole fractions in Eqs. (22a) and (22b) for this effect. Model expressions for the rational activity coefficient as a function of the mole fraction of one of the exchanger phase have been established to account for the composition dependence of K_V . The rational activity coefficients are expressed in terms of power series which, for example, in the case of the Na/K exchange is given by:

$$\ln f_{\text{NaX}} = a_1 x_{\text{KX}} + a_2 x_{\text{KX}}^2 + a_3 x_{\text{KX}}^3 + a_4 x_{\text{KX}}^4 \quad (24a)$$

$$\ln f_{\text{KX}} = a_1 x_{\text{NaX}} + a_2 x_{\text{NaX}}^2 + a_3 x_{\text{NaX}}^3 + a_4 x_{\text{NaX}}^4 \quad (24b)$$

We refer to Sposito (1981) for a detailed discussion and adequate treatment of the model expressions given in Eqs. (24a) and (24b).

3.3 *Empirical cation exchange models*

Other cation exchange models have been established in order to account for the composition dependence of equilibrium constants. These models are usually based on some empirical, chemical picture of the ion exchange reaction. A further characteristic of these models is that the activities of the exchanger components are modelled mathematically instead of modelling the rational activity coefficients. The Gaines and Thomas model and the so-called Gapon model for cation exchange reactions are based on the definition of an activity-equivalent fraction relationship given by Gaines and Thomas (1953):

$$(i) = g_i E_i \quad (25)$$

with E_i as the equivalent fraction of the exchanger cation and g_i as an "activity coefficient". The relationship given in Eq. (25) is a non-thermodynamic correction of the non-ideal behaviour of exchanger phases. As shown by Sposito (1977) and Sposito and Mattigod (1979), the coefficients g_A and g_B are not true activity coefficients since the equivalent fraction concentration scale may not be used to define rational activity coefficients.

Eqs. (19) and (20) for homo- and heterovalent ion exchange reactions can be expressed in terms of the Gaines and Thomas convention:

$$\text{homovalent: } K_x^\circ = K_{GT} \frac{(g_{KX})}{(g_{NaX})} \quad (26a)$$

$$\text{with } K_{GT} = \frac{(E_{KX})(a_{Na})}{(E_{NaX})(a_K)}$$

$$\text{heterovalent: } K_x^\circ = K_{GT} \frac{(g_{CaX_2})}{(g_{NaX})^2} \quad (26b)$$

$$\text{with } K_{GT} = \frac{(E_{CaX_2})(a_{Na})^2}{(E_{NaX})^2(a_{Ca})}$$

The parameters used in the Gaines and Thomas convention can be compared with those defined by the solid solution model (Table 1). The parameters of the two conventions are identical in the case of homovalent exchange, but significantly different in the case of heterovalent ion exchange reactions. It is evident from Table 1 that K_{GT} will not be constant if K_V is constant for a heterovalent ion exchange reaction, and that g_{CaX_2} and g_{NaX} will not be equal to 1 when f_{CaX_2} and f_{NaX} are equal to 1. This means that the parameter values of the Gaines and Thomas convention cannot be directly compared with those resulting from the solid solution model. This also holds if the parameters of the Gapon model and the solid solution model are compared.

Table 1: Comparison of the Gaines and Thomas convention and the solid solution model for expressing selectivity coefficients in cation exchange reactions.

	homovalent	heterovalent
equivalent fraction E_A	$E_{KX} = x_{KX}$	$E_{CaX_2} = 2 x_{CaX_2} / (1 + x_{CaX_2})$
equivalent fraction E_B	$E_{NaX} = x_{NaX}$	$E_{NaX} = x_{NaX} / (2 - x_{NaX})$
selectivity coefficient K_{GT}	$K_{GT} = K_V$	$K_{GT} = K_V \times (2 x_{CaX_2} + x_{NaX})$
coefficient g_{KX}, g_{CaX_2}	$g_{KX} = f_{KX}$	$g_{CaX_2} = 0.5 f_{CaX_2} \times (1 + x_{CaX_2})$
coefficient g_{NaX}	$g_{NaX} = f_{NaX}$	$g_{NaX} = f_{NaX} \times (2 - x_{NaX})$

3.4 *Applicability of the cation exchange models*

Ideal or non-ideal behaviour of the exchanger is revealed in the composition dependence of the Vanselow selectivity coefficient, K_V , using the thermodynamic convention as given in the solid solution model. If K_V is constant regardless of the variation in the surface composition, the exchanger is termed ideal. Composition dependence of K_V , however, indicate non-ideal ion exchange behaviour. Following the Gaines and Thomas convention (or the Gapon model, respectively), the same criteria are met for homovalent ion exchange reactions. In the case of heterovalent ion exchange, however, the different bases of the Gapon and of the Gaines and Thomas models on one hand and the solid solution model on the other hand become evident: The composition dependence of K_{GT} in the Gaines and Thomas model (or K_G used in the Gapon model) would indicate a non-ideal exchanger phase when the solid solution model predicts ideality.

We investigate the ion exchange characteristics of Na-smectite used in the study of Yajima (1993) by calculating the Vanselow selectivity coefficient, K_V , of the Na/K exchange. As discussed in the previous sections, a proper evaluation of the thermodynamic equilibrium constants for the other ion exchange reactions, i.e., $\text{Na}^+ \rightarrow \text{H}^+$, $\text{Na}^+ \rightarrow \text{Ca}^{2+}$ and $\text{Na}^+ \rightarrow \text{Mg}^{2+}$ exchange, is not possible based on the experimental data presented in this study. In these experiments, simultaneously occurring adsorption reactions, e.g., proton adsorption on edge and layer sites in the case of Na/H exchange reactions and adsorption of Ca^{2+} and CaCl^+ in the case of Na/Ca exchange reactions account for the overall observed ion exchange process and, hence, the equilibrium constants derived from the experimental data are not attributable to single ion exchange reactions.

The Vanselow selectivity coefficient of the Na/K exchange is evaluated from the experimental data measured at pH = 3 (range 3.0 - 3.3), pH = 4.5 (range 4.4 - 4.7) and pH = 11 (range 10.8 - 11.0). Figure 7 shows that, within the scatter of the data, the Vanselow selectivity coefficient, K_V , can be assumed to be constant at pH = 11. The composition dependence of K_V at pH = 3 and pH = 4.5 at low values of the mole fraction of adsorbed K, x_{KX} , presumably reflects the composition dependence of the competitive exchange reactions $\text{Na}^+ \rightarrow \text{K}^+$ and $\text{Na}^+ \rightarrow \text{H}^+$. Note that at high values of x_{KX} , the Vanselow selectivity coefficient is constant within the scatter of the data. Hence the results indicate the possibility of ideality of the Na/K exchange on Na-smectite. Using all the data shown in Figure 7, the Vanselow selectivity coefficient can be estimated to $K_V = (1.58 \pm 0.39)$. In the case of homovalent ion exchange, the

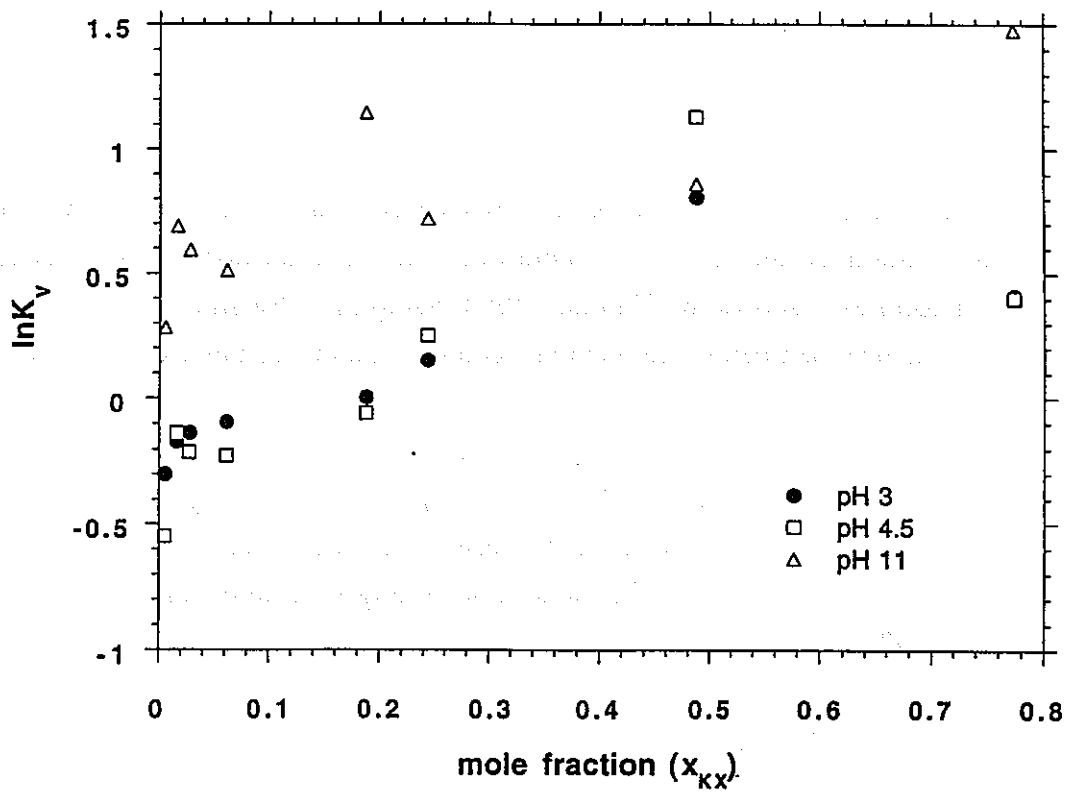


Figure 7 Graph of $\ln K_v$ as a function of the mole fraction of $KX(s)$, x_{KX} , for Na/K exchange on montmorillonite at different pH values.

Vanselow selectivity coefficient corresponds to the thermodynamic equilibrium constant, K_X° .

4 Leaching of purified bentonite (Na-smectite) and Kunipia F and Kunigel V1 bentonite in distilled water

4.1 Purified bentonite (Na-smectite)

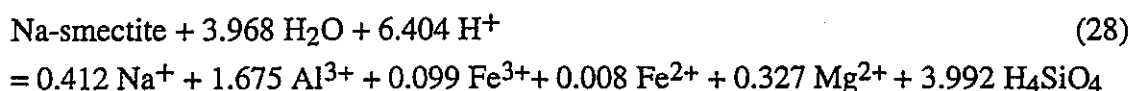
Purified bentonite was prepared from Kunipia F bentonite by washing the elutriated Kunipia F bentonite with $\text{CH}_3\text{COOH} / \text{CH}_3\text{COONa}$ and subsequently with $\text{C}_2\text{H}_5\text{OH}$ in order to minimize the content of impurities. The montmorillonite was converted into the Na-form as described by Yajima (1993). Samples of Na-smectite were used in the ion exchange experiments (see previous sections) and in leaching experiments.

The ratio of the elemental composition of the so prepared Na-smectite is given in Table 2. The CEC was determined to 107.2 meq/100g, 108.1 meq/100g and 110.2 meq/100g Yajima (1993). The formula of the Na-form of montmorillonite is obtained from the elemental composition given in Table 2 according to a procedure described by van Olphen (1977):



The formula weight of the half unit cell and the Si/Al ratio are 374.60 and 2.38, respectively.

Dissolution of the Na-smectite in slightly acidic media (pH 5 - 6) occurs according to:



The reaction given in Eq. (28) represents stoichiometric and congruent dissolution of the mineral. However, the experimental data of the leaching test (Yajima, 1993) suggest that the solubility of amorphous Al hydroxide controls the Al concentration in solution in the near neutral pH range in all the experiments, accounting for an incongruent dissolution of Na-smectite. We hence expect incongruent dissolution of Na-smectite and the formation of amorphous Al hydroxide giving rise to the experimentally observed constancy of the Al concentration over time. In a similar manner, precipitation of Fe hydroxide controls the concentration of free Fe in solution. The stoichiometric formula for Na-smectite indicates that Fe, Mg, Ca, Na and K are present in trace amounts. Hence the high and relatively constant concentrations of Na^+ and K^+ ($4 - 6 \times 10^{-4}$ M and $1 - 2 \times 10^{-4}$ M, respectively) observed in the leaching test of Yajima

(1993) most likely indicate the presence of minor traces of impurities. The release of silicon from montmorillonite represents the dissolution of the Na-smectite structure. However, since the initial concentration of Si is very high ($3 - 4 \times 10^{-4}$ M), an increase of Si over time cannot be observed in the leaching tests conducted at 25° and 60°C. A dissolution rate of 10^{-8} mol g⁻¹ h⁻¹ can be determined from the experimental data measured at 90°C. The rate can be compared with the dissolution rates determined for K-montmorillonite and for kaolinite. From the release of Si, Furrer et al. (1993) determined a dissolution rate of 2.51×10^{-8} mol g⁻¹ h⁻¹ for K-montmorillonite at pH = 5 and t = 25°C. The dissolution rate of kaolinite has been reported to be 1.5×10^{-8} mol g⁻¹ h⁻¹ at pH = 6 and t = 25°C (Wieland and Stumm, 1992). Both studies show that in the near neutral pH range, the dissolution reactions of K-montmorillonite and kaolinite occur at edge surface sites.

In order to extract more information from the dissolution measurements of Na-smectite, a slight modification of the experimental setup is required. Prior to dissolution, the Na-smectite suspension can be "conditioned" by preexposing it for a limited period of time in bidistilled water. During the preconditioning step, highly reactive material is removed from the surface of Na-smectite causing a reduction of the initial concentration of the elemental composition in solution. A pretreatment procedure for K-montmorillonite was reported by Furrer et al. (1993). Preconditioning of Na-smectite facilitates the observation of a time-dependent increase of the element concentrations in solution. Furthermore, using "mixed-flow" reactors instead of batch reactors would offer a possibility to reduce the concentration of Fe and Al in solution below saturation with respect to Fe and Al hydroxides (Furrer et al., 1993).

Table 2: Elemental composition of Na-smectite used in the experiments (weight-%).

SiO ₂	62.3 %	MgO	3.42 %
TiO ₂	0.16 %	CaO	0.01 %
Al ₂ O ₃	22.2 %	Na ₂ O	3.22 %
Fe ₂ O ₃	2.05 %	K ₂ O	0.03 %
FeO	0.14 %	P ₂ O ₅	0.07 %
MnO	< 0.01 %	total-S	0.015 %
Cl ⁻	0.02 %	ignition loss	6.10 %
SO ₄ ²⁻	< 0.001 %		
CO ₂	< 0.005 %		

4.2 *Kunipia F and Kunigel V1 bentonite*

Leaching tests with Kunipia F bentonite were conducted in distilled water with the bentonite/water ratio (0.01 - 1 g/ml) and the reaction time (3, 14, 28, 70 and 100 days) as variable parameters (Sasaki, 1993). Kunipia F contains > 95% Na-montmorillonite. These experiments allow to derive the contents of soluble impurities in Kunipia F, assuming that, after an equilibration time of 14 days, the soluble impurities are completely dissolved. The percentages of impurities, KCl, NaCl, CaSO₄ and NaNO₃, are listed in Table 3. These percentage values are derived from the increase of the concentrations of K⁺, Cl⁻, SO₄²⁻ and NO₃⁻ in the leaching tests. The choice of the

Table 3: Impurities in Kunipia F (weight-%).

solid/water ratio [g/ml]	% KCl	% NaCl	% CaSO ₄	% NaNO ₃
1	0.0034	0.1094	1.0629	7.68E-03
1	0.0031	0.1064	0.9779	1.33E-02
0.5	0.0036	0.0961	1.0204	4.25E-03
0.5	0.0029	0.0835	0.7937	4.11E-03
0.2	0.0044	0.0765	0.6519	3.56E-04
0.2	0.0045	0.0756	0.7795	9.60E-05
0.1	0.0032	0.0337	0.6944	<5.48E-05
0.1	0.0061	0.0710	0.7370	6.85E-04
0.1 *	0.0036	0.0467	0.6250	6.17E-04
0.02	0.0086	0.0650	0.4110	<5.48E-05
0.02	0.0086	0.0625	0.4110	<5.48E-05
0.01	0.0057	0.0483	0.4535	<5.48E-05
0.01	0.0076	0.0468	0.3543	6.85E-05
average	0.0050	0.0712	0.6935	
	±0.002	±0.024	±0.244	

* Average values from the measurements after 3, 14, 28, 70 and 100 days.

respective counter ions is based on assumptions. It is difficult to distinguish between KCl and NaCl, because K^+ is an exchangeable ion, and part of the KCl impurity may have reacted with the montmorillonite surface. Table 3 shows NaCl and $CaSO_4$ as the major impurities with contents ranging from 0.05 - 0.1 % and 0.4 - 1%, respectively. Since the Kunipia F bentonite is reported to be 100% in the Na-form, the increase in the K^+ concentration in solution is probably due to a soluble potassium impurity. It should be mentioned that $CaCO_3$ is another impurity found in bentonites. The solubility of $CaCO_3$ is low, however, and the degree of its dissolution depends to a large extent on the ion exchange reactions. The analyses in Table 3 might suggest a systematic decrease of the relative amounts of dissolved impurities with decreasing solid/water ratio. However, the difference in dissolved NaCl and $CaSO_4$ at a solid/water ratio between 1 g/ml and 0.01 g/ml is only a factor of 2. We therefore consider it justified to average the values and define a mean percentage of impurities, as indicated in the last row of Table 3. It should also be mentioned that an experiment carried out to determine

Table 4: Impurities in Kunigel V1 (weight-%) after 14 days of reaction time.

solid/water ratio [g/ml]	% KCl	% NaCl	% $CaSO_4$	% $NaNO_3$
0.5	0.0015	0.0017	0.284	2.33E-03
0.5	0.0015	0.0017	0.284	2.33E-03
0.2	0.0028	0.0011	0.404	1.00E-03
0.2	0.0027	0.0013	0.404	1.01E-03
0.1	0.0034	0.0008	0.383	4.93E-04
0.1	0.0036	0.0010	0.411	4.93E-04
0.02	0.0057	0.0011	0.369	9.60E-05
0.02	0.0056	0.0009	0.390	8.22E-05
0.01	0.0075	0.0005	0.411	4.11E-05
0.01	0.0094	0.0004	0.496	4.11E-05
average	0.0044 ± 0.0026	0.0011 ± 0.0004	0.38 ± 0.06	

the reaction time shows constant solution concentration over a period of 3 to 100 days, indicating that the dissolution of impurities is not subject to any serious kinetic constraints. The dissolution of nitrate shows large variations with the solid/water ratio, its concentration is in general very low, and in some cases even below the detection limit. Based on the present knowledge, the comparatively small amounts of nitrate that may be released from the bentonite can be neglected in the safety analysis or in the assessment of long-term behaviour.

Leaching tests with Kunigel V1 bentonite were conducted in distilled water with bentonite/water ratios varying between 0.01 - 0.5 g/ml and the reaction times ranging from 3 to 180 days (Sasaki, 1993). A similar analysis as above shows that CaSO₄ is the

Table 5: Impurities in 0.1 g/ml Kunigel V1 (weight-%) as a function of time.

Reaction time [days]	% KCl	% NaCl	% CaSO ₄	% NaNO ₃
3	0.0032	0.0004	0.3260	4.25E-04
3	0.0029	0.0006	0.3260	4.11E-04
7	0.0032	0.0006	0.3401	4.66E-04
7	0.0034	0.0001	0.3118	4.80E-04
14	0.0034	0.0008	0.3827	4.93E-04
14	0.0036	0.0010	0.4110	4.93E-04
28	0.0040	0.0002	0.5244	4.52E-04
28	0.0038	0.0003	0.5102	4.93E-04
42	0.0042	0.0005	0.5102	4.39E-04
42	0.0042	0.0003	0.5244	4.11E-04
70	0.0045	0.0002	0.6944	4.52E-04
70	0.0047	0.0004	0.6944	4.80E-04
100	0.0051	0.0003	0.7795	4.11E-04
100	0.0049	0.0003	0.7511	3.29E-04
180	0.0064	0.0001	0.7937	3.56E-04
180	0.0061	0.0002	0.7795	3.15E-04

major impurity in Kunigel V1 with contents ranging from 0.3 - 0.8 %. The analyses show a fairly constant proportion of NaCl, KCl and CaSO₄ over a solid/water ratio ranging from 0.01 g/ml to 0.5 g/ml. Again, the nitrate content varies considerably, however, as mentioned above for Kunipia F, the dissolution of such small amounts of nitrate may not be important for the assessment of the long-term behaviour of bentonite. Table 5 shows the time dependence of the dissolution of impurities at a solid/water ratio of 0.1 g/ml, suggesting that the dissolution reactions may not be completed after 14 days. Even after 180 days, the solution concentration of sulfate and potassium are still rising. The same trend is observed at other solid/water ratios. However, it is obvious that a large part of the impurities dissolves in a very short time (3 days) and that thereafter the increase in the concentration of dissolved impurities is comparatively small.

5 Conclusions and Recommendations

The goal of this work was to interpret the ion exchange processes on Na-smectite using the experimental data reported by Yajima (1993) and a thermodynamic model for the montmorillonite/water interaction. The thermodynamic model is based on the concept of hypothetical surface complex formation and is compatible with ion-association models such as MINEQL (Wanner, 1986) or MIN_SURF. The modelling procedure can be used to simulate simultaneous ion exchange reaction, surface complex formation, as well as speciation in solution and at the solid/water interface. The modelling approach outlined in this study is flexible and thermodynamically self-consistent.

In general the model predictions are in good agreement with the experimental results of Yajima (1993). The model computations correctly predict the Na/K exchange on Na-smectite in a chloride background medium of increasing ionic strength. Na/K exchange was modelled at pH = 3, 4.5 and 11 according to the pH conditions reported in the experimental study. For modelling the exchange isotherm at pH = 11, we also include the possible interaction of K⁺ with negatively charged edge surface sites. Model computations predict that the three exchange isotherms should overlap. Since the density of edge surface sites is small compared to the CEC and the concentration of K⁺ comparatively large, the association of K⁺ with edge surface sites has little effect on the exchange isotherm of K⁺ at pH = 11. The deviation of the experimental and modelled exchange isotherms at pH = 3 and 4.5 can possibly be attributed to the competitive exchange reactions of Na/K and H/K occurring at the Na-smectite surface in the acidic

pH range. The proton balance in the acidic pH range is determined by three coinciding reactions: Ion exchange (e.g., Na/H and K/H exchange), protonation of edge surface sites and, in the strongly acidic pH range, dissolution of the montmorillonite structure. Hence a proper determination of the equilibrium constant for the Na/H exchange requires the evaluation of all three reactions and their contribution to the overall proton balance within the experimental time scale.

In the model computations of Na/Ca and Na/Mg exchange reactions in chloride background medium, we emphasize the effect of anion adsorption on the Ca²⁺ and Mg²⁺ exchange isotherms which has been reported previously by Fletcher and Sposito (1989). In general, the experimental results of the Na/Ca and Na/Mg exchange reactions

Table 6: Parameters used to model purified Na-smectite.

Cation exchange capacity	108.1 meq/100 g
Exchangeable ions	100 % Na
Ion exchange reactions at layer sites: Value of the constant K_X° : 1)	
$K^+ + NaX = KX + Na^+$	1.8
$H^+ + NaX = HX + Na^+$	1.26 / 8.9 *
$Ca^{2+} + 2 NaX = CaX_2 + Na^+$	1.48
$Mg^{2+} + 2 NaX = MgX_2 + Na^+$	1.48
$Ca^{2+} + Cl^- + NaX = CaClX + Na^+$	193
$Mg^{2+} + Cl^- + NaX = MgClX + Na^+$	181
Surface complexation at edge sites:	
$K^+ + NaE = KE + Na^+$	1.8 / 18 *

1) The constants for ion exchange reactions on montmorillonite are reported by Fletcher and Sposito (1989) except those indicated with an asterisk. (*) denotes estimated values. The constants refer to equilibrium expressions given in mole fractions of the adsorbed species. We assume that beidellite and nontronite which are also present in Na-smectite behave like montmorillonite.

on Na-smectite are predicted adequately. In media with complexing anions (e.g., chloride and nitrate), an increased selectivity for divalent cations has been observed (Fletcher and Sposito, 1989). Therefore the simulations were conducted by implementing ion exchange reactions with Ca^{2+} , CaCl^+ and Mg^{2+} and MgCl^+ , respectively. The effect of chloride on the Na/Ca and Na/Mg exchange isotherms is adequately reflected in the model computations. The simulations reveal that cation exchange experiments with divalent cations (e.g., Ca^{2+} and Mg^{2+}) must be conducted in a medium with non-complexing anions (e.g., perchlorate) for a proper determination of the Ca^{2+} and Mg^{2+} exchange constants. The parameters used in modelling the ion exchange reactions on Na-smectite are summarized in Table 6.

The chemical significance of activity coefficients of surface complexes is discussed in the context of the composition dependence of the conditional equilibrium constant, i.e., the Vanselow selectivity coefficient, K_V . Based on the solid solution model, the activity coefficient of surface complexes, denoted as rational activity coefficient, f , is defined on a thermodynamic activity-concentration relationship. The chemical significance of the rational activity coefficient is parallel to that developed for the aqueous-species activity coefficient.

An exchanger phase is said to be an ideal solid solution if the rational activity coefficient of each component of the solid-phase mixture is equal to 1 regardless of the composition of the mixture. Ideal ion exchange is consistent with the compositional independence of the Vanselow selectivity coefficient. Hence, based on this definition of an ideal exchanger phase, the mole fractions alone are adequate to reflect the composition dependence of the thermodynamic equilibrium constant. Furthermore, the conditional equilibrium constant, i.e., the Vanselow selectivity coefficient, and the thermodynamic equilibrium constant are identical and take a constant value. Ideality on montmorillonite is supported generally by a range of experimental studies (Fletcher and Sposito, 1989). We have investigated the possibility of ideality on montmorillonite using the experimental results of the Na/K exchange reactions. In view of the scatter of the experimental results determined at pH = 11 and the uncertainty in the data measured in the acidic pH range (competition of the K/H exchange reaction), the Vanselow selectivity coefficient for the Na/K exchange appears to be relatively constant. Hence the Na-smectite used in the experimental study of Yajima (1993) is likely to conform to ideal behaviour.

Leaching tests of Kunipia F and Kunigel VI reported by Sasaki (1993) allow the determination of soluble impurities in these two bentonites. The knowledge of these

impurities is important for predictive modelling, especially when the contacting aqueous phase has a low degree of mineralisation. Kunipia F is found to contain 0.69% CaSO_4 , 0.071% NaCl and 0.005% KCl as soluble impurities. The impurities of Kunigel VI are 0.38% CaSO_4 , 0.0011% NaCl and 0.0044% KCl .

The model computations presented in this report point to a few recommendations regarding a possible extension of the experimental studies. In the following, we would like to briefly outline these recommendations :

a) Experimental protocol

Ion exchange experiments should be conducted at constant pH and constant ionic strength (e.g., $I = 0.1$ or 0.05 M). Under these conditions, higher surface coverages of the exchangeable cations can be achieved.

b) Electrolyte background

The electrolyte medium chosen as an ionic background in the experiments may significantly affect the experimental results. The presence of chloride, for example, leads to the adsorption of CaCl^+ and MgCl^+ in Na/Ca and Na/Mg adsorption studies. We hence recommend that the cation exchange experiments with divalent cations (Ca^{2+} , Mg^{2+} etc.) may also be conducted in background media containing non-complexing anions (e.g., perchlorate). The exchange constants of Ca^{2+} and Mg^{2+} determined in perchlorate background ionic media can then be used to evaluate the exchange constants for CaCl^+ and MgCl^+ in chloride background ionic media. It appears that in dilute electrolyte solutions monovalent cations (e.g., Na^+ , K^+ , etc.) do not encourage this type of adsorption.

c) pH dependence of ion exchange reactions

Protons in solution react with the layer and edge surface sites of Na-smectite and therefore may interfere with ion exchange reactions. An extension of the experimental programme regarding the pH dependence of ion exchange reactions should address the problem of separating ion exchange reactions (e.g., Na/H exchange at layer sites) and protonation of edge surface sites.

Ternary ion exchange reactions occurring in the acidic pH range may further complicate the determination of equilibrium constants of cation exchange reactions. In this pH range, layer sites are partially occupied by protons reducing the apparent CEC. Studying the exchange of cations, e.g., Na/K exchange, in the acid pH range hence requires an appropriate evaluation of K/H and Na/K exchange reactions. This again

leads back to the problem of separating protonation of layer and edge surface sites over the entire pH range.

Although the amount of edge sites in montmorillonite is about an order of magnitude smaller than that of the layer sites, it is very likely that they play an important role in retarding certain radionuclides through the formation of stable surface complexes. In order to form a basis for evaluating the retardation capabilities of the edge sites, it is necessary to investigate their reactivities. This can be done by alkalimetric and acidimetric titrations of the edge sites.

d) Presentation of the experimental data

The Vanselow convention suggests the determination of the conditional equilibrium constant in terms of mole fractions instead of equivalent fractions. The convention is consistent with a thermodynamic definition of the rational activity coefficient of surface components. The problem of ideality or non-ideality of the exchanger phase can be addressed by evaluating the composition dependence of the Vanselow selectivity coefficient. We hence recommend to present the experimental data of ion exchange experiments in a graph showing the Vanselow coefficient (determined from the experimental data) as a function of the mole fraction of a surface component. Ideal behaviour is indicated by a constant Vanselow selectivity coefficient regardless of the composition of the exchanger phase. If the selectivity coefficient depends on the composition, chemical thermodynamic methods can then be applied to derive equations for activity corrections as a function of the composition of the exchanger phase. The modelling approach presented in this report is flexible enough to accommodate exchanger-phase activity coefficients if required.

e) Total carbonate control

The amount of carbonate in solution is an important parameter in modelling solution speciation in the alkaline pH range. Hence the control of CO₂ during the experiments, i.e., maintaining a constant partial pressure of CO₂ or complete absence of CO₂ facilitates model computations.

e) Leaching experiments

We recommend to carry out similar leaching tests for each type of bentonite considered in the selection process of backfill material for radioactive waste repositories. The experiments should be designed in such a manner that dissolution processes related to the presence of small amounts of impurities and related to the long-term stability of the montmorillonite structure can be distinguished and quantified.

6 Acknowledgment

We would like to express our thanks to Prof. L. Charlet (University of Grenoble) for helpful discussions.

7 References

- Berner, U. (1986). MIN-SURF. PSI version of MINEQL code, Würenlingen.
- Fletcher, P., and Sposito, G. (1989). The chemical modelling of clay/electrolyte interactions for montmorillonite. *Clay Minerals* **24**, 375 - 391.
- Furrer, G, Zysset, M., and Schindler, P.W. (1993). Weathering kinetics of montmorillonite: Investigations in batch and mixed-flow reactors. In: *Geochemistry of Clay-Pore Fluid Interactions* (eds. D.A.C. Manning, P.L. Hall and C.R. Hughes). Chapman & Hall, London.
- Gaines, G.L., and Thomas, H.C. (1953). Adsorption studies on clay minerals. II. A formulation of the thermodynamics of exchange adsorption. *J. Chem. Phys.* **21**, 714 - 718.
- Gast, R.G. (1971). Alkali metal cation exchange on Chambers montmorillonite. *Soil Sci. Soc. Am. Proc.* **36**, 14 - 18.
- Gast, R.G., Van Bladel, R., and Deschpande, K.B. (1969). Standard heats and entropies of exchange for alkali metals on Wyoming bentonite. *Soil Sci. Soc. Am. Proc.* **33**, 661 - 669.
- Guggenheim, E.A. (1952). *Mixtures*. Oxford University Press, London.
- Sasaki, T. (1993). Personal communication to H. Wanner, Power Reactor and Nuclear Fuel Development Corporation (PNC), Tokai-mura, Japan.
- Shaviv A., and Mattigod, S.V. (1985). Cation exchange equilibria in soils expressed as cation-ligand complex formation. *Soil. Sci. Soc. Am. J.* **49**, 569 - 578.
- Sierro, N. (1992). MIN_SURF. MBT PC-version of MINEQL code, Zürich.
- Sposito, G. (1977). The Gapon and the Vanselow selectivity coefficients. *Soil Sci. Soc. Am. J.* **41**, 1205 - 1206.
- Sposito, G., and Mattigod, S.V. (1979). Ideal behavior in Na⁺-trace metal cation exchange on Camp Berteau montmorillonite. *Clays Clay Minerals* **27**, 125 - 128.

Sposito, G. (1981). *The thermodynamics of soil solutions*. Oxford University Press, New York, 223 pp.

Sposito, G., Holtzclaw, K.M., Johnston, C.T., and LeVesque, X. (1981). Thermodynamics of sodium-copper exchange on Wyoming bentonite at 298 K. *Soil Sci. Soc. Am. J.* **45**, 1079 - 1085.

Sposito, G., Holtzclaw, K.M., Charlet, L., Jouany, C., and Page, A.L. (1983a). Sodium-calcium and sodium-magnesium exchange on Wyoming bentonite in perchlorate and chloride background ionic media. *Soil Sci. Soc. Am. J.* **47**, 51 - 56.

Sposito, G., Holtzclaw, K.M., Jouany, C., and Charlet, L. (1983b). Cation selectivity in sodium-calcium, sodium-magnesium, and calcium-magnesium exchange on Wyoming bentonite at 298 K. *Soil Sci. Soc. Am. J.* **47**, 917 - 921.

Sposito, G., Jouany, C., Holtzclaw, K.M., and LeVesque, X. (1983c). Calcium-magnesium exchange in the presence of adsorbed sodium. *Soil Sci. Soc. Am. J.* **47**, 1081 - 1085.

Sposito, G. (1984). *The surface chemistry of soils*. Oxford University Press, New York, 235 pp.

Van Olphen, H. (1977). *Clay colloid chemistry*. Wiley-Interscience, New York.

Vanselow, A.P. (1932). Equilibria of the base-exchange reactions of bentonites, permutites, soil colloids, and zeolithes. *Soil Sci.* **33**, 95 - 113.

Wanner, H. (1986). Modelling interaction of deep groundwaters with bentonite and radionuclide speciation. Nagra NTB 86-21, Baden, Switzerland. NTP 86-21.

Wieland, E., and Stumm, W. (1992). Dissolution kinetics of kaolinite in acidic aqueous solutions at 25°C. *Geochim. Cosmochim. Acta* **56**, 3339 - 3355.

Yajima, T. (1993). Personal communication to H. Wanner, Mitsubishi Material Corporation, Naka-gun, Japan.

卷末資料 (2)

卷末資料 2

拡散試験データ集

- (1) ウランの定常拡散試験データ
- (2) アメリシウム²⁴¹の定常拡散試験データ

672	5.7×10^{-5}	7.9×10^{-4}
696	5.6×10^{-5}	8.3×10^{-4}
720	5.7×10^{-5}	8.6×10^{-4}
744	5.4×10^{-5}	8.9×10^{-4}
768	5.0×10^{-5}	9.1×10^{-4}
792	5.4×10^{-5}	9.4×10^{-4}
816	5.3×10^{-5}	9.1×10^{-4}
840	4.3×10^{-5}	9.4×10^{-4}
	試験終了	

巻末資料2 アメリシウムの定常拡散試験データ

表2.1 ~2.3 にアメリシウムの定常拡散試験の測定データを示す。▨の部分には定常状態と判断し、実効拡散係数の解析を行ったデータ部分である。

資料2.1-(1) Am定常拡散試験データ
(0.8 g/cm³, フィルタ)

資料2.1-(2) Am定常拡散試験データ
(0.8 g/cm³, 本試験)

経過時間 (hr)	高濃度側濃度 C ₀ (cpm/ml)	低濃度側への 積算通過量 Q(t) (cpm)
0	11809	2026
2	11874	3964
6	11722	5599
24	11561	11050
32	11503	12789
47	11516	13009
120	11405	37040
144	11515	49108
168	11414	55137
192	11405	65222
216	11392	69491
288	11301	87420
312	11100	88724
336	11046	94720
360	11098	102706
	試験終了	

経過時間 (hr)	高濃度側濃度 C ₀ (cpm/ml)	低濃度側への 積算通過量 Q(t) (cpm)
0	1.17×10 ³	2.13×10 ³
7	1.15×10 ³	1.72×10 ³
24	1.13×10 ³	2.95×10 ³
48	1.12×10 ³	3.42×10 ³
72	1.10×10 ³	2.39×10 ³
96	1.12×10 ³	1.91×10 ³
168	1.09×10 ³	3.95×10 ³
192	1.08×10 ³	4.79×10 ³
264	1.07×10 ³	4.44×10 ³
336	1.04×10 ³	4.70×10 ³
432	1.02×10 ³	5.81×10 ³
528	1.01×10 ³	7.09×10 ³
600	9.85×10 ⁴	8.99×10 ³
672	9.66×10 ⁴	1.10×10 ⁴
768	9.53×10 ⁴	1.67×10 ⁴
840	9.30×10 ⁴	2.09×10 ⁴
888	1.05×10 ³	2.25×10 ⁴
1008	1.02×10 ³	2.96×10 ⁴
1176	9.84×10 ⁴	4.05×10 ⁴
1344	9.41×10 ⁴	5.55×10 ⁴
1440	1.05×10 ³	6.19×10 ⁴
1512	1.05×10 ³	7.02×10 ⁴

資料2.3-1) Am定常拡散試験データ
(1.8 g/cm^3 , フィルタ)

経過時間 (hr)	高濃度側濃度 C_0 (cpm/ml)	低濃度側への 積算通過量 $Q(t)$ (cpm)
0	11741	0
2	11674	318
6	11737	6509
24	11713	11145
32	11594	9238
47	11700	17233
120	11500	24669
144	11547	31900
168	11326	35587
192	11281	44881
216	11375	49745
288	11264	62661
312	11165	67147
336	11121	73430
360	11138	77572
	試験終了	

資料2.3-2) Am定常拡散試験データ
(1.8 g/cm^3 , 本試験)

経過時間 (hr)	高濃度側濃度 C_0 (cpm/ml)	低濃度側への 積算通過量 $Q(t)$ (cpm)
0	1.15×10^4	7.96×10^1
7	1.14×10^4	2.61×10^1
24	1.12×10^4	2.63×10^2
48	1.12×10^4	8.11×10^2
72	1.10×10^4	5.99×10^0
96	1.11×10^4	5.99×10^0
168	1.07×10^4	1.29×10^3
192	1.07×10^4	1.25×10^3
264	1.05×10^4	3.11×10^2
336	1.01×10^4	1.50×10^3
432	9.91×10^3	2.73×10^3
528	9.59×10^3	3.99×10^3
600	9.51×10^3	4.85×10^3
672	9.34×10^3	7.47×10^3
696	9.19×10^3	7.68×10^3
720	1.04×10^4	9.46×10^3
840	1.03×10^4	1.49×10^4
1008	9.80×10^3	2.23×10^4
1176	9.33×10^3	3.03×10^4
1344	1.01×10^4	3.83×10^4
1440	9.97×10^3	4.16×10^4
1512	9.72×10^3	4.75×10^4
1680	9.28×10^3	5.78×10^4
1776	1.05×10^4	6.23×10^4
1848	1.02×10^4	6.82×10^4
1896	1.01×10^4	7.32×10^4

資料2.3-1) Am定常拡散試験データ
(1.8 g/cm³, フィルタ)

経過時間 (hr)	高濃度側濃度 C ₀ (cpm/ml)	低濃度側への 積算通過量 Q(t) (cpm)
0	11741	0
2	11674	318
6	11737	6509
24	11713	11145
32	11594	9238
47	11700	17233
120	11500	24669
144	11547	31900
168	11326	35587
192	11281	44881
216	11375	49745
288	11264	62661
312	11165	67147
336	11121	73430
360	11138	77572
	試験終了	

資料2.3-2) Am定常拡散試験データ
(1.8 g/cm³, 本試験)

経過時間 (hr)	高濃度側濃度 C ₀ (cpm/ml)	低濃度側への 積算通過量 Q(t) (cpm)
0	1.15×10 ⁴	7.96×10 ¹
7	1.14×10 ⁴	2.61×10 ¹
24	1.12×10 ⁴	2.63×10 ²
48	1.12×10 ⁴	8.11×10 ²
72	1.10×10 ⁴	5.99×10 ⁰
96	1.11×10 ⁴	5.99×10 ⁰
168	1.07×10 ⁴	1.29×10 ³
192	1.07×10 ⁴	1.25×10 ³
264	1.05×10 ⁴	3.11×10 ²
336	1.01×10 ⁴	1.50×10 ³
432	9.91×10 ³	2.73×10 ³
528	9.59×10 ³	3.99×10 ³
600	9.51×10 ³	4.85×10 ³
672	9.34×10 ³	7.47×10 ³
696	9.19×10 ³	7.68×10 ³
720	1.04×10 ⁴	9.46×10 ³
840	1.03×10 ⁴	1.49×10 ⁴
1008	9.80×10 ³	2.23×10 ⁴
1176	9.33×10 ³	3.03×10 ⁴
1344	1.01×10 ⁴	3.83×10 ⁴
1440	9.97×10 ³	4.16×10 ⁴
1512	9.72×10 ³	4.75×10 ⁴
1680	9.28×10 ³	5.78×10 ⁴
1776	1.05×10 ⁴	6.23×10 ⁴
1848	1.02×10 ⁴	6.82×10 ⁴
1896	1.01×10 ⁴	7.32×10 ⁴